Analysis of 13C and 15N isotopes from Eurasian Quaternary fossils: Insights in diet, climate and ecology
Kuitems, M.

Cover Page

Universiteit Leiden

Author: Kuitems, M.
Title: Analysis of 13C and 15N isotopes from Eurasian Quaternary fossils: Insights in diet, climate and ecology
Issue Date: 2020-05-14

Analysis of ^{13}C and ^{15}N isotopes from Eurasian Quaternary fossils

Insights in diet, climate and ecology

Proefschrift

ter verkrijging van
de graad van Doctor aan de Universiteit Leiden,
op gezag van Rector Magnificus prof.mr. C.J.J.M. Stolker,
volgens besluit van het College voor Promoties
te verdedigen op donderdag 14 mei 2020
klokke 13.45 uur

door

Margot Kuitems
geboren te Houten
in 1985

Supervisors
Prof. dr. T. van Kolfschoten (Leiden University)
Prof. dr. J. van der Plicht (University of Groningen)

Assessment committee
Prof. dr. J. Kolen (Leiden University)
Prof. dr. M. Soressi (Leiden University)
Prof. dr. J.W.M. Roebroeks (Leiden University)
Prof. dr. A.M. Lister (Natural History Museum London, United Kingdom)
Dr. A.N. Tikhonov (Zoological Institute, Russian Academy of Sciences, Saint Petersburg, Russia)
Dr. L. Llorente Rodriguez (Leiden University)

Contents

CHAPTER 1
INTRODUCTION

The environmental context in which the cultural and physical evolution of humans took place is a crucial aspect of archaeological research. Copious numbers of papers are devoted to the palaeoenvironmental reconstruction of the hominin niche during the Quaternary; a period that is characterized by major climatic changes as can be deduced from the different proxies preserved in the geological record.

A powerful tool to investigate the palaeoecological conditions in which hominins operated is the analysis of the stable carbon and nitrogen isotope signals in fossil bones and teeth. Fossil tissue reflects the chemical composition of the food that an organism ingested during its life. The stable carbon and nitrogen isotope compositions in the bone collagen of for instance herbivores are related to the isotopic composition of the plants they are eating, and in turn, the stable carbon and nitrogen values in these plants (and soils) are controlled by climatic and (local) environmental parameters. With the growing interest in environmental and dietary issues, combined with major technological innovations, the application of stable isotope studies increased dramatically since the publication of one of the first stable isotope papers written by Vogel and van der Merwe (1977) about the use of stable carbon isotope signals to distinguish between consumption of so-called C3 and C4 plants.

Stable isotope analysis is, nowadays, more commonly used in modern archaeological research. These studies are not limited to human fossils. Stable isotope data of co-occurring animals are also a valuable source of information for the reconstruction of the palaeoenvironment in which humans operated and a big advantage is that animal fossils are much more numerous than hominin remains. The application of stable isotope analysis offers an additional or another perspective on results achieved by other archaeological methods. Given the current sophistication of isotope measurement technology, low costs and fast sample throughput, large data sets are available nowadays.

1.1 Research foci

During the past years, the author was involved in several research projects, amongst others the investigation of fossils from Late Pleistocene Eurasia, from the North Sea region and from the archaeological site Schöningen (Germany). This thesis presents a compilation of several stable isotope case studies executed in the frame of these projects. These studies are mainly based on data from samples collected and chemically prepared by the author and on $\delta^{15}N$ and $\delta^{13}C$ data that were available at the Centre for Isotope Research, University of Groningen. The discussed dataset is extensive and allows to detect and compare inter- and intraspecific, diachronic and spatial patterns of feeding behaviour and habitat use. The dataset is valuable not only for its size, but also for the species it represents, the age of the samples and their geographical origin. The geographical distribution of the investigated samples is presented in Fig. 1.1.

Figure 1.1 The geographical distribution of all investigated samples. Regions are marked with a number that corresponds to the chapter in which the samples are discussed.

The focuses of the case studies are larger herbivores from: 1) the Late Pleistocene and Early Holocene fossil record from a number of regions within the Eurasian mammoth steppe biome, and 2) the Lower Palaeolithic and late Middle Pleistocene archaeological sites at Schöningen (Germany). The mammoth steppe biome and Schöningen are introduced in the sections 1.1.1 and 1.1.2, respectively.

1.1.1 The mammoth steppe ecosystem

The stable isotope data (except those from Schöningen) are from ^{14}C dated samples and are, therefore, mostly Holocene or Late Pleistocene in age with a maximum of ca. 50,000 years (which equals 45,000 yr BP (uncalibrated radiocarbon years BP) or ~ 50,000 cal yr BP, see Reimer *et al.*, 2013; van der Plicht and Palstra, 2016). A timespan that includes the Upper Palaeolithic, during which the Neanderthal got extinct and modern

humans expanded their distribution range to north of the Arctic Circle. Numerous cave paintings, from for instance France, date from this period. Many of them depict typical ice age mammals, such as woolly mammoth, woolly rhinoceros, giant deer, and aurochs.

The woolly mammoth (*M. primigenius*), with its large size, long tusks and thick fur, became worldwide an icon for the ice age. Its remains have been recovered abundantly throughout its distributional range that, during the Late Pleistocene, covered geographically a huge territory stretching from Western Europe via Eurasia and Beringia to Alaska and northern North America (Guthrie, 1990). The species inhabited a dry and highly productive environment with cold winters and warm summers (Guthrie, 1982, 1990, 2001); an unrivalled biotope that is characterized by its non-analogue combination of plant and animal species. This former 'tundra-steppe' or 'steppe-tundra' consisted of mosaic-like landscapes dominated by grass and herbs communities, with patches of shrub-tundra and forest (Sher *et al.*, 2005). This biotope is often referred to as 'mammoth steppe' (Guthrie, 1990), after its most famous dweller: the woolly mammoth.

There has been a specific relationship between hominins and woolly mammoths throughout the Palaeolithic. For instance, woolly mammoths have been depicted in paintings and sculptures, have formed an important food source, and their bones have been used as construction materials in dwellings and in modified form as tools (Soffer *et al.*, 1997; Svoboda *et al.*, 2005; Braun and Palombo, 2012; Agam and Barkai, 2018; Guil-Guerrero *et al.*, 2018).

At the end of the Pleistocene, climatic ameliorations from cold and arid to warmer and wetter circumstances caused sea level rise and replacement of the original 'mammoth steppe' vegetation by less productive mesic tundra in the north and (larch) forest further south (Lozhkin, 1993; Hoffecker and Elias, 2007; Andreev *et al.*, 2011). The environmental alterations were critical for the geographical distribution of many plant and animal species. Several typical mammoth steppe faunal elements, including the woolly mammoth, became extinct (Guthrie, 2001; Stuart *et al.*, 2002; Lister and Stuart, 2008; Stuart, 2015; Puzachenko *et al.*, 2017).

The mammoth steppe ecosystem has been subject to extensive multidisciplinary investigations, using 'classical' palaeontological methods and applying 'modern' techniques to study changes in different proxies. The adaptation of flora and fauna to the changes in climate during the Late Pleistocene-Early Holocene is an important research topic.

Insights into the geographical distribution of mammoths during the last 50,000 years have been obtained by analysing huge datasets of radiocarbon (^{14}C) dated remains from more than a thousand localities which yielded woolly mammoth remains (Stuart, 2005; Puzachenko *et al.*, 2017; Lister and Stuart, 2019). Moreover, extensive stable carbon and nitrogen isotope studies on various mammoth steppe dwellers from numerous localities across Eurasia and Alaska have been performed (Iacumin *et al.*, 2000; Bocherens, 2003; Drucker *et al.*, 2003b, 2014; Richards and Hedges, 2003; Stevens and Hedges, 2004; Fox-Dobbs *et al.*, 2008; Szpak *et al.*, 2010).

1.1.2 The Lower Palaeolithic sites of Schöningen

Successful stable isotope research is not restricted to samples within the ^{14}C age range. As long as collagen is well preserved, older samples can also yield reliable stable isotope data that can be used to reconstruct for instance the diet of specific species and their palaeoenvironmental conditions further back in time. Even Lower Palaeolithic samples can be good enough as indicated by the investigations of the fossils from Schöningen (Germany), assessed to be about 300,000 years old (van Kolfschoten *et al.*, 2012; Lang *et al.*, 2012).

The Schöningen Lower Palaeolithic sites are located east of the German village Schöningen, in an area with remnants of huge quarries; the result of opencast brown coal exploitation. In order to reach the Tertiary lignite, the overlying Quaternary sediments had to be removed. This resulted in the discovery of a number of sites yielding important archaeological finds. Most famous are the Palaeolithic wooden throwing sticks and perfectly shaped wooden spears discovered in 1995 (Thieme, 1997). The spears were found at the so-called Schö 13 II-4 site, referred to as the 'spear horizon', amongst thousands of remains of butchered horses (Voormolen, 2008; van Kolfschoten *et al.*, 2015a).

The fossil remains are extremely well preserved, allowing a detailed study of the bone surface displaying numerous cut marks, (long) scraping marks and small and large impact notches indicative for hominin activities such as dismembering, intensive marrow extraction and the use of bones as tools (van Kolfschoten *et al.*, 2015b). The excellent preservation is also reflected in the state of the fossil bone collagen. The collagen of many bones is in pristine condition which allows to investigate the stable isotope signal of the Lower Palaeolithic bones.

1.2 Research objectives

This research contributes to our understanding of the palaeoecological conditions during the Pleistocene/Early Holocene in Eurasia by analysing the stable isotope compositions of fossils from specific mammalian species which inhabited Eurasia. More specifically, the case studies in this thesis contribute - directly or indirectly - to answering the following research questions (RQs):

1. *What are the geographical as well as temporal differences in the stable isotope signals of the woolly mammoth fossils?*
2. *Does the stable isotope signal of the fossil bone tissue of the last surviving woolly mammoths in North-Eastern Siberia show similar changes as detected in Eastern Europe?*
3. *Was climate change the fatal blow for the woolly mammoth?*
4. *Which regional palaeoenvironmental conditions might have prevented an earlier human migration to the east?*
5. *What are the factors behind the observed discrepancy in $\delta^{15}N$ values between herbivores?*

6. *What was the diet of the* Elasmotherium sibiricum*, and how might this have contributed to its extinction?*

7. *What is the preservation state of the collagen from the Schöningen fossils like?*

8. *What was the proportion of forest versus open landscape during the deposition of different levels in Schöningen?*

9. *What was the diet of the Schöningen horses like, leading to such a distinct molar wear pattern?*

The research topics are elaborated in the following two sections.

1.2.1 Research questions concerning the mammoth steppe ecosystem

Although our knowledge of the mammoth steppe ecosystem has increased over the last decades, there are still several questions unanswered. Key questions concern the uniformity of the mammoth steppe biome through time and space (**RQ 1**). Studies on various proxies revealed interregional differences, which are in particular clear if one compares Eurasia and Alaska (Guthrie, 2001; Bocherens, 2003; Rivals *et al.*, 2010; Szpak *et al.*, 2010). Stable isotope studies indicate a distinctive pattern of elevated stable nitrogen values and depleted stable carbon values in mammal samples from Siberia compared to the values in samples from Europe, as well as from Alaska (Bocherens, 2003; Szpak *et al.*, 2010).

Diachronic differences in stable carbon and nitrogen isotope values have been observed in mammoth steppe faunal species other than woolly mammoths that occurred in North-western Europe and, although less pronounced, in Alaska. The changing isotope compositions have been linked to changes in environmental circumstances, especially those that were driven by major climatic changes that took place around the Last Glacial Maximum (LGM) and the Pleistocene/Holocene transition dating to roughly 25,000 and 11,000 years ago, respectively (Drucker *et al.*, 2003b, 2008; Richards and Hedges, 2003; Stevens and Hedges, 2004; Fox-Dobbs *et al.*, 2008).

Indeed, several regions of the woolly mammoth steppe biome have been extensively studied. However, in specific regions there are often chronological hiatuses in the stable isotope record and/or low sampling density within parts of the mammoth steppe biotope, which hampers a comparison of the data and the observation of possible changes through time (Fox-Dobbs *et al.*, 2008). For instance, published stable nitrogen and carbon data of woolly mammoth samples with a post-LGM age and in particular with an LGM age are scarce. However, it is interesting to know if the diet of the mammoth and hence, the stable isotope signal in the fossil bone tissue changed when the species approached its extinction (**RQ 2, 3**). North-eastern Siberia (number 3 in Fig. 1.1) was more or less continuously inhabited by the woolly mammoth from its first presence (~ 400,000 years ago) until its very extinction (~ 4,000 years ago). The most recent woolly mammoth remains with an age of 3685 ± 60 ^{14}C yr BP (Vartanyan *et al.*, 2008) are from Wrangel Island.

There is an ongoing debate about what caused the megafauna extinctions (including

the woolly mammoth) towards the end of the Pleistocene (for example, Lorenzen *et al.*, 2011; Stuart, 2015). Among the predominant hypotheses for the extinction of the woolly mammoth, are a) the overkill hypotheses stating that mainly human hunters are responsible for the extinction whereas other scholars assume that b) climate change played a major role; a third option is that the combination of overkill and climate change led to the megafauna extinction (for example, Martin, 1984; Koch and Barnosky, 2006; Haynes, 2007; Nikolskiy *et al.*, 2011; Braje and Erlandson, 2013; Cooper *et al.*, 2015). A dramatic shift in the stable carbon and nitrogen isotope values, observed in woolly mammoth fossils from the central East European Plains, coincide with the local extinction of the species. The shift in isotope values is associated with changing diet and environmental change and points to niche competition with other large herbivores. The changing circumstances possibly made in particular the woolly mammoths susceptible to overhunting (Drucker *et al.*, 2014, 2018).

It is very unlikely that niche competition with other large herbivores or human presence played a role in the extinction of the woolly mammoths at Wrangel Island (Gerasimov *et al.*, 2006; Nikolskiy *et al.*, 2011; Zimov *et al.*, 2012). If climate change is the major trigger that led to the extinction of the woolly mammoth, it is most probably reflected as changes in the stable carbon and nitrogen values in the fossil bones (**RQ 3**).

North-eastern Siberia is of major interest from an archaeological point of view, because humans crossed the area on their way from Eurasia to North America. Humans inhabited North-eastern Siberia (western Beringia) well before the onset of the LGM (for example, Pitulko *et al.*, 2004). Recent data support previous indications that show that humans were present even north of the polar circle as early as ca. 45,000 years ago (Pitulko, 2016). The timing of the human migration to the Americas, via Beringia, is a topic of an ongoing debate. There seems to be a general consensus, based on archaeological data, that the dispersal into North America did not take place until ca. 14,000 years ago (Guthrie, 2006; Wooller *et al.*, 2018). However, Vachula *et al.* (2019) suggest, based on for example recent genetic data and on the discovery of faecal biomarkers in the sediment archive of Lake E5 (Alaska), that humans might have been present in eastern Beringia (the American Arctic) already by ca. 32,000 years ago. The Late Pleistocene palaeoenvironmental conditions in Beringia play a crucial role in the debate on the timing and the pathway of human migration into North America and include among others the restricted geographical distribution of species such as the woolly rhinoceros, which flourished throughout Eurasia, but never crossed the Beringian land bridge between Eurasia and America (Guthrie, 2001; **RQ 4**).

The concentration of the stable carbon and nitrogen stable isotopes in, for instance bone collagen, is influenced by natural fractionation processes and depends heavily on the diet of the individual. The nitrogen values depend heavily on the trophic level of a species (DeNiro and Epstein, 1981; Schoeninger and DeNiro, 1984). However, stable nitrogen isotope data from Late Pleistocene mammals often show dramatic differences between those values of the extinct Pleistocene woolly mammoth and those of coeval

living large herbivores (Bocherens, 2003; **RQ 5**).

Another impressive mammoth steppe dweller, the giant rhinoceros or Siberian unicorn (*Elasmotherium sibiricum*), raised questions that demand stable isotope research. It was generally assumed that this Pleistocene megafauna species survived in the steppic zone of eastern Europe and Asia until ca. 200,000 years ago (see number 5 in Fig. 1.1). However, new ¹⁴C data of specimens from a number of localities convincingly indicate an extinction during the Late Pleistocene (Kosintsev *et al.*, 2019). The unique morphology of the dentition of the animal suggests a highly specialised diet (**RQ 6**).

1.2.2 Research questions concerning the Palaeolithic sites at Schöningen

The application of stable isotope research on older material is challenging. The Middle Pleistocene bones, botanical remains, and even insect remains collected at the sites in Schöningen are extraordinary well-preserved (see number 6 in Fig. 1.1). In case the collagen is preserved as well (**RQ 7**), stable isotope studies can contribute to the debate on environmental and morphological issues at the Schöningen sites. Since the discovery in 1992 of Palaeolithic bones and wooden- and stone artefacts, the focus of the ongoing multidisciplinary research has been on (bio)stratigraphical dating of the sites and the individual find horizons, on reconstructing the palaeoenvironment in which the hominins operated, and on subsistence strategies of the hominins. The Lower Palaeolithic finds are from a period of changing climate: from an interglacial optimum at the base of a sequence of successive depositional levels to the next cold stage at the top of the sequence. Botanical proxies are indicative for the occurrence of warm deciduous forest during the warm phase and for boreal forest and steppe vegetation during the colder periods. However, such a climate and environmental change within the different successive deposits is less obvious in the mammalian faunal record (**RQ 8**).

In addition, the macro- and microwear patterns of the horse molars from Schöningen diverge from those found in most other periods and sites in Central Europe (Rivals *et al.*, 2015). They show unusual pointed cusps indicating an abnormal diet (**RQ 9**).

1.3 Outline of the thesis

After the Introduction (**Chapter 1**), **Chapter 2** discusses the basic principles of ¹³C and ¹⁵N stable isotope research and its applications, and the applied analytical methods. The following chapters (3 - 6) present stable isotope research that has been published in different journals. The data and conclusions presented in the chapters match those in the original publications. However, the text presented in the chapters 3-6 has been modified in order to enhance coherence and consistency and prevent repetition throughout the thesis, and occasionally extra (background) information is provided. That is, parts of the introduction of the original articles have been incorporated in this thesis in the section on research goals and site description (Chapter 1), and most of the

methodological aspects from the articles have been aggregated in Chapter 2.

Chapter 3 discusses an extensive stable isotope record of Late Pleistocene and Holocene woolly mammoths from North-eastern Siberia. Aim of the stable isotope studies of the east Siberian mammoth, presented in **Chapter 3**, is to track possible shifts within the stable carbon and nitrogen record coinciding with global climatic changes as were observed in other parts of the mammoth steppe biotope. Special focus is drawn to the Holocene data of fossils from Wrangel Island, in order to increase our understanding of the conditions under which the last mammoths lived.

Chapter 3 provides us with information about the conditions in the central part of the mammoth steppe biome, whereas **Chapter 4** presents stable isotope data from the western part of the mammoth steppe ecosystem, that is, the North Sea area (see number 4 in Fig. 1.1). During the Weichselian, the sea-level dropped dramatically and a landmass, that can be regarded as the western extension of the North European Plain (Schild, 1976), connected the European Continent and Great Britain. This landmass was intersected by large rivers (Hijma *et al.*, 2012) and covered by a characteristic mammoth steppe vegetation. The large amount of (mainly unstratified) fossils, including Neanderthal and anatomically modern human remains, indicate that the area was roamed by the typical mammoth steppe fauna with species such as the woolly mammoth, the woolly rhinoceros and large carnivores such as cave hyenas and lions. In the past decades, thousands of fossil remains have been collected, often from a stratigraphically disturbed context. In order to place the finds within a chronological context, many fossils have been ^{14}C dated. This resulted in a large set of ^{14}C data as well as stable isotope data, both from animals and humans. These data are discussed in **Chapter 4**.

Fossil remains from the characteristic Pleistocene megafauna in South-eastern Europe and adjacent areas in Asia indicate that the mammoth steppe biome stretched well into these regions. **Chapter 5** presents Late Pleistocene data of an extinct species that lived in the southern part of the mammoth steppe, the giant rhinoceros (*Elasmotherium sibiricum*). New ^{14}C data of fossils from the giant rhinoceros convincingly show that the species became extinct much later than assumed, that is during the Late Pleistocene (Kosintsev *et al.*, 2019). Changes within the environmental conditions might explain the extinction of the species. An additional, interesting topic is the diet of Elasmotherium. The species has extremely high-crowned rootless molars; a feature that is regarded as an adaptation to very abrasive food. The stable isotope data as examined in **Chapter 5** are an important proxy in the debate on the diet of the 'Siberian unicorn'.

Good quality collagen in bones that are way older than 50,000 years is scarce. In 2009, a pilot study, financially supported by the Leiden University Foundation (LUF), was executed to investigate whether the bones from the Middle Pleistocene archaeological sites in Schöningen, despite their age, contain collagen that potentially could be used for isotope research. Because of the very promising results (van der Plicht *et al.*, 2011) more fossils from different taxa and from different stratigraphical horizons were sampled for

stable carbon and nitrogen isotope analyses in order to gain additional environmental and dietary information of the various animal species in Schöningen. **Chapter 6** presents and discusses the carbon and nitrogen isotope data from the faunal remains from Schöningen (~ 300,000 years old). Because of the age of the samples, special attention is given to preservation issues of the collagen.

The results and conclusions of the case studies presented in the **Chapter 3-6** are integrated and discussed in **Chapter 7**.

Centre for Isotope Research, photo: R. Zijlstra

CHAPTER 2

STABLE ISOTOPES: PRINCIPLES AND ANALYTICAL METHODS

2.1 Introduction

This chapter is an introduction to the Chapters 3 to 6, addressing the principles and basics of the application of stable carbon and nitrogen isotopes as a tool for dietary and environmental reconstruction. The popularity of stable isotopes analysis increased almost exponentially over the last few decades (Szpak *et al.*, 2017) and the method is nowadays routinely applied in archaeological investigations. It is, however, important to realize that specific factors have an effect on the stable isotope signals in the different body tissues. The main factors will be discussed in this chapter.

The majority of the stable isotope data discussed in this thesis have been produced at the Centre for Isotope Research (CIO), University of Groningen, the Netherlands. The way the samples are prepared and measured at the CIO is concisely described in this chapter.

2.2 Fundamentals of stable isotope analysis

2.2.1 Isotopes of carbon and nitrogen in nature

In order to understand the behaviour of isotopes, we have to look at atoms first. All atoms consist of a heavy nucleus and a number of electrons moving 'in orbit' around this nucleus. The nucleus consists of protons (charged particles) and neutrons (neutral particles). The number of protons is equal to the atomic number by which a chemical element is identified. However, the mass of a chemical element can differ depending on the number of neutrons in the nucleus. The nucleus of carbon, with 6 protons, can have 6, 7 or 8 neutrons. Hence, there are in nature 3 different carbon isotopes: carbon-12 (^{12}C; 6 protons plus 6 neutrons), carbon-13 (^{13}C; 6 protons plus 7 neutrons), and carbon-14 (^{14}C or radiocarbon; 6 protons and 8 neutrons). Their abundances in nature are respectively 98.9, 1.1 and 10-10%. Nitrogen has two natural isotopes: ^{14}N and ^{15}N, with respective abundances of 99.6 and 0.4%.

The isotopes ^{12}C, ^{13}C, ^{14}N and ^{15}N are stable. ^{14}C is instable or radioactive, and decays through time with a regular pace. Therefore, the amount of ^{14}C in a fossil depends on its age, making this isotope well-known for dating organic samples. The ^{14}C dating method can be applied for organic materials up to around 50,000 years old.

Examples of elements of archaeological interest with more than one stable isotope are carbon (C), nitrogen (N), oxygen (O), hydrogen (H), and sulphur (S), important building blocks of biological molecules. This thesis focusses on carbon and nitrogen.

The different isotopes of a single element have similar chemical properties, and hence, behave chemically more or less the same. However, physically they behave in a different way. The dissimilarity in number of neutrons between isotopes causes different atomic masses. These lead to difference in reaction rates, creating small (predictable) differences in the natural abundances of isotopes in different materials. The lighter

isotopes (that is, the isotopes with the lower mass number) tend to react faster than the heavier, more resistant isotopes which affects the distribution. This process of isotope discrimination is called 'fractionation'. Fractionation leads to an unequal distribution in isotope ratio between the sources (generally more heavier isotopes) and products (generally more lighter isotopes). This is the essence of stable isotope analysis.

A well-known example of a process in which fractionation occurs is photosynthesis. A tree is depleted in ^{13}C (and in ^{14}C) compared to the atmosphere in which it lives, because photosynthesis causes fractionation: photosynthesis is a mass-dependent effect. The heavier isotopes are 'hindered' relative to the lighter ones. This results in a lower $^{13}C/^{12}C$ ratio in the tree than in its surrounding atmosphere.

2.2.2 Stable isotopes of carbon and nitrogen in the laboratory

Stable isotope values can be measured in samples extracted from all kinds of body tissues of both humans and animals, such as hair, bone, and teeth. The main material that is analysed in studies presented in this thesis is (bulk) collagen. Collagen is rich in carbon and nitrogen. It is the main protein found in mammals and facilitates the elasticity of bones. The collagen has to be chemically isolated before its stable isotope values can be investigated.

Stable isotope measurements are performed by mass spectrometry (MS; de Groot, 2004). For isotope ratios, a special form of MS is developed: Isotope Ratio Mass Spectrometry (IRMS). The machinery is based on molecular gases, which means that for this technique, the collagen of the target sample has to be combusted into the gases CO_2 and N_2 before isotope values of respectively carbon and nitrogen can be measured.

After combustion, the gas sample is led via an inlet system into an ion source. This produces a molecular ion beam (CO_2^+ or N_2^+) which is accelerated and steered into the mass analyser (Fig. 2.1). Here, ion beams with different masses are separated by a magnetic field. Heavier isotopes ($^{13}CO_2$ and $^{14}N^{15}N$ as the most relevant examples) follow a straighter flight path than the lighter isotope ($^{12}CO_2$, $^{14}N_2$) beams. The beam intensities of the different ion currents are measured by Faraday-cups. Based on these beam intensities, the isotope ratios are determined.
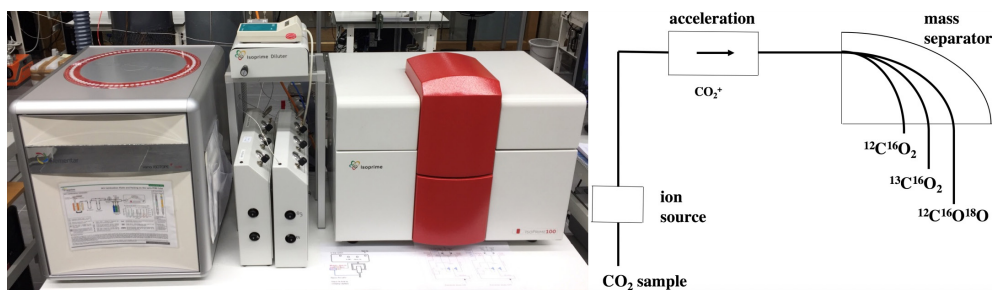
Figure 2.1 Left: Picture of the Elemental Analyser and the IRMS equipment at Groningen, respectively. Right: schematic representation of the way the IRMS operates.

The isotope composition of a sample is given in so-called δ-values. These values are defined as the deviation of the isotope ratio obtained from a sample and that of reference material for normalisation, which is taken along with each measurement. For the carbon and nitrogen isotope ratios these are:

$$^{13}\delta = \frac{(^{13}C/^{12}C)_{sample}}{(^{13}C/^{12}C)_{reference}} - 1 (\times 1000‰) \qquad \text{and} \qquad ^{15}\delta = \frac{(^{15}N/^{14}N)_{sample}}{(^{15}N/^{14}N)_{reference}} - 1 (\times 1000‰)$$

The numerical values for δ are very small. Therefore, they are expressed in per mill (‰, equivalent to 10^{-3}). The notation $\delta^{13}C$ and $\delta^{15}N$ is used in the literature and throughout this thesis instead of $^{13}\delta$ and $^{15}\delta$.

Each time samples are measured by IRMS, the gas of a specific amount of reference material is measured as well. Reference materials consist of 'control standards' and 'normalisation standards', with known isotopic compositions. Control standards are used to monitor the accuracy of the entire pretreatment and measurement procedure and the analytical precision. The measured isotopic value of the normalisation standard has to be 'normalised' and reported relative to the value of internationally recognised reference material. For carbon, this is Vienna PeeDee Belemnite (V-PDB), and for nitrogen, this is ambient inhalable reservoir (AIR). The absolute isotope contents of the reference materials is well known and have been measured very accurately (Mook, 2006 and references therein).

2.3 Principal concepts of the application of stable carbon and nitrogen analysis in archaeological research

Isotope analysis can provide a wide range of information. For instance, $\delta^{13}C$ and $\delta^{15}N$ values can be used as dietary tracers and can serve as indicators for past climatic and environmental conditions. In short, plant $\delta^{13}C$ and $\delta^{15}N$ values are directly controlled by climate and environment (for example, soil processes). Via food consumption, $\delta^{13}C$ and $\delta^{15}N$ values of plants are transferred to their consumers, and finally incorporated into their body tissues.

2.3.1 Stable isotopes of carbon and nitrogen: palaeodiet

Carbon is the universal building block of life. It is a constituent of atmospheric CO_2 and is dissolved in ocean water. Atmospheric carbon forms the key carbon source for terrestrial plants, which they take up by means of photosynthesis, and which is subsequently incorporated by other organisms in the food chain.

Also, nitrogen is a crucial component for all organisms. With a share of about 80% it is the most abundant element in the atmosphere. It is also present (in dissolved form) in ocean water. The N_2 gas is converted by micro-organisms in the soil to ammonium (NH4+; ammonification) or nitrate (NO3-; nitrification) before it is assimilated by

terrestrial plants, or it is made available to plants by nitrogen-fixing microbes living in symbiosis with the plant. In the body of animals and humans, nitrogen is mainly supplied by dietary protein.

$\delta^{13}C$ and $\delta^{15}N$ values, measured in body tissues, can reveal indirect information about the diet of an individual. Food sources have different isotope compositions. Through consumption, these isotopic compositions are incorporated into body tissues, considering some (predictable) change due to fractionation. In turn, stable isotopes in body tissues can provide information on the diet by examining their δ-values.

The entity of analysis - $\delta^{13}C$ and $\delta^{15}N$ values of a single sample - is the individual. It allows to determine differences in diet between individuals. Moreover, isotope composition can also vary between groups. Sample sets representing larger numbers of individuals can provide information at for instance community-scale (for example, about economic or social aspects) or about regional or temporal variability (Schoeninger and Moore, 1992).

For archaeology, the most well-known application of stable isotope research concerns the reconstruction of palaeodiet (Michener and Lajtha, 2007). Based on the $\delta^{13}C$ and $\delta^{15}N$ values of (fossil) animal and human remains it is possible to distinguish herbivores, omnivores, carnivores, C3 and C4 plant consumers, and consumers of aquatic diet - to mention the main categories. This is best illustrated by the famous phrase "you are what you eat (plus a few ‰)" (DeNiro and Epstein, 1976; Kohn, 1999).

It is a general ecological rule that the cohabitation of species leads to niche differentiation that minimises direct competition. Such differentiation is often well reflected in a bivariate diagram that shows the specific $\delta^{13}C$ and $\delta^{15}N$ values. Indeed, a general (and more or less standard) way to present $\delta^{13}C$ and $\delta^{15}N$ data, is to plot the data in a consistent way - $\delta^{13}C$ horizontally, and $\delta^{15}N$ vertically, which enables an easy comparison. Figure 2.2 shows a schematic plot, where the various dietary groups are indicated by their hypothetical, general $\delta^{13}C$ and $\delta^{15}N$ values.

The consumption of C3 or C4 plants, in particular, leads to clearly distinguishable $\delta^{13}C$ signals. Plants using the C3 photosynthetic pathway show a range of $\delta^{13}C$ values around -27‰, whereas C4 plants have much higher $\delta^{13}C$ values of around -13‰ (Marshall *et al.*, 2007). In addition, there is a category known as CAM plants, with $\delta^{13}C$ values in between those of C3 and C4. Most plants are of the C3 type. Prime archaeological examples of C4 plants are corn and millet. Distinctive increases of $\delta^{13}C$ value are also observed in the food chain. There is an enrichment of the $\delta^{13}C$ value by about 1‰ for each trophic level shift (Lanting and van der Plicht, 1998; Fig. 2.2).

More pronounced differences between trophic levels are observed in $\delta^{15}N$ values. The isotopic enrichment of the $\delta^{15}N$ value is about 3-5‰ for each trophic level shift (Bocherens and Drucker, 2003; Hedges and Reynard, 2007). This means for instance, that the bone collagen of a carnivore is enriched in ^{15}N relative to ^{14}N in comparison with the amount of ^{15}N and ^{14}N originally present in their prey species, and herbivores have higher $\delta^{15}N$ values than the plants they consume (Schoeninger and Moore, 1992;
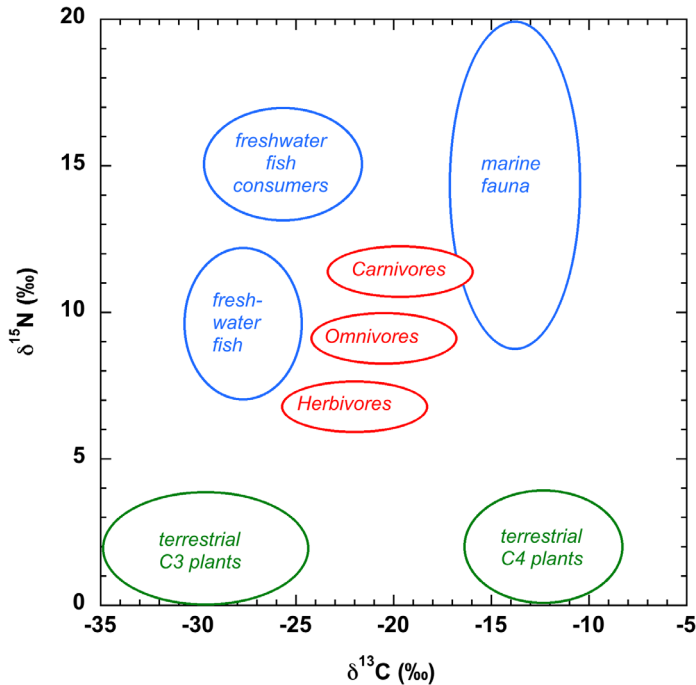
Figure 2.2 Schematic representation of (part of) the food web, indicating the ranges of hypothetical $\delta^{13}C$ and $\delta^{15}N$ values for terrestrial fauna (red), aquatic fauna (blue) and terrestrial plants (green).

Gannes *et al.*, 1998; Sealy, 2001).

Identification of the exploitation of terrestrial and aquatic resources is based on observable differences between organisms living in an aquatic (with in general higher $\delta^{15}N$ values) and terrestrial environment (in general lower $\delta^{15}N$ values) mainly due to differences in the nitrogen and carbon sources within the two systems. For freshwater reservoirs, typical values for animals and humans are around -25‰ and +13‰ for $\delta^{13}C$ and $\delta^{15}N$, respectively (Arneborg *et al.*, 1999; Cook *et al.*, 2001; Philippsen, 2013). For a marine reservoir, these $\delta^{13}C$ and $\delta^{15}N$ values are around -11‰ and +13‰, respectively (for example, van der Plicht *et al.*, 2016).

Diet composition also plays an important role in establishing $\delta^{13}C$ and $\delta^{15}N$ values in tissues of coeval living species from the same trophic level, for instance terrestrial herbivores. In brief, their $\delta^{15}N$ values vary due to nitrogen fixation and type of mycorrhizal associations between consumed plants, and even different $\delta^{15}N$ values can be observed between plant organs of a single plant. In general, grasses and sedges have higher $\delta^{15}N$ values than lichens, mosses and shrubs, and the values in trees are even lower than those in shrubs (Högberg *et al.*, 1996; see summary in Bocherens [2003] and Drucker *et al.* [2010]). Therefore, browsers tend to have lower $\delta^{15}N$ values than grazers (Ambrose, 1991; Drucker *et al.*, 2010).

Specifically, the protein content of consumed plants affects $\delta^{15}N$ values in herbivore tissues. Animals cannot store amino acids to any great extent in their tissues. The higher the protein throughput, the more the body needs to get rid of excess nitrogen by urea

excretion. Due to fractionation, the isotopically lighter ^{14}N is favoured during excretion compared to the heavier ^{15}N, resulting in the retention of heavier ^{15}N in the body. Therefore, protein rich diets lead to higher $\delta^{15}N$ values in body tissues than nutrient poor diets (Ambrose, 1991; Sponheimer *et al.*, 2003a; Fuller *et al.*, 2005).

On the other hand, higher $\delta^{15}N$ values are also found in studies on animals which had very nitrogen-poor diets (Hobson *et al.*, 1993). No consensus has been found explaining the exact mechanism behind the enrichment of ^{15}N in the body of animals that live under extremely nitrogen-poor conditions and/or during water stress. Recycling of internal (body) nitrogen resources for nitrogen concentration purposes is suggested to be contributory, since this would result in the excretion of (small amounts of) concentrated ^{14}N-depleted urea (Sealy *et al.*, 1987; Adams and Sterner, 2000). However, this violates the model of isotopic mass balance: if nitrogen is conserved rather than excreted, ^{15}N enrichment is no option (Ambrose, 1991).

2.3.2 Stable isotopes of carbon and nitrogen: palaeoenvironment

The $\delta^{13}C$ values in plants are primarily determined by the measure of exchange of CO_2 and moisture between the plant leaves and the atmosphere (so-called stomatal conductance; Marshall *et al.*, 2007), which is consecutively affected by various factors. In the terrestrial biosphere, fractionation of $^{13}C/^{12}C$ is mainly governed by the type of the photosynthetic pathway used by plants. In the mammoth steppe, plants used the C3 photosynthetic pathway (Blinnikov *et al.*, 2011). The $\delta^{13}C$ values of C3 plants are mainly determined by (local) environmental factors, such as humidity, atmospheric CO_2 concentrations (Polley *et al.*, 1993), and the occurrence of dense forest (van der Merwe and Medina, 1991). These factors cause geographical gradients in $\delta^{13}C$ values observed on the continent. In addition, there are also altitudinal gradients (van Klinken *et al.*, 1994; Kohn, 2010).

In forests, the 'canopy effect' produces ^{13}C-depleted plants and a gradient of leaf $\delta^{13}C$ values from ground to canopy; the most negative values are near the ground. Explanations for this phenomenon include recycling of ^{13}C-depleted CO_2 in the forest, fractionation due to photosynthesis in low light, and other plant physiological aspects (van der Merwe and Medina, 1991; Noe-Nygaard *et al.*, 2005). Thus, in densely forested regions, the $\delta^{13}C$ values of vegetation tend to be more negative than in open landscapes. In turn, the canopy effect is recognizable in the $\delta^{13}C$ values of bones of animals that feed on plants from a forested habitat (Bocherens and Drucker, 2007; Drucker *et al.*, 2008; Doppler *et al.*, 2017).

Within the terrestrial biosphere, $\delta^{15}N$ values in plants are determined by various biogeochemical processes within the plant and in their surrounding soil, including nitrogen cycling. But also nutrient availability and the type of mycorrhizal fungi living in symbiosis with the plant play a role (Nadelhoffer *et al.*, 1996; Högberg, 1997; Hobbie and Högberg, 2012; Szpak, 2014). Most of these processes are linked to one another and relate to climatic conditions such as humidity and temperature.

Fluctuations in $\delta^{13}C$ and $\delta^{15}N$ values in terrestrial herbivores have been observed that could be linked to changing climatological aspects, such as temperature (Bocherens *et al.*, 2006a,b) and aridity (Kohn, 2010). Besides aspects related to (isotopic) diet composition, climatic and environmental conditions, species-specific physiological aspects can cause differences in $\delta^{15}N$ and $\delta^{13}C$ values between herbivores (Gannes *et al.*, 1998; Schoeller, 1999; Sponheimer *et al.*, 2003b).

2.3.3 Isotope signals in different tissues

Stable isotope analyses can be performed on samples that vary in size from tens or hundreds of milligrams (for example, bone), a few milligrams (for example, hair), to molecular-scale level (for example, individual amino acids). Each sample strategy and sample type have their own possibilities and constraints. Sampling strategy should therefore be carefully considered prior to sample taking, bearing in mind aspects such as research question and properties and conditions of the available material (Phillips *et al.*, 2014).

The signals can represent different time-windows, from days or months up to an average of several years, depending on the turnover time of the sampled tissue and sample strategy. For instance, bone is constantly renewed throughout life and the measured signals in bulk samples of bone reflect dietary records of several years. Short-term dietary signals, such as seasonal change in food supply, can be observed in smaller, serially taken samples from for instance hair.

Among sample types, skeletal elements such as bone, antler and tooth dentine are routinely used for dietary reconstruction. Bone (and antler and bone dentin) is composed of an interconnected mineral and organic structure, which is built from molecules present in food. The mineral component ($\pm$ 70%) is called bio-apatite. The organic part of bone is mainly made up of collagen (that is, collagen type I). Furthermore, bone consists of other proteins and water (Jans, 2005).

The collagen fraction (including collagen of bone, antler and dentine, henceforward referred to as 'bone collagen' or simply 'collagen') is predominantly used for stable isotope analysis to determine past diet. It can be chemically isolated and since it does not, in principal, exchange carbon with the environment, it is the most inert fraction of bones for ^{14}C dating. The main fraction used throughout this thesis is (bulk) collagen.

2.3.4 Quality aspects of collagen used for isotope analysis

Bone collagen is sensitive to degradation and this explains why the majority of stable isotope analyses using collagen has been carried out on geologically young material with a Holocene or Late Pleistocene age (usually within the ^{14}C time scale, that is, up to 50,000 years ago). The occurrence of good quality collagen in bones that are older than 50,000 years decreases with age. However, if one were excluding bone collagen examination on forehand based on the age, one might miss out on possible valuable

information from the fossils, such as stable isotope or DNA data.

After deposition, bones can be contaminated with exogenous biomolecules and other foreign substances. Several kinds of taphonomical processes, such as hydrolysis, wear and attack by soil bacteria and fungi cause bone degradation or so-called 'diagenesis'. Diagenesis can lead to contamination with exogenous matter from surrounding deposits and/or loss of crystalline or organic components such as collagen. The change in physical and chemical properties of fossils caused by diagenesis may alter the isotope values of proteins, in particular in the case that fossils have a low collagen content. The degree of diagenesis- and in turn preservation state- is related to numerous factors, including local groundwater level, porosity of the skeletal element, temperature, sediment type, and time. Therefore bone (collagen) preservation varies from one burial environment to another (Hedges and Millard, 1995; Bocherens *et al.*, 1997b; Jans, 2005; Harbeck and Grupe, 2009).

It is essential for the validity of the isotope data that the collagen is well enough preserved, or in other words, that the collagen is pure enough and of good quality (Jans, 2005; Koch, 2007; Smith *et al.*, 2007; Harbeck and Grupe, 2009). In order to get rid of potential contaminants, the collagen extraction procedure includes chemical steps with the purpose of removing as many potential contaminants. In general, an organic solvent pretreatment is applied prior to the routine pretreatment in case the sample is covered with glues or preservations. Procedures may vary depending on sample type and properties, and between laboratories.

Collagen integrity can be estimated in different ways. The most common indicators are the carbon and nitrogen extraction yields of the collagen, denoted as respectively %C and %N. These are automatically provided by the mass spectrometer. Also, the atomic C/N ratio ($C:N_{atomic} = \%C/\%N \times 14/12$) is a widely accepted quality parameter, with values of 2.9-3.6 to be considered acceptable (Szpak *et al.*, 2017). In addition, based on comparison with the chemical composition of collagen extracted from fresh bone using the same purification treatment, the carbon content of genuine collagen should be around 30-40% and its nitrogen content around 11-16% for the results to be reliable (van Klinken, 1999).

The weight proportion of the extracted collagen in relation to the initial sample weight (% yield) is preferably minimally 0.5% (according to van Klinken, 1999) or 1% (according to Ambrose, 1993). For fresh bone, this yield is about 20%. Prior to the collagen extraction, the % yield can be guesstimated by measuring the proportion of the percentage of nitrogen in the initial sample (Bocherens *et al.*, 2005). Such a technique may be efficient to select promising samples in an early stage (with percentages close to the 4% N found in fresh bones [Brock *et al.*, 2010]), and rejecting samples which are examined to yield low quality collagen (Brock *et al.*, 2010, 2012). However, a deficiency is that the high percentage of nitrogen in 'promising' samples might partly be derived from nitrogen-containing contaminants present in the sample (Brock *et al.*, 2012). This can even result in varying nitrogen percentages within one bone. Indeed, ambiguity

exists in the relationship between %N and collagen content (Jacob *et al.*, 2018). Another proxy used to assess the integrity of the collagen is amino acid analysis; for instance, by comparing the amino acid profiles in the extracted collagen with such profiles of a fresh bone (Harbeck and Grupe, 2009).

2.4 Isotope measurements at the Centre for Isotope Research (CIO), Groningen

Chemical preparation, ^{14}C dating, and stable isotope measurements of the samples discussed throughout this thesis were, unless mentioned otherwise, performed at the Centre for Isotope Research (CIO), Groningen University, the Netherlands, following standard procedures (Mook and Streurman, 1983; see for a recent update Dee *et al.*, 2019).

In short, the bone, antler and dentine samples are decalcified over at least a 24-h period using weak acid (HCl, 4% w/vol). When CO_2 release has ceased and the fragments have become soft and pliable they are rinsed thoroughly with distilled water (DW). Following the demineralisation, the samples are soaked into NaOH (1%, > 30 min) to eliminate humic acids, rinsed to neutrality and treated once more with acid (HCl, 4% w/vol, 15 min). The raw collagen fraction is then denatured to gelatine in acidified DW (pH 3) at 90 ºC for 18 h. Before drying, the dissolved gelatine is filtered through a 50 μm mesh to eliminate any remaining foreign particulates.

The collagen product is combusted to obtain CO_2 using an Elemental Analyser (Isocube, Elementar) connected to an IRMS (Isoprime 100, Elementar), providing the isotope ratios $^{13}C/^{12}C$ and $^{15}N/^{14}N$ (Fig. 2.1). For carbon, the international standards NBS 18, NBS 19 and LSVEC are used to calibrate by two-point normalisation relative to V-PDB. For nitrogen, IAEA-N1 and IAEA-N$_2$ are the international standards used to calibrate relative to AIR. The combined uncertainty is about 0.3‰ for $\delta^{13}C$ and 0.2‰ for $\delta^{15}N$. To monitor analytical accuracy and precision, (internal) normalisation standards and control references are used. For $\delta^{13}C$, these are oxalic acid (-17.6‰), caffeine (-38.2‰), CaN (caffeine mixed with $\delta^{15}N$-enriched caffeine, +0.61‰) and collagen (-19.87‰); for $\delta^{15}N$ these are CaN (+19.04‰), caffeine (-6.61‰) and collagen (+10.07‰).

Before 2013, the isotope ratios $^{13}C/^{12}C$ and $^{15}N/^{14}N$ were measured in separate samples by using another Elemental Analyser (NEA). The $\delta^{15}N$ values were measured in duplicate. To monitor analytical accuracy and precision, slightly different (internal) normalisation standards and control references were used. For $\delta^{13}C$, these are oxalic acid (-17.6‰), caffeine (-38.2‰), anthracite (-23.25‰); for $\delta^{15}N$, these are N1 (+0.43‰), N2 (+20.32‰), collagen (+9.8‰) and flower (+1.7‰). The $\delta^{13}C$ and $\delta^{15}N$ values discussed in this thesis and measured at the CIO, have been measured either by using this older Elemental Analyser or by the previous mentioned Isocube.

Throughout the thesis, the $\delta^{13}C$ and $\delta^{15}N$ values are often reported and discussed in conjunction with ^{14}C dates. Most ^{14}C dates in the tables are from Groningen; they can be recognized by the laboratory reference numbers with the following prefixes:

- GrN: conventional (radiometry by proportional gas counters), used until 2011
- GrA: AMS (3 MV Tandetron accelerator, High Voltage Engineering), used from 1994 to 2017
- GrM: AMS (200 kV compact accelerator [MICADAS], IonPlus AG), used since 2017.

^{14}C dates are reported in BP, which by convention means that the ^{14}C radioactivity is measured relative to the Oxalic Acid standard, that the dates are calculated using the Libby half-life of 5568 years, and that isotope fractionation is corrected for using the ^{13}C isotope to $\delta^{13}C = -25‰$ (Mook and van der Plicht, 1999).

2.5 Application of stable isotope analysis from an historical perspective

Today, $\delta^{13}C$ and $\delta^{15}N$ analyses of bones and teeth are almost standardly implemented within archaeological research. However, half a century ago, stable isotope analysis was used only occasionally. The intensification of the use of stable isotopes analysis within the last few decades is partly related to developments within the archaeological discipline itself and to the improved application of chemical, physical, environmental and mathematical research methods. Moreover, the enhanced sophistication and user-friendliness of IRMS, the development of quality controls, the accumulation of available stable isotope datasets and a substantial progress concerning the interpretation of the data have been of crucial value for a useful implementation of isotope studies within an archaeological research context.

Since the invention of the mass spectrometer by Thompson in 1910, several types of IRMS have been developed. The first models required samples to be purified manually before entering the mass spectrometer. In the course of the 1980s-1990s, semi-automated and later fully automated combustion systems (EA, Elemental Analyzer) combined with the mass spectrometer were developed: EA-IRMS.

These technological developments are related to those in the ^{14}C dating realm. ^{14}C fractionates, and hence, ^{14}C dates need to be corrected for this effect. This is done by measuring not only the ^{14}C isotope, but also, in the same sample, the abundance of ^{13}C (Mook and Streurman, 1983). IRMS was introduced in the ^{14}C laboratories in the 1960s. The dating of (archaeological) samples resulted automatically in additional $\delta^{13}C$ data. This became soon supplemented by $\delta^{15}N$ analysis of the same bone (Schoeninger *et al.*, 1983). Initially, this required analysis of a second bone sample - a sample for both C isotopes, and one for ^{15}N. Later, EA-IRMS systems could provide both $\delta^{13}C$ and $\delta^{15}N$

values for one sample. Today, even systems for combined $^{13}C/^{14}C/^{15}N$ analysis (EA-IRMS-AMS) exist (Synal *et al.*, 2013).

Initial applications of $\delta^{13}C$ and $\delta^{15}N$ analysis in archaeology were mainly used to identify the consumption of different resources. In particular, $\delta^{13}C$ values were primarily used to distinguish between consumption of C3 and C4 plants (Vogel and van der Merwe, 1977). This application is based on the observation by the geochemist Craig (1953) who discovered that plants that use different photosynthetic pathways show distinct stable carbon isotope ratios. In the beginning, $\delta^{15}N$ values were mainly used for the determination of trophic levels and discrimination between the exploitation of terrestrial and aquatic resources (Minagawa and Wada, 1984; Schoeninger and DeNiro, 1984; Walker and DeNiro, 1986; Yesner, 1987). The application has expanded since and includes a huge range of research topics including animal husbandry practices (Doppler *et al.*, 2017; Makarewicz, 2017; Cubas *et al.*, 2019) and the estimation of weaning age (Reynard and Tuross, 2015; Guiry *et al.*, 2016). Another significant application of $\delta^{13}C$ and $\delta^{15}N$ of fossil bone is providing information about reservoir effects in ^{14}C dated bone. Aquatic reservoirs are depleted in ^{14}C relative to atmospheric and terrestrial reservoirs. Therefore, archaeological bone of fish consumers date too old on the BP-timescale. The $\delta^{13}C$ and $\delta^{15}N$ values of such bones can be used as proxies in order to estimate the size of the reservoir effect, which can be hundreds of ^{14}C years (Cook *et al.*, 2001; Philippsen, 2013; Wood *et al.*, 2013; van der Plicht *et al.*, 2016).

The sophistication of the IRMS technology over the years has today resulted in lower prices for isotope analysis, faster sample throughput, and smaller sample sizes, allowing to measure on a completely different scale and addressing questions that initially could not be answered.

CHAPTER 3

**WOOLLY MAMMOTH
δ^{13}C AND δ^{15}N VALUES
REMAINED AMAZINGLY STABLE
THROUGHOUT THE LAST ~50,000 YEARS
IN NORTH-EASTERN SIBERIA**

3.1 Introduction

3.1.1 The mammoth steppe ecosystem and its collapse

The woolly mammoth (*Mammuthus primigenius*) originated about 400,000 years ago in North-eastern Asia, and dispersed during the late Middle Pleistocene westwards (Lister and Sher, 2001, 2015; Lister *et al.*, 2005). *M. primigenius* inhabited a biotope that occurred during its maximal expansion in a geographically extensive area stretching from western Europe, via northern Eurasia to northern America. This biotope is often referred to as 'mammoth steppe' (Guthrie, 1990; see also Chapter 1, section 1.1.1).

At the end of the Pleistocene, the mammoth steppe biotope started to collapse. The disintegration of the mammoth steppe biome did not occur simultaneously throughout its entire geographical range. *M. primigenius* changed its distribution range repeatedly during the Middle and Late Weichselian, often triggered by climatic and/or environmental changes. In general, its range increased in size during colder episodes (stadials) and decreased during most of the interstadials, and finally it fell apart into isolated patches (Puzachenko *et al.*, 2017).

Woolly mammoth remains have been recovered abundantly throughout its distributional range. Insights into the dynamics of geographical distribution of mammoths during the last 50,000 years (that is, the ¹⁴C time scale) were obtained by analysing extensive datasets of ¹⁴C dated remains from more than a thousand localities (Stuart, 2005; Nikolskiy *et al.*, 2011; Puzachenko *et al.*, 2017; Stuart *et al.*, 2019). In parts of its biome, *M. primigenius* went extinct as early as the Late Glacial (~ 21,000 years ago in Southwestern Europe, Puzachenko *et al.*, 2017), whereas relict populations of (small-sized) mammoths survived longer on isolated islands.

On Wrangel Island, an island situated north of Chukotka mainland, the youngest dated woolly mammoth remains are found (3685 ± 60 ¹⁴C yr BP; Vartanyan *et al.*, 2008). Hence, Wrangel Island plays an important role in the debate about the cause of the final extinction of the woolly mammoth and the nature of refugial areas.

3.1.2 Stable C and N isotope analysis of the mammoth steppe ecosystem

Stable isotope data from mammoth steppe mammals have been measured and investigated, in order to gain insights in different aspects of the mammoth steppe ecosystem. Significant variations through time and space are observed in the δ¹³C and δ¹⁵N records of Late Pleistocene and Holocene fossils of diverse mammoth steppe dwellers from Eurasia and Alaska (Iacumin *et al.*, 2000; Bocherens, 2003; Drucker *et al.*, 2003b, 2014; Richards and Hedges, 2003; Stevens and Hedges, 2004; Fox-Dobbs *et al.*, 2008; Szpak *et al.*, 2010). Mammal samples from North-eastern Siberia show, compared to the values in samples from Europe, and in particular compared to values in samples from Alaska, elevated δ¹⁵N values and depleted δ¹³C values (Bocherens, 2003; Szpak *et al.*, 2010). These differences in values are linked to generally more arid conditions and lower temperatures in North-eastern Siberia throughout the Late Pleistocene, opposed

to more mesic components in the habitats of Alaska (Szpak *et al.*, 2010). Other proxies, including palaeoentomological data and dental wear patterns of ungulate species also point to ecological differences between respectively Alaska and North-eastern Siberia (Szpak *et al.*, 2010) and between Europe and Alaska (Rivals *et al.*, 2010) during the Late Pleistocene.

The diachronic isotope variations are observed in a number of species from North-western Europe and, although less pronounced, in species from Alaska. The changing isotope compositions, predominantly reflected as a trend towards lower $\delta^{13}C$ and $\delta^{15}N$ values at the onset of the Late Glacial, are linked to changing environmental circumstances, especially those that were driven by major climatic deteriorations that took place around the Last Glacial Maximum (LGM) and the Pleistocene/Holocene transition. These changing environmental circumstances include changes in atmospheric CO_2 concentration (Richards and Hedges, 2003; Stevens and Hedges, 2004), climatic variation on a local-scale including soil moisture conditions (Stevens and Hedges, 2004; Fox-Dobbs *et al.*, 2008), and forest development (Drucker *et al.*, 2008; Drucker and Bocherens, 2009).

Unfortunately, there are chronological hiatuses in stable isotope records and/or low sampling density within parts of the mammoth steppe biome, hampering the data interpretation and the observation of possible trends in time (Fox-Dobbs *et al.*, 2008). For instance, published $\delta^{15}N$ and $\delta^{13}C$ records of woolly mammoth samples with a post-LGM age and in particular with an LGM age are scarce.

3.1.3 North-eastern Siberia

The area of North-eastern Siberia was more or less continuously inhabited by the woolly mammoth (Puzachenko *et al.*, 2017). Not only the numerous sites with woolly

Figure 3.1 Map of the study area. The locations of the fossil data are indicated with black open circles.

mammoth remains and the long-term survival of the woolly mammoth in that area, but also its geographical position and the fact that it was for a long period part of the Beringia Land Bridge - providing a corridor between continents for some species, but prohibiting crossing by others (Hopkins 1982; Guthrie, 2001; Elias and Crocker, 2008; Meiri *et al.*, 2014)- makes this an attractive study area.

The investigated dataset comprises an unprecedented amount of $\delta^{15}N$ and $\delta^{13}C$ values of directly dated woolly mammoth samples from North-eastern Siberia, including many samples dating to the post-LGM and a number to the LGM. The majority of the samples date to the Late Pleistocene, but also a relatively large number have a Holocene age. The latter samples are mainly from Wrangel Island.

The study focuses on North-eastern Siberia (Fig. 3.1). A large number of new $\delta^{15}N$ and $\delta^{13}C$ values have been analysed in order to track possible shifts within the woolly mammoth $\delta^{13}C$ and $\delta^{15}N$ record towards its time of extinction.

3.2 Material and methods

3.2.1 Material

The study presents $\delta^{15}N$ and $\delta^{13}C$ values from 109 woolly mammoth samples from an area located north of 70° N. The dataset includes new measurements (n = 62) and published data (n = 47, see Table SI Chapter 3.1: Bocherens *et al.*, 1996; Iacumin *et al.*, 2000, 2010; Szpak *et al.*, 2010). Geographically, the samples can roughly be divided into three regions of provenance (Fig. 3.1): from west to east - Taimyr Peninsula, Yakutia (predominantly Lena River Delta, New Siberian Archipelago and Yana-Indigirka Lowland), and Wrangel Island (specifically Gusinaya River in the west of the island, Peak in the centre, and Mamontovaya River in the southwest).

Samples were taken from different skeletal parts. Samples from tusks form the majority of the new data (n = 42), the rest of the samples is bone (n = 16) or molar dentine (n = 3). For one sample the material was not specified, but it is highly probable that it was taken from either bone or tusk. In tusks, seasonal variation in isotope signals can be recorded (Rountrey *et al.*, 2007). However, the tusk samples, used for the present study, are bulk samples, in which the isotope signal of several seasons is averaged. The current analysis assumes that the stable isotope signals of the collagen from these three different material categories are comparable to each other. The $\delta^{13}C$ value of all samples was measured, and for 58 samples the $\delta^{15}N$ value has been determined as well.

The age of the samples is summarized in Table 3.1. It shows the number of records per period relative to the LGM. Most samples (n = 98) date to the last part of the Late Pleistocene or to the succeeding Holocene. Eleven samples have 'infinite ¹⁴C ages', which means they are older than 45,000 ¹⁴C yr BP (Table SI Chapter 3.1). Their age is not specified.

Table 3.1 Number of woolly mammoth samples from North-eastern Siberia, arranged per time interval relative to the LGM.

N	n (new)*	period	used abbreviation	¹⁴C age (yr BP)	cal yr BP**
54	(21)	Pre-Last Glacial Maximum	Pre-LGM	> 45,000-24,600	>50,000-28,660
10	(5)	Last Glacial Maximum	LGM	24,600- 17,000	28,660-20,520
45	(36)	Post-Last Glacial Maximum	Post-LGM	<17,000	<20,520
109	(62)				

*Numbers of newly provided samples by the current paper are shown between brackets
**cal yr BP = calendar ages relative to 1950

3.2.2 Methods

Chemical preparation, ^{14}C dating, and stable isotope measurements of the new samples were performed at the Centre for Isotope Research in Groningen, the Netherlands, following the Groningen procedures as described in Chapter 2 (section 2.4).

General patterns in the dataset were visually examined using bivariate plots. Further, differences in the means and trends were tested for by statistical modelling. Differences in the means of δ^{13}C and δ^{15}N values were examined by using One-way ANOVA: a parametric statistical test at the 95% confidence level, with H_0 = all means are the same and H_0 is rejected when p-value < 0.05. Normal distribution and homogeneity of variance were checked by applying the Shapiro-Wilk test and Bartlett test, respectively. A linear regression model was used to test if δ^{13}C or δ^{15}N values show a linear trend with time.

3.3 Results

The atomic C/N ratio of the collagen samples is 2.9-3.6 (%C = 37.7-50.1 and %N = 13.4-18.4). These percentages indicate good quality collagen (Ambrose, 1990). Eight samples have a somewhat higher %C value (> 47; see the italic values in Table SI Chapter 3.1). These samples are included in the current investigations since the %C values fall between 45 and 50, a range that is regarded as indicative for good quality collagen suitable for ^{14}C dating (Mook and Streurman, 1983).

The results of the stable isotope measurements are shown in chronological order in Table SI Chapter 3.1. The δ^{13}C and δ^{15}N values of samples from Taimyr Peninsula, Yakutia and Wrangel are plotted relative to time in Fig. 3.2. The δ^{13}C values range from -23.2‰ to -20.1‰, with an average of -22.0‰ and a standard deviation of 0.5. The δ^{15}N values range from +5.6‰ to +12.1‰, with an average of +9.4‰ and a standard deviation of 1.2.
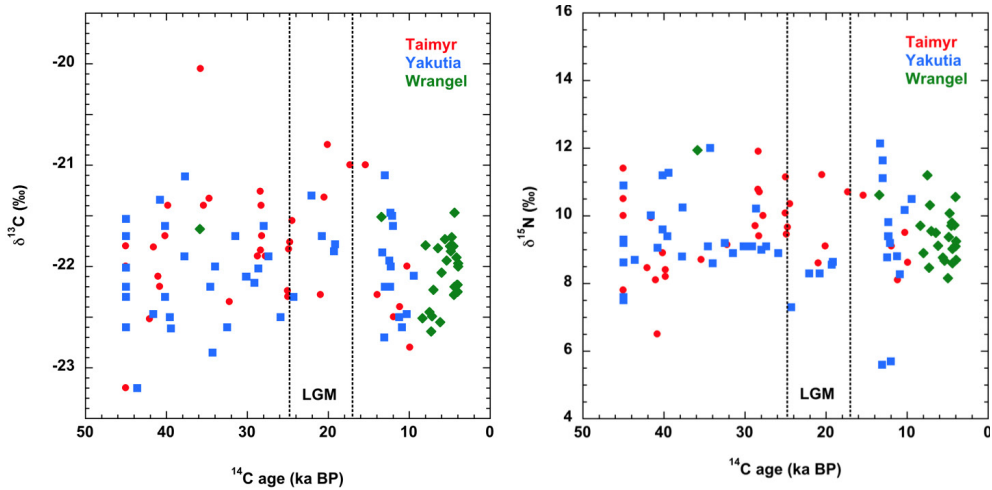
Figure 3.2 The δ¹³C values (left) and δ¹⁵N values (right) of samples from Taimyr Peninsula, Yakutia and Wrangel through time.

Table 3.2 gives an overview of the average δ¹³C and δ¹⁵N values, standard deviations and number of available samples for the different regions (that is, Taimyr, Yakutia and Wrangel). It aggregates all data together and compares between regions irrespective of the age of the samples. Table 3.2 shows that both the mean δ¹³C values and δ¹⁵N values of the samples from the three regions are very similar (< 0.3‰ difference). No statistically significant difference was found at the 95% confidence level between the mean δ¹³C values (ANOVA, p = 0.13) and δ¹⁵N values (ANOVA, p-value = 0.59) of the regions. Therefore, the data are further discussed irrespective of the region of provenance of the samples.

Table 3.2 Averages and standard deviations of δ¹³C and δ¹⁵N values for different regions.

	δ¹³C (‰)			δ¹⁵N (‰)		
	mean	st dev	n	mean	st dev	n
Taimyr	-21.8	0.6	37	9.4	1.2	34
Yakutia	-22.1	0.5	46	9.3	1.4	46
Wrangel	-22	0.3	26	9.5	0.9	25
All areas	-22	0.5	109	9.4	1.2	105

Table 3.3 gives an overview of the average δ¹³C and δ¹⁵N values, standard deviations and number of samples for different time slices relative to the LGM, and for the Pleistocene and Holocene (> 11,000 ¹⁴C yr BP). Table 3.3 shows that both the mean δ¹³C values and δ¹⁵N values of the samples are very similar throughout the different periods.
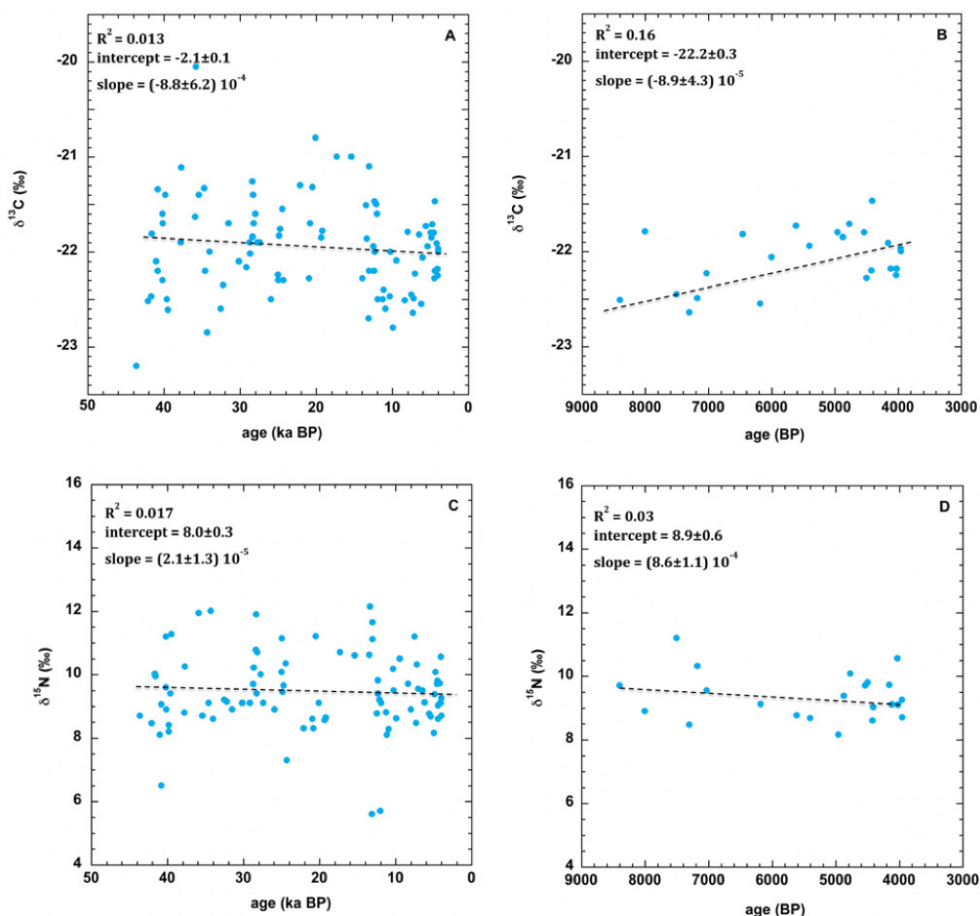
Figure 3.3 The $\delta^{13}C$ and $\delta^{15}N$ values of samples with a finite age (> 45,000 ^{14}C yr BP) through time. A: $\delta^{13}C$ values of samples from North-eastern Siberia; B: $\delta^{13}C$ values of samples from Wrangel Island; C: $\delta^{15}N$ values of samples from North-eastern Siberia; D: $\delta^{15}N$ values of samples from Wrangel Island.

Indeed, we cannot conclude at the 95% significance level that there is a temporal trend in the $\delta^{13}C$ values (p = 0.157; Fig. 3.3A) or in the $\delta^{15}N$ values (p = 0.1; Fig. 3.3C).

Also, in the $\delta^{13}C$ and $\delta^{15}N$ values of woolly mammoths from Wrangel Island no significant temporal correlation is observed. The variation through time is on average very small, in particular considering the analytical uncertainty for $\delta^{13}C$ and $\delta^{15}N$ measurement (see Chapter 2). It cannot be concluded at the 95% confidence level that there is a temporal trend in the $\delta^{13}C$ values (p = 0.051; Fig. 3.3B) or in the $\delta^{15}N$ values (p = 0.43; Fig. 3.3D). So, the values provide no evidence to reject the hypothesis that they remain constant. But even if there were a significant statistical correlation, an increase through time of ~ 0.5‰ is not very significant biologically and in terms of analytical precision.

Table 3.3 Averages and standard deviations of woolly mammoth $\delta^{13}C$ and $\delta^{15}N$ values for different time intervals.

	$\delta^{13}C$ (‰)			$\delta^{15}N$ (‰)		
	mean	st dev	n	mean	st dev	n
Pre-LGM	-22.0	0.5	54	9.5	1.2	52
LGM	-21.6	0.5	10	9.1	1.2	10
Post-LGM	-22.1	0.4	45	9.4	1.2	43
Pleistocene	-21.9	0.5	80	9.4	1.3	77
Holocene	-22.1	0.3	29	9.4	0.7	28

3.4 Discussion

3.4.1 Spatial and temporal distribution

Mainland

The current data set reveals stability in $\delta^{13}C$ and $\delta^{15}N$ values of woolly mammoth skeletal remains from North-eastern Siberia throughout the last part of the Late Pleistocene. This is even the case in periods in which in other regions the stable isotope values change considerably. The post-LGM $\delta^{13}C$ and $\delta^{15}N$ values from North-eastern Siberia are similar to those of the pre-LGM, and even fairly similar to those of the LGM.

The dataset of a previous study by Iacumin *et al.* (2010) comprised two woolly mammoth samples from Yakutia, dating to post-LGM, which appeared to have low $\delta^{15}N$ values (+5.6‰ and +5.7‰) relative to older samples. This depletion was attributed to higher precipitation rates during the post-LGM period (Iacumin *et al.*, 2010), and seemed to be part of a trend towards lower $\delta^{15}N$ values after the LGM. However, the two samples with low values form, when compared to the newly obtained data from the present study and other recently published data, an exception for some unknown reason: all other samples from Yakutia with a post-LGM age (n = 17) have $\delta^{15}N$ values between +8.62‰ and +12.14‰, and are comparable to $\delta^{15}N$ values of samples with a pre-LGM and LGM age. Hence, the current data are consistent with information revealed from other ecological proxies such as pollen and entomological data from Taimyr and Yakutia, which indicate that after the LGM, but pre-dating the start of the Holocene, climatic and environmental conditions resembled those during pre-LGM times (Nikolskiy *et al.*, 2011).

At the start of the Holocene, temperatures started to rise in different regions inhabited by the woolly mammoth, including Taimyr and Yakutia; a temperature rise that resulted in, amongst others, a rise in sea level. A marked paludification is recorded in palynological, macrobotanical and insect assemblages (Nikolskiy *et al.*, 2011). Around that time, the woolly mammoths went extinct on the North-eastern Siberian mainland (Nikolskiy *et al.*, 2011; Puzachenko *et al.*, 2017).

Wrangel Island

The $\delta^{13}C$ and $\delta^{15}N$ values of the Holocene woolly mammoth remains from Wrangel Island are well within the range of $\delta^{13}C$ and $\delta^{15}N$ values of the Late Pleistocene mammoths from the North-eastern Siberian mainland. Moreover, the $\delta^{13}C$ and $\delta^{15}N$ values from Wrangel Island remain consistent through time. Changes in habitat and/or diet at some point cannot be absolutely ruled out based on diachronic similarity of stable isotope data. But since $\delta^{13}C$ and/or $\delta^{15}N$ values of C3 plants are mainly determined by (local) environmental factors, such as humidity, temperature and atmospheric CO_2 concentration, some kind of change is to be expected in the tissues of the consumers of these plants in times of changing conditions. Especially, because other parts of the mammoth steppe did show significant changes in $\delta^{13}C$ and $\delta^{15}N$ values from herbivore tissues following climatic and environmental changes.

The $\delta^{13}C$ and $\delta^{15}N$ values of woolly mammoth samples from Wrangel Island (Fig. 3.3B and D) show less variation than the woolly mammoths which lived on the North-Siberian mainland (Fig. 3.3A and C). This might partly be explained by the fact that the woolly mammoths on Wrangel Island exploited a much more restricted, and likely more uniform area -despite the supposed local variation in vegetation cover on the island- over a much shorter time span than their Late Pleistocene mainland counterparts.

Different hypotheses/models are launched to explain the disappearance of the woolly mammoth: a) the 'overkill' model (Martin, 1984; Haynes, 2007;) or 'Blitzkrieg' model (Martin, 1984) in which mainly human hunters are held responsible, b) models in which climate change played a major role (Koch and Barnosky, 2006; Nikolskiy *et al.*, 2011; Cooper *et al.*, 2015), c) pandemic theories, and d) models which involve (a combination of) ecological changes, habitat reduction, and reduction of genetic diversity (for example, Palkopoulou *et al.*, 2015; Graham *et al.*, 2016).

The stable isotope data do not give direct information about the extinction of the woolly mammoth on Wrangel Island. But the consistency in $\delta^{13}C$ and $\delta^{15}N$ values through time implies that Holocene mammoths living on Wrangel Island were feeding on resources with the same isotopic composition as their Late Pleistocene counterparts from the North-eastern Siberian mainland throughout their existence. The stable isotope data from Wrangel Island support the hypothesis that climate change was not the (main) cause of the ultimate extinction of the woolly mammoth. These results are in line with conclusions from Fox *et al.* (2007): climate signals recorded in oxygen isotope values in serially sampled tusks from North-eastern Eurasia, including Holocene tusks from Wrangel Island do not point to climate change that could be regarded as the direct cause of the woolly mammoth extinction.

The local extinction of the woolly mammoth often co-occurred with environmental changes and habitat expansion of humans. However, the interference of early man is not likely to have driven the mammoths on Wrangel Island to extinction, since there is no clear evidence that humans occupied the island before the mammoth's disappearance (Nikolskiy *et al.*, 2011). The absence of humans and other predators

allowed the woolly mammoths to reduce in size, which is a well-known phenomenon for islands. Pleistocene bones from Wrangel all belong to normal-sized mammoths, but between 8000 and 6000 BP, the mammoths started to reduce in size. After 6000 BP, all mammoths were small-sized (Vartanyan *et al.*, 1993).

Recent investigation on the genome of one of the last surviving Wrangel mammoths (dated to about 4300 yr BP) demonstrates reduced genetic variation (Palkopoulou *et al.*, 2015). In the course of the Holocene, the reduced genetic variation was probably harmful for the reproductive success of the Wrangel mammoths and might have contributed to their extinction (Palkopoulou *et al.*, 2015).

Late Pleistocene fossils from woolly mammoth, horse, and woolly rhinoceros indicate that Wrangel Island was inhabited by a mammalian assemblage comparable to that of Late Pleistocene Yakutia and Taimyr (Zimov *et al.*, 2012). However, during the Early Holocene the woolly mammoth was by far the most dominant large herbivore species. Only one bison fossil with an Holocene age, has been discovered so far. Based on the number of ¹⁴C dated fossils, the Wrangel woolly mammoth population even seems to have increased in number compared to the Late Pleistocene population (Zimov *et al.*, 2012).

First, the continued existence of woolly mammoths on the one hand, and the extinction of many other species on the island on the other hand, indicates a high degree of resilience of the woolly mammoth to changing conditions. Second, it
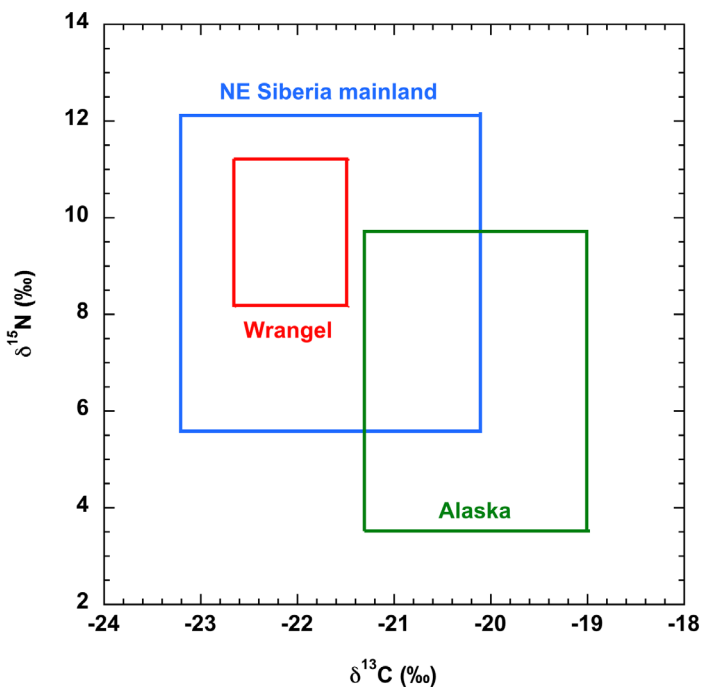
Figure 3.4 The δ^{13}C and δ^{15}N ranges of woolly mammoth samples from Wrangel Island (in red), compared to these from North-eastern Siberia mainland (in blue) and from Alaska (green; Debruyne *et al.*, 2008; Szpak *et al.*, 2010; Graham *et al.*, 2016; see Table SI Chapter 3.2 for raw data).

indicates that conditions which disallowed survival of other large species on the island, did not (negatively) affect the habitats which were suitable for the woolly mammoth. This is supported by the current stable isotope results, since the $\delta^{13}C$ and $\delta^{15}N$ values of Holocene woolly mammoth samples from Wrangel Island are similar to these of Late Pleistocene North-eastern Siberia mainland and remain the same throughout the Holocene.

Since the woolly mammoth was virtually the only large herbivore species that lived on Wrangel Island during the Holocene, niche competition did not play a role (Zimov *et al.*, 2012). It was hypothesized by Zimov *et al.* (2012) that woolly mammoths might have occupied the ecological niches of bison and horse which became available in the Holocene. Indications for niche change are found in the isotope record of Pleistocene woolly mammoths from Mezhyrich (Drucker *et al.*, 2014). Late-Glacial samples of woolly mammoths from this Ukrainian site show $\delta^{15}N$ values similar to those of horses from the same spatiotemporal range. These overlapping $\delta^{15}N$ values of woolly mammoths and horses were associated with niche competition (Drucker *et al.*, 2014). However, the Wrangel data differ. The lack of other large herbivores on Wrangel prohibits comparison of isotope data of the woolly mammoth with such species. Drucker *et al.* (2014) observed significantly higher $\delta^{15}N$ values prior to the Late Glacial, in the bone collagen of the woolly mammoths from Mezhyrich. Such a shift in $\delta^{15}N$ values pointing to a change of the ecological niche is not observed in the isotope data of the woolly mammoth from Wrangel Island.

Beringia

By including data from Wrangel Island, the current study presents crucial stable isotope data from the border region between Siberia and Alaska. Wrangel Island is, geopolitically part of Siberia, but it is geographically closer to Alaska (Fig. 3.1). Wrangel is nowadays an island in the Arctic Ocean, but it was connected to the mainland until about 12,000 ^{14}C yr BP (Keighwin *et al.*, 2006; Vartanyan *et al.*, 2008). From the onset of the Holocene to about 6000 years ago, the Long Strait (that is, the water body that separates Wrangel from the Siberian mainland) was so narrow that mammoths might still have crossed the strait during winter. During the Weichselian, the Beringia Land Bridge connected North-eastern Siberia and Alaska. The conditions in Central Beringia are supposed to have been much more mesic than at either side of the land bridge, that is, West Beringia/North-eastern Siberia and East Beringia/Alaska (Guthrie, 2001; Elias and Crocker, 2008).

The $\delta^{13}C$ and $\delta^{15}N$ values of samples from Wrangel Island fall entirely within the range of values from North-eastern Siberia (Fig. 3.4) and hardly overlap with the $\delta^{15}N$ and $\delta^{13}C$ values from Alaska. Hence, the stable isotope data suggest that the stable isotope composition of vegetation on Wrangel Island was similar to that of other parts of West-Beringia and not to that in Alaska, despite the proximity to Central Beringia and Alaska. A remarkable difference between Wrangel Island and Central Beringia

and Alaska is also observed in the mammalian fauna, in the occurrence of the woolly rhinoceros. The woolly rhinoceros (*Coelodonta antiquitatis*) inhabited Wrangel during the Pleistocene (Vartanyan *et al.*, 2008) but fossils of this species have never been recovered at the east side of the Bering Land Bridge. Central Beringia might have acted as ecological barrier that prevented this xerophilic species to migrate to East Beringia (Elias and Crocker, 2008).

3.4.2 Comparison with other species from North-eastern Siberia

It is interesting to compare the results of our analyses with data of other mammalian species from North-eastern Siberia. The $\delta^{13}C$ and $\delta^{15}N$ values of musk oxen are well documented, in particular in a publication by Raghavan *et al.* (2014). They analysed the $\delta^{13}C$ and $\delta^{15}N$ values of 160 Pleistocene and Holocene musk oxen samples from across the Holarctic, and observed similarity in the $\delta^{13}C$ and $\delta^{15}N$ values between Holocene and Pleistocene musk oxen from Taimyr (n = 52). In contrast to the samples from Taimyr, $\delta^{13}C$ and $\delta^{15}N$ values of Canadian musk oxen are lower during the Holocene compared to the Pleistocene values. The authors explain the observed differences in the muskoxen from Canada by an increase in precipitation during the Holocene, and conclude that Canada might have experienced a more pronounced increase in precipitation during the Holocene than Taymir (Raghavan *et al.*, 2014).

From North-eastern Siberia, the number of ¹⁴C dated samples of mammalian species other than mammoth and musk oxen, of which the $\delta^{13}C$ and $\delta^{15}N$ values are published, are scarce. Making statements about temporal variations based on these few samples is not justified, because of lack of continuity of relevant data through time. However, the observed continuity through time in the $\delta^{13}C$ and $\delta^{15}N$ values of musk oxen from Taimyr, whilst change at the Pleistocene/Holocene transition is observed in other parts of their biome (Raghavan *et al.*, 2014), corresponds to the results of the current study.

3.5 Conclusion

The data set reveals a remarkable stability in $\delta^{13}C$ and $\delta^{15}N$ values of woolly mammoth skeletal remains throughout the last part of the Late Pleistocene in North-eastern Siberia. Minor differences are observed in samples with an LGM age, but the post-LGM $\delta^{13}C$ and $\delta^{15}N$ values from North-eastern Siberia are similar to those pre-dating the LGM. This continuity or recovery of stable isotope values sharply contrasts to published data of woolly mammoths and other large herbivores from Europe and Alaska, which revealed significant changes in $\delta^{13}C$ and $\delta^{15}N$ values; changes that are related to climatic fluctuations during and/or after the LGM.

Even more remarkable, woolly mammoths maintained similar $\delta^{13}C$ and $\delta^{15}N$ values throughout their Holocene existence, as demonstrated by results of woolly mammoth fossils from the legendary Wrangel Island, where they survived until around 2100 BCE.

The $\delta^{13}C$ and $\delta^{15}N$ values of the Holocene woolly mammoths from Wrangel Island are similar to the $\delta^{13}C$ and $\delta^{15}N$ values of the Late Pleistocene mammoths from the North-eastern Siberian mainland. They diverge from $\delta^{13}C$ and $\delta^{15}N$ values of woolly mammoth samples from Alaska, despite the fact that both regions are geographically rather close.

The stable isotope data indicate that Holocene mammoths from Wrangel Island were feeding on isotopically the same resources as they did on the North-eastern Siberian mainland throughout the last part of the Late Pleistocene, and suggest, at least in broad sense, that these mammoths were able to maintain the same diet throughout their whole existence on the island.

North Sea, photo: M. Kuitems

CHAPTER 4

FOSSIL BONES FROM THE NORTH SEA: STABLE ISOTOPES

The research described in this chapter is based on the following studies:
Kuitems, M., van der Plicht, J., forthcoming. Fossil bones from the North Sea: stable isotopes. *Paleontos*, accepted.

van der Plicht, J., Kuitems, M., forthcoming. Fossil bones from the North Sea: radiocarbon dates. *Paleontos*, accepted.

Kuitems, M., van Kolfschoten, T., De Loecker, D., Busschers, F.S., 2015. Geoarchaeological and palaeontological research in the Maasvlakte 2 sand extraction zone and on the artificially created Maasvlakte 2 beach: a synthesis. B*OORrapporten* **48**.

4.1 Introduction

The North Sea is today a domain of mammoth tankers, but once it was dominated by the woolly mammoths and other Ice-Age creatures. During the Weichselian, when the sea level was much lower than today, the North Sea area was land and thousands of recovered fossil remains witness the past occurrence of hominins and mammals.

This chapter presents an inventory of the stable isotope values of North Sea finds that have been measured by the Centre for Isotope Research in Groningen. A general overview of the stable isotope results is given, and some aspects are discussed in more detail.

4.1.1 The North Sea basin in the Pleistocene

Alternations of cold and warm periods are characteristic for the Pleistocene epoch. During glacials, large volumes of water were stored in continental ice caps. Each glacial/interglacial climatic cycle changed the eustatic sea level significantly. Since the southern North Sea shelf has a rather flat surface, sea level changes affected the North Sea Basin palaeolandscapes dramatically (Peeters *et al.*, 2009; Cohen *et al.*, 2011; Hijma *et al.*, 2012). Sea level fluctuations resulted in temporal changes in the palaeocoastline and the tributaries of large river systems. During the Weichselian, the sea level dropped more than 100 meters below the current sea level, and the area of the present-day North Sea and the English Channel was part of the mammoth steppe ecosystem. The changes in climate had also a major impact on the local flora and fauna.

4.1.2 The North Sea finds

In the last few decades, thousands of Pleistocene and Holocene animal remains have been recovered from the North Sea bottom. Indeed, the North Sea can be regarded as one of the richest palaeozoological sites in the world. The site also yielded hominin remains (Roebroeks, 2014; Meiklejohn *et al.*, 2015; van der Plicht *et al.*, 2016). Occasionally, recovered fossils show traces of human modification, or even have been made into bone and antler artefacts. Also, lithic tools have been found, in particular near the coast of Great Yarmouth (see for example Glimmerveen *et al.*, 2004, 2006; De Loecker, 2010; Pieters *et al.*, 2010; Momber *et al.*, 2011; Tizzard *et al.*, 2014, 2015; Niekus *et al.*, 2019). These finds witness the presence of humans in this area during the Palaeolithic and Mesolithic era. Moreover, excavations at coastal sites near Happisburgh (Norfolk) and Pakefield (Suffolk) (UK) revealed that hominins lived in the North Sea area as early as the late Early Pleistocene (Happisburgh) and during the early Middle Pleistocene (Pakefield; Parfitt *et al.*, 2005, 2010).

Numerous human skeletal remains have been found, but finds of Pleistocene hominin fossils from the North Sea bottom are extremely rare. About ten years ago, the first Neanderthal remains (*Homo neanderthalensis*) ever found in Dutch North Sea waters were brought to the surface. It was a skull fragment of a young male, probably Late

Pleistocene in age (Hublin *et al.*, 2009). Many human fossils date to the Mesolithic era, when humans inhabited a delta landscape that developed during the Early Holocene.

Natural history museums such as Naturalis Biodiversity Centre in Leiden and Het Natuurhistorisch in Rotterdam store a large collection of North Sea fossils. But also extensive private collections exist. These collections consist of abundant amount of species, varying in age from Pliocene up to modern. They include spectacular finds, such as fossils with carnivore gnawing marks, coprolites, and fossils of specimens that are rare in the fossil record such as the sabre tooth cat (*Homotherium* species), and artefacts. Numerous finds have been published in (prominent) journals (see for example, Parfitt *et al.*, 2005; Tizzard et al, 2014; Niekus *et al.*, 2019).

4.1.3 Lack of (primary) context data

The recovered finds inform us about the past biota in the now submerged landscape. However, the (stratigraphical, geographical, and archaeological) context of the vast majority of the finds is missing due to the methods in which the archaeological and palaeontological material was retrieved (Peeters, 2011). Most fossils are found when fishermen, coincidentally, catch them in their nets (see for example, van Kolfschoten and Laban, 1995; Mol and de Vos, 1995; Glimmerveen *et al.*, 2004; Mol *et al.*, 2007). Others are collected on the artificial beaches formed by sediments dredged from the bottom of the North Sea (see for example, Hublin *et al.*, 2009; Peeters *et al.*, 2009; Tizzard *et al.*, 2014, 2015). These circumstances hamper the assignment of the palaeontological and archaeological finds to a specific stratigraphical unit. The original geographical position of a number of finds collected during special private 'fossil hunting' boat trips or those carried out in the frame of the expansion of the Port of Rotterdam- the construction of Maasvlakte 2- (Mol and Post, 2010; Kuitems *et al.*, 2013) is roughly known. However, these rather detailed data about the location and depth are far from precise enough to link a find to a specific stratigraphical layer (Kuitems *et al.*, 2015b).

Moreover, most of the fossil remains were, when collected, not in primary context due to natural erosion and sedimentation processes. Recent investigations have increased our insights into geographical aspects of this now submerged landscape (Gaffney *et al.*, 2007; Sturt *et al.*, 2013; Cohen *et al.*, 2014; van Heteren *et al.*, 2014). A detailed stratigraphic framework has been made for the Eurogully region (Hijma *et al.*, 2012) and for the Maasvlakte 2 area (Busschers *et al.*, 2013). The defined lithostratigraphic units show signs of repeated, severe reworking during various fluviatile and/or marine depositional phases.

The geological data presented by Hijma *et al.* (2012) indicate that all Late Pleistocene terrestrial mammals that are older than ca. 30,000 years must have been redeposited. The skeletal remains from the North Sea are, however, rather well preserved with only minor signs of weathering and little or no rounding (Kuitems *et al.*, 2013); taphonomic features that indicate that the skeletal material was not exposed for a long time, nor that it was transported over large distances. Therefore, many finds may derive from eroded,

large lumps of reworked or frozen sediments (Hijma *et al.*, 2012; Kuitems *et al.*, 2015b). One can, therefore, assume that most of the North Sea assemblages, including the samples discussed in this chapter, are mixed. Nonetheless, several areas in the southern North Sea, for instance the Brown Bank and Eurogully, known as palaeontological and/ or archaeological 'hot spots', have been subject to targeted 'fishing' expeditions. An exception is the *in situ* research carried out in the Yangtzehaven (Rotterdam-Maasvlakte 2, the Netherlands) (Moree and Sier, 2015).

Due to the lack of context data, it is, however, impossible to carry out an in-depth study of for example the correlation between human subsistence and the palaeolandscape. But a number of finds may be assigned to a specific lithological unit if one combines a) the age of the finds, b) geological information of the area and the coordinates of the original place where it has been collected, and c) the knowledge of the ecological preference and restriction of a species.

4.1.4 Isotope investigation

It is uttermost important to know the age of the fossil finds and hence, many fossils have been ^{14}C dated. This resulted in an extensive dataset, including different species dating from Pleistocene up to modern. An overview of ^{14}C dated fossils from the North Sea is presented by van der Plicht and Kuitems (forthcoming). It is a catalogue of samples dated by ^{14}C, both by the conventional method and by AMS. Most samples are dated at Groningen.

Along with ^{14}C, δ^{13}C and δ^{15}N values have been measured for many of the skeletal remains. These isotope data provide additional information about for example the palaeoenvironmental conditions, the diet of organisms and ^{14}C reservoir effects. The stable isotope dataset of fossils from the North Sea is extensive. The majority consists of data from mammal fossils, which can shed light on ecological aspects of the North Sea area in the past. Moreover, in particular together with stable isotope data of similar species from adjacent areas, the Late Pleistocene data enhance our knowledge of the western part of the mammoth steppe ecosystem. The dataset also contains data of numerous Holocene human remains, which can shed light on (changes in) human subsistence in the North Sea region.

4.2 Material and methods

Sample preparation and isotope measurement were performed at the Groningen Centre for Isotope Research (CIO) following the standard CIO procedures described in Chapter 2 (section 2.4). The current dataset consists of directly ^{14}C dated samples of numerous mammalian species, representing marine carnivores, terrestrial carnivores, omnivores (incl. humans), herbivores, and one bird (Table 4.1). A grand total of 281 samples is presented: 157 animals, and 124 humans.

Table 4.1 Overview of analysed species, environment and average values of the stable isotope ratios δ¹³C and δ¹⁵N.

species (English)	species (Latin)	environment & diet	n	δ¹³C (‰)	n	δ¹⁵N (‰)
hare	*Lepus* sp.	terrestrial herbivore	1	-21.3	0	
beaver	*Castor fiber*	terrestrial herbivore	1	-22.1	1	4.8
dog/wolf	*Canis lupus/*sp.	terrestrial carnivore	2	-22.5	2	9.0
arctic fox	*Alopex lagopus*	terrestrial carnivore	1	-20.7	1	8.5
bear	*Ursus arctos/*sp.	terrestrial omnivore	2	-21.3	2	5.6
cave hyena	*Crocuta crocuta spelaea*	terrestrial carnivore	1	-20.1	0	
cave lion	*Panthera spelaea*	terrestrial carnivore	2	-19.3	2	8.5
wolverine	*Gulo gulo*	terrestrial carnivore	1	-21.2	0	
otter	*Lutra lutra*	freshwater carnivore	2	-25.5	1	8.6
walrus	*Odobenus rosmarus*	marine carnivore	5	-13.3	4	12.1
grey seal	*Halichoerus grypus*	marine carnivore	2	-13.6	1	14.5
harp seal	*Pagophilus groenlandica*	marine carnivore	2	-15.4	0	
woolly mammoth	*Mammuthus primigenius/*sp.	terrestrial herbivore	24	-22.0	20	7.1
straight-tusked elephant	*Palaeoloxodon antiquus*	terrestrial herbivore	7	-20.7	7	9.9
horse	*Equus caballus/*sp.	terrestrial herbivore	6	-21.2	6	4.3
woolly rhinoceros	*Coelodonta antiquitatis*	terrestrial herbivore	3	-20.7	1	4.5
Balaenidae	*Balaenidae*	marine carnivore	1	-16.7	1	9.3
bowhead whale	*Balaena mysticetus*	marine carnivore	1	-14.8	1	14.3
common rorqual	*Balaenoptera physalus*	marine carnivore	1	-12.6	0	
grey whale	*Eschrichtius robustus*	marine carnivore	14	-14.3	12	14.2
white-beaked dolphin	*Lagenorhynchus albirostris*	marine carnivore	2	-12.2	2	15.9
killer whale	*Orcinus orca*	marine carnivore	2	-12.0	2	16.4
bottlenose dolphin	*Tursiops truncatus*	marine carnivore	2	-11.9	2	15.4
beluga whale	*Delphinapterus leucas*	marine carnivore	4	-15.5	3	15.2
wild boar	*Sus scrofa*	terrestrial omnivore	3	-21.7	2	5.1
giant deer	*Megaloceros giganteus*	terrestrial herbivore	4	-20.0	3	4.9
red deer	*Cervus elaphus*	terrestrial herbivore	14	-21.6	9	3.5
moose	*Alces alces*	terrestrial herbivore	5	-21.0	5	3.2
reindeer	*Rangifer tarandus*	terrestrial herbivore	16	-19.9	12	3.8

| roe deer	*Capreolus capreolus*	terrestrial herbivore	2	-21.8	2	2.7
aurochs	*Bos primigenius*	terrestrial herbivore	5	-22.1	5	5.3
bison	*Bison priscus*/sp.	terrestrial herbivore	3	-20.4	1	3.9
bovids	*Bovidae*	terrestrial herbivore	5	-22.0	5	5.6
muskox	*Ovibos moschatus*	terrestrial herbivore	1	-20.1	0	
Caprinae	*Caprinae*	terrestrial herbivore	1	-19.2	1	7.5
human	*Homo sapiens*	terrestrial omnivore	124	-20.0	123	12.1
great auk	*Pinguinus impennis*	marine carnivore	3	-14.5	3	17.1
unknown	unknown	unknown	6	-21.7	6	5.2
			281		248	
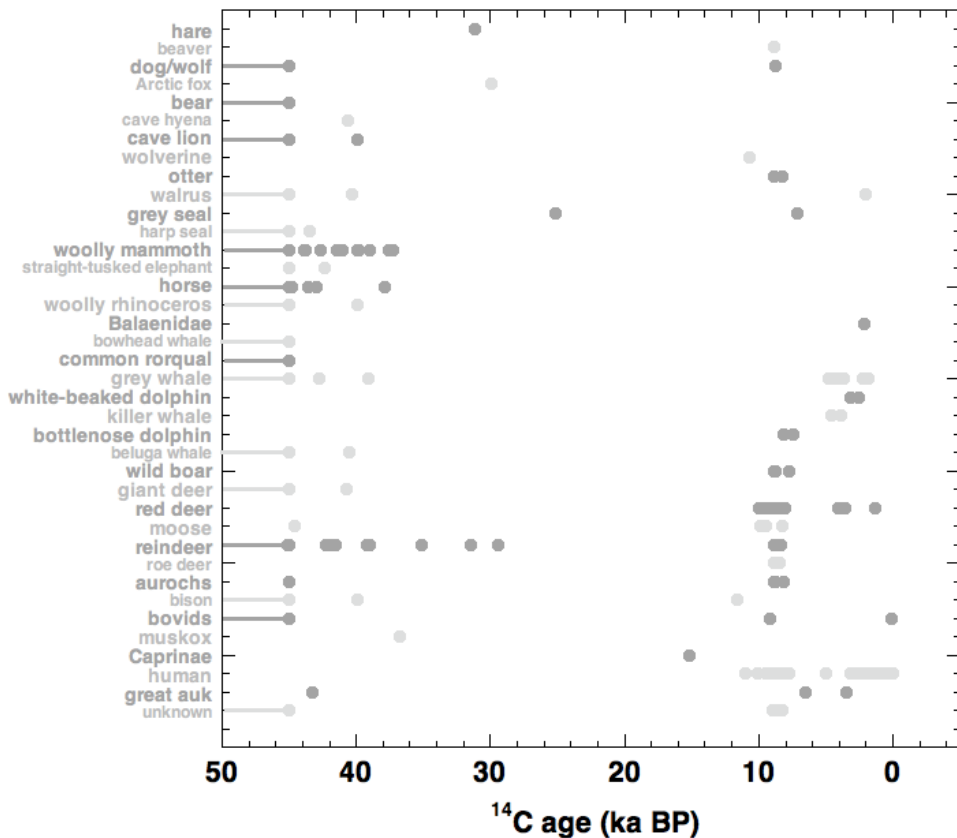
Figure 4.1 Age distribution of all analysed samples from the North Sea, taxonomically ordered. A grand total of 281 dates is plotted. The horizontal lines at the left side of the figure correspond to ages larger than 45,000 ^{14}C yr BP. Dates reported as finite and older than 45,000 ^{14}C yr BP are truncated at 45,000 ^{14}C yr BP.

Figure 4.1 shows the age distribution of all analysed samples from the North Sea area. The majority of the samples have a Pleistocene age (n = 96; all non-humans) and many samples are from species that are part of the typical Late Pleistocene mammoth steppe fauna: woolly mammoth, cave lion, arctic fox, hyena, woolly rhinoceros, horse, giant deer, reindeer and bison. The dataset includes, in addition, 19 marine animals with a Pleistocene age, such as bowhead whale, common rorqual, beluga whale, grey whale, grey seal, harp seal, walrus, and great auk. The rest of the samples (n = 185) are Holocene in age. These include both human (n = 124) and animal fossils (n = 61), the latter including at least 25 artefacts/worked items made of antler and bone.

This dataset gives an impression of the variety of species which lived in this area throughout the last 50,000 years. However, the composition of the current dataset is biased. Aspects such as taphonomic processes, the mesh size of fishing nets but also the selection of sediments used for sand deposition projects and the decision of collectors to focus on specific (rare) species determine the type of North Sea finds that are finally submitted for ^{14}C dating and hence, affects the representation of species.

Many finds come from a relatively limited number of areas in the North Sea basin, specifically locations that are frequently exploited by fishermen and that are suitable for sand extraction purposes (see Table SI Chapter 4). About one third of the samples come from the important fishing areas Brown Bank (n = 53) and Eurogully (n = 43). Also, a large part (n = 38) comes from beaches along the Dutch province South-Holland, where in recent years, several large-scale sand deposition projects took place. The Brown Bank and Eurogully yielded the highest number of species. Human remains are found at different localities, but the majority of them come from the coast of the Dutch province South-Holland and from the Wadden Sea in the North of the Netherlands. Moreover, all main find localities within the North Sea area yielded remains of both marine and terrestrial animals.

4.3 Results

Table 4.1 shows the analysed species, number of samples, the biotope (marine or terrestrial) and trophic level, and the (averaged) δ^{13}C and δ^{15}N values. For the results of the isotopic measurements of each individual sample, the reader is referred to Table SI Chapter 4. Figure 4.2 shows the mean δ^{13}C and δ^{15}N values for the samples, roughly ordered per trophic level and environment. In general, the isotope signals of most species fit into the broad clusters as shown in Fig. 2.2 (Chapter 2).

As expected, the marine carnivores show the highest δ^{13}C and δ^{15}N values. Their δ^{13}C values range between -16.7 and -11.4‰, and the δ^{15}N values between +9.3 and +17.7‰. The δ^{13}C values of the terrestrial herbivores range from -23.3 to -18.9‰. Their δ^{15}N values cover a large range of 9.9‰, the lowest being +1.7‰ and the higher δ^{15}N values being higher than those of the terrestrial omnivorous animals and terrestrial
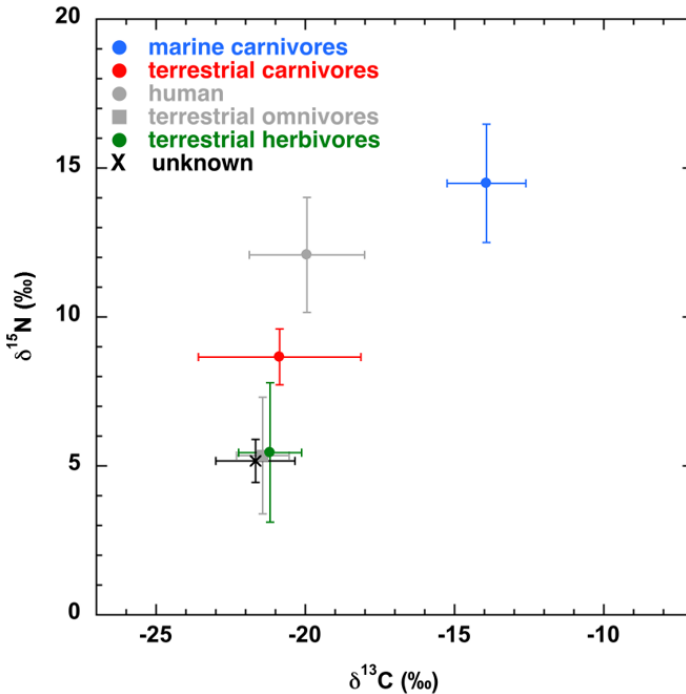
Figure 4.2 Mean $\delta^{13}C$ and $\delta^{15}N$ values with 1 σ-standard deviation for all samples, ordered per trophic level (herbivore, carnivore, omnivore) and habitat (marine, terrestrial).

carnivores in the current dataset. Apart from the humans, the terrestrial omnivores values fall within the range of these of terrestrial herbivores; $\delta^{13}C$ values range between -22.3 and -20.3‰, and $\delta^{15}N$ between +3.5 and +7.7‰. The human samples show large ranges of both isotope values. Their $\delta^{13}C$ values range between -24.7 and -13.4‰, and the $\delta^{15}N$ values range all except one (that is +4.5‰) between +8.0 and +17.4‰. The terrestrial carnivores have $\delta^{13}C$ and $\delta^{15}N$ values between -25.6 and -19.2‰ and between +7.7 and +10.2‰, respectively. The dataset consists of two samples of a freshwater carnivore, an otter, with $\delta^{13}C$ values of -26.2‰ and -24.8‰, and a $\delta^{15}N$ value of +8.6‰ (the $\delta^{15}N$ was measured for only one of these samples).

The trophic level/habitat clusters are composed of a variety of species from different time periods. The results of certain species will be discussed in more detail in the next paragraph. This selection is primarily based on the number of available samples per species.

4.4 Discussion

4.4.1 Stable isotope signatures of the Pleistocene animals

An overview of the data of the Pleistocene animals is shown in Fig. 4.3. It shows that the $\delta^{15}N$ values of the straight-tusked elephant (+7.5 to +11.6‰) and many of the woolly
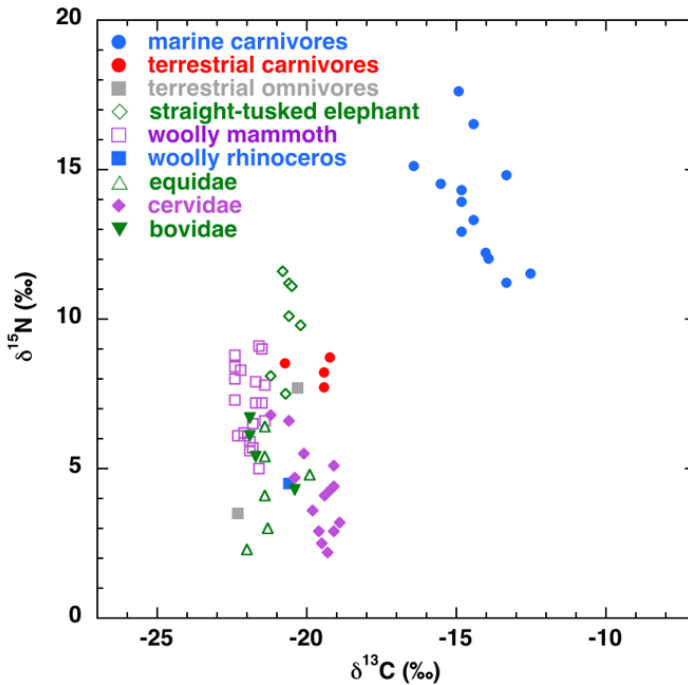
Figure 4.3 δ^{13}C and δ^{15}N values for Pleistocene mammal samples from the North Sea.

mammoth (+5.0 to +9.1‰) exceed these of other herbivores. Relatively high δ^{15}N values are commonly observed for woolly mammoth (for example, Bocherens, 2003; Kuitems *et al.*, 2015c) and have also been observed for Middle Pleistocene straight-tusked elephants from Germany (Kuitems *et al.*, 2015a; see Chapter 6). The current dataset also includes woolly mammoth samples with lower δ^{15}N values. Relatively low δ^{15}N values were also observed for Late-Glacial woolly mammoths in the Ukraine (Drucker *et al.*, 2014). The lowering of the values has been associated with changing environments and/or climates and changes in niche occupation after the LGM. Pre-LGM values of mammoths from Europe (including samples from the Ukraine (Drucker *et al.*, 2014)) show higher δ^{15}N values, ranging between +6.7 and +11.1‰. The current dataset of the North Sea contains only mammoth samples with a pre-LGM age; the majority being older than the ^{14}C background for fossil bone collagen (> 45,000 yr BP). The woolly mammoth samples with the lowest δ^{15}N values (between +5.0 and +6.0‰) are older than 45,000 years BP.

The δ^{13}C values of woolly mammoths (-22.4 to -21.4‰) are rather negative, in particular compared to those of other herbivores, including straight-tusked elephants (-21.2 to -20.2‰). Also, this picture (woolly mammoths are depleted in δ^{13}C compared to other herbivores) is known for other localities, and has tentatively been linked to seasonal metabolism of fat (Bocherens, 2003; Szpak *et al.*, 2010).

A number of the walrus samples have a nitrogen isotope ratio (n = 4; average = +12.1‰) that is low compared to most other marine mammals (average = +14.8‰;

Fig. 4.5). This might be explained by a low trophic level diet, such as clams and other molluscs (Dehn *et al.*, 2007).

As mentioned in Chapter 3, well-defined temporal changes in the distribution of $\delta^{13}C$ and $\delta^{15}N$ values have been observed for several species inhabiting North-western Europe; changes that are related to the climatic and environmental changes during the Late-Glacial and/or at the Pleistocene-Holocene transition. Indeed, the Pleistocene-Holocene boundary is characterised by severe climatic and environmental change in the North Sea region. The onset of the Holocene is, generally speaking, characterised by wetter and warmer climatic conditions, sea level rise and the development of forest. The current stable isotope North Sea record does not allow statements on temporal trends: samples from the last part of the Late Pleistocene, specifically, the LGM and the Late Glacial, are lacking (see Fig. 4.1 and Table SI Chapter 4) and the number of Pleistocene and Holocene records of a specific species is too low to draw solid conclusions.

4.4.2 Stable isotope signatures of the Holocene animals

In contrast to the characteristic Pleistocene 'mammoth steppe fauna', generally thriving in open landscapes, the Holocene samples represent forest dwellers that lived under temperate conditions. This is clearly illustrated by the North Sea Cervidae samples: Pleistocene samples are mainly from reindeer; other species are giant deer and moose. The Holocene cervid samples are predominantly from red deer; other species are moose and roe deer. As shown in Fig. 4.4, the $\delta^{13}C$ values of samples from Holocene
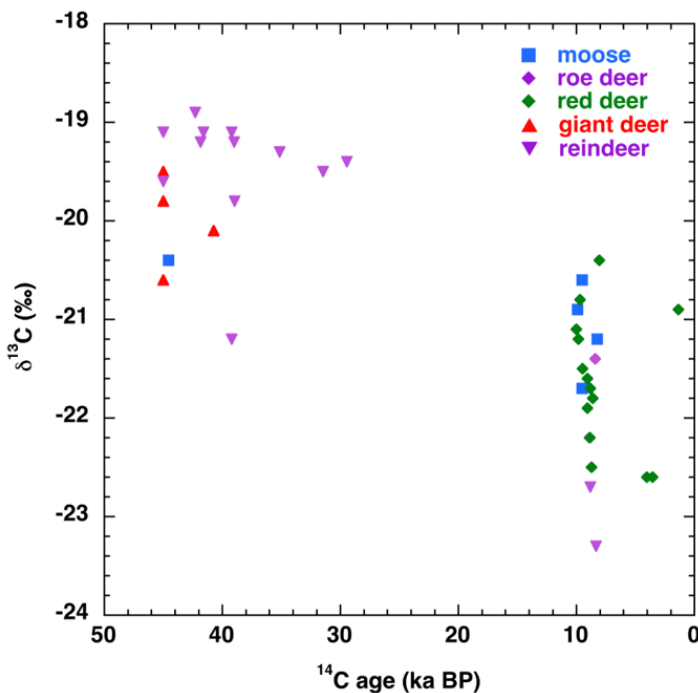
Figure 4.4 $\delta^{13}C$ values for samples of cervids from the North Sea through time.
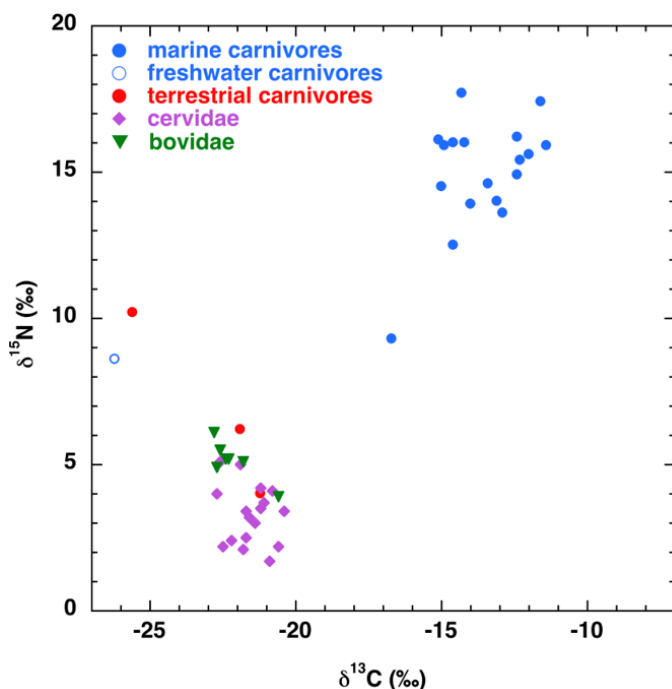
Figure 4.5 $\delta^{13}C$ and $\delta^{15}N$ values for Holocene animal samples from the North Sea.

cervids (n = 22, average = -21.7‰) are considerably more negative than those of the Pleistocene cervids (n = 20, average = -19.7‰). This difference can partly be ascribed to the changed $\delta^{13}C$ values in plants caused by the climate shift from the Pleistocene to the Holocene. Moreover, this difference can be explained by dissimilarities between the species, such as niche occupation, dietary composition, and physiology. For instance, the reindeer diet consists in general, for a significant part of lichens, which commonly yield higher $\delta^{13}C$ values than vascular plants (Ben-David *et al.*, 2001; Drucker *et al.*, 2003b). Fig. 4.4 shows that the $\delta^{13}C$ values from the Holocene reindeer (even though n = 2) are much lower in $\delta^{13}C$ than the Pleistocene ones. This might be explained by a dietary change, but a mistake in species identification cannot be excluded.

Due to the sea level rise, samples of marine mammals recur in the Holocene record. The only Holocene freshwater species is the otter. However, the stable isotopes of the Holocene dog/wolf (*Canis* sp.; GrA-24209) also show a mainly freshwater signal (Fig. 4.5). This is not surprising, since the Holocene dog lived together with humans (Noe-Nygaard, 1983, 1988; Schulting and Richards, 2002; Fischer *et al.*, 2007) and freshwater fish was an important part of the Mesolithic human diet. Dogs might have consumed the 'leftovers' of the human meal (Noe-Nygaard, 1983).

Not only human skeletal remains, also stone and bone tools indicate the presence of Mesolithic humans of the North Sea area. Archaeological sites such as Hardinxveld-Giessendam De Bruin indicate that the Mesolithic inhabitants lived on the higher
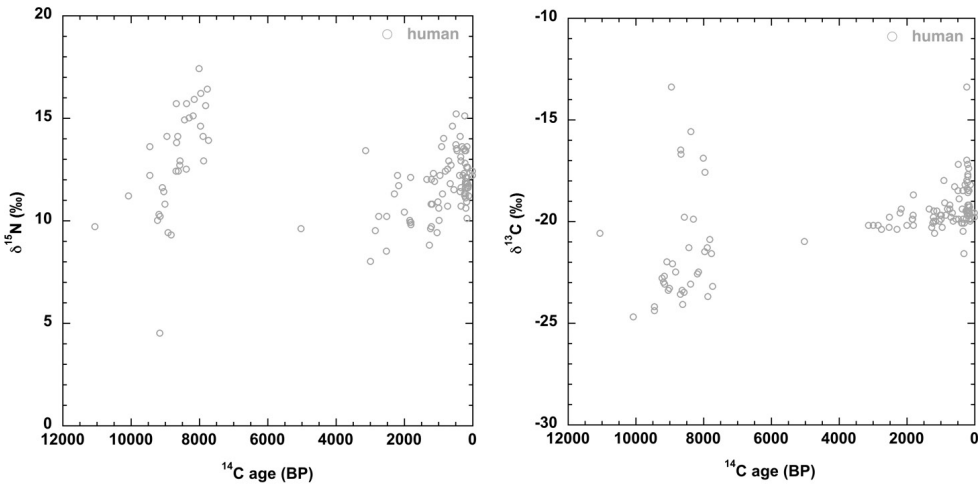
Figure 4.6 δ^{15}N and δ^{13}C values of human bones from the North Sea through time. Left: δ^{15}N versus ^{14}C age (yr BP); Right: δ^{13}C versus ^{14}C age (yr BP).

areas such as river dunes (Louwe Kooijmans *et al.*, 2001). The worked bone and antler artefacts are made from long bones of bovids, equids, and cervids, and from antler, predominantly of red deer. Six objects could not be assigned to a specific species. The δ^{13}C and δ^{15}N values of the bone artefacts fall within those of the terrestrial herbivore ranges.

4.4.3 The human stable isotope signature

The dataset with more than hundred human skeletal remains include bones from the sea floor found by fishing or dredging (Amkreutz *et al.*, 2018a,b) as well as finds collected on the beach (Storm, 2010). Recently, an overview of 56 human bone remains was published (van der Plicht *et al.*, 2016); 33 are Mesolithic in age (including a few Late Palaeolithic), the remaining 23 specimens range between Roman age and recent. The main conclusion of the stable isotope analysis is that the Mesolithic humans were predominantly consumers of freshwater protein (van der Plicht *et al.*, 2016).

   Since the publication in 2016, the dataset of human finds has significantly increased. The fossils are either Mesolithic in age, or ranging between late Roman time and recent (see Fig. 4.6 and see Table SI Chapter 4). There is only one exception: a find from the island of Texel with an age of 5,020 ^{14}C yr BP (GrM-10161). The average δ^{13}C and δ^{15}N values of the human bones are shown in Fig. 4.2; the δ^{13}C and δ^{15}N values for the individual human samples are plotted against time in Fig. 4.6. Abundant fish remains from archaeological coastal sites such as at Hardinxveld-Giessendam reveal that fish may have been the most important dietary resource for Mesolithic humans, in particular pike (Louwe Kooijmans, 2005). Many of the humans have δ^{15}N values which are often indicative for aquatic dietary resources, in particular those with δ^{15}N values higher than

+12‰. However, $\delta^{15}N$ values can be affected in many ways. For instance, it is known from other Holocene sites in the Netherlands, that cattle grazing on the coastal salt marshes may have considerably high $\delta^{15}N$ values (Prummel *et al.*, forthcoming; Kamjan *et al.*, forthcoming). These high $\delta^{15}N$ values are passed on to humans who are eating the cattle's meat. Since there is no proper baseline available for isotope values of different food recourses in this area, only cautious statements about dietary resources can be made.

As visible in Fig. 4.6 (right), there is a discrepancy between the Mesolithic and later inhabitants of the North Sea area. The low $\delta^{13}C$ values point to a significant component of freshwater fish in the diet of Mesolithic humans. The $\delta^{13}C$ values of the non-Mesolithic human bones have intermediate $\delta^{13}C$ values, generally indicative of a mixed marine/freshwater/terrestrial food source. This can be expected in a delta region like the coastal Netherlands.

Compared to the other samples of the current dataset, there is one exceptionally low $\delta^{15}N$ value of 4.5‰. This is not necessarily an ingenuine result, as the human $\delta^{15}N$ ranges generally between 4 to 10‰ for terrestrial diets, depending on the trophic level of the food protein (Richards and Hedges, 1999). Such low $\delta^{15}N$ values for human bones have been observed before, for example in Mesolithic bones from Germany (Terberger *et al.*, 2012).

4.4.4 Radiocarbon dates of the current dataset

The present tables contain partly published but for a major part of unpublished ^{14}C, ^{13}C, ^{15}N data. The $\delta^{13}C$ and $\delta^{15}N$ dataset discussed in this chapter includes skeletal remains of both terrestrial and aquatic organisms. The age determination of the latter ones needs special attention. The ^{14}C convention is defined for terrestrial material, which is in equilibrium with atmospheric CO_2. Reservoirs like oceans, rivers and lakes generally contain less ^{14}C than the atmosphere. This causes older apparent ages for organisms acquiring their carbon from these reservoirs through the food chain: the so-called 'reservoir effect'. ^{14}C dates of aquatic organisms need a correction for the reservoir effect in order to derive absolute calendar ages. This also applies to terrestrial organisms with a significant amount of aquatic food in their diet. The general marine offset is about 400 years towards older, but riverine or a mixture of marine and fresh water resources may have considerably large and obscure consequences for the age determination. Since the actual share of aquatic versus terrestrial food and the share of marine versus fresh water resources of for instance humans is unknown, the reservoir effect cannot be quantified. Thus, the dates cannot be calibrated. To avoid reservoir effect ambiguities, the age of the samples discussed in this chapter are given in ^{14}C ages (BP) instead of calibrated dates (cal BP).

Figure 4.1 suggests that the LGM is more or less devoid of fossils. There is an ongoing discussion about the conditions in the North Sea area during the LGM, but the absence or scarcity of fossils supports the idea that the North Sea basin has been a

harsh environment in this period (Carr *et al.*, 2006). One should note, however, that this dataset reflects a biased composition of inhabitants of the North Sea area in the past. Aspects such as taphonomic processes, choices for sediment used for substantial sand deposition projects, mesh size of fishing nets, detection of finds by (often amateur) collectors, and the glamour of specific finds dramatically determine the type of North Sea finds that are finally submitted for ^{14}C dating. For instance, small, fragile fish and bird bones are just sporadically submitted for ^{14}C dating. The possibility to recover these finds in the North Sea area is very limited and the quantity and/or quality of the collagen from these remains is often not enough to date the remains. In contrast to smaller animals, many human remains have been submitted for ^{14}C dating. A large number of samples are human bones thought to be Neanderthal based on the degree of fossilization. However, none of these appeared Neanderthal; they are all Mesolithic or Late Palaeolithic. Today, the only Neanderthal from the North Sea is 'Krijn' (Hublin *et al.*, 2009), known to be Neanderthal because of its distinctive skull features. Since the fossil did not yield collagen, it is not datable by [14]C. Moreover, samples of cervids (often pieces of modified antlers) are represented in relatively high numbers in the ^{14}C dataset.

As expected, many of the (Late) Pleistocene fossils are from species that are part of the so-called mammoth steppe fauna. Moreover, a large number of Pleistocene fossils are from marine mammals. The set of large marine mammal ^{14}C dates have raised questions, which still need to be resolved. Many whales date between 35,000 and 45,000 ^{14}C yr BP and walruses between 25,000 and 30,000 ^{14}C yr BP. However, these ages conflict with the results of geological and stratigraphical studies executed in the North Sea area; studies that show that the sea level was low during these periods and the area where the fossils have been collected was land instead of sea. Hijma *et al.* (2012) show the marine fauna must be either older than ~ 80,000 years or Holocene in age. The obtained ^{14}C dates have, therefore, been criticised, and compared with ^{14}C dates of shells (Rijsdijk *et al.*, 2013; Busschers *et al.*, 2014). The datable fraction of shells is their carbonate. In contrast to bones, fossil corals and shells can recrystallize, enabling exchange of carbon (including ^{14}C) from different sources. Shell ^{14}C dates can, therefore, be in conflict with other dating methods, in particular racemization. It may be worth re-dating a number of the marine mammals remains by compound specific ^{14}C dating.

4.5 Conclusion

The North Sea region was dry land during the last glacial period, and was inhabited by a rich fauna. With the onset of the Holocene, the eustatic sea level raised and Mesolithic people inhabited the higher parts of the new-developed coastal North Sea area. Large quantities of fossil bones have been recovered from the present seabed. Over the years, the $\delta^{13}C$ and $\delta^{15}N$ values of almost 300 human and non-human animal remains have been measured. Since the context of the finds is unclear, the ^{14}C dates are crucial to

establish the age of the fossils. The δ^{13}C and δ^{15}N values of the dated bone collagen yield information about for example palaeodiet, palaeoclimate and palaeoenvironment.

The isotope signals are, in general, comparable to those that are known from omnivores, herbivores and carnivores inhabiting past marine and terrestrial biotopes elsewhere in North-western Europe. This large North Sea dataset consists of species for which δ^{13}C and δ^{15}N data are not abundant such as straight-tusked elephant, otter, wolverine and great auk, numerous large marine mammals and humans.

The stable isotope data can be used to further zoom in on questions related to fossil remains from the North-western mainland and the United Kingdom. Moreover, a vast amount of new stable isotope data for human remains from the North Sea is presented. Most human bones have δ^{15}N values that point to an aquatic diet. The δ^{13}C values of the Mesolithic humans are generally indicative for freshwater food resources. The δ^{13}C values of human bones from later periods point towards a mixed diet of marine, freshwater, and terrestrial food resources. This analysis, based on a large database obtained over the years, illustrates that a collection of stray finds without context nevertheless can lead to inference of inhabitants from past environments in a multidisciplinary approach.

Irtysh River, photo: P. Kosintsev

STABLE ISOTOPES
OF THE SIBERIAN UNICORN

The stable isotope research in this chapter describes the stable isotope research published in the following articles:

Kosintsev, P. Mitchell, K. Devièse, T. van der Plicht, J., Kuitems, M., Petrova, E., Tikhonov, A., Higham, T., Comeskey, D., Turney, C., Cooper, A., van Kolfschoten, T., Stuart, A., Lister, A., 2019. Evolution and extinction of the giant rhinoceros *Elasmotherium sibiricum* sheds light on late Quaternary megafaunal extinctions. *Nature Ecology & Evolution* **3** (1), 31-38.

Kuitems, M., van der Plicht, J., van Kolfschoten, T., 2019. *Elasmotherium sibiricum*: de uitgestorven Siberische Eenhoorn – uitkomsten van opzienbarend onderzoek. *Cranium* **36** (1), 34-43.

5.1 Introduction

A rather unknown inhabitant of Mammoth Steppe was *Elasmotherium sibiricum*, the so-called 'Siberian unicorn'. The Siberian unicorn was a giant rhinoceros that lived in Eastern Europe and Central Asia. The Siberian unicorn, which appeared in the Early Pleistocene, was the youngest representative of the 40-million-year-old Elasmotherinae branch. With its extinction, the last representative of the once successful subfamily disappeared. The *Elasmotherium* has been used in Eastern Europe as a guiding 'chronospecies' for a specific biostratigraphic unit (Schvyreva, 2015). Based on the fossil data, the extinction was generally assumed to have happened during the Middle Pleistocene around 200,000 years ago (Zhegallo *et al.*, 2005).

The co-occurrence of a few remains of *E. sibiricum* and Late Pleistocene species within the same fossil assemblages, suggested that their existence may have extended to the Late Pleistocene. However, the fossil assemblages consist often of remains that originate from multiple stratigraphic layers. For example, at the site Pyshma near Yekaterinburg in the Southern Urals, it was assumed that *E. sibiricum* fossils represented older material that had ended up in a mixed fossil assemblage. A sample for dating was nevertheless taken. The result was surprising; the age of the fossil turned out to be within ^{14}C range and to be as old as the other dated remains from the same site (that is, GrA-53424; 33380 ± 205 ^{14}C yr BP). This was the incentive to date more *Elasmotherium* fossils from that region, and led to an intensive international research cooperation.

Recently, a paper on this extinct unicorn was published in Nature Ecology and Evolution (Kosintsev *et al.*, 2019), revealing (1) that the *E. sibiricum* went extinct much later than previously thought, (2) that the Elasmotherinae and Rhinocerotinae lineages split already ~ 40 million years ago, and (3) that this animal had a distinct diet. The latter was discovered by stable isotope analysis of *Elasmotherium* fossils, carried out by this thesis' author, in combination with analysis of the species' characteristic morphology.

This chapter focusses on the stable isotope investigation. First, some general background information on the species is provided and the results of the genetic and dating studies are summarised.

5.1.1 The Siberian unicorn

E. sibiricum is an odd-toed ungulate (order Perissodactyla) belonging to the rhinoceros family, the Rhinocerotidae; a group of about 250 described, mostly extinct, species that were very diverse and successful in the past. With a length of approximately 4.5 meters, a withers height of over 2 meters, and a weight of ~ 3.5 tonnes, *E. sibiricum* was a true giant. However, it was not the largest rhinoceros that lived in Eurasia during the Pleistocene. Its predecessor, *E. caucasicum* was with a length of 5.0 - 5.2 meters, a withers height of about 2.4 meters and a weight of about 5 tonnes even larger (Zhegallo *et al.*, 2005; Schvyreva, 2015).

The skeleton of the Siberian unicorn (Fig. 5.1) is in many ways similar to that of

Figure 5.1 Skeleton of an *Elasmotherium sibiricum* specimen in the Stavropol regional museum (Schvyreva, 2016).

other rhinos, but it has a number of clear diagnostic features. For instance, bones of the front and rear legs are relatively slender. This is seen as an evolutionary adaptation whereby the animal, despite its weight, was able to move quickly and thus travel large distances (Schvyreva, 2014; 2015; 2016).

Another distinctive feature is the huge skull, which was bent downward. On its forehead (the frontal bone), the Siberian unicorn had a striking dome (Fig. 5.2) that forms the basis of a large horn. The Siberian unicorn differs, also in this respect, from rhinos such as the woolly rhino where the basis of the horns is more anterior, i.e., the nasal bone. A cross section through the skull (Fig. 5.2) shows that the bump on the forehead does not consist of solid bone, but has a spongy, cellular structure similar to skulls of elephants. Traces of well-developed blood vessels, especially at the base of the dome, suggest strong blood flow. According to some researchers, this may indicate a well-developed sense of smell. The bump has a rough surface; a phenomenon that we also see in other rhinos where the horns are attached to the muzzle.

There are different opinions about the shape and the size of the horn of the Siberian unicorn; fossil remains of the horn have never been found (Zhegallo *et al.*, 2005). Also, the dentition is very specific and characteristic for the species. The teeth are reduced in terms of elements; both the upper jaw and lower jaw lack the incisors and canines as well as the anterior two premolars. The permanent teeth consist of five very high-
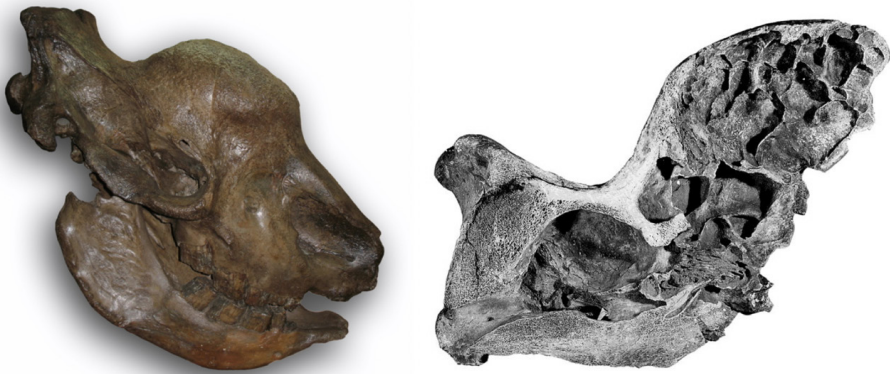
Figure 5.2 Left: Cranium of an *E. sibiricum* specimen from the collection of the Zoological Museum in St. Petersburg (Russia). (Photo: Alexei Tikhonov). Right: Longitudinal section of the cranium of an *E. sibiricum* specimen (Schvyreva, 2016).

Figure 5.3 Surface (left) and lateral view (right) of an upper M3 of *E. sibiricum* specimen from the Lower Don Region, late Middle Pleistocene. Collection Azov museum-reserve (Photos: Vadim Titov).

crown molars (2 premolars, 3 molars). The rootless, permanent growing molars have remarkably undulated enamel (Fig. 5.3).

Zhegallo *et al.* (2005) present an extensive overview of the different hypotheses on the species' habitat and diet. Inhabiting swampy areas along rivers and lakes have been suggested, but primarily the dry areas of steppes are proposed as the habitat of the Siberian unicorn (Zhegallo *et al.*, 2005; Schryreva, 2016). The characteristic hypsodont teeth of the Siberian unicorn are seen by many as an adaptation to a diet that causes exceptional rapid wear (Schryreva, 2016). The food itself can be the cause of the rapid abrasion, but also sand or grit, which comes with the food, can cause substantial part of the molar wear.

5.1.2 Genetic data and age

During the Miocene (~ 23-5 million years ago), the Rhinocerotidae dominated the large mammalian fauna of Africa, Eurasia and North America (Kosintsev *et al.*, 2019). They are subdivided into two subfamilies: 1) the Rhinocerotinae, to which the five recently living species belong as well as the Pleistocene species of rhinoceros that lived in Western Europe (for example the steppe rhino *Stephanorhinus hemitoechus* and the woolly rhino *Coelodonta antiquitatis*), and 2) the extinct Elasmotherinae, with a geographical range limited to Eastern Europe and Central Asia, and a number of geographically
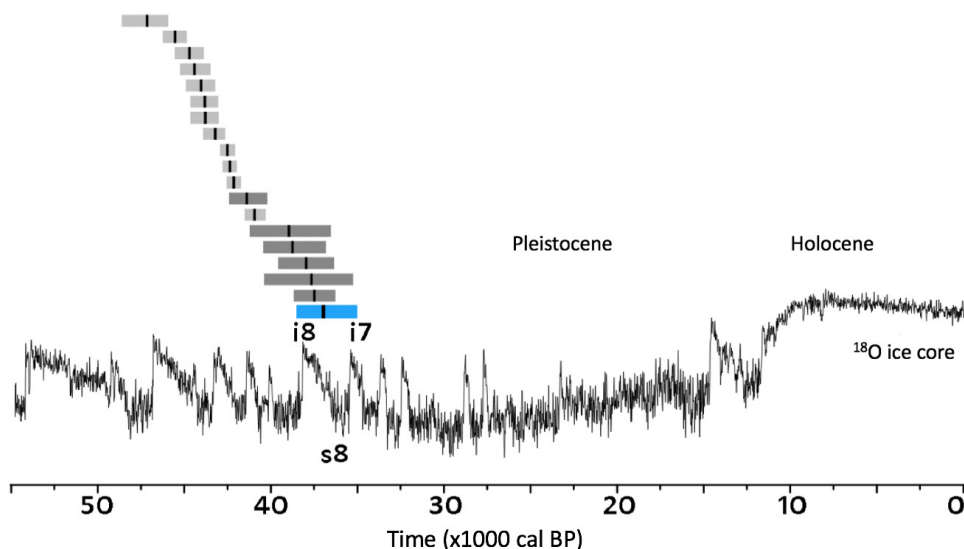
Figure 5.4 Calibrated ¹⁴C dates of *E. sibiricum*, compared to the chronology and temperature of Greenland ice. The blue area marks the extinction event, as determined from modelled ¹⁴C dates. Calibration and modelling were performed using respectively IntCal13 and the function Single Phase model in OxCal version 4.3.2 (Bronk Ramsey, 2009; Reimer *et al.*, 2013). From Kosintsev *et al.* (2019).

isolated areas in Mongolia and China. Based on the fossil record, it was assumed that the split between the two subfamilies took place very early, during the Eocene (around 56-34 million years ago). The analysis of the fossil DNA in the recently examined bones has confirmed the earlier assumption with a calculated genetic divergence of about 47.4 million years ago (Kosintsev *et al.*, 2019).

Radiocarbon dates clearly show that *E. sibiricum* got extinct much later than previously thought. The species still lived during the late Quaternary. There are no finds of *Elasmotherium* known from an LGM (or younger) context. The extinction of the Siberian unicorn can therefore be seen as belonging to the 'Late Quaternary megafaunal extinctions' during the Weichselian (Stuart, 2015).

In Fig. 5.4 the dates are compared with ^{18}O data from Greenland ice cores (Rasmussen *et al.*, 2014). The relative concentration of the oxygen isotope ^{18}O (δ^{18}O) in ice is a proxy for temperature and climate; more positive values correspond to relatively warm periods, more negative to colder periods. Holocene and Pleistocene are clearly distinguishable and indicated in the figure. The Pleistocene is characterized by climate fluctuations called the Greenland Stadials and Interstadials. The extinction of the *Elasmotherium* took place during an era of extreme climate fluctuations, known as Marine Isotope Stage (MIS) 3, as can be observed in deep sea core record and in Greenland ice cores as the alternation of interstadials and stadials (Fig. 5.4; interstadials GI-7, GI-8 and stadial GS-8). It is striking that the extinction of *Elasmotherium* roughly coincides with GS-8 (Fig. 5.4) and also with a period in which extreme 'ice rafting' occurs in the North Atlantic, a period known as the Heinrich Event H4 (Bassis *et al.*, 2017).

5.2 Material and Methods

A total of 25 fossils from various locations throughout the Siberian unicorn's distribution area were sampled (Table 5.1, Fig. 5.5). Sample preparation and measurement of the δ^{13}C and δ^{15}N values that are discussed in this chapter (Table 5.2) was carried out at Groningen, CIO, following procedures as described in Chapter 2 (section 2.4).

^{14}C dating was performed at Groningen and Oxford. The youngest samples according to the original Groningen data set were subsequently also dated in Oxford. In case ^{14}C results of a fossil were different (within the mutual measurement error) for Groningen and Oxford, the specific fossil was dated again by hydroxyproline (or HYP). In this method, developed at Oxford to improve dating of potentially contaminated samples, the amino acid hydroxyproline is extracted from the collagen. This method was chosen because hydroxyproline is unique to mammals, thus minimises contamination. In Table 5.2, the stable isotope values (measured at Groningen) are shown in combination with what was considered the best current date for each specimen.

The δ^{13}C and δ^{15}N values are compared with those of other coeval living species, specifically data from woolly rhinoceros (*C. antiquitatis*; Stuart and Lister, 2012) and saiga

Table 5.1 Information about the *E. sibiricum* samples taken for isotope analysis.

museum & number	locality	skeletal element	latitude	longitude
C/M 12836	Irbit	cranium	57.67	63.07
IPAE 420/111	Smelovskya	molar	53.60	58.90
NHM M7099	Saratov	molar	51.54	46.01
ZIN 36330	Hydroelectric pwr. st., Ship Canal #32, Eur. Russia	cranium		
IPAE 915/2804	Tobolsk	radius	58.00	68.00
IPAE 2388/2	Bashkiriya	cranium	54.50	56.33
ZIN 31791	Samara district	cranium	53.20	50.14
IPAE 2388/1	Bashkiriya	cranium	55.00	55.83
IPAE 17-5703/7	Samara district	femur	53.20	50.14
IPAE 5-147	Samara district	tooth	53.20	50.14
IPAE 12-001	Samara district	cranium	53.20	50.14
IPAE 10-5566	Samara district	cranium	53.20	50.14
IPAE 897/200	Borovlyanka	molar	56.80	62.87
ZIN 36331	unknown	cranium		
ZIN (26021) 3963	Luchka (Svetliy Yar), Volgograd Region	cervical vertebra	48.47	44.77
ZIN 3986	Incineration factory of bones, European Russia	cervical vertebra		
ZIN 10794	Luchka (Svetliy Yar), Volgograd Region	cranium	48.47	44.77
IPAE 2388/3	Bashkiriya	cranium	54.00	56.50
IPAE 2388/5	Bashkiriya	mandible/molar	53.17	56.00
IPAE 1871/200	Voronovka	cranium	55.45	65.33
IPAE 897/172	Borovlyanka	metacarpal	56.80	62.87
IPAE 897/123	Borovlyanka	molar	56.80	62.87
NHM M12429	Sarepta	cranium	48.52	44.51
IPAE 2388/4	Bashkiriya	cranium	53.67	56.08
IPAE 9-133	Odessa	tooth	46.47	30.73

antelope (*Saiga tatarica*; Jürgensen *et al.*, 2017). Only data from pre-LGM central Asia were used for direct comparison with *E. sibiricum*. Also, published $\delta^{13}C$ and $\delta^{15}N$ data of other fossil rhinoceroses, specifically, Merck's rhinoceros (*Stephanorhinus kirchbergensis*) and indeterminate *Stephanorhinus* specimens were used for comparison with the stable isotope data of the Siberian unicorn.
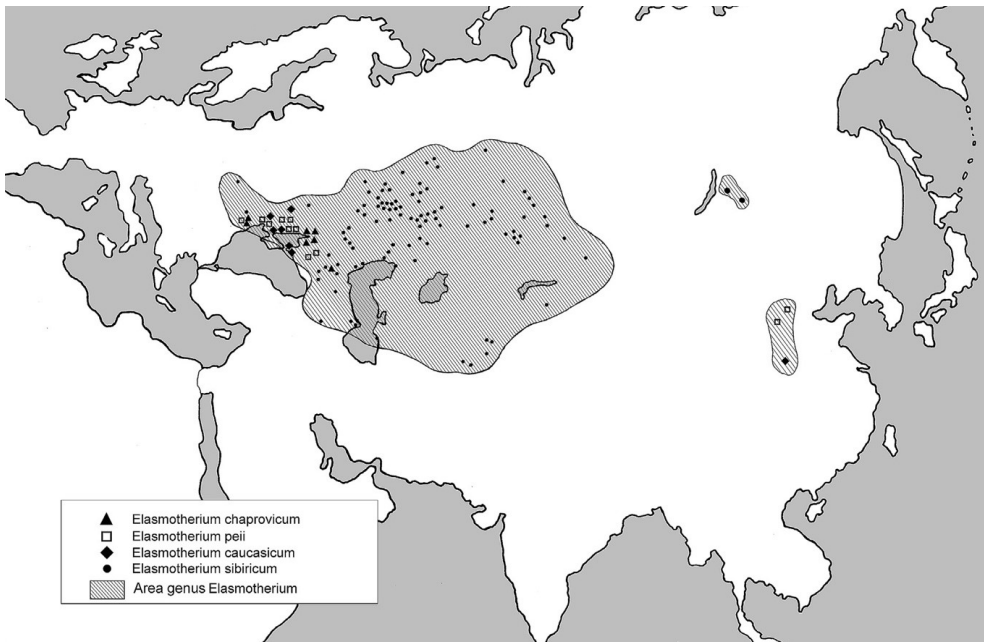
Figure 5.5 Geographical distribution of *E. sibiricum* and related species (Schvyreva, 2016).

5.3 Results and discussion

Of the 25 samples, 23 samples yielded enough collagen for ^{14}C dating and stable isotope analysis. The atomic C:N ratio of these samples (3.0-3.2) were within the acceptable range, with the exception of sample IPAE 420-111, which was just outside the range and was excluded from further analyses. The *Elasmotherium* δ^{13}C values (n = 22) range from −21.5 to −16.3‰ with a mean of −18.1 ± 0.3‰. The δ^{15}N values (n = 21) range from +6.5 to +12.8‰ with a mean of +9.4 ± 0.3‰ (Table 5.2). The differences in the stable isotope values might partly be due to geographic or temporal variation, although no trend through time or correlation with latitude was observed in the data (Fig. 5.6).

High δ^{13}C and δ^{15}N values, as seen in *E. sibiricum*, are observed in mammals inhabiting dry steppes or deserts (Bocherens, 2003). The *Elasmotherium* δ^{13}C and δ^{15}N values clearly differ from those of other fossil Rhinocerotidae from Eurasia (Fig. 5.7). Most of the samples had higher δ^{13}C and δ^{15}N values compared with the woolly rhinoceros (*Coelodonta antiquitatis*) from within the temporal and geographical range of the *Elasmotherium* material. Moreover, the majority of *E. sibiricum* samples were relatively higher in both δ^{13}C and δ^{15}N than narrow-nosed and/or Merck's rhinoceroses (*Stephanorhinus hemitoechus* and *S. kirchbergensis*, respectively) from the Middle Pleistocene sites of Schöningen, Germany. Among other rhinoceros species, morphological and

Table 5.2 Isotope measurement results for collagen (rejected collagen crossed out) from investigated samples of *E. sibiricum*.

museum & nr	laboratory nr	¹⁴C age (yr BP)	σ	%C	%N	C:N	δ¹³C (‰)	δ¹⁵N (‰)
C/M 12836	OxA-X-2750-15	51,100	>	48.4	17.6	3.2	-17.4	10.1
	OxA-X-2750-14	49,000	>					
~~IPAE 420/111~~	~~GrA-32606~~	~~45,000~~	~~>~~	~~35.9~~	~~15.2~~	~~2.8~~	~~-15.8~~	~~11.0~~
NHM M7099	OxA-X-2762-57	45,700	>	45.0	16.5	3.2	-17.3	11.6
ZIN 36330	OxA-X-2750-38	50,300	2,700	32.4	11.9	3.2	-16.6	10.4
IPAE 915/2804	OxA-34900	49,200	>	42.2	16.0	3.2	-18.8	12.8
IPAE 2388/2	GrA-55451	43,900	575	45.0	16.2	3.2	-16.4	9.6
ZIN 31791	GrA-62202	42,230	370	41.8	15.6	3.1	-17.2	9.6
IPAE 2388/1	GrA-55450	41,220	445	47.8	17.2	3.2	-17.8	6.5
IPAE 17-5703/7	GrA-61035	40,860	455	42.9	15.5	3.2	-17.3	8.8
IPAE 5-147	GrA-61030	40,470	445	42.0	15.1	3.2	-17.7	10.2
IPAE 12-001	GrA-61033	40,200	445	41.3	15.0	3.2	-18.7	10.0
IPAE 10-5566	GrA-61031	40,180	445	42.2	15.4	3.2	-21.5	8.4
IPAE 897/200	GrA-53425	39,480	355	43.4	17.1	3.0	-18.8	9.4
ZIN 36331	GrA-62203	38,440	295	45.2	16.7	3.2	-16.9	10.3
ZIN (26021) 3963	GrA-62200	38,230	285	42.3	15.6	3.2	-18.2	10.1
ZIN 3986	GrA-62197	37,850	285	43.3	15.9	3.2	-17.8	7.2
ZIN 10794	OxA-X-2750-13	36,850	650	44.3	16.4	3.2	-18.3	9.5
IPAE 2388/3	GrA-55452	36,290	275	45.4	17.5	3.0	-18.2	10.4
IPAE 2388/5	OxA-X-2756-57	34,400	1,000	44.4	16.9	3.1	-19.2	7.2
IPAE 1871/200	OxA X-2677-55	34,250	700	45.4	16.6	3.2	-18.7	8.6
IPAE 897/172	OxA-X-2756-56	33,300	1,100	43.5	16.3	3.1	-18.6	9.6
IPAE 897/123	OxA X-2677-54	33,650	650	35.2			-20.9	
NHM M12429	OxA X-2677-52	33,250	500	46.4	17.0	3.2	-16.3	7.8
IPAE 2388/4	no collagen							
IPAE 9-133	no collagen							

tooth-wear data show that *S. kirchbergensis* and *S. hemitoechus* were browse- and graze-dominated mixed feeders, respectively, while *C. antiquitatis* was predominantly a grazer (Boeskorov *et al.*, 2011; Pushkina *et al.*, 2014; Rivals and Lister, 2016; Saarinen *et al.*, 2016; see also Chapter 6).

In contrast to other rhinoceroses, *E. sibiricum* δ¹³C and δ¹⁵N values overlap strongly with those of samples of saiga antelope (*Saiga tatarica*) from the same spatiotemporal range (Fig. 5.7). Both fossil and modern saiga antelopes are well adapted to inhabit
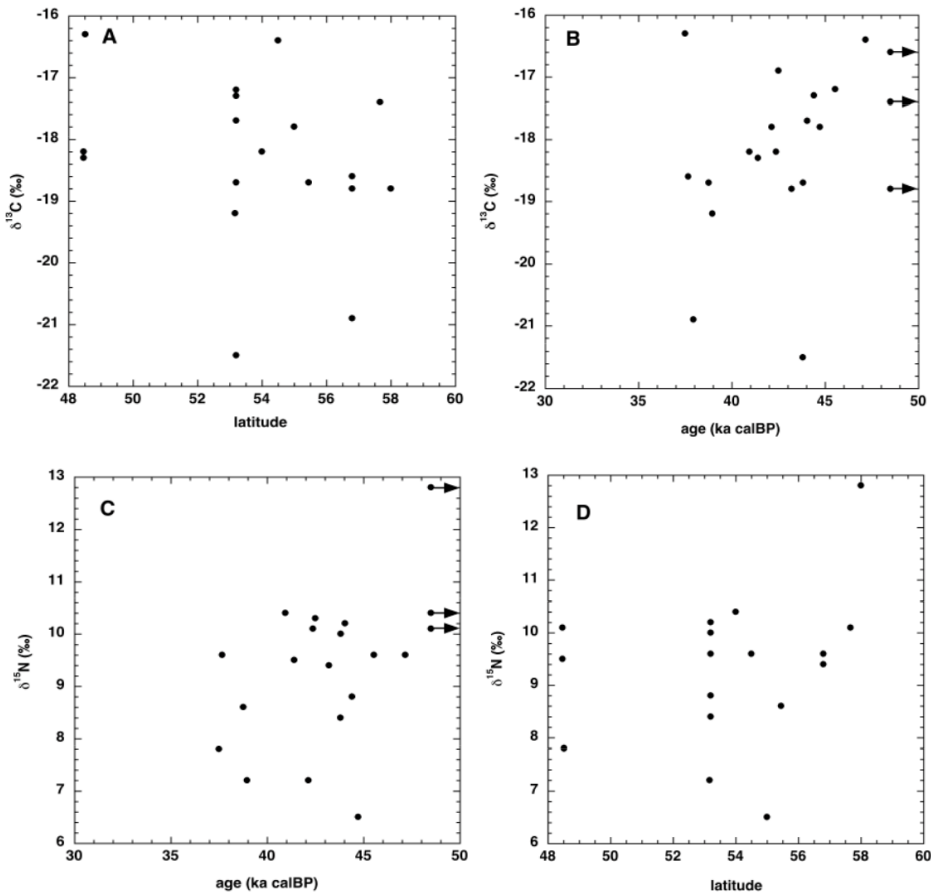
Figure 5.6 Stable isotope values of *E. sibiricum* versus latitude and ^{14}C age: (A) δ^{13}C versus latitude of samples; (B) δ^{13}C versus ^{14}C date of samples; (C) δ^{15}N versus ^{14}C date of samples; (D) δ^{15}N versus latitude of samples.

dry steppe. The δ^{13}C values of modern *S. tatarica* may have been influenced by the consumption of Chenopodiaceae (C4 photosynthesizers), but the mammoth steppe flora is considered to have consisted of C3 plants only (Jürgensen *et al.*, 2017).

Another aspect that may have affected the high δ^{13}C values of *E. sibiricum* is consumption of underground plant parts, since these tend to contain higher δ^{13}C values than photosynthetic plant parts (Badeck *et al.*, 2005), and/or the pulling up and consumption of roots (as suggested for *E. sibiricum*; Schvyreva, 2015). It would also explain why the molars of *E. sibiricum* are extremely high-crowned and without roots, giving them unlimited growth: when eating tubers, a lot of sand comes along, which means that the animal's teeth are likely to wear down at a high rate.

The extinction of *Elasmotherium* may have been linked to its high degree of
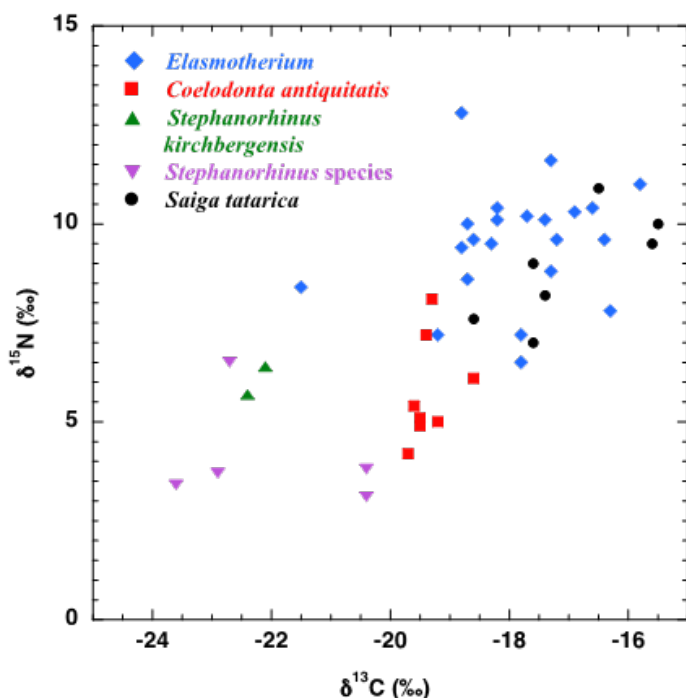
Figure 5.7 δ^{13}C and δ^{15}N values of various species. *E. sibiricum* samples are compared with those of the Late Pleistocene woolly rhinoceros (*C. antiquitatis*; Stuart and Lister, 2012), Middle Pleistocene Merck's rhinoceros (*S. kirchbergensis*; Kuitems *et al.*, 2015a), indeterminate Middle Pleistocene *Stephanorhinus* specimens (*S. kirchbergensis* or narrow-nosed rhinoceros (*S. hemitoechus*; Kuitems *et al.*, 2015a) and Late Pleistocene saiga antelope (*Saiga tatarica*; Jürgensen *et al.*, 2017). *Coelodonta* and *Saiga* data are restricted to the spatiotemporal extent of the *E. sibiricum* samples.

specialization, including extreme dietary adaptations (Schvyreva, 2015). Previous stable isotope studies on mammalian herbivore species from Europe have illustrated change in ecological niches during the pre-LGM (Drucker *et al.*, 2015) and the late glacial (Drucker *et al.*, 2014). Both *Coelodonta antiquitatis* and *Saiga tatarica* survived the MIS 3 extinction of *E. sibiricum*: *C. antiquitatis* with an isotopic signature implying a dietary niche consistently different from that of *E. sibiricum*, *S. tatarica* with a shift in its range of isotopic values. While *Saiga* samples from pre-LGM central Asia show δ^{13}C and δ^{15}N values overlapping strongly with contemporary *Elasmotherium* (Fig. 5.7), samples from later periods (LGM to GI-1), and those from other regions, include lower δ^{15}N values (down to +2.8‰), indicating dietary flexibility (Jürgensen *et al.*, 2017). The implication is that both *Coelodonta* and *Saiga* could cope with the environmental change that began around 38ka, but *E. sibiricum* could not. In addition to this, the persistently restricted geographical range of *Elasmotherium* (also probably linked to its specialized habitat), as well as the assumed low population size and slow reproductive rate associated with its large body size (Johnson, 2009) would have predisposed it to extinction in the face of environmental change, while the ecologically similar, but much smaller species (*S. tatarica*) survived. The extinction of *E. sibiricum* could in theory have been exacerbated by human hunting pressure. However, there is currently no record of the hunted/butchered species' remains from any archaeological site.

Schöningen, photo: T. van Kolfschoten

CHAPTER 6

CARBON AND NITROGEN STABLE ISOTOPES OF WELL-PRESERVED MIDDLE PLEISTOCENE BONE COLLAGEN FROM SCHÖNINGEN (GERMANY) AND THEIR PALAEOECOLOGICAL IMPLICATIONS

6.1 Introduction

Most of the Middle Pleistocene fossils from Schöningen are macroscopically very well preserved, while the preservation at the microscopic level needed further investigation. To determine if the bone collagen was well preserved enough to retrieve reliable $\delta^{13}C$ and $\delta^{15}N$ data to decipher the environmental conditions hominins experienced at Schöningen, a pilot study was executed in 2009 at Leiden University. Based on the very promising results (van der Plicht *et al.*, 2011), further isotopic research on material from the site of Schöningen was conducted in a joint project with the University of Tübingen and published (Kuitems *et al.*, 2015a).

6.1.1 The Schöningen sites and the stratigraphic position of the different assemblages

The Quaternary deposits exposed in the lignite quarry east of the village of Schöningen (Fig. 6.1) during the past two decades, have yielded a large amount of Palaeolithic material, such as artefacts made out of flint and wood, stone and bone tools, and a large number of vertebrate skeletal remains. The exposed Quaternary deposits cover the late Middle Pleistocene up to the Holocene (Mania, 1995; Lang *et al.*, 2012). The Elsterian till forms the base of the Quaternary sedimentary sequence (Fig. 6.1C). On top of the Elsterian till lies a series of so-called channels (Mania, 1995; Thieme, 1999) (Fig. 6.1B). Channels I-III date from the period between the Elsterian and the Saalian (Drenthe) glaciations. The majority of the fossil material studied for this paper is from deposits of the second channel. Channel II contains five depositional levels of organic muds and peats with loess deposits on top, dating from the second half of the Reinsdorf Interglacial and the ensuing Fuhne cold stage. The Reinsdorf Interglacial is generally correlated with MIS 9 with an age of around 300,000 years (Lang *et al.*, 2012; van Kolfschoten, 2012, 2014). For more detailed information about the Reinsdorf sedimentary sequence the reader is referred to Urban *et al.* (2011) and Lang *et al.* (2012). Within Channel II, there are two spatially separated concentrations of sites: Schö 12 and Schö 13, each with a number of sites/depositional levels. The notation of the different sites and depositional levels (for example, Schö 13 II-4) refers to a specific geographical position in the investigated area (Schö 13), to a particular channel (II), and to a specific depositional level within the sedimentary sequence (4; see for example Serangeli *et al.*, 2012b). Most of the larger mammal material was collected from the Schö 13 II site, in particular Schö 13 II-4: more than 12,000 large mammal remains are recorded from the Schö 13 II-4 site representing a variety of species. The famous wooden spears are also from the Schö 13 II-4 site.

The botanical (Urban, 2007a,b) and malacological (Mania, 2007) record from the successive depositional levels in Channel II levels 1-5 indicate an environmental and/or climatic shift from an interglacial climatic optimum at the base of the sequence (level 1) with vegetation that is characterized by the occurrence of warm deciduous forest to the beginning of the following cold stage at the top of the sequence with a dominance of boreal forest and steppe vegetation (Urban, 2007a). However, the changes in the
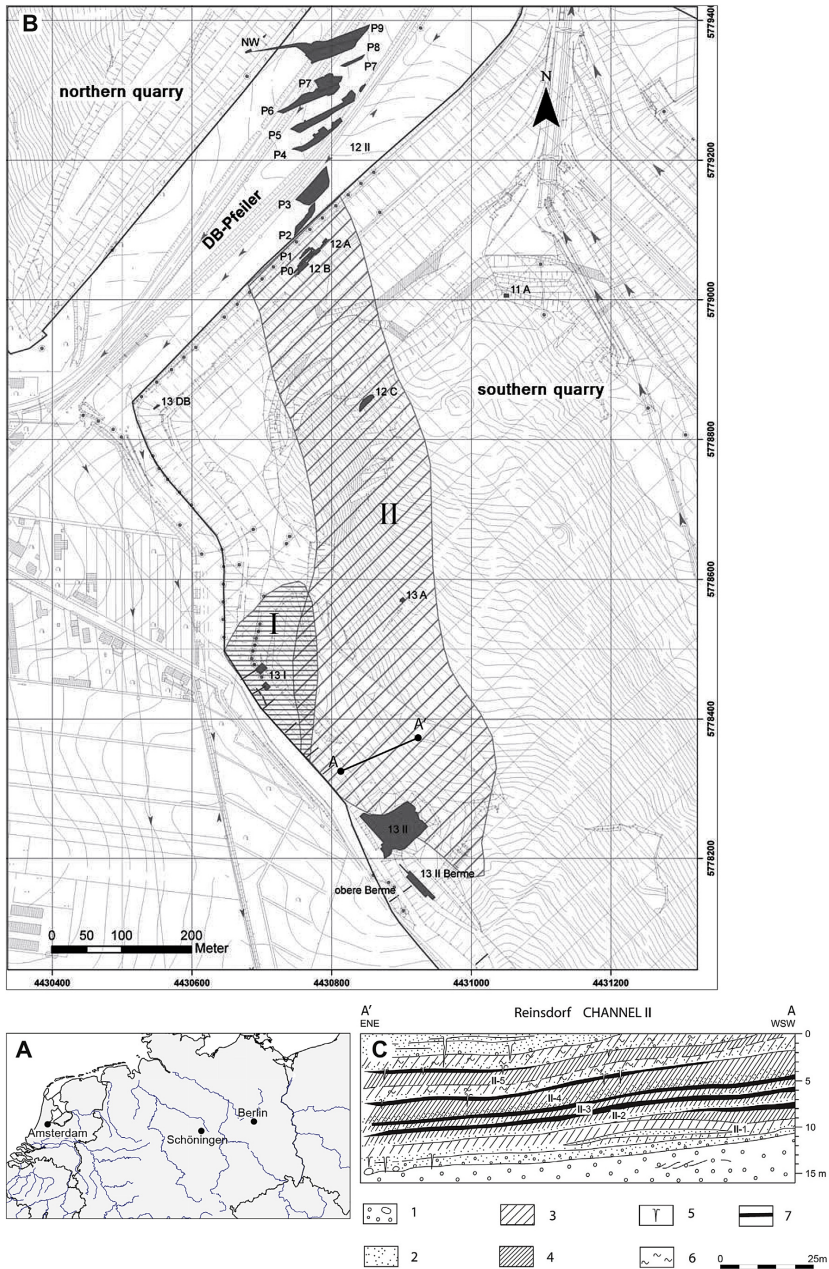
Figure 6.1 Origin of the samples discussed in this chapter. A: Geographical position of the locality Schöningen. B: Horizontal distribution of the sites mentioned in the text (after Serangeli *et al.*, 2012b: 14). C: General lithology of the Reinsdorf stratigraphic sequence, discordantly overlying Elsterian glacial sediments. Key: 1) Elsterian till, gravel and fluvioglacial sediments, 2) sand, 3) basin silt, 4) silty and calcareous mud, 5) ice wedges, 6) solifluction layers, 7) fen peat (Urban *et al.*, 2011: 130).

mammalian record are not as obvious as one would expect (van Kolfschoten, 2014). The Channel II sequence did not yield mammal assemblages that clearly indicate climatic deterioration and the occurrence of glacial conditions. Several assumed forest dwellers (for example *S. kirchbergensis*, *Sus scrofa*) that occur in Channel II level 1 are also represented in the faunal assemblage of Channel II level 4 (van Kolfschoten *et al.*, 2007; van Kolfschoten, 2014). The faunal assemblages from level 1 indicate interglacial conditions and a forested environment alternating with areas of more open, steppe vegetation, while the mammalian fauna from Schö 13 II-4 also suggests the occurrence of forested areas in a steppe landscape.

The environmental context of hominin activities at Schöningen is still a matter of debate, in particular the proportion of forest versus open landscape during the deposition of different levels in Schöningen. Therefore, the aim of this study was to investigate the ecological preference of the different herbivores represented in the Schöningen assemblages using stable isotope data. This isotopic study was preceded by a thorough examination of the preservation of the collagen from such an old context.

6.2 Materials and methods

6.2.1 Material

For this study skeletal material of 69 specimens including bones and antlers has been selected. The specimens are from Schöningen 12 and 13 and belonged to different taxa of large herbivorous mammals: Elephantidae, Rhinocerotidae, Equidae, Cervidae, and Bovidae (Table 6.1).

The Elephantidae were represented by eight samples of the straight-tusked elephant (*Palaeoloxodon antiquus*). Samples of Rhinocerotidae (n = 18) included Merck's rhinoceros (*Stephanorhinus kirchbergensis*), narrow-nosed rhinoceros (*S. hemitoechus*), and *Stephanorhinus* sp. Skeletal material of 20 horses (*Equus mosbachensis*) was sampled; 10

Table 6.1 Overview of the number of samples per taxonomic group and per site and layer/level.

	Level 1		Level 2		Level 3		Level 4		
	Schö 13 II-1	Schö 12B	Schö 12 II-1	Schö 13 II-2	Schö 12A	Schö 13 II-3	Schö 13 II-4	Schö 13 II A	
Elephantidae	4	1					1		6
Rhinocerotidae	1	4				1	1		7
Equidae	1	1			1	1	10	1	15
Cervidae	1	2	1	1		4	3		12
Bovidae				1		3	3		7
	7	8	1	2	1	9	18	1	47

bone samples originated from Schö 13 II-4. Among the 16 Cervidae samples, red deer (*Cervus elaphus*/cf. *C. elaphus*) is most frequent. Furthermore, four samples of giant deer (*Megaloceros giganteus*) were taken. The seven Bovidae samples were represented by bison (*Bison priscus*) and a number of samples that could not be determined as either aurochs or bison (hereafter designated as *Bos/Bison*).

6.2.2 Methods

Collagen extraction and isotopic analysis was undertaken, and the stable isotope concentrations were measured by IRMS at the CIO in Groningen following the procedure as described in Chapter 2 and at the Department of Geosciences of Tübingen University following the method published by Bocherens *et al.* (1997a).

All 'collagen' samples with atomic C:N ratios outside the widely accepted range of 2.9-3.6 were excluded from further analyses. Besides examining the C% and N% and the atomic C:N ratio with the aim of assessing the quality of the collagen, five representative samples were ^{14}C dated by AMS in order to confirm the antiquity of the collagen samples and, in particular, determine if the samples have been contaminated by geologically young material. The ^{14}C activities are reported in conventional activities ($^{14}a_N$), that is, they are measured relative to oxalic acid standard and corrected (normalised) for isotopic fractionation using the stable isotope ratio $^{13}C/^{12}C$ to $\delta^{13}C =$ -25‰, using a half-life value of 5568 years (Mook and van der Plicht, 1999). From the normalised activities, the conventional ^{14}C ages (in BP) are calculated. In the following, the normalised activities will be indicated by ^{14}a.

6.3 Results and discussion

6.3.1 Collagen preservation

A number of preliminary chemical composition determinations following the approach of Bocherens *et al.* (2005), measuring the percentage of nitrogen in whole bones, were performed and yielded values up to 2-3%, close to the 4% nitrogen found in fresh bones. Collagen was successfully extracted for 72% of the samples, a very high percentage given the geological age of the fossils. However, not all of these samples meet the collagen quality criteria and to determine which samples have good collagen and thus can be considered to produce reliable stable isotope ratios for ecological interpretation, the %C, %N, and C:N ratios were examined.

Figure 6.2 presents the carbon and nitrogen content of the extracted bone collagen and shows that 47 samples have %C between 31.1 and 47.0, %N between 10.2 and 16.3, and an atomic C:N ratio between 3.1 and 3.6. These 47 samples are considered to have good quality collagen, with collagen yield varying between 0.5% and 7.8% (mean = 2.9%). The collagen of the other three samples does not meet the quality criteria, and the stable isotope ratios of these samples are therefore disregarded in the final

Figure 6.2 Carbon content relative to nitrogen content in the samples. The samples with both acceptable C:N ratios and %C and %N values are shown in black triangles (▼), while rejected samples are represented by open circles (o).
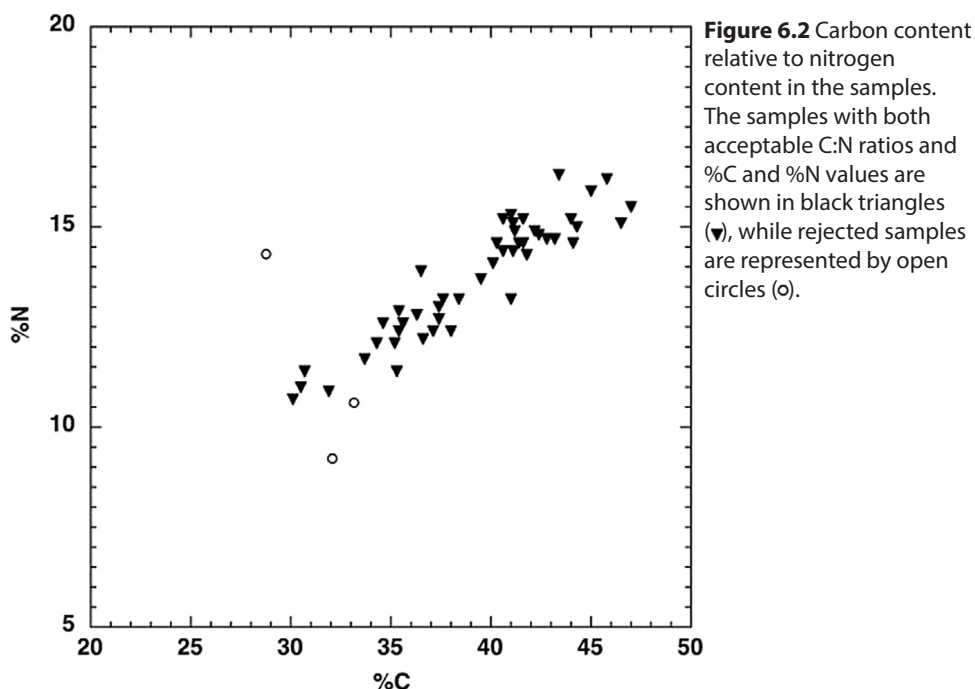
palaeobiological interpretation. The final result is that 68% of the Schöningen samples yielded reliable collagen.

The ^{14}C activities measured are shown in Table 6.2. The background for this batch showed an activity of ^{14}a = 0.20%, corresponding with a ^{14}C age of > 50,000 yr BP. Based on laboratory experience, the background for fossil bone is determined as 45,000 yr BP. There is one sample (GrA-49107) showing a finite age of 47,000 yr BP when using anthracite as a background; we report this age as > 45,000 yr BP. It appears impossible to have proper blanks (that is, infinite age and the same quality or degradation properties as the bone sample) for fossil bone of this age. All results are at the ^{14}C background level, which means they are reported as older than 45,000 yr BP (van der Plicht and Palstra, 2016). This convincingly shows that the Schöningen bones are not contaminated with younger carbon.

Table 6.2 Results of ^{14}C dating.

species	site layer	laboratory nr	^{14}a (%)	^{14}C age (yr BP)
Palaeoloxodon antiquus	Schö 12B	GrA-49111	0.20 ± 0.03	>45,000
Palaeoloxodon antiquus	Schö 13 II-4	GrA-49249	0.00 ± 0.02	>45,000
Stephanorhinus kirchbergensis	Schö 12B	GrA-49107	0.27 ± 0.03	>45,000
Equus mosbachensis	Schö 13A	GrA-49110	0.03 ± 0.03	>45,000
Cervus elaphus	Schö 13 II-3	GrA-49112	-0.02 ± 0.02	>45,000
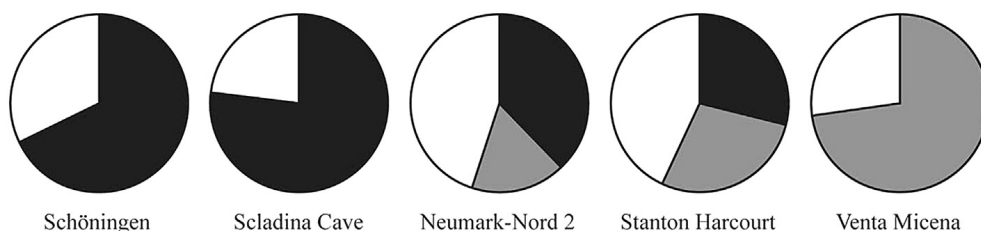
Figure 6.3 Proportions of extracted collagen in bones older than 50,000 yr in different archaeological sites. Reliable collagen samples (collagen with %C and %N values that are within the range of fresh collagen) are shown in black. Collagen samples classified as reliable in other studies but that are or may be outside the range of fresh collagen are shown in grey. Samples that did not yield collagen are shown in white.

The occurrence of good quality collagen in bones that are older than 50,000 years is remarkable but not unique. Stable isotope data have also been recorded from archaeological sites such as Scladina Cave in Belgium (ca. 120,000 years old, Eemian interglacial [MIS 5e], n = 36/47 [77%]: Bocherens *et al.*, 1999), Stanton Harcourt in southern Britain (ca. 200,000 years old [MIS 7], n = 4/7 [57%]: Jones *et al.*, 2001), Neumark-Nord 2 in Germany (ca. 120,000 years old, Eemian interglacial [MIS 5e], n = 23/42 [55%]: Britton *et al.*, 2012), and Venta Micena in southeastern Spain (ca. 1.500,000 years old, n = 77/105 [73%]: Palmqvist *et al.*, 2003, 2008).

The quality of the collagen of skeletal remains from Stanton Harcourt was estimated by analysing the amino acid profiles of the mammoth and elephant remains and by considering the atomic C:N ratio. However, two out of four samples that have been considered to yield qualitatively good collagen had low %C and %N values (*B. priscus*: %C = 23.2 and %N = 8.5; *P. antiquus*: %C = 23.9 and %N = 8.2). For Neumark-Nord, Britton and colleagues (2012) also included samples (n = 7) in their isotope analysis with collagen having low %C (12.6-27.0) and low %N (4.2-9.5), values that are outside of the range of values that are considered in the present study to correspond to good quality collagen. For Venta Micena, Palmqvist and colleagues (2003) performed amino acid analysis on a small number of samples (n = 4) and only considered samples with C:N ratios between 2.9 and 3.6 to constitute good quality collagen. However, the authors did not report the %C and %N for the samples. For the analyses of the Schöningen data we restrict ourselves to collagen with %C and %N values that are within the range of fresh collagen. Despite the fact that such restrictive conditions are applied, quite a high proportion (68%; Fig. 6.3) of the Schöningen fossils fulfil those criteria.

The data indicate that a large part of the Schöningen vertebrate remains is well preserved, not only at a macroscopic level but also at a molecular level. An explanation for the excellent conservation could be the high groundwater level (Lang *et al.*, 2012; Serangeli *et al.*, 2012a). Until very recently the groundwater table at many Schöningen sites was above the find horizons, and the fossil remains were located in waterlogged sediments. This buffered depositional setting offered favourable conditions for the preservation of faunal and botanical remains (Hedges and Millard, 1995; Bocherens

et al., 1997b; Prummel and Niekus, 2011; Lang *et al.*, 2012; Serangeli *et al.*, 2012a). Furthermore, the ground water that partly originates from springs in the Elm ridge is rich in calcium carbonate (Huckriede, 1967; Lang *et al.*, 2015), which also has a positive effect on the preservation of organic material.

6.3.2 Stable isotopic values

The results of the stable isotope measurements are shown in Table 6.3. The data set of good quality collagen samples consists of 47 fossil bones (the black down pointing triangle data points in Fig. 6.2), representing different mammal species and different sites and/or stratigraphical levels. More than a third of these samples are derived from the famous spear horizon (Schö 13 II-4, n = 18). In Table 6.3 the samples that have not been accepted (the open circles in Fig. 6.2) are eliminated.

The $\delta^{15}N$ values from all collagen samples ranged from +2.5‰ to +8.7‰, with an average of +4.8‰ and a standard deviation of 1.6. The $\delta^{13}C$ values from all collagen samples ranged from -23.6‰ to -19.8‰, with an average of -21.4‰ and a standard deviation of 0.9. Although the $\delta^{13}C$ and $\delta^{15}N$ ranges of several mammal species show some overlap, certain trends among species are visible. For example, the $\delta^{13}C$ values of Elephantidae (-22.9‰ to -21.4‰) are all lower than those of Bovidae (-21.2‰ to -19.8‰), whereas the $\delta^{15}N$ values of Elephantidae (+6.6‰ to +8.7‰) exceed the $\delta^{15}N$ values of all other analysed herbivores, except for some Bovidae (+3.6‰ to +7.1‰). The significance of the differences observed in $\delta^{13}C$ and $\delta^{15}N$ values between the families was determined with the Mann-Whitney U test, where H0 = not significantly different and H1 = significantly different (Shennan, 1997). As shown in Table 6.4, the $\delta^{13}C$ values were significantly different for Elephantidae compared to Bovidae, Elephantidae compared to Cervidae, Equidae compared to Cervidae, and Equidae compared to Bovidae. Between all families, the $\delta^{15}N$ values were significantly different, except for these of Rhinocerotidae compared to Equidae, and Rhinocerotidae compared to Bovidae.

The data show interesting patterns in respect to the environmental conditions (forest versus open landscape) experienced by hominins at Schöningen. In Fig. 6.4, the $\delta^{15}N$ and $\delta^{13}C$ values, respectively, are shown for the different taxonomic families during depositional level 1 (indicated with black circles; samples derived from Schö 12B, Schö 12 II-1, and Schö 13 II-1) and depositional level 4 (indicated with open circles; samples derived from Schö 13 II A and Schö 13 II-4). Based on, for example, botanical and malacological data, depositional level 1 is assumed to represent the Reinsdorf Interglacial climatic optimum during which the environment was quite closed with forest dominated by oak, ash, and linden, whereas depositional level 4 is characterized by a boreal continental climate and an open steppe-like landscape with some pine, spruce, larch, and birch (Urban, 2007b). As Fig. 6.4 shows, no divergent pattern in $\delta^{15}N$ values exists between the two depositional levels. The $\delta^{15}N$ values of rhinoceroses, horses, and cervids seem to alternate with each other in the different periods. The highest $\delta^{15}N$

Table 6.3 Stable isotope ratios δ¹³C and δ¹⁵N for fossil bones from Schöningen with accepted collagen and rejected collagen (crossed out).

species	layer	material	%C	%N	C:N	δ¹³C (‰)	δ¹⁵N (‰)
Elephantidae							
Palaeoloxodon antiquus	Schö 12 B	bone	40.6	14.4	3.3	-22.0	7.3
Palaeoloxodon antiquus	Schö 13 II-1	bone	36.6	12.2	3.5	-22.4	7.8
Palaeoloxodon antiquus	Schö 13 II-1	bone	30.1	10.7	3.3	-22.9	6.6
Palaeoloxodon antiquus	Schö 13 II-1	bone	35.3	11.4	3.6	-22.5	7.0
Palaeoloxodon antiquus	Schö 13 II-1	bone	37.5	13.2	3.3	-21.8	7.2
Palaeoloxodon antiquus	Schö 13 II-4	bone	41.6	15.2	3.2	-21.4	8.7
					mean	-22.2	7.4
					st dev	0.5	0.7
Rhinocerotidae							
Stephanorhinus kirchbergensis	Schö 12 B	molar root	43.2	14.7	3.4	-22.1	6.4
Stephanorhinus kirchbergensis	Schö 12 B	molar root	40.6	15.2	3.1	-22.4	5.7
cf. *Stephanorhinus kirchbergensis*	Schö 12 B	bone	36.3	12.8	3.3	-22.7	6.5
cf. *Stephanorhinus kirchbergensis*	Schö 12 B	bone	40.3	14.6	3.2	-22.9	3.7
Stephanorhinus species	Schö 13 II-1	bone	35.6	12.6	3.3	-23.6	3.4
Stephanorhinus species	Schö 13 II-3	bone	42.4	14.8	3.3	-20.4	3.1
Stephanorhinus species	Schö 13 II-4	bone	44.0	15.2	3.4	-20.4	3.8
~~*Stephanorhinus species*~~	~~Schö 13 II-3~~	~~bone~~	~~32.1~~	~~9.2~~	~~4.1~~	~~-21.2~~	~~4.3~~
~~*Stephanorhinus species*~~	~~Schö 13 II-3~~	~~bone~~	~~33.2~~	~~10.6~~	~~3.7~~	~~-22.2~~	~~2.8~~
					mean	-22.1	4.7
					st dev	1.2	1.5
Equidae							
Equus mosbachensis	Schö 12 A	bone	38.4	13.2	3.4	-22.7	3.6
Equus mosbachensis	Schö 12 B	bone	34.3	12.1	3.3	-23.2	4.6
Equus mosbachensis	Schö 13 A	bone	37.1	12.4	3.5	-21.9	3.2
Equus mosbachensis	Schö 13 II-1	bone	35.4	12.4	3.3	-20.9	2.5
Equus mosbachensis	Schö 13 II-3	bone	33.7	11.7	3.4	-21.5	3.6
Equus mosbachensis	Schö 13 II-4	bone	46.5	15.1	3.6	-21.2	3.1
Equus mosbachensis	Schö 13 II-4	bone	44.3	15.0	3.4	-21.4	3.1
Equus mosbachensis	Schö 13 II-4	bone	44.1	14.6	3.5	-21.4	3.0
Equus mosbachensis	Schö 13 II-4	bone	34.6	12.6	3.2	-21.6	4.2
Equus mosbachensis	Schö 13 II-4	bone	47.0	15.5	3.5	-21.9	2.7

Equus mosbachensis	Schö 13 II-4	bone	41.1	15.1	3.2	-21.1	2.8
Equus mosbachensis	Schö 13 II-4	bone	45.8	16.2	3.3	-22.1	2.8
Equus mosbachensis	Schö 13 II-4	bone	41.0	13.2	3.6	-20.0	4.5
Equus mosbachensis	Schö 13 II-4	bone	37.4	13.0	3.4	-21.8	3.2
Equus mosbachensis	Schö 13 II-4	bone	39.5	13.7	3.4	-21.4	2.9
~~*Equus mosbachensis*~~	~~Schö 13 B~~	~~bone~~	~~28.8~~	~~14.3~~	~~2.3~~	~~-25.7~~	~~3.7~~
					mean	-21.6	3.3
					st dev	0.8	0.7
Cervidae							
Cervus elaphus	Schö 12 B	antler	30.5	11.0	3.2	-23.0	4.8
Cervus elaphus	Schö 12 B	bone	36.5	13.9	3.1	-20.7	3.9
Megaloceros giganteus	Schö 12 II-1	bone	42.2	14.9	3.3	-21.5	5.4
Cervus elaphus	Schö 13 II-1	antler	30.7	11.4	3.2	-20.5	3.5
Cervus elaphus	Schö 13 II-2	bone	38.0	12.4	3.6	-20.9	4.9
Cervus elaphus	Schö 13 II-3	antler	41.8	14.3	3.4	-20.1	5.2
Cervus elaphus	Schö 13 II-3	antler	42.8	14.7	3.4	-20.6	4.8
Cervus elaphus	Schö 13 II-3	antler	41.6	14.6	3.3	-20.5	4.9
Megaloceros giganteus	Schö 13 II-3	bone	37.4	12.7	3.4	-20.5	5.1
cf. *Cervus elaphus*	Schö 13 II-4	antler	35.4	12.9	3.2	-21.2	4.3
cf. *Cervus elaphus*	Schö 13 II-4	antler	35.2	12.1	3.4	-21.8	3.7
Megaloceros giganteus	Schö 13 II-4	molar root	31.9	10.9	3.4	-20.6	5.5
					mean	-21.0	4.7
					st dev	0.8	0.7
Bovidae							
Bos/Bison	Schö 13 II-2	bone	45.0	15.9	3.3	-20.6	3.6
Bison species	Schö 13 II-3	bone	40.1	14.1	3.3	-20.4	6.5
Bos/Bison	Schö 13 II-3	bone	41.1	14.4	3.3	-19.8	6.6
Bos/Bison	Schö 13 II-3	bone	41.4	14.6	3.3	-20.2	6.4
Bos/Bison	Schö 13 II-4	bone	41.0	15.3	3.1	-21.1	5.5
Bos/Bison	Schö 13 II-4	bone	41.2	14.9	3.2	-20.9	5.2
Bison species	Schö 13 II-4	bone	43.4	16.3	3.1	-21.2	7.1
					mean	-20.6	5.8
					st dev	0.5	1.2

value (+8.7‰) was measured from the sample of a young straight-tusked elephant from level 4 and might reflect the effect of suckling of a not yet weaned individual, as has been observed in woolly mammoths (Metcalfe *et al.*, 2010; Bocherens *et al.*, 2013). The three bovids in Fig. 6.4 are all derived from level 4, and no samples were taken from Bovidae living during the Reinsdorf Interglacial optimum. The Rhinocerotidae and Elephantidae have low $\delta^{13}C$ values (-23.6‰ to -22.1‰ and -22.9‰ to -21.8‰, respectively) during the Reinsdorf Interglacial optimum and higher values in level 4 (-20.4‰ and -21.4‰, respectively; Fig. 6.4). Since only one measurement is available for each of these species from level Schö 13 II-4, a conclusion that we are dealing with a significant difference in $\delta^{13}C$ values between the two periods is not justified. The $\delta^{13}C$ values of the horses and cervids from level 1 overlap with those from level 4.

Since the $\delta^{15}N$ and $\delta^{13}C$ values in bone collagen are related to the food consumed by the animal, the variation in plant $\delta^{15}N$ and $\delta^{13}C$ values is reflected in the tissues of the herbivore eating the plants. For example, fungi and grasses/sedges have relatively higher $\delta^{15}N$ values than lichens, mosses, and shrubs/trees (see summary in Bocherens [2003] and Drucker *et al.* [2010]), and understory vegetation in dense forest usually has more negative $\delta^{13}C$ values (that is, the so-called 'canopy effect') than plants growing in open environments (for example, Drucker *et al.*, 2008). The fact that the $\delta^{15}N$ values do not seem to diverge between depositional level 1 and 4 points to a quite similar dietary plant preference for these mammal species during both periods. The $\delta^{13}C$ values indicate relative stability in the diet despite climatic change but also point to an environmental change. As shown in Fig. 6.4, seven samples have $\delta^{13}C$ values of -22.5‰ and lower, which might suggest that they reflect the canopy effect. This canopy effect is only seen in samples from level 1, the Reinsdorf Interglacial optimum. The $\delta^{13}C$ values thus indicate that the landscape was more densely forested during depositional level 1 and more open during level 4. However, the majority of samples from level 1 have $\delta^{13}C$ values between

Table 6.3 Results of Mann-Whitney U test for $\delta^{13}C$ and $\delta^{15}N$ values between the largest taxonomical families.

Families	$\delta^{13}C$	$\delta^{15}N$
Elephantidae-Rhinocerotidae	H0	H1
Elephantidae-Equidae	H0	H1
Elephantidae-Cervidae	H1	H1
Elephantidae-Bovidae	H1	H1
Rhinocerotidae-Equidae	H0	H1
Rhinocerotidae-Cervidae	H0	H0
Rhinocerotidae-Bovidae	H0	H0
Equidae-Cervidae	H1	H1
Equidae-Bovidae	H1	H1
Cervidae-Bovidae	H0	H1
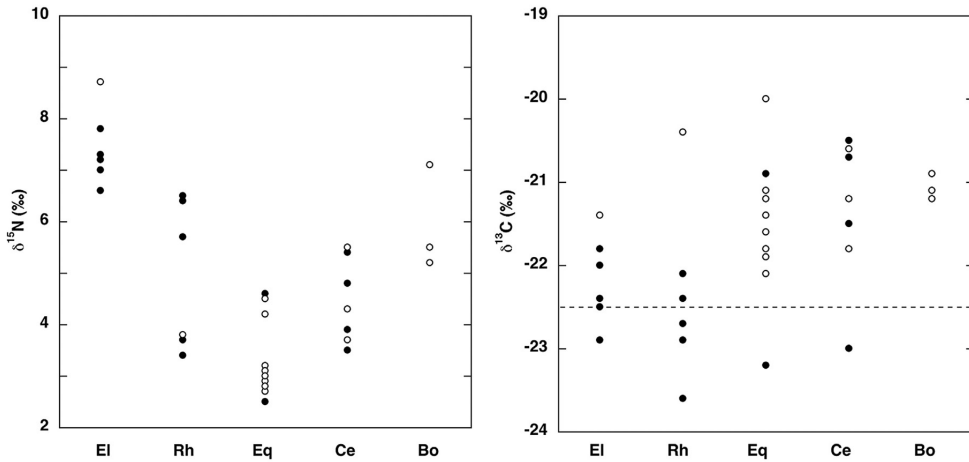
Figure 6.4 Left: δ^{15}N values for Elephantidae (El), Rhinocerotidae (Rh), Equidae (Eq), Cervidae (Ce), and Bovidae (Bo) for the Reinsdorf Interglacial optimum (closed circles) and the colder, fourth depositional phase (open circles). More grass in the diet leads to higher δ^{15}N values, while a browsing diet results in lower δ^{15}N values. Right: δ^{13}C values for Elephantidae (El), Rhinocerotidae (Rh), Equidae (Eq), Cervidae (Ce), and Bovidae (Bo) for the Reinsdorf Interglacial optimum (closed circles) and the colder, fourth depositional level (open circles). Below the dotted line (at -22.5‰), values are expected to reflect the canopy effect.

-22.4‰ and -20.5‰, indicating that these animals mainly fed in an environment that was not densely forested. Thus, the δ^{13}C values suggest that during level 1 at least part of the landscape was forested and alternated with a substantial part that was more open, whereas during level 4 the landscape was more open. However, although the δ^{13}C values of several species point to a relatively open landscape, these δ^{13}C values seem to be too low to reflect a steppe landscape similar to the mammoth steppe-tundra (Bocherens, 2003). This is supported by the zoological data, since remains of typical steppe dwellers such as ground squirrels and hamsters have so far not been recorded in the Schöningen mammalian record.

The isotope data suggest that the Schöningen landscape was inhabited by herbivorous species with different ecological niches, which is reflected, for example, in habitat choice (densely forested versus open landscape) and dietary preferences (browsing, grazing, and mixed feeding). The horses from Schöningen have the lowest δ^{15}N values of all species. The dental wear pattern observed in the horse molars diverges from that seen in horses from other periods and sites, with evidence that browsing formed a substantial part of the horse diet at Schöningen (see Rivals *et al.* [2015] for a microwear and mesowear analysis on the horse molars from Schö 13 II-4). The low δ^{15}N values also support a browsing diet for the Schöningen horses. This browsing role is remarkable, as horses are generally considered to be typical obligate grazers.

The δ^{15}N values of the straight-tusked elephants are remarkably higher than those

of the other species, except for one bovid. Several studies (for example Bocherens *et al.*, 1994; Iacumin *et al.*, 2000) demonstrated that the extinct woolly mammoth (*Mammuthus primigenius*) had remarkably high $\delta^{15}N$ values in comparison with other contemporary living herbivores. The results of this study suggest a similar pattern for the stable nitrogen values of straight-tusked elephants from Schöningen. The driving force behind the discrepancy of $\delta^{15}N$ values between woolly mammoth and contemporaneous herbivores is not well understood but may be induced by dietary selection, physiology, or coprophagy (for more detailed information see Bocherens, 2003; Kuitems *et al.*, 2015c). These factors might also explain the elevation of the straight-tusked elephant $\delta^{15}N$ values in this study. In contrast to the woolly mammoth, the straight-tusked elephant is generally assumed to be a browser preferring wooded environments (Stewart, 2004; Stuart, 2005). Usually, browsers tend to have lower $\delta^{15}N$ values than grazers (and lower $\delta^{13}C$ values; for example, Drucker *et al.*, 2010). However, recent investigations of microwear patterns on the teeth of Pleistocene proboscideans showed that *Palaeoloxodon antiquus* exhibits variable dietary preferences similar to those of *Mammuthus primigenius* (Rivals *et al.*, 2012). Therefore, it seems possible that the high $\delta^{15}N$ values of the Schöningen elephants might be linked to a high proportion of ^{15}N-enriched grass in their diet.

Merck's rhinoceros (*Stephanorhinus kirchbergensis*) is also believed to have been a browser supplementing its diet by grazing, dwelling in both forest and open landscape (Loose, 1975). In contrast, the narrow-nosed rhinoceros (*S. hemitoechus*) was a true grazer (Loose, 1975). Fossils of both species have been found in Schöningen. Unfortunately, it was not possible to identify all skeletal elements in the sample to the species level. The rhinoceroses from Schöningen have quite a large range in $\delta^{15}N$ values. Within this spread, it looks as if two groups exist: four lower values (+3.1‰ to +3.8‰) and three values that are more enriched (+5.7‰ to +6.5‰). Of course, the number of data is limited and there is the risk of over interpretation. However, since the samples with a $\delta^{15}N$ value of +3.4‰ and +6.4‰ both belong to Merck's rhinoceros, it is unlikely that the difference in values should (only) be explained by grazing versus browsing. The $\delta^{13}C$ values of the Schöningen rhinoceroses diverge in another way than the $\delta^{15}N$ values, having five lower values (-23.6‰ to -22.1‰) and two (*Stephanorhinus* sp.) higher values of both -20.4‰.

The cervids have quite low $\delta^{15}N$ values. One should take into account, however, that seven out of the nine red deer samples have been derived from antler instead of bone. Since antlers re-grow every year, the isotope values in antler reflect a shorter time period than the isotope values in bone material (which reflect the mean isotope signal of several years). Based on stomach content analysis, the red deer is known to be a mixed feeder (Gebert and Verheyden-Tixier, 2001) able to incorporate both browsing and grazing in its diet. This is supported by the isotope data of this study. While the $\delta^{13}C$ value of one red deer (Schö 12B) is low and seems to reflect the canopy effect (-23.0‰, measured in antler), the eleven other values of red deer (n = 8) and giant deer remains

(n = 3) from different sites/levels (including another red deer sample from Schö 12B: -20.7‰) are considerably higher (-21.8‰ to -20.1‰). Among the cervids, giant deer seem to have higher $\delta^{15}N$ values than most red deer. This could indicate that the diet of giant deer included grass in a higher proportion than that of red deer.

Six of the seven bovids (from Schö 13 II-3 and Schö 13 II-4) have both high $\delta^{15}N$ (+5.2‰ to +7.1‰) and $\delta^{13}C$ (-21.2‰ to -20.5‰) values compared with the other species. Both $\delta^{15}N$ and $\delta^{13}C$ values indicate a grazing diet in an open environment. One bovid (from Schö 13 II-2) has a $\delta^{15}N$ value of +3.6‰ and $\delta^{13}C$ value of -20.6‰ and may have supplemented its diet by browsing.

The results of the stable isotope investigations are an important contribution to the debate on the interpretation of the large concentration of fossil horse remains in Schö 13 II-4. It was hypothesized that the Schö 13 II-4 horse assemblage may be the result of a single event during which Palaeolithic hominins killed a group of horses. However, the large variation in the isotope values of the horse bones does not support this hypothesis. The ten horse samples from Schö 13 II-4, the famous spear horizon, have $\delta^{13}C$ values ranging from -22.1‰ to -20.0‰ and $\delta^{15}N$ values ranging from +2.7‰ to +4.5‰. These ranges of isotopic values seem too large for a homogenous population (Lovell *et al.*, 1986), indicating that more than one horse population is represented in the Schö 13 II-4 assemblage. This conclusion supports the suggestion that we are dealing with multiple events and that, in turn, suggests a scenario in which there is a large concentration of horse remains in a landscape with scattered vertebrate remains from a variety of large mammal species including horses (van Kolfschoten *et al.*, 2015a).

6.4 Conclusions

This chapter presents the study of remarkably well-preserved bone collagen of skeletal remains from Schöningen, Germany with an age of 300,000-400,000 years. Our investigation indicates that a large part of the vertebrate remains exhibit excellent preservation, not only at a macroscopic level but also at a molecular level. Stable isotope ratios ($\delta^{13}C$ and $\delta^{15}N$) of material derived from five taxonomic groups (Elephantidae, Rhinocerotidae, Equidae, Cervidae, and Bovidae) have been measured. The isotopic data indicate that during the Reinsdorf Interglacial the hominins at Schöningen lived in a mosaic-like landscape: during the Reinsdorf Interglacial climatic optimum the landscape seems to have been forested, alternating with open areas, whereas during depositional level 4 the isotopic data give the impression that the landscape was more open, although not steppe-like. These mosaic landscapes were inhabited by herbivorous species with different ecological niches, which is reflected in habitat choice (forest versus open landscape) and diet (browsing, grazing, and mixed feeding). The stable isotope values of the horses from the spear horizon Schö 13 II-4 seem too variable to represent one homogenous population and suggest multiple accumulation events.
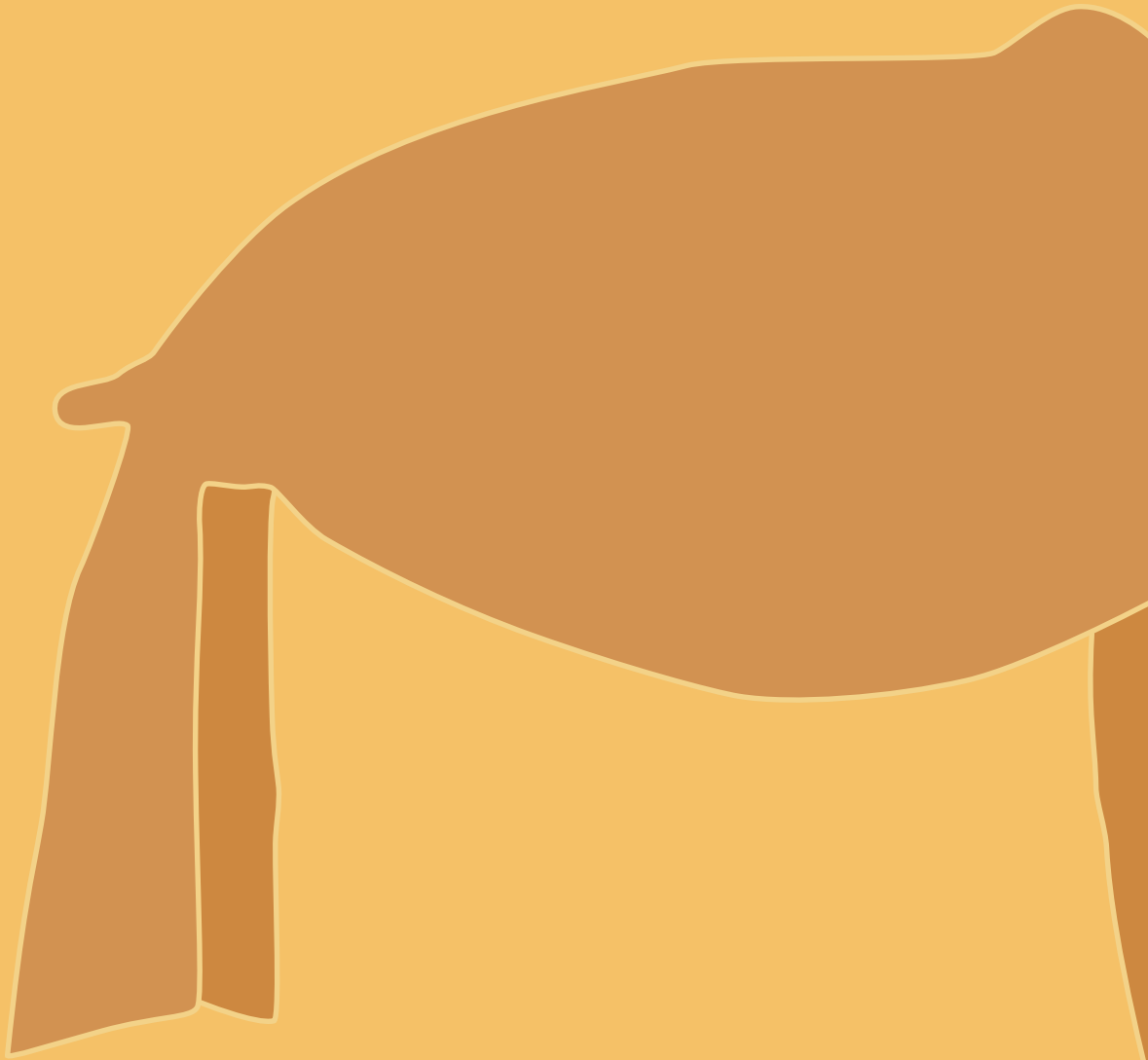
CHAPTER 7
DISCUSSION AND SYNTHESIS

The thesis presents research that is based on unique δ^{15}N and δ^{13}C datasets, often in combination with the ^{14}C age of the fossil remains. Unique not only because of the large amount of data, but also because of the species represented in the dataset, the age of the samples and their geographical origin.

These datasets, presented in a number of articles and discussed in chapters 3-6, consists predominantly of isotope data from mammalian fossils. These data give information about diet, environment and climate through time and space for numerous animal species: information that also indirectly gives valuable insights in the living circumstances of coeval living hominins.

Moreover, results raised new questions and data from the individual chapters require mutual comparison. The integrated data offer the possibility to discuss a number of intriguing topics as there are a) unexpected δ^{15}N results, b) difficulties using appropriate model species, and c) questions concerning the Late Quaternary megafaunal extinction. These topics will be discussed in this chapter.

7.1 High δ¹⁵N values observed in proboscidean tissues

Throughout most of the Late Pleistocene, woolly mammoths (*M. primigenius*) have remarkably high bone collagen δ¹⁵N values compared to other contemporaneous large herbivores. This phenomenon is not the result of a regional effect; a comparable pattern (that is, a discrepancy of roughly the same magnitude between the δ¹⁵N values of mammoths and other coeval herbivores) manifests in Europe (Bocherens *et al.*, 1997a), Siberia (Bocherens *et al.*, 1996) and Alaska (Bocherens *et al.*, 1994; Bocherens, 2003). Some evidence has been found that δ¹⁵N values of mammoths became more comparable to those of coeval living herbivores towards the end of their existence in certain locations, such the Ukraine (Drucker *et al.*, 2014). But in general, the phenomenon remains visible through time and space.

Different factors are suggested to have determined the relatively high δ¹⁵N values in woolly mammoths, such as aspects related to (isotopic) diet composition, digestive physiology and feeding habits (Schoeller, 1999; Sponheimer *et al.*, 2003a; Kuitems *et al.*, 2015c). Diet-related aspects concern, for example, consumption of high amounts of ¹⁵N-enriched plant parts and/or species (Bocherens, 2003; Metcalfe *et al.*, 2013). However, considering the bulk amounts of food a mammoth probably consumed on a daily basis to fulfil its nutritional needs, it seems more likely that the mammoth ate all appropriate and preferred plants that it came across rather than selecting specific plant parts. A suggested option is though that the mammoth's tusks would have served as a tool to get access to ¹⁵N-enriched partly decayed vegetation under the snow, that would have been inaccessible for other inhabitants of the mammoth steppe biome (Schwartz-Narbonne *et al.*, 2015). However, the amount of snow in major parts of the area they inhabited was limited. Therefore, it is unlikely that the consumption of plants under the snow caused the widely observed pattern of high δ¹⁵N values of woolly mammoths.

Investigations of for example intestinal remains recovered in the Siberian permafrost from woolly mammoth and other hindgut fermenters such as horse and rhinoceros, and the dental wear patterns of these species from Europe and Alaska (Rivals *et al.*, 2010) showed that these animals were feeding predominantly on grasses and other herbaceous plants and -in particular during winter- on some amounts of browse (Olivier, 1982; Vereshchagin and Baryshnikov, 1982; Guthrie, 1990; Ukraintseva, 1993; Putshkov, 2003; Mol *et al.*, 2006; van Geel *et al.*, 2008; Willerslev *et al.*, 2014). Based on these results, a difference in diet between Pleistocene horse, woolly mammoth and woolly rhinoceros does not seem to be the major cause for the discrepancy in δ¹⁵N values between woolly mammoth and the other species. To some extent, however, variation in δ¹⁵N values between ungulates sharing the mammoth steppe biotope must be explained by resource partitioning. As a general rule in ecology, the cohabitation of species leads to niche differentiation in order to avoid direct competition. Such differentiation is often well reflected in a bivariate diagram of inter-specific δ¹³C and δ¹⁵N values. Indeed, studies on dental wear patterns show that resource partitioning existed within the mammoth

steppe. However, although for instance the amount of browse in the diet differed to some extent between species (Rivals *et al.*, 2010), such studies do not explain why the difference in $\delta^{15}N$ values between woolly mammoths and other hindgut fermenters is larger than the variation in $\delta^{15}N$ values between other hindgut fermenting species, nor why the $\delta^{15}N$ values of specifically woolly mammoths tend to be high.

The higher the protein throughput, the more the body needs to get rid of excess nitrogen, that is, by urea excretion. Due to fractionation, the isotopically lighter ^{14}N is favoured during excretion over the heavier ^{15}N, resulting in the retention of heavier ^{15}N in the body. Therefore, protein rich diets lead to higher $\delta^{15}N$ values in body tissues than nutrient poor diets (Ambrose, 1991; Sponheimer *et al.*, 2003a; Fuller *et al.*, 2005). Analysis of cementum from fossil mammoth molars suggests that woolly mammoths faced food deficiency on an annual basis (Guthrie, 1990; Wang *et al.*, 2018). In addition to the beforementioned protein-rich diets, protein shortage has been found to correlate with enrichment of ^{15}N in body tissues (Sealy *et al.*, 1987; Hobson *et al.*, 1993; Adams and Sterner, 2000). However, it seems unlikely that temporal enrichment of ^{15}N in body tissues alone is 'strong' enough to have caused the observed high $\delta^{15}N$ values in bone collagen, which has a turnover time of years. Moreover, the mammoth has been a successful species for a time range of hundred-thousands of years. Therefore, a significant part of the population must have had access to sufficient amounts of nutrients on a yearly basis, in order to reproduce and to maintain the population's fitness.

Woolly mammoths may have had specific (metabolic) adaptations to compensate for low digestion efficiency (Kuitems *et al.*, 2015c), or to cope with periods of winter starvation (Bocherens *et al.*, 1996). Results of investigations by van Geel *et al.* (2008, 2011) on frozen mammoth dung from Alaska (ca. 12.300 yr BP) and from intestinal remains from a mammoth carcass from Yakutia (ca. 18.500 ^{14}C yr BP) reveal evidence for coprophagy, and even suggest that this might have been a routine practise amongst woolly mammoths. Dung must have contained considerable amounts of undigested food. Coprophagy may lead to slightly higher $\delta^{15}N$ values in body tissues, in particular if it enhances the digestive efficiency substantially (Ugan and Coltrain, 2011). Faecal consumption is observed amongst free ranging modern African elephants, but not as a common practice (van Geel, 2011).

The results of a stable isotope study by the author of nail samples, collected from modern herbivores, showed that the nails of captive elephants, rhinoceroses and horses have similar $\delta^{15}N$ values (Kuitems *et al.*, 2015c). These animals lived predominantly in Dutch zoos and never had to cope with food and water stress, competition for resources nor niche partitioning leading to dietary differentiation. Instead, the animals got all the nutritional components they need and all got roughly the same food. It is known that young elephants, living in the zoos where the nail samples came from, occasionally eat dung. It concerns mainly faeces from their mother but also from other elephants of their group. The analysed nail samples came from adult elephants that had never been observed eating any dung at an advanced age.

The obtained results indicate that aspects related to diet and physiology, as well as coprophagy are indeed possible explanations for differentiation in stable isotope values, but they do not explain the observed discrepancy of δ^{15}N values between Pleistocene herbivores. Probably, neither results of the analysis of nail keratin, nor of δ^{15}N values in bulk collagen will ever point to the specific discriminating factor(s) (McMahon and McCarthy, 2016), since equifinality (that is the principle that a specific end state - here the high δ^{15}N values - can be reached via many potential pathways) is inherent to stable isotope values of fossils from free-ranging animals in the past.

Analysis of the δ^{15}N composition of single compounds, that is, individual amino acids in collagen, may be an important and valuable addition to this discussion in future, since it allows discrimination between ^{15}N-enrichment in 'source' amino acids and 'trophic' amino acids (Schwartz-Narbonne *et al.*, 2015; McMahon and McCarthy, 2016). The idea is, that 'source' amino acids have nitrogen isotopic values that are closer related to those of same amino acid in the consumed food than 'trophic' amino acids, whose amino-nitrogen is part of a metabolic amino-nitrogen pool. A study of compound-specific isotopes of different Pleistocene large herbivore and carnivore species carried out by Schwartz-Narbonne *et al.* (2015) pointed towards a dietary (as opposed to a physiological) explanation for the high mammoth δ^{15}N values. However, more study is necessary to get precise insight into the complex cycling of single amino acids through the metabolic network, that is the underlying metabolic drivers for the observed nitrogen isotopic patterning in amino acids (McMahon and McCarthy, 2016; O'Connell, 2017). In support of a dietary explanation, and not a proboscidean-specific physiological adaptation, is the fact that mastodons (*Mammut americanum*) tend to have lower δ^{15}N values than woolly mammoths, which might be explained by a species-specific diet (Metcalfe *et al.*, 2013, 2016).

However, mastodons are not elephantids. Therefore, a physiological adaptation that is elephantid-specific, such as a possible (metabolic) adaptation to compensate for low digestion efficiency (Kuitems *et al.*, 2015c), remains a credible explanation for the high δ^{15}N values observed in woolly mammoths. Data from this thesis are even in favour of such an explanation. As shown in Chapter 4 and 6, samples from straight-tusked elephant (*Palaeoloxodon antiquus*) reveal that these older elephantids do yield higher δ^{15}N values than those of coeval living large herbivores; a similar pattern as observed for woolly mammoths.

In addition to the data presented in Chapter 6, stable isotopes of three omnivores and two carnivores from Schöningen have been measured (Table 7.1). These new data are interesting to compare with the herbivore data. The δ^{15}N values for straight-tusked elephants and/or woolly mammoths are shown in Fig. 7.1, relative to the δ^{15}N values of other terrestrial herbivores, omnivores and carnivores from the same region (specifically, North Sea and Schöningen). The figure shows that in both regions the δ^{15}N values of straight-tusked elephants are higher than those of most other, non-proboscidean herbivores, and more similar to those of carnivores. The range of δ^{15}N values of woolly

Table 7.1 Isotope results of omnivorous and carnivorous mammals from Schöningen.

species (Latin)	species (English)	layer	material	%C	%N	C:N	δ¹³C (‰)	δ¹⁵N (‰)
Canis lupus	wolf	Schö 13 II-4	bone	37.1	13.1	3.3	-20.1	8.7
Vulpus vulpus	fox	Schö 13 II-4	bone/dentine	34.7	12.3	3.3	-20.3	9.3
Ursus spelaeus	cave bear	Schö 12B	bone	41.4	14.8	3.3	-22.9	4.7
Sus scrofa	wild boar	Schö 12B	bone/dentine	38.8	13.7	3.3	-22.0	6.0
Sus scrofa	wild boar	Schö 12B	bone/dentine	40.9	14.5	3.3	-22.4	4.3

mammoths from the North Sea partly overlaps with the lowest values of the straight-tusked elephants and the highest values of the non-proboscidean herbivores.

In contrast to the woolly mammoth, the straight-tusked elephant is assumed to be a browser preferring wooded environments (Stuart, 2005). Recent tooth wear investigations on straight-tusked elephants from other Middle Pleistocene localities correlated with MIS 11 in Germany (Steinheim; Rivals and Ziegler, 2018) and in England (Clacton, Hoxne, and Swanscombe; Rivals and Lister, 2016) support that the straight-tusked elephant's diet consisted partly or predominantly -depending on the location- of browse (Rivals and Ziegler, 2018). In general, browsers tend to have lower δ¹⁵N values than grazers (Ambrose, 1991, Drucker *et al.*, 2010). This, and the fact that straight-tusked elephants are believed to have inhabited quite humid and temperate environments, makes the high δ¹⁵N values of straight-tusked elephant tissues even more intriguing
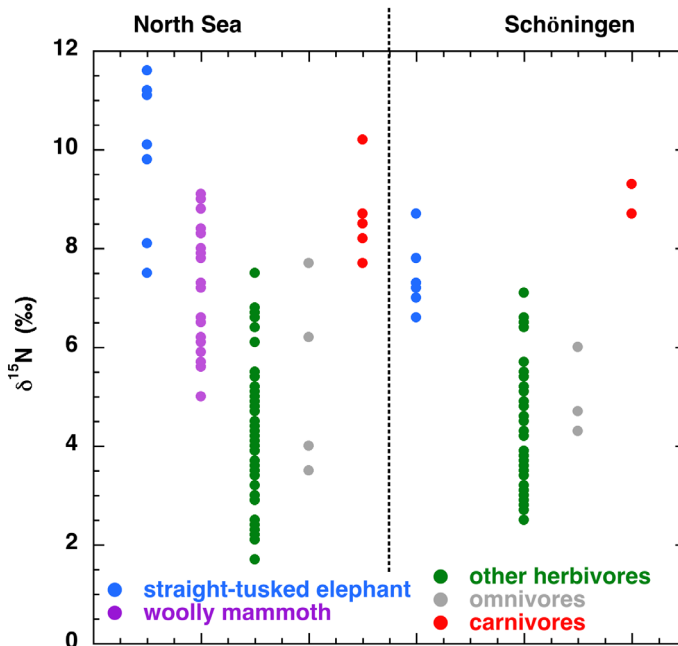

Figure 7.1 δ¹⁵N values of straight-tusked elephants and woolly mammoths compared to δ¹⁵N values of other terrestrial herbivores, omnivores and carnivores. Blue dots indicate δ¹⁵N values of mammals from Schöningen; open circles indicate δ¹⁵N values of mammals from the North Sea area.

than those of the woolly mammoth. These data make a family-wide physiological cause for the observed high δ^{15}N values more plausible and form a promising basis for further investigation and debate.

7.2 Looking for a model of the past

Ambrose and DeNiro (1986) showed that the δ^{15}N value in collagen of a free-ranging wild modern African elephant living in East Africa is higher than stable δ^{15}N values of other ungulates and almost as high as the δ^{15}N values of the carnivorous species in the same study. This result resembles the pattern observed in Pleistocene herbivores inhabiting the mammoth steppe environment, and was the incentive to use extant relatives of the woolly mammoth, the African elephant (*Loxodonta africana*) and in particular Asian elephant (*Elephas maximus*) in order to get information about the δ^{15}N values in modern elephantids living under controlled conditions in Kuitems *et al.* (2015c).

In addition to considering results in the context of what is known from other proxies, δ^{13}C and δ^{15}N values are practically always discussed relative to those from the same species in different times or areas, or to other species that live in the same area and period or share certain characteristics. Also, in order to gain insights into potential factors underlying specific isotopic compositions of extinct species, one needs to use modern 'model' species. The use of (modern) models is not confined to stable isotope studies, but is inherent to any study that attempts to make assumptions about what might have happened in the past. Appropriate model species share relevant characteristics with the 'target' species (that is, here, the species one attempts to decipher by information obtained from the model species).

However, choosing an appropriate model is not always straightforward and may sometimes even be problematic, as becomes also clear from various examples throughout the current thesis. The species chosen will usually meet a determined taxonomic equivalency, but as examples in the present thesis show, the best fitting model is not per se genetically the closest related. Also, a target species may have various model species, each of them being most suitable for a particular situation or purpose. The appropriateness certainly depends on the research question, but also on availability. Finally, comparison with model species can be informative, but care must be taken when generalizing from one species to another. For instance, a species in the past may have had characteristics that differ from what is generally assumed. In that case, the fundamental idea or 'baseline' which is used for comparison with the target species is already biased.

The choice of appropriate baselines becomes dramatically clear when using models in order to convert stable isotope values into estimates of the proportion of different food sources in a diet. The use of isotope mixing models for these purposes has taken off during the last decade. Although recently developed models allow more and more

for a certain amount of uncertainties, using inappropriate priors and/or interpreting the outcomes as hard evidence, lead to erroneous conclusions (Caut *et al.*, 2008; Phillips *et al.*, 2014).

Controlled feeding studies proved to be valuable for interpreting stable isotope results and for understanding specific fractionation processes (Ambrose, 2000; Sponheimer *et al.*, 2003a; Nardoto *et al.*, 2006; O'Connell *et al.*, 2012), and would have been excellent to get insights in the high mammoth $\delta^{15}N$ values. Performing such a study with extinct animals would be impossible for obvious reasons. Also in other studies, physical or ecological aspects of modern elephants are compared to those of extinct proboscideans. Sometimes the authors make explicit why the comparison between extinct elephants and modern elephants is appropriate and relevant (see for example, Olivier, 1982; Valente, 1983; Marchant and Shoshani, 2007; Smith *et al.*, 2017), but other do not (e.g., Cammidge *et al.*, 2019). Recently, Meyer *et al.* (2017) discovered that the straight-tusked elephant's genome was closely to the genome of the extant African elephant than previously thought. Would this mean the African elephant would be, in a comparison study, an appropriate model for the straight-tusked elephant?

An example from this dissertation where the choice of a model was not obvious, can be found in Chapter 5, in which the isotope composition of Siberian unicorn (*Elasmotherium sibiricum*) samples have been discussed. This extinct kind of rhinoceros had enormous, continuously-growing cheek-teeth. This extreme form of hypselodonty is an adaptation to dietary components which lead to major dental abrasion. Its dental morphology and the angle of its neck and head indicate adaptation to feeding close to the ground or even consumption of underground plant parts such as plant bulbs and roots. Until recently, very little was known about this peculiar animal. Not only its morphology, but also its stable isotope values diverge from other Pleistocene rhinoceroses and many other large herbivores, including those from woolly rhinoceros and woolly mammoth from the same spatio-temporal range. A modern inhabitant of this region, which today is characterized by dry steppe environments and (semi) deserts, is the saiga antelope (*Saiga tatarica*). Also, Late Pleistocene fossil remains of the saiga antelope have been found in this region. Surprisingly, their $\delta^{13}C$ and $\delta^{15}N$ values overlap considerably with those of Siberian unicorn. This overlap could be interpreted as an indication of sharing (parts of) a dietary niche, but in contrast to the Siberian unicorn, saiga antelope is medium-sized, has different (digestive) physiology and is not specialised in eating underground plant parts. The relation between $\delta^{13}C$ values and the consumption of underground plant parts would be an interesting topic for further investigation.

An animal that does include underground plant parts in its diet is the wild boar (*Sus scrofa*). Wild boars have brachyodont molars and the species is generally a forest dweller, and did not inhabit the mammoth steppe. As discussed in Chapter 6, one of the reasons not to assume that the landscape in Schöningen was completely open and glacial conditions prevailed during depositional level 4, is the presence of fossils of wild

boar (for example, Schö 13 II-4). Recently, stable isotopes were measured in two wild boar samples (see Table 7.1). The samples originate from depositional level 1 (Schö 12 B), the assumed interglacial optimum. Their $\delta^{13}C$ values (-22.0‰ and -22.4‰) agree with the $\delta^{13}C$ values of other animals from the interglacial optimum (n = 17, average -22.2‰).

However, according to the threshold presented in Chapter 6, these $\delta^{13}C$ values do not reflect the canopy effect. Of course, a number of two samples is very limited and there is a significant risk of over-interpretation. But among the possible explanations for the fact that the wild boar samples do not reflect the canopy effect, is that the value below which $\delta^{13}C$ values are expected to reflect the canopy effect (-22.5‰) must be somewhat adjusted towards a less negative number in the case of the Schöningen fossils. This $\delta^{13}C$ value of -22.5‰ is based on the results of previous studies on fossil remains and modern samples from different large herbivores, ages and localities by Drucker and colleagues, such as Late-Glacial and Early Holocene red deer samples from the French Jura (Drucker *et al.*, 2003a; Drucker and Bocherens, 2009). The circumstances in these localities may have not been a suitable equivalent for those in Middle Pleistocene Schöningen. As for $\delta^{13}C$ values from fossils, the canopy effect-$\delta^{13}C$ threshold may be expected to vary through time and space. Hence, this canopy effect-threshold was indicated with a dotted line and must be considered as an estimation for the canopy effect-threshold for the Schöningen fossils, instead of as a strict boundary.

Another possible explanation is that the consumption of underground plant parts, which seem to have higher $\delta^{13}C$ values than photosynthetic plant parts (Badeck *et al.*, 2005) make the visibility of the canopy-effect on the $\delta^{13}C$ values less clear. Other possible explanations are that the Schöningen wild boars inhabited forested parts of the landscapes which were not densely closed (N.B. more open forest types would not cause the canopy effect), or these Middle Pleistocene wild boars were less restricted to forest than their modern counterparts. In the latter case, the characteristics of the species have changed over time.

The fact that characteristics such as habitat or diet of a modern species does not have to match those in previous times, becomes clear from the isotope signatures of horses from Schöningen (see Chapter 6). Horses are generally considered to be typical obligate grazers. However, the $\delta^{15}N$ values of the horses from Schöningen, which are lower than all other investigated species from the same locality, provide supporting evidence for a browsing diet. Morphologically, the horse molars diverge from those found in other periods and sites, with unfamiliar pointed cusps and a dental wear pattern indicative that browsing formed a substantial part of the diet (Rivals *et al.*, 2014). Besides, the study of Rivals *et al.* (2014) shows that the variety of dental wear of horses across time and space is extremely wide. Richards *et al.* (2017) found that $\delta^{13}C$ and $\delta^{15}N$ values of collagen of horses from an archaeological site in France changed considerably between ~ 150,000 and 50,000 years ago following environmental and/or climatic changes. The wide variety in isotope values they found seems to support flexibility in diet. But as the

authors state, it is unclear whether the range of $\delta^{13}C$ and $\delta^{15}N$ values from collagen reflects either changing isotope compositions of diachronic similar dietary components, or reflects dietary change (Richards *et al.*, 2017). The horse stable isotope data show a flexibility that is most probably not restricted to horses. One can assume that also other mammalian species have a degree of flexibility in their diet and their environmental constraints. A flexibility that is important, in particular for herbivores, to survive the Pleistocene changes in climatic conditions and vegetation. A lack of flexibility might lead to extinction.

7.3 The fatal blow for woolly mammoths

Many of the data discussed in this thesis come from fossils of now extinct animal species. Most of these species vanished as part of the 'Late Quaternary megafaunal extinctions' (Stuart, 2005; Stuart and Lister, 2012; Kosintsev *et al.*, 2019; Lister and Stuart, 2019). During the Weichselian and the Early Holocene, about 65% of the terrestrial large mammals (weighing more than 45 kg) became extinct across various continents (Mann *et al.*, 2015, 2018; Di Febbraro *et al.*, 2017; Rabanus-Wallace *et al.*, 2017). There is a long and still ongoing debate about what caused the megafauna extinctions that started towards the end of the Pleistocene (Koch and Barnosky, 2006; Haynes, 2009; Stuart, 2015). The Late Quaternary is a period characterized by major climate fluctuations. In addition, humans developed more advanced hunting techniques and they expanded their geographical range into three new continents and farther more to the north (Sykes, 2018; Hufthammer *et al.*, 2019; Ineshin and Teten'kin, 2019; Pitulko *et al.*, 2019; Vachula *et al.*, 2019). These factors have undoubtedly been critical for the extinction of certain species. But despite the number of species that became extinct within the Late Quaternary, the reasons for extinction may need to be studied per species and per region rather than a common explanation to be sought for the entire complex of extinctions (Broughton and Weitzel, 2018). Inter- and intraspecies spatiotemporal differences are observed for their extinction dates, and hence, it is obvious that they did not suffer a synchronous collapse (Lorenzen *et al.*, 2011; Stuart, 2015; Puzachenko *et al.*, 2017; Puzachenko and Markova, 2019). The disappearance of certain species may itself have triggered the extinction of other species, occasionally dramatically altering the functioning of entire ecosystems (Rule *et al.*, 2012; Gill, 2014).

Also, the mammoth steppe ecosystem, including many of its inhabitants came to an end in this period. Among the prevailing hypotheses explaining the extinction of the woolly mammoth, are 1) the hypothesis that humans are mainly responsible (over-hunting and introducing diseases; Martin, 1984; Braje and Erlandson, 2013; Boivin *et al.*, 2016), 2) the idea that climate change played major part (Cooper *et al.*, 2015; Rabanus-Wallace *et al.*, 2017), and 3) the assumption that both humans and climate played a crucial role (Haynes, 2007; Nikolskiy *et al.*, 2011; Wan and Zhang, 2017). Moreover, exotic

causes have been suggested, such as impacts from the cosmos (Firestone *et al.*, 2007; Pinter *et al.*, 2011). Frequently-mentioned problems include the numerous preceding glacial-interglacial cycles that the species did survive, the long-term coexistence of woolly mammoths and hominins in some of their geographical regions dismissing prey naivety as contributing factor over there, the surviving of numerous coeval living species, and the lack of enough diachronic high-quality data (Stuart, 2015; Di Febbraro *et al.*, 2017; Rabanus-Wallace *et al.*, 2017; Vachula *et al.*, 2019).

At the margins of a biotope, significant information can be found about determining factors for the maximum spread of that specific biotope (Chase and Leibold, 2003), albeit potentially a reflection of predominantly suboptimal conditions (Braunisch *et al.*, 2008). Several biotic and abiotic factors, rather than behaviour and habitat selection, limit the distribution a species. These include vegetation type, sea level rise, widespread peat formation and the configuration of impassable rivers, mountain chains and ice sheets (Lister and Stuart, 2008; Kahlke, 2015).

Changes challenge the tolerance of a species, their niche breadth, rather than on the preference of the species; tolerance draws the line between survival and extinction. The disappearance of a species might be triggered by several factors. The ability to (episodically) expand or shift the actual range of a species into other areas within its potential range (that is, where it can survive and reproduce) often plays an essential role for survival. Habitat loss and fragmentation are inextricably linked to climate change, but geographically interconnected areas of suitable habitat are critical for maintaining the survival of a species (Aitken and Whitlock, 2013; Di Febbraro *et al.*, 2017).

The woolly mammoths survived numerous climatic changes caused by alternating glacials/stadials and interglacials/interstadials throughout their existence in the Pleistocene. Though their range was contracted into refugia during interglacials, woolly mammoths inhabited a gigantic geographic region with local variations due to natural features such as mountain ranges and rivers, which shows that woolly mammoths had a high level of flexibility and the ability to adapt to a range of environmental conditions.

Although situated on the northern peripheries of the mammoth steppe biotope, North-eastern Siberia was more or less continuously occupied by the woolly mammoth (Puzachenko *et al.*, 2017). Apparently here, life conditions remained suitable enough throughout the various Late Pleistocene stadials and interstadials. Favourable circumstances were served by, for instance, the lowlands of many parts of North-eastern Siberia remaining ice-free due to aridity during the LGM, whereas many other regions along the Northern Hemisphere were then covered by ice sheets (Gualtieri *et al.*, 2005; Hoffecker and Elias, 2007; Stauch and Gualtieri, 2008; Möller *et al.*, 2015).

It was also North-eastern Siberia where the woolly mammoth survived the longest before getting extinct. This also applies to various other mammoth steppe dwellers (Boeskorov, 2006; Di Febbraro *et al.*, 2017), such as woolly rhino (Stuart and Lister, 2012), steppe bison (Stuart, 2015) and wild horse (Boeskorov *et al.*, 2018). Indeed, whereas mammoths started to disappear from different parts of their range between

around 20,000 and 11,000 years ago, fossils from much younger mammoth populations are recovered from islands in the Bering Sea, such as St Lawrence, St Matthew, the Pribilof Islands, and in particular Wrangel. The fact that the mammoth survived so long on Wrangel Island, and the fact that there is no clear evidence that humans occupied the island before the mammoth's disappearance (Gerasimov *et al.*, 2006; Nikolskiy *et al.*, 2011), makes Wrangel Island an interesting area to study the conditions under which the very last woolly mammoths became extinct.

As presented and discussed in Chapter 3, the $\delta^{13}C$ and $\delta^{15}N$ values of woolly mammoth samples from Wrangel remain similar through time. Recently, these conclusions were confirmed by Arppe *et al.* (2019). The stable isotope data do not give direct information about the extinction of the woolly mammoth on Wrangel Island. But the stable isotope composition of samples from woolly mammoth show no changes that point to any changes in for instance the moisture or nutrient availability on the island, as was previously suggested for St. Paul Island (Graham *et al.*, 2016). These results are in line with conclusions from Fox *et al.* (2007): climate signals recorded in oxygen isotope values in serially sampled tusks from North-eastern Eurasia, including Holocene tusks from Wrangel Island do not point to climate change that could be regarded as the direct cause of the woolly mammoth extinction (Fox *et al.*, 2007). Also our mammoth stable isotope data from Wrangel do not indicate any climate change just before its ultimate extinction.

Although the current dataset and results of study of various other proxies point to stability through time in this region, changes in habitat and/or diet at some point cannot be absolutely ruled out based on diachronic similarity of stable isotope data. For instance, a transition to another diet would go unnoticed in the stable isotope values of the tissues of the consumer, if the isotope values of the new food have more or less the same isotope values as the other diet. A stable isotope value of fossil tissue of a consumer can be generated by many potential means, instigated by for instance soil processes, dietary isotope composition, physiological aspects. However, also the opposite is true. Variation in $\delta^{13}C$ and $\delta^{15}N$ values in an herbivore tissue following environmental and/or climatic changes, could reflect either variation in isotope values of the consumed plants in response to the climate fluctuations, or a switch to another diet (Rabanus-Wallace *et al.*, 2017; Richards *et al.*, 2017). The latter would indicate adaptability and flexibility of the animal, whereas the previous would not per se.

Nevertheless, climate change is not likely to have been the direct cause of the woolly mammoth extinction on Wrangel Island. Nutrition and the absence of predators are not the only factors critical for a species' survival. The small population size in combination with the dispersal barriers of Wrangel- inextricably linked to the isolated nature of an island- has probably been the bottleneck for the Wrangel mammoths. Recent investigation on the genome of one of the last surviving Wrangel mammoths (dated to about 4,300 yr BP) demonstrates reduced genetic variation. It also shows that the last mammoths on Wrangel Island likely suffered from genetic diseases that reduced

fitness (Palkopoulou *et al.*, 2015; Pečnerová *et al.*, 2016; Rogers and Slatkin, 2017; Fry *et al.*, 2018). The actual population size might have been large considering the small size of the island and might even have increased dramatically around the onset of the Holocene (Zimov *et al.*, 2012). But it was not large in terms of the measure of genetic exchange, which hampers maintaining a healthy and reproductive population. Already 12,000 years ago, at about the time when Wrangel became separated from the mainland (Brigham-Grette and Gualtieri, 2004; Keigwin *et al.*, 2006), the woolly mammoth genome indicates a major reduction in effective population size (Palkopoulou *et al.*, 2015). Along the way, the reduced genetic variation was probably harmful for the reproductive success of the Holocene Wrangel mammoths. That must have had a disastrous impact on their viability and might have contributed to their extinction (Palkopoulou *et al.*, 2015).

The youngest dated mammoth from Wrangel is dated to 3685 ± 60 ^{14}C yr BP (Ua-13366; Vartanyan *et al.*, 2008), which calibrates to 2276-1905 BCE (at 95.4% probability by using IntCal13, Reimer *et al.*, 2013). This youngest find does not represent the last animal per se, since in theory, younger remains may be found at a later stage, in particular considering the incompleteness of the fossil record or so-called 'Signor-Lipps effect' (Signor and Lipps, 1982). But an estimation for the extinction date of the woolly mammoth produced by Bayesian age modelling, indicates that this youngest find belonged to one of the very last representatives of this species. So far, 153 ^{14}C dates of woolly mammoth fossils from Wrangel Island have been published, including the new dates as presented in Chapter 3. The majority (n = 132) are younger than 12,000 years ago, and therefore date to the time after Wrangel became an island isolated from the mainland (Brigham-Grette and Gualtieri, 2004; Keigwin *et al.*, 2006). The 132 Holocene ^{14}C dates of woolly mammoths from Wrangel Island can be incorporated within a Single Phase model in OxCal version 4.3.2 (Bronk Ramsey, 2009). In the model, the end boundary provides an estimate of the last appearance of the woolly mammoth on the basis of the 132 ^{14}C data. The callibration curve IntCal13 was used for calibrating the ^{14}C dates (Reimer *et al.*, 2013). The model (see SI Chapter 7 for the code) generates an end boundary of 4218-3886 cal BP (at 95.4% probability). This means that the last appearance for the woolly mammoth was around 2269-1937 BCE and means the very end of this intriguing species.

Summarising conclusions

In this dissertation, a vast amount of $\delta^{13}C$ and $\delta^{15}N$ data from bulk collagen of Quaternary mammalian bone, tusk, antler and teeth samples are presented and discussed. Most of these data are measured at the Centre for Isotope Research (CIO), Groningen (n > 400). The dataset consists of samples from various localities within Eurasia and are taken from human fossils, but mainly from fossils of various animal taxa including extinct species such as woolly mammoth (*Mammuthus primigenius*), straight-tusked elephant (*Palaeoloxodon antiquus*), wild horse (*Equus mosbachensis*), Siberian unicorn (*Elasmotherium sibiricum*), woolly rhinoceros (*Coelodonta antiquitatis*) and giant deer (*Megaloceros giganteus*). Many of these faunal species belong to the typical 'mammoth steppe fauna'.

The results shed light on dietary and habitat characteristics of these animals through time and space. But also on the habitat characteristics of coeval living hominins, as they were exposed to the same environmental and climatological circumstances. Moreover, dietary information of animals is relevant for hominins sharing the same region, as in turn the animals may have been part of the hominins' diets, or the animals may have competed for the same food resources. Fossil skeletal remains are abundantly found at archaeological sites.

Archaeologists reconstruct the past, usually based on a limited amount of available data. Stable isotope analyses, however, offer a relatively cheap, fast, objective, controllable and nowadays widely available, valuable and unique contribution to the palaeoenvironmental reconstruction and to the scientific debates. For instance, the numerous $\delta^{13}C$ and $\delta^{15}N$ data from Holocene woolly mammoths from Wrangel Island provide a clearer picture of the circumstances in which mammoths lived just before the ultimate extinction of the species (see Chapter 3). The Holocene $\delta^{13}C$ and $\delta^{15}N$ values remain remarkably similar through time and are the same as those of Late Pleistocene woolly mammoths from the Northeastern Siberian mainland (**RQ 2**). Minor differences are observed in samples with an LGM age, but the post-LGM $\delta^{13}C$ and $\delta^{15}N$ values from North-eastern Siberia are similar to those pre-dating the LGM. This continuity or recovery of stable isotope values sharply contrasts to published data of woolly mammoths and other large herbivores samples from Europe and Alaska, which revealed significant changes in $\delta^{13}C$ and $\delta^{15}N$ values; changes that are related to climatic fluctuations during and/or after the LGM. Moreover, the data reveal that the $\delta^{13}C$ and $\delta^{15}N$ values of the Holocene woolly mammoths from Wrangel Island are similar to these of the Late Pleistocene mammoths from the North-eastern Siberian mainland, while they diverge from $\delta^{13}C$ and $\delta^{15}N$ values of woolly mammoth samples from Alaska, despite the fact that both regions are geographically rather close (**RQ 1**). The stable isotope data indicate that the stable isotope composition of vegetation on Wrangel Island was similar to that of other parts of West-Beringia and not to that in Alaska, despite the proximity to Central Beringia and Alaska. The difference in $\delta^{13}C$ and $\delta^{15}N$ values between Wrangel Island and Central Beringia and Alaska can be used

in further research on the way in which Central Beringia might have acted as ecological barrier that prevented (an earlier) migration of specific species to East Beringia (**RQ 4**).

Although changes in habitat and/or diet cannot be unconditionally ruled out based on diachronic similarity of stable isotope data, climate change would most probably be reflected as changes in the $\delta^{13}C$ and $\delta^{15}N$ values in the fossil bones. Therefore, the stable isotope data provide supporting evidence that climate change was not the direct cause of the ultimate extinction of the woolly mammoth. This way, the stable isotope data add to the debate on the cause of the megafauna extinctions towards the end of the Pleistocene (**RQ 3**).

Another example of a valuable contribution of stable isotope research to the scientific debate, forms the analysis of $\delta^{13}C$ and $\delta^{15}N$ data of fossil material from various mammal taxa and multiple find horizons from the key archaeological site Schöningen (see Chapter 6). Seemingly contradicting results achieved by analysis of different proxies, hampered the possibility to get a clear picture of the environmental circumstances in which the hominins operated at this locality. The isotopic data from faunal remains indicate that during the climatic Reinsdorf Interglacial optimum the landscape was forested, alternating with open areas, whereas during depositional level 4 the landscape was more open. The $\delta^{13}C$ values seem to be too low to be indicative for a steppe landscape. This is supported by the faunal record of depositional level 4 that does not include species that are indicative for glacial conditions (**RQ 8**).

Moreover, the results show the important addition that stable isotope analysis can make to results achieved by other archaeological methods. The application of stable isotope analysis is not limited to the individual but suitable for detecting and comparing inter- and intraspecific, diachronic and spatial patterns of feeding behaviour and habitat use (see Chapter 3 and 5). Stable isotope data offer another perspective on, and form a valuable addition to, results achieved by analytic methods focussing on for instance morphology, dental wear, and dental calculus analyses. This is illustrated by the stable isotope data from the Siberian unicorn (*Elasmotherium sibiricum*), presented in Chapter 4. The species has extremely high-crowned rootless molars. This morphological feature is regarded as an adaptation to very abrasive food, such as eating tubers. When eating plant roots, a lot of sand comes along, which means that the animal's teeth are likely to wear down fast. The $\delta^{13}C$ and $\delta^{15}N$ values from the Siberian unicorn point to a very specialised diet and $\delta^{13}C$ values support the consumption of underground plant parts. Its very specialised diet, its specialized habitat, the assumed low population size and its slow reproductive rate may have made the Siberian unicorn prone to extinction in the face of environmental change (**RQ 6**).

Another example of a significant addition to dental morphological information is the $\delta^{15}N$ values of the horses from Schöningen (see Chapter 6), which are lower than all other investigated herbivore species at the site. Although horses are generally considered to be typical obligate grazers, the $\delta^{15}N$ values may point to a browsing diet for the horses at Schöningen. Morphologically, the horse molars diverge from these found in

other periods and sites, with unfamiliar pointed cusps and a dental wear pattern indeed indicative for a substantial part of browse in their diet (**RQ 9**).

The Schöningen results from well-preserved bone collagen (**RQ 7**) illustrate, in addition, that the age of fossils does not have to be per se a limiting factor to analyse their stable isotope ratios. Instead, the current research makes clear that it is worth examining the organic fraction from fossils (far) beyond the radiocarbon timescale, in cases that the burial context or the physical appearance of the fossil remains suggest good preservation. Indeed, if the $\delta^{13}C$ and $\delta^{15}N$ analysis of bone collagen from old samples were categorically on forehand excluded because of their age, we would mistakenly miss potentially important information.

For instance, stable isotope information of the straight-tusked elephant would never have been recovered if fossils with an age higher than 50 ka were disregarded. The straight-tusked elephant samples from Schöningen (see Chapter 6) and the North Sea area (see Chapter 4) revealed that these elephantids show a distinctive pattern of $\delta^{15}N$ values higher than those of coeval living herbivorous large mammals. A similar discrepancy of $\delta^{15}N$ values between woolly mammoths and co-occurring Late Pleistocene herbivores is commonly observed. An all-encompassing explanation for the divergence is not yet established. Likely, $\delta^{13}C$ and $\delta^{15}N$ analysis of bulk collagen samples will not be good enough to solve this puzzle. Although more study is necessary to get precise insight into the complex cycling of single amino acids through the metabolic network (McMahon and McCarthy, 2016; O'Connell, 2017), analysis of the $\delta^{15}N$ composition of single compounds from woolly mammoths and straight-tusked elephants may eventually give the solution. A study of compound-specific isotopes of different Pleistocene large herbivore and carnivore species carried out by Schwartz-Narbonne *et al.* (2015) pointed towards a dietary (as opposed to a physical) explanation for the high mammoth $\delta^{15}N$ values. However, the data from straight-tusked elephants make an elephantid-specific physiological adaptation a more plausible cause for the observed high $\delta^{15}N$ values and form a promising basis for further investigation and debate (**RQ 5**).

The research in this thesis emphasises the importance of sufficient amounts of data. As shown in the case of the extensive dataset of Siberia, prior claims based on just a few data showed to be off the point. Outliers occur, but the problem is that others build on such data, whilst the data do not form a good base. We must continue to look extremely critically at claims made on the basis of a small amount of data. To date, discussing small datasets of stable isotopes from bulk collagen can actually be avoided for many species and localities. Given the current sophistication of isotope measurement technology, low costs and fast sample throughput, statements should nowadays be based on relatively large data sets. In addition to create a sound base for outlier analysis and other statistical evaluation, large data sets ensure that diachronic and spatial patterns can be analysed. Often, $\delta^{13}C$ and $\delta^{15}N$ is automatically measured with collagen ^{14}C dating. Much of the data presented in this dissertation has been obtained in this way. By publishing such

data, it would be easier to discuss a (few) stand-alone data point(s) in comparison to relevant readily available δ^{13}C and δ^{15}N values. Also, applications such as isotope mixing models and estimating reservoir effects likely benefit from higher amounts of available ^{14}C dated δ^{13}C and δ^{15}N data. Moreover, techniques such as ZooMS probably increases the future amount of δ^{13}C and δ^{15}N data, since it enables to identify bone parts which lack morphological diagnostic features relatively simply at species level (Richter *et al.*, 2011; Stewart *et al.*, 2014; Welker *et al.*, 2015). Therefore, likely more frequently bone fragments will be sent in for ^{14}C, δ^{13}C and δ^{15}N analysis. This way, ZooMS opens the possibility to investigate δ^{13}C and δ^{15}N data of bone assemblages that may be important but that previously, without morphological species identification, would have been ignored. It will improve our understanding of associated assemblages that itself may be inappropriate or too valuable for destructive δ^{13}C and δ^{15}N analysis, and to feed isotope mixing models with valuable data of potential important, but otherwise overlooked, dietary resources.

Samenvatting

Fossielen van wolharige mammoeten op een eiland waar de soort uiteindelijk uitsterft, menselijke en dierlijke fossielen op de bodem van de Noordzee, resten van Siberische eenhoorns en uitzonderlijk goed bewaarde botten van 300.000 jaar geleden uit de beroemde archeologische vindplaats Schöningen in Duitsland: dit zijn de hoofdonderwerpen die in dit proefschrift aan bod komen.

De fossiele botten en tanden zijn bestudeerd aan de hand van hun chemische samenstelling, namelijk de relatieve stabiele koolstof- en stikstofisotopenconcentraties. Stabiele isotopengegevens in fossielen van mensen en dieren vormen een waardevolle informatiebron voor de reconstructie van hun dieet en van het milieu waarin zij leefden. Fossiel weefsel is gelinkt aan de chemische samenstelling van het voedsel dat een organisme tijdens zijn leven heeft opgenomen. De stabiele isotopenwaarden van koolstof en stikstof in het botcollageen van bijvoorbeeld herbivoren zijn gerelateerd aan de isotopensamenstelling van dezelfde elementen in de planten die ze eten. Op hun beurt worden de stabiele koolstof- en stikstofwaarden in deze planten (en bodems) beïnvloed door klimatologische en (lokale) omgevingsparameters.

Dit proefschrift bundelt een aantal stabiele isotopenstudies die de auteur de afgelopen jaren heeft uitgevoerd. Het onderzoeksdoel van deze studies is bijdragen aan het begrip van de ecologische omstandigheden tijdens het Pleistoceen/Vroeg-Holoceen in Eurazië door de stabiele isotopensamenstellingen te analyseren van fossielen van zoogdieren die in delen van Eurazië leefden. De focus ligt op fossielen van grote herbivoren uit: 1) een aantal regio's in het Euraziatische deel van het zogenaamde 'mammoetsteppe'-bioom ten tijde van het Laat-Pleistoceen (het Laat-Pleistoceen begint ongeveer 125.000 jaar geleden) en het Vroeg-Holoceen (het Holoceen begint ongeveer 11.700 jaar geleden en is het tijdvak waarin we nu leven), en 2) de paleolithische vindplaatsen bij Schöningen, met een laat Midden-Pleistoceen ouderdom (het Midden-Pleistoceen begint ongeveer 780.000 jaar geleden en gaat vooraf aan het Laat- Pleistoceen).

De meeste stabiele isotopengegevens (behalve die van Schöningen) zijn afkomstig van monsters waarvan de ouderdom is vastgesteld door middel van koolstofdatering (^{14}C-datering). De monsters stammen daarom meestal uit het Holoceen of Laat-Pleistoceen en hebben vaak een maximale ouderdom van ca. 50.000 jaar (dat is namelijk het ^{14}C-dateringsbereik, wat overeenkomt met 45.000 ^{14}C jaar BP of ~ 50.000 jaar geleden). Succesvol stabiele isotopenonderzoek blijft niet beperkt tot monsters binnen het ^{14}C-dateringsbereik. Zolang collageen goed bewaard is gebleven, kunnen ook oudere monsters betrouwbare stabiele isotopengegevens opleveren. Die kunnen vervolgens worden gebruikt om bijvoorbeeld het dieet van specifieke soorten en de milieuomstandigheden verder terug in de tijd te reconstrueren. Dit gaat zelfs terug tot het Vroeg-Paleolithicum (of Oude Steentijd), zoals het onderzoek van de fossielen uit Schöningen - geschat op een ouderdom van ongeveer 300.000 jaar oud - laat zien.

Na de inleiding (**Hoofdstuk 1**), bespreekt **Hoofdstuk 2** de basisprincipes van het onderzoek van stabiele koolstof- en stikstofisotopen, de toepassingen ervan en de gebruikte analytische methoden. Het merendeel van de stabiele isotopengegevens die in dit proefschrift worden besproken, is afkomstig van het Centrum voor Isotopenonderzoek (CIO) van de Universiteit Groningen. De manier waarop de monsters zijn voorbehandeld en gemeten bij het CIO, wordt in het kort beschreven in dit hoofdstuk.

Stabiele isotopenwaarden kunnen worden gemeten in monsters die afkomstig zijn van allerlei lichaamsweefsels van mensen en dieren, zoals haar, botten en tanden. De hier gepresenteerde studies maken voornamelijk gebruik van (bulk)collageen uit bot. Collageen is rijk aan koolstof en stikstof. Het is het meest voorkomende eiwit in zoogdieren en het draagt bij aan de elasticiteit van beenderen. Voordat collageen geschikt is voor onderzoek naar stabiele isotopen wordt het chemisch geïsoleerd in een laboratorium.

Stabiele isotopen worden gemeten met behulp van massaspectrometrie (MS). Voor isotopenverhoudingen is een speciale vorm van MS ontwikkeld: isotopenratio massaspectrometrie (IRMS). De machine werkt met moleculaire gassen. Daarom moet het collageen van het beoogde monster eerst worden verbrand, waarbij de gassen CO_2 en N_2 vrijkomen. Pas dan kunnen de isotopenwaarden van respectievelijk koolstof en stikstof gemeten worden. De isotopenverhouding verkregen uit een monster wordt vergeleken met die van referentiemateriaal en wordt weergegeven in zogenaamde δ-waarden (deltawaarden). De numerieke waarden voor δ zijn erg klein. Daarom worden ze uitgedrukt in promille (‰, gelijk aan 10^{-3}).

Hoofdstuk 3 bespreekt een grote dataset van $\delta^{13}C$-waarden (stabiele koolstofwaarden) en $\delta^{15}N$-waarden (stabiele stikstofwaarden) van wolharige mammoeten (*Mammuthus primigenius*) uit het Laat-Pleistoceen en het Holoceen uit Noordoost-Siberië. Dit gebied werd min of meer continu bewoond door de wolharige mammoet vanaf zijn verschijnen (~ 400.000 jaar geleden) tot zijn uitsterven (~ 4.000 jaar geleden).

De meest recente wolharige mammoet met een leeftijd van 3685 ± 60 ^{14}C jaar BP komt van het legendarische eiland Wrangel in de Noordelijke IJszee, ten noorden van het vasteland van het Russische district Tsjoekotka. Het doel van de stabiele isotopenstudies van de Oost-Siberische mammoet, is het volgen van mogelijke verschuivingen in de stabiele koolstof- en stikstofdata die samenvallen met wereldwijde klimaatveranderingen, zoals waargenomen in andere delen van het mammoetsteppe-bioom. Bovendien wijzen de studies uit of het dieet van de mammoet en daarmee het stabiele isotopensignaal in het fossiele botweefsel veranderde toen de soort zijn uitsterven naderde. Speciale aandacht wordt gevestigd op de Holocene gegevens van fossielen afkomstig van Wrangel; gegevens die bijdragen aan onze kennis van de omstandigheden waaronder de laatste mammoeten leefden.

De data onthullen een opmerkelijke stabiliteit in δ^{13}C- en δ^{15}N-waarden van skeletresten van de wolharige mammoet in Noordoost-Siberië tijdens het laatste deel van het Laat-Pleistoceen. Deze continuïteit van stabiele isotopenwaarden staat in schril contrast met de gepubliceerde gegevens van monsters van wolharige mammoeten en andere grote herbivoren uit Europa en Alaska. Nog opmerkelijker, wolharige mammoeten handhaafden vergelijkbare δ^{13}C- en δ^{15}N-waarden gedurende het Holoceen. Dat blijkt met name uit de resultaten van gemeten fossielen van wolharige mammoeten van het eiland Wrangel, waar ze tot ongeveer 2100 v.Chr. leefden. De stabiele isotopengegevens geven aan dat Holocene mammoeten van Wrangel zich met bronnen voedden die dezelfde isotopenverhouding hadden als die op het vasteland van Noord-Siberië tijdens het laatste deel van het Laat-Pleistoceen. Dit suggereert, althans in brede zin, dat het dieet van de mammoeten op Wrangel niet wezenlijk veranderde gedurende het Laat-Pleistoceen en Holoceen.

Waar Hoofdstuk 3 gegevens over de omstandigheden van de oostkant van het mammoetsteppe ecosysteem beschrijft, richt **Hoofdstuk 4** zich op isotopengegevens van fossielen afkomstig uit het westelijk deel van de mammoetsteppe, namelijk het Noordzeegebied. Tijdens het Weichselien (de laatste ijstijd) daalde de zeespiegel drastisch en een landmassa, die kan worden beschouwd als de westelijke uitbreiding van de Noord-Europese vlakte, verbond het Europese continent met Groot-Brittannië. Deze landmassa werd doorsneden door grote rivieren en was begroeid met een karakteristieke mammoetsteppevegetatie. De grote hoeveelheid fossielen, waaronder overblijfselen van de Neanderthaler en anatomisch moderne mens, geven aan dat het gebied werd bewoond door de typische mammoetsteppefauna met soorten als de wolharige mammoet, de wolharige neushoorn (*Coelodonta antiquitatis*) en grote carnivoren zoals holenhyena's (*Crocuta spelaea*) en holenleeuwen (*Panthera spelaea*). In de afgelopen decennia zijn duizenden fossiele overblijfselen verzameld, vaak vanuit een stratigrafisch verstoorde context. Om de vondsten desondanks in een chronologische context te kunnen plaatsen, is de ouderdom van veel fossielen bepaald met behulp van de koolstofdatering. Dit heeft geresulteerd in een grote dataset met ^{14}C-gegevens en δ^{13}C- en δ^{15}N-waarden, van zowel dieren als mensen. Deze gegevens worden gepresenteerd en besproken in Hoofdstuk 4.

Een deel van de resultaten van de stabiele isotopenmetingen is vergelijkbaar met die van gepubliceerde data van omnivoren, herbivoren en carnivoren die in het verleden elders in Noordwest-Europa vergelijkbare gebieden bewoonden. Daarnaast bevat deze grote Noordzee-dataset soorten waarvan δ^{13}C- en δ^{15}N-gegevens voorheen niet of nauwelijks bekend waren, zoals bosolifant (*Palaeoloxodon antiquitatis*), otter (*Lutra lutra*), veelvraat (*Gulo gulo*) en reuzenalk (*Pinguinus impennis*).

De stabiele isotopengegevens kunnen worden gebruikt om verder in te zoomen op vragen met betrekking tot dierlijke fossiele overblijfselen van het Noordwestelijke Europese vasteland en het Verenigd Koninkrijk. Bovendien wordt een grote hoeveelheid

nieuwe stabiele isotopengegevens voor grote zeezoogdieren en menselijke resten uit de Noordzee gepresenteerd. De meeste menselijke botten hebben δ^{15}N-waarden die wijzen op een dieet bestaande uit onder andere aquatische voedselbronnen. De δ^{13}C-waarden van de Mesolithische mensen zijn over het algemeen indicatief voor zoetwatervoedsel. De δ^{13}C-waarden van menselijke botten uit latere periodes wijzen op een gemengd dieet van mariene, zoetwater en terrestrische voedselbronnen.

Deze studie, gebaseerd op een grote hoeveelheid meetgegevens, illustreert dat een verzameling van losse vondsten zonder een stratigrafische context toch een waardevolle bijdrage kan leveren aan de reconstructie van de leefomgeving in het verleden.

Fossiele overblijfselen van de karakteristieke Pleistocene megafauna in Zuidoost-Europa en aangrenzende gebieden in Azië tonen aan dat het mammoetsteppe-bioom zich ook tot in die regio's uitstrekte. **Hoofdstuk 5** presenteert gegevens van een zeer tot de verbeelding sprekende uitgestorven diersoort die leefde in het zuidelijke deel van de mammoetsteppe, namelijk de 'Siberische eenhoorn' (*Elasmotherium sibiricum*). Algemeen werd aangenomen dat deze gigantische soort neushoorn in de steppezone van Oost-Europa en Azië leefde tot ca. 200.000 jaar geleden. Recent gepubliceerde ^{14}C-gegevens van fossielen van verschillende vindplaatsen leveren echter overtuigend bewijs dat deze diersoort pas veel later uitstierf, namelijk tijdens het Laat-Pleistoceen. Veranderingen in de omgevingscondities kunnen mogelijk het uitsterven van de soort verklaren. Een bijkomend, interessant onderwerp is het dieet van *Elasmotherium*. De soort heeft extreem hoogkronige kiezen zonder wortel; een kenmerk van een aanpassing aan voedsel dat een zeer hoge mate van slijtage aan het gebit veroorzaakt. Bij het eten van plantenwortels komt er veel zand mee, wat betekent dat de tanden van het dier snel slijten. De δ^{13}C- en δ^{15}N-waarden van de Siberische Eenhoorn vormen een belangrijke proxy in het debat over het dieet van deze Siberische eenhoorn. De gegevens wijzen op een zeer gespecialiseerd dieet en ondersteunen het idee van de consumptie van ondergrondse plantendelen. De δ^{13}C- en δ^{15}N-waarden van de Siberische eenhoorn verschillen sterk van die van andere fossiele neushoorns uit Eurazië.

De conservering van collageen in fossielen met een ouderdom tot 50.000 jaar is vaak beter dan die van fossielen die veel ouder zijn. **Hoofdstuk 6** bespreekt de koolstof- en stikstofisotopengegevens die succesvol zijn gemeten in dierlijke fossielen uit Schöningen in de Duitse deelstaat Nedersaksen. Vanwege de leeftijd van de botmonsters (~ 300.000 jaar oud) is speciale aandacht besteed aan de conserveringsgraad van het collageen. Schöningen is een zeer belangrijke archeologische vindplaats die in de jaren '90 van de vorige eeuw wereldwijde bekendheid kreeg door de ontdekking van zorgvuldig vervaardigde houten speren. Deze werden gevonden te midden van een grote hoeveelheid fossielen van geslachte dieren, met name van paarden.

Het onderzoek toont aan dat een groot deel van de fossielen een uitstekende conservering heeft, niet alleen op macroscopisch niveau, maar ook op moleculair

niveau. $\delta^{13}C$- en $\delta^{15}N$-waarden zijn gemeten aan fossielen van vijf taxonomisch verschillende groepen: Elephantidae, Rhinocerotidae, Equidae, Cervidae en Bovidae. De isotopengegevens geven onder andere informatie over hoe het landschap er toentertijd uitzag en dan met name over de mate van bebossing.

De resultaten van de in de hoofdstukken 3-6 gepresenteerde casestudies zijn geïntegreerd en bediscussieerd in **Hoofdstuk 7**. Bovendien wordt naar aanleiding van de gepresenteerde gegevens een aantal intrigerende onderwerpen extra uitgelicht, zoals afwijkende $\delta^{15}N$-resultaten, problemen met betrekking tot het gebruik van geschikte modelsoorten, en het uitsterven van de wolharige mammoet tijdens het Laat-Pleistoceen.

De gepresenteerde resultaten leveren een bijdrage aan bestaande wetenschappelijke debatten. Zo geven de grote hoeveelheid $\delta^{13}C$- en $\delta^{15}N$-waarden van Holocene wolharige mammoeten van het eiland Wrangel een duidelijker beeld van de omstandigheden waarin mammoeten leefden vlak voor het uitsterven van de soort. Daarnaast leveren de $\delta^{13}C$- en $\delta^{15}N$-waarden van fossielen uit Schöningen een bijdrage aan het debat over de omgevingsfactoren waarin de mensachtigen opereerden.

   Bovendien tonen de resultaten dat stabiele isotopenanalyse een belangrijke aanvullende bijdrage kan leveren op resultaten die verkregen zijn met andere archeologische methoden. Dit wordt geïllustreerd door de stabiele isotopengegevens van de Siberische eenhoornfossielen en die van de paarden uit Schöningen. Zo ondersteunen de $\delta^{15}N$-gegevens dat het dieet van de paarden uit Schöningen voor een aanzienlijk deel uit bladeren en twijgen bestond. Hun morfologisch afwijkende kiezen wijzen tevens in die richting.

   Ook illustreren de resultaten van Schöningen dat de ouderdom van fossielen op zichzelf geen beperkende factor hoeft te zijn voor het verkrijgen van $\delta^{13}C$- en $\delta^{15}N$-data. Als de $\delta^{13}C$- en $\delta^{15}N$-analyse van botcollageen van oude monsters op voorhand wordt uitgesloten op basis van hun ouderdom, missen we mogelijk belangrijke informatie. Stabiele isotopengegevens van de bosolifanten zou dan bijvoorbeeld niet gemeten zijn. Terwijl die van bosolifanten uit Schöningen (zie Hoofdstuk 6) en het Noordzeegebied (zie Hoofdstuk 4) echter onthulden dat deze olifanten opvallend hogere $\delta^{15}N$-waarden hebben ten opzichte van die van andere, gelijktijdig levende, grote terrestrische herbivoren. Dit patroon doet sterk denken aan een veelbesproken fenomeen van hogere $\delta^{15}N$-waarden van wolharige mammoeten ten opzichte van andere Laat-Pleistocene herbivoren. Deze nieuwe informatie wijst erop dat dit $\delta^{15}N$-fenomeen karakteristiek voor olifantachtigen kan zijn.

Al met al draagt dit proefschrift, een studie van stabiele isotopengegevens van zoogdierfossielen, bij aan onze kennis van de ecologische omstandigheden tijdens het Pleistoceen/Vroeg-Holoceen in Eurazië.

References

Adams, T.S., Sterner, R.W., 2000. The effect of dietary nitrogen content on trophic level ^{15}N enrichment. *Limnology and Oceanography* **45** (3), 601-607.

Agam, A., Barkai, R., 2018. Elephant and Mammoth Hunting during the Paleolithic: A Review of the Relevant Archaeological, Ethnographic and Ethno-Historical Records. *Quaternary* **1** (3), 1-28.

Aitken, S.N., Whitlock, M.C., 2013. Assisted gene flow to facilitate local adaptation to climate change. *Annual review of ecology, evolution, and systematics* **44**, 367-388.

Ambrose, S.H., 1990. Preparation and characterization of bone and tooth collagen for isotopic analysis. *Journal of Archaeological Science* **17**, 431-451.

Ambrose, S.H., 1991. Effects of diet, climate and physiology on nitrogen isotope abundances in terrestrial foodwebs. *Journal of Archaeological Science* **18**, 293-317.

Ambrose, S.H., 1993. Isotopic analysis of palaeodiets: methodical and interpretive considerations. In: Sandford, M.K. (Ed.) *Investigation of ancient human tissue: chemical analysis in anthropology*. Gordon & Breach (New York), 59–130.

Ambrose, S.H., 2000. Controlled diet and climate experiments on nitrogen isotope ratios of rats. In: Ambrose, S.H., Katzenberg, M.A. (Eds.). *Biogeochemical approaches to paleodietary analysis*. Kluwer Academic/Plenum Publishers (New York), 243-259.

Ambrose, S.H., DeNiro, M.J., 1986. The isotopic ecology of East African mammals. *Oecologia* **69**, 395-406.

Amkreutz, L., Verpoorte, A., Waters-Rist, A., Niekus, M., van Heekeren, V., van der Merwe, L., van der Plicht, J., Glimmerveen, J., Stapert, D., Johansen, L., 2018a. What lies beneath… Late Glacial human occupation of the submerged North Sea landscape. *Antiquity* **92**, 22-37.

Amkreutz, L., Verpoorte, A., Waters-Rist, A., Niekus, M., van Heekeren, V., van der Merwe, L., van der Plicht, J., Glimmerveen, J., Stapert, D., Johansen, L., 2018b. IJstijdjagers op de bodem van de Noordzee. *Cranium* **35**, 41-45.

Andreev, A.A., Schirrmeister, L., Tarasov, P.E., Ganapolski, A., Brovkin, V., Siegert, C., Wetterich, S., Hubbertsen, H.-W., 2011. Vegetation and climate history in the Laptev Sea region (Arctic Siberia) during Late Quaternary inferred from pollen records. *Quaternary Science Reviews* **30**, 2182-2199.

Arneborg, J., Heinemeier, J., Lynerup, N., Nielsen, H.L., Rude, N., Sveinbjornsdotir, A.E., 1999. Change of diet of the Greenland Vikings determined from stable carbon isotope analysis. *Radiocarbon* **41**, 157-168.

Arppe, L., Karhu, J.A., Vartanyan, S., Drucker, D.G., Ehu-Sihvola, H., Bocherens, H., 2019. Thriving or surviving? The isotopic record of the Wrangel Island woolly mammoth population. *Quaternary Science Reviews* **222**, 105884.

Badeck, F.-W., Tcherkez, G., Nogués, S., Piel, C., Ghashghaie, J., 2005. Postphotosynthetic fractionation of stable carbon isotopes between plant organs—a widespread phenomenon. *Rapid Communications in Mass Spectrometry* **19**, 1381–1391.

Bassis, J.N., Petersen, S.V., Mac Cathles, L., 2017. Heinrich events triggered by ocean forcing and modulated by isostatic adjustment. *Nature* **542**, 332.

Ben-David, M., Shochat, E., Adams, L., 2001. Utility of stable isotope analysis in studying foraging ecology of herbivores: examples from moose and caribou. *Alces* **37**, 421-434.

Blinnikov, M.S., Gaglioti, B.V., Walker, D.A., Wooller, M.J., Zazula, G.D., 2011. Pleistocene graminoid-dominated ecosystems in the Arctic. *Quaternary Science Reviews* **30** (21-22), 2906-2929.

Bocherens, H, Drucker, D., Billiou, D., Moussa, I., 2005. Une nouvelle approche pour évaluer l'état de conservation de l'os et du collagène pour les mesures isotopiques (datation au radiocarbone, isotopes stables du carbone et de l'azote). *L'Anthropologie* **109** (3), 557-567.

Bocherens, H., 2003. Isotopic biogeochemistry and the paleoecology of the mammoth steppe fauna. In: Reumer, J.W.F., de Vos, J., Mol, D. (Eds.). Advances in mammoth research (Proceedings of the Second International Mammoth Conference, Rotterdam, May 16–20 1999). *Deinsea* **9**, pp. 57–76.

Bocherens, H., Billiou, D., Patou-Mathis, M., Bonjean, D., Otte, M., Mariotti, A., 1997a. Paleobiological implications of the isotopic signatures (^{13}C, ^{15}N) of fossil mammal collagen in Scladina Cave (Sclayn, Belgium). *Quaternary Research* **48**, 370-380.

Bocherens, H., Billiou, D., Patou-Mathis, M., Otte, M., Bonjean, D., Toussaint, M., Mariotti, A., 1999. Palaeoenvironmental and palaeodietary implications of isotopic biogeochemistry of late interglacial Neandertal and mammal bones in Scladina Cave (Belgium). *Journal of Archaeological Science* **26** (6), 599-607.

Bocherens, H., Drucker, D., 2003. Trophic level isotopic enrichments for carbon and nitrogen in collagen: case studies from recent and ancient terrestrial ecosystems. *International Journal of Osteoarchaeology* **13**, 46-53.

Bocherens, H., Drucker, D.G., 2007. Terrestrial Teeth and Bones. In: Elias, S.A. (Ed.). *Encyclopedia of Quarternary Research*, 309–317.

Bocherens, H., Fizet, M., Mariotti, A., Gangloff, R.A., Burns, J.A., 1994. Contribution of biochemistry (^{13}C, ^{15}N, ^{18}O) to the paleoecology of mammoths (*Mammuthus primigenius*). *Historical Biology* **7** (3), 187-202.

Bocherens, H., Germonpré, M., Toussaint, M., Semal, P., 2013. XVII. Stable isotopes. In: Semal, P., Hauzeur, A. (Eds.). *Spy Cave: State of 125 Years of Pluridisciplinary Research on the Betche-aux-Rotches from Spy (Jemeppe-sur-Sambre, Province of Namur, Belgium).* Royal Belgian Institute of Natural Sciences, 357-371.

Bocherens, H., Michaux, J., Garcia Talavera, F., van der Plicht, J., 2006b. Extinction of endemic vertebrates on islands: the case of the giant rat Canariomys bravoi (Mammalia, Rodentia) on Tenerife (Canary Islands, Spain). *Comptes Rendus Palévol* **5** (7), 885-891.

Bocherens, H., Pacaud, G., Lazarev, P.A., Mariotti, A., 1996. Stable isotope abundances (^{13}C, ^{15}N) in collagen and soft tissues from Pleistocene mammals from Yakutia:

Implications for the palaeobiology of the mammoth steppe. *Palaeogeography, Palaeoclimatology, Palaeoecology* **126**, 31–44.

Bocherens, H., Tresset, A., Wiedemann, F., Giligny, F., Lafage, F., Lanchon, Y., Mariotti, A., 1997b. Bone diagenetic evolution in two French Neolithic sites. *Bulletin de la Société Géologique de France* **168** (5), 555-564.

Bocherens, K., Drucker, D.G., Billiou, D., Geneste, J.M., van der Plicht, J., 2006a. Bears and humans in Chauvet Cave (Vallon-Pont-d'Arc, Ardèche, France): insights from stable isotopes and radiocarbon dating of bone collagen. *Journal of Human Evolution* **50**, 370-376.

Boeskorov, G. G., Lazarev, P.A., Sher, A.V., Davydov, S.P., Bakulina, N.T., Shchelchkova, M.V., Binladen, J., Willerslev, E., Buigues, B., Tikhonov, A.N., 2011. Woolly rhino discovery in the lower Kolyma River. *Quaternary Science Reviews* **30**, 2262–2272.

Boeskorov, G.G., 2006. Arctic Siberia: refuge of the Mammoth fauna in the Holocene. *Quaternary international* **142**, 119-123.

Boeskorov, G.G., Potapova, O.R., Protopopov, A.V., Plotnikov, V.V., Maschenko, E.N., Shchelchkova, M.V., Petrova, E.A., Kowalczyk, R., van der Plicht, J., Tikhonov, A.N., 2018. A study of a frozen mummy of a wild horse from the Holocene of Yakutia, East Siberia, Russia. *Mammal Research* **63** (3), 307-314.

Boivin, N.L., Zeder, M.A., Fuller, D.Q., Crowther, A., Larson, G., Erlandson, J.M., Denham, T., Petraglia, M.D., 2016. Ecological consequences of human niche construction: Examining long-term anthropogenic shaping of global species distributions. *Proceedings of the National Academy of Sciences* **113** (23), 6388-6396.

Braje, T.J., Erlandson, J.M., 2013. Human acceleration of animal and plant extinctions: A Late Pleistocene, Holocene, and Anthropocene continuum. *Anthropocene* **4**, 14-23.

Braun, I.M., Palombo, M.R., 2012. *Mammuthus primigenius* in the cave and portable art: An overview with a short account on the elephant fossil record in Southern Europe during the last glacial. *Quaternary International* **276**, 61-76.

Braunisch, V., Bollmann, K., Graf, R.F., Hirzel, A.H., 2008. Living on the edge—modelling habitat suitability for species at the edge of their fundamental niche. *Ecological modelling* **214** (2-4), 153-167.

Brigham-Grette, J., Gualtieri, L., 2004. Response to Grosswald and Hughes (2004), Brigham-Grette et al. (2003), "Chlorine-36 and [14]C Chronology support a limited last glacial maximum across central Chukotka, northeastern Siberia, and no Beringian ice Sheet," and Gualtieri et al. (2003), "Pleistocene raised marine deposits on Wrangel Island, northeastern Siberia: implications for Arctic ice sheet history". *Quaternary Research* **62**, 227-232.

Britton, K., Gaudzinski-Windheuser, S., Roebroeks, W., Kindler, L., Richards, M.P., 2012. Stable isotope analysis of well-preserved 120,000-year-old herbivore bone collagen from the Middle Palaeolithic site of Neumark-Nord 2, Germany reveals niche separation between bovids and equids. *Palaeogeography, Palaeoclimatology, Palaeoecology* **333-334**, 168-177.

Brock, F., Higham, T., Bronk Ramsey, C., 2010. Pre-screening techniques for identification of samples suitable for radiocarbon dating of poorly preserved bones. *Journal of Archaeological Science* **37**, 855–865.

Brock, F., Wood, R., Higham, T.F.G., Ditchfield, P., Bayliss, A., Bronk Ramsey C., 2012. Reliability of nitrogen content (% N) and carbon: nitrogen atomic ratios (C:N) as indicators of collagen preservation suitable for radiocarbon dating. *Radiocarbon* 54, 879–886.

Bronk Ramsey, C., 2009. Bayesian analysis of radiocarbon dates. Radiocarbon **51**, 337–360.

Broughton, J.M., Weitzel, E.M., 2018. Population reconstructions for humans and megafauna suggest mixed causes for North American Pleistocene extinctions. *Nature communications* **9**, 5441.

Busschers, F., Westerhof, W., van Heteren, S., 2013. *Het stratigrafisch raamwerk voor de geologische opbouw van het zandwingebied Maasvlakte 2. Rapport 1 van het geoarcheologisch en paleontologisch onderzoek zandwingebied en buitencontour Maasvlakte 2.* TNO (Utrecht).

Busschers, F.S., Wesselingh, F., Kars, R.H., Versluijs-Helder, M., Wallinga, J., Bosch, J.H.A., Timmner, J., Nierop, K.G.J., Meijer, T., Bunnik, F.P.M., De Wolf, H., 2014. Radiocarbon Dating of Late Pleistocene Marine Shells from the Southern North Sea. *Radiocarbon* **56**, 1151-1166.

Cammidge, T., Kooyman, B., Theodor, J.M., 2019. Diet reconstructions for end-Pleistocene *Mammut americanum* and *Mammuthus* based on comparative analysis of mesowear, microwear, and dental calculus in modern Loxodonta africana. *Palaeogeography, Palaeoclimatology, Palaeoecology*, 109403.

Carr, S.J., Holmes, R.V.D., van der Meer, J.J.M., Rose, J., 2006. The Last Glacial Maximum in the North Sea Basin: micromorphological evidence of extensive glaciation. *Journal of Quaternary Science* **21** (2), 131-153.

Caut, S., Angulo, E., Courchamp, F., 2008. Caution on isotopic model use for analyses of consumer diet. *Canadian Journal of Zoology* **86** (5), 438-445.

Chase, J.M., Leibold, M.A., 2003. *Ecological niches: linking classical and contemporary approaches.* University of Chicago Press (Chicago).

Cohen, K.M., Gibbard, P.L., Weerts, H.J.T., 2014. North Sea palaeo-geographical reconstructions for the last 1 Ma. *Netherlands Journal of Geosciences* **93**, 7-29.

Cohen, K.M., MacDonald, K., Joordens, J.C.A., Roebroeks, W., and Gibbard, P.L., 2011. Earliest occupation of north-west Europe: a coastal perspective. *Quaternary International* **271**, 70-83.

Cook, G.T., Bonsall, C., Hedges, R.E.M., McSweeney, K.M., Boronean, V., Pettitt, P.B., 2001. A freshwater diet-derived ^{14}C reservoir effect at the Stone Age sites in the Iron Age gorge. *Radiocarbon* **43**, 453-460.

Cooper, A., Turney, C., Hughen, K.A., Brook, B.W., McDonald, H.G., Bradshaw, C.J.A., 2015. Abrupt warming events drove Late Pleistocene Holarctic megafaunal turnover. *Science* **349**, 602-606.

Craig, H., 1953. The geochemistry of the stable carbon isotopes. *Geochimica et Cosmochimica Acta* **3** (2-3), 53-92.

Cubas, M., Peyroteo-Stjerna, R., Fontanals-Coll, M., Llorente-Rodríguez, L., Lucquin, A., Craig, O.E., Colonese, A.C., 2019. Long-term dietary change in Atlantic and Mediterranean Iberia with the introduction of agriculture: a stable isotope perspective. *Archaeological and Anthropological Sciences* **11**, 3825-3836.

Debruyne, R., Chu, G., King, C.E., Bos, K., Kuch, M., Schwarz, C., Szpak, P., Gröcke, D.R., Matheus, P., Zazula, G., Guthrie, D., Froese, D., Buigues, B., de Marliave, C., Flemming, C., Poinar, D., Fisher, D., Southon, J., Tikhonov, A.N., MacPhee, R.D.E., Poinar, H.N., 2008. Out of America: ancient DNA evidence for a New World origin of Late Quaternary woolly mammoths. *Current Biology* **18**, 1320-1326.

Dee, M.W., Palstra, S.W.L., Aerts-Bijma, A.Th., Bleeker, M.O., de Bruijn, S., Ghebru, F., Jansen, H.G., Kuitems, M., Paul, D., Richie, R.R., Spriensma, J.J., Scifo, A., van Zonneveld, D., Verstappen-Dumoulin, B.M.A.A., Wietzes-Land, P., Meijer, H.A.J., 2019. Radiocarbon Dating at Groningen: New and Updated Chemical Pretreatment Procedures. *Radiocarbon*, 1-12. DOI:10.1017/RDC.2019.101.

Dehn, L.A., Sheffield, G.G., Follmann, E.H., Duffy, L.K., Thomas, D.L., O'Hara, T.M., 2007. Feeding ecology of phocid seals and some walrus in the Alaskan and Canadian Arctic as determined by stomach contents and stable isotope analysis. *Polar Biology* **30**, 167-181.

De Loecker, D., 2010. *Great Yarmouth dredging license Area 240, Norfolk, United Kingdom. Preliminary report on the lithic artefacts.* Unpublished manuscript, Faculty of Archaeology, Leiden University (Leiden).

DeNiro, M.J., 1985. Postmortem preservation and alteration of in vivo bone collagen isotope ratios in relation to paleodietary reconstruction. *Nature* **317** (6040), 806-809.

DeNiro, M.J., Epstein, S., 1976. You are what you eat (plus a few ‰): the carbon isotope cycle in food chains. *Geological Society of America* **6**, 834.

DeNiro, M.J., Epstein, S., 1981. Influence of diet on the distribution of nitrogen isotopes in animals. *Geochimica et Cosmochimica Acta* **45**, 341–351.

Di Febbraro, M., Carotenuto, F., Castiglione, S., Russo, D., Loy, A., Maiorano, L., Raia, P., 2017. Does the jack of all trades fare best? Survival and niche width in Late Pleistocene megafauna. *Journal of Biogeography* **44**, 2828-2838.

Doppler, T., Gerling, C., Heyd, V., Knipper, C., Kuhn, T., Lehmann, M.F., Pike, A.W.G., Schibler, J., 2017. Landscape opening and herding strategies: Carbon isotope analyses of herbivore bone collagen from the Neolithic and Bronze Age lakeshore site of Zurich-Mozartstrasse, Switzerland. *Quaternary International* **436**, 18-28.

Drucker, D.G., Bocherens, H., Péan, S., 2014. Isotopes stables (^{13}C, ^{15}N) du collagène des mammouths de Mezhyrich (Epigravettien, Ukraine): implications paléoécologiques. *L'Anthropologie* **118**, 504–517.

Drucker, D., Bocherens, H., Bridault, A., Billiou, D., 2003a. Carbon and nitrogen isotopic composition of red deer (*Cervus elaphus*) collagen as a tool for tracking

palaeoenvironmental change during the Late-Glacial and Early Holocene in the northern Jura (France). *Palaeogeography, Palaeoclimatology, Palaeoecology* **195** (3-4), 375-388.

Drucker, D.G., Bocherens, H., 2009. Carbon stable isotopes of mammal bones as tracers of canopy development and habitat use in temperate and boreal contexts. In: Creighton, J.D., Roney, P.J. (Eds.). *Forests canopies: Forest production, ecosystem health, and climate conditions.* Nova Science Publishers (USA), 103-109.

Drucker, D.G., Bocherens, H., Billiou, D., 2003b. Evidence for shifting environmental conditions in Southwestern France from 33000 to 15000 years ago derived from carbon-13 and nitrogen-15 natural abundances in collagen of large herbivores. *Earth and Planetary Science Letters* **216**, 163–173.

Drucker, D.G., Bridault, A., Hobson, K.A., Szuma, E., Bocherens, H., 2008. Can carbon-13 abundances in large herbivores track canopy effect in temperature and boreal ecosystems? Evidence from modern and ancient ungulates. *Palaeogeography, Palaeoclimatology, Palaeoecology* **266**, 69-82.

Drucker, D.G., Hobson, K.A., Ouellet, J.-P., Courtois, R., 2010. Influence of forage preferences and habitat use on ^{13}C and ^{15}N abundance in wild caribou (*Rangifer tarandus caribou*) and moose (*Alces alces*) from Canada. *Isotopes in Environmental and Health Studies* **46**, 107-121.

Drucker, D.G., Stevens, R.E., Germonpré, M., Sablin, M.V., Péan, S., Bocherens, H., 2018. Collagen stable isotopes provide insights into the end of the mammoth steppe in the central East European plains during the Epigravettian. *Quaternary Research* **90** (3), 457-469.

Drucker, D.G., Vercoutere, C., Chiotti, L., Nespoulet, R., Crépin, L., Conard, N.J., Münzel, S.C., Higham, T., van der Plicht, J., Lázničková-Galetová, M. and Bocherens, H., 2015. Tracking possible decline of woolly mammoth during the Gravettian in Dordogne (France) and the Ach Valley (Germany) using multi-isotope tracking (^{13}C, ^{14}C, ^{15}N, ^{34}S, ^{18}O). *Quaternary International* **360**, 304–317.

Elias, S.A., Crocker, B., 2008. The Bering Land Bridge: a moisture barrier to the dispersal of steppe–tundra biota? *Quaternary Science Reviews* **27**, 2473–2483.

Firestone, R.B., West, A., Kennett, J.P., Becker, L., Bunch, T.E., Revay, Z.S., Schultz, P.H, Belgya, T., Kennett, D.J., Erlandson, J.M., Dickenson, O.J., Goodyear, A.C., Harris, R.S., Howard, G.A., Kloosterman, J.B., Lechler, P., Mayewski, P.A., Montgomery, J., Poreda, R., Darrah, T., Que Hee, S.S., Smith, A.R., Stich, A., Topping, W., Wittke, J.H., Wolbach, W.S., 2007. Evidence for an extraterrestrial impact 12,900 years ago that contributed to the megafaunal extinctions and the Younger Dryas cooling. *Proceedings of the National Academy of Sciences* **104** (41), 16016-16021.

Fischer, A., Olsen, J., Richards, M., Heinemeier, J., Sveinbjornsdottir, A.E., Bennike, P., 2007. Coast-inland mobility and diet in the Danish Mesolithic and Neolithic: evidence from stable isotope values of humans and dogs. *Journal of Archaeological Science* **34**, 2125-2150.

Fox-Dobbs, K., Leonard, J.A., Koch, P.L., 2008. Pleistocene megafauna from eastern Beringia: Paleoecological and paleoenvironmental interpretations of stable carbon and nitrogen isotope and radiocarbon records. *Palaeogeography, Palaeoclimatology, Palaeoecology* **261**, 30–46.

Fox, D.L., Fisher, D.C., Vartanyan S., Tikhonov, A.N., Mol, D., Buigues, B., 2007. Paleoclimatic implications of oxygen isotopic variation in late Pleistocene and Holocene tusks of *Mammuthus primigenius* from northern Eurasia. *Quaternary International* **169–170**, 154–165.

Fry, E., Kim, S.K., Chigurapti, S., Mika, K.M., Ratan, A., Dammermann, A., Mitchell, B.J., Miller, W., Lynch, V.J., 2018. Functional architecture of deleterious genetic variants in the Wrangel Island mammoth genome. *BioRxiv* 137455, DOI: https://doi.org/10.1101/137455.

Fuller, B.T., Fuller, J.L., Sage, N.E., Harris, D.A., O'Connell, T.C., Hedges, R.E.M., 2005. Nitrogen balance and δ^{15}N: why you're not what you eat during nutritional stress. *Rapid Communication in Mass Spectrometry* **19**, 2497–2506.

Gaffney, V., Thomsen, K., Fitch, S. (Eds.). 2007. Mapping Doggerland: the Mesolithic landscapes of the southern North Sea. *Archaeopress* (Oxford).

Gannes, L.Z., Martínez del Rio C., Koch, P., 1998. Natural abundance variations in stable isotopes and their potential uses in animal physiological ecology. *Comparative Biochemistry and Physiology* **119A** (3), 725–737.

Gebert, C., Verheyden-Tixier, H., 2001. Variations of diet composition of red deer (*Cervus elaphus* L.) in Europe. *Mammal Review* **31**, 189-201.

van Geel, B., Aptroot, A., Baittinger, C., Birks, H.H., Bull, I.D., Cross, H.B., Evershed, R.P., Gravendeel, B., Kompanje, E.J.O., Kuperus, P., Mol, D., Nierop, K.G.J., Pals, J.P., Tikhonov, A.N., van Reenen, G., van Tienderen, P.H., 2008. The ecological implications of a Yakutian mammoth's last meal. *Quaternary Research* **69**, 361-376.

van Geel, B., Guthrie, R.D., Altmann, J.G., Broekens, P., Bull, I.D., Gill, F.L., Jansen, B., Nieman, A.M., Gravendeel, B., 2011. Mycological evidence of coprophagy from the feces of an Alaskan Late Glacial mammoth. *Quaternary Science Reviews* **30**, 2289-2303.

Gerasimov, D.V., Giria, E.Y., Pitul'ko, V.V., Tikhonov, A.N., 2006. New Materials for the interpretation of the Chertov Ovrag Site on Wrangel Island. In: Dumond, D.E, Bland, R.L. (Eds.). *Archaeology in Northeast Asia: on the pathway to Bering Strait*. Museum of Natural and Cultural History, and Department of Anthropology, University of Oregon, 203-206.

Gill, J.L., 2014. Ecological impacts of the late Quaternary megaherbivore extinctions. *New Phytologist* **201**, 1163-1169.

Glimmerveen, J., Mol, D., Post, K., Reumer, J.F.W, van der Plicht, J., de Vos, J., van Geel, B., van Reenen, G., Pals, J.P., 2004. The North Sea project: the first paleontological, palynological and archaeological results. In: Flemming, N.C. (Ed.) *Submarine prehistoric archaeology of the North Sea*. CBA Research Report **141**, 43-52.

Glimmerveen, J., Mol, D., van der Plicht, J., 2006. The Pleistocene Reindeer of the North

Sea: initial paleontological data and archaeological remarks. *Quaternary International* **142-143**, 242-246.

Graham, R.W., Belmecheri, S., Choy, K., Culleton, B.J., Davies, L.J., Froese, D., Heintzman, P.D., Hritz, C., Kapp, J.D., Newsom, L.A., Rawcliffe, R., Saulnier-Talbot, É., Shapiro, B., Wang, Y., Williams, J.W., Wooller, M.J., 2016. Timing and causes of mid-Holocene mammoth extinction on St. Paul Island, Alaska. *Proceedings of the National Academy of Sciences* **113**, 9310–9314.

de Groot, P.A., 2004. *Handbook of Stable Isotope Analytical Techniques*. Elsevier (Amsterdam).

Gualtieri, L., Vartanyan, S.L., Brigham-Grette, J., Anderson, P.M., 2005. Evidence for an ice-free Wrangel Island, northeast Siberia during the Last Glacial Maximum. *Boreas* **34**, 264-273.

Guil-Guerrero, J.L., Tikhonov, A., Ramos-Bueno, R.P., Grigoriev, S., Protopopov, A., Savvinov, G., González-Fernández, M.J., 2018. Mammoth resources for hominins: from omega-3 fatty acids to cultural objects. *Journal of Quaternary Science* **33**, 455-463.

Guiry, E.J., Hepburn, J.C. and Richards, M.P., 2016. High-resolution serial sampling for nitrogen stable isotope analysis of archaeological mammal teeth. *Journal of Archaeological Science* **69**, 21-28.

Guthrie R.D., 2006. New carbon dates link climatic change with human colonization and Pleistocene extinctions. *Nature* **441**, 207–209.

Guthrie, R.D., 1982. Mammals of the mammoth steppe as paleoenvironmental indicators. In: Hopkins, D.M., Matthews, J.V., Schweger, C.E., Young S.B. (Eds.). *Paleoecology of Beringia*. Academic Press (New York), 179-191.

Guthrie, R.D., 1990. *Frozen fauna of the mammoth steppe: The story of Blue Babe*. University of Chicago Press, (Chicago and London).

Guthrie, R.D., 2001. Origin and causes of the mammoth steppe: a story of cloud cover, woolly mammoth tooth pits, buckles, and inside-out Beringia. *Quaternary Science Reviews* **20**, 549-574.

Harari, Y.N., 2015. *Sapiens: A Brief History of Humankind*. Anchor books.

Harbeck, M., Grupe, G., 2009. Experimental chemical degradation compared to natural diagenetic alteration of collagen: implications for collagen quality indicators for stable isotope analysis. *Archaeological and Anthropological Sciences* **1** (1), 43-57.

Haynes, G., 2007. A review of some attacks on the overkill hypothesis, with special attention to misrepresentations and doubletalk. *Quaternary International* **169-170**, 84-94.

Haynes, G., 2009. Introduction to the volume. In: Haynes, G., (Ed.). *American Megafaunal Extinctions at the End of the Pleistocene*. Springer (Dordrecht), pp. 1-20.

Hedges, R.E.M., Millard, A.R., 1995. Bones and groundwater: Towards the modelling of diagenetic processes. *Journal of Archaeological Science* **22**, 155-164.

Hedges, R.E.M., Reynard, L.M., 2007. Nitrogen isotopes and the trophic level of humans in archaeology. *Journal of Archaeological Science* **34**, 1240-1251.

van Heteren, S., Meekes, J.A.C., Bakker, M.A.J., Gaffney, V., Fitch, S., Gearey, B.R., Paap,

B.F., 2014. Reconstructing North Sea palaeolandscapes from 3D and high-density 2D seismic data: an overview. *Netherlands Journal of Geosciences* **93**, 31-42.

Hijma, M., Westerhoff W., Roebroeks W., van Kolfschoten, Th., Cohen, K., 2011. Cultureel erfgoed in de Noordzee: hoe gaan we er mee om? *ARCHEObrief* **15** (3), 31-6.

Hijma, M.P., Cohen, K.M., Roebroeks, W., Westerhoff, W.E., Busschers, F.S., 2012. Pleistocene Rhine-Thames landscapes: geological background for hominin occupation of the southern North Sea region. *Journal of Quaternary Science* **27** (1), 17-39.

Hobbie, E.A., Högberg, P., 2012. Nitrogen isotopes link mycorrhizal fungi and plants to nitrogen dynamics. *New Phytologist* **196**, 367–382.

Hobson, K.A., Alisauskas, R.T., Clark, R.G., 1993. Stable-nitrogen isotope enrichment in avian tissues due to fasting and nutritional stress: implications for isotopic analyses of diet. *The Condor* **95** (2), 388-394.

Hoffecker, J.F., Elias, S.A., 2007. *Human ecology of Beringia*. Columbia University Press (New York).

Högberg, P., 1997. Tansley Review No. 95. ^{15}N natural abundance in soil-plant systems. *New Phytologist* **137**, 179–203.

Högberg, P., Högbom, L., Schinkel, H., Högberg, M., Johannisson, C., Wallmark, H., 1996. ^{15}N abundance of surface soils, roots and mycorrhizas in profiles of European forest soils. *Oecologia* **108**, 207-214.

Hopkins, D.M., 1982. Aspects of the paleogeography of Beringia during the Late Pleistocene. In: Hopkins, D.M., Matthews, J.V., Schweger, C.E., Young, S.B. (Eds.). *Paleoecology of Beringia*. Academic Press, 3-28.

Huckriede, R., 1967. Neues zur Geologie des Elms (Niedersachsen). *Geologica et Palaeontologica* **1**, 87-95.

Hufthammer, A.K., Svendsen, J.I., Pavlov, P., 2019. Animals and humans in the European Russian Arctic towards the end of the last Ice Age and during the mid☐ Holocene time. *Boreas* **48** (2), 387-406.

Iacumin, P., Di Matteo, A., Nikolaev, V., Kuznetsova, T.V., 2010. Climate information from C, N and O stable isotope analyses of mammoth bones from northern Siberia. *Quaternary International* **212**, 206–212.

Iacumin, P., Nikolaev, V., Ramigni, M., 2000. C and N stable isotope measurements on Eurasian fossil mammals, 40 000 to 10 000 years BP: Herbivore physiologies and palaeoenvironmental reconstruction. *Palaeogeography, Palaeoclimatology, Palaeoecology* **163**, 33–47.

Ineshin, E.M., Teten'kin, A.V., 2019. Humans and the environment in northern Baikal Siberia during the Late Pleistocene. *Cambridge Scholars Publishing* (Newcastle upon Tyne, UK).

Jacob, E., Querci, D., Caparros, M., Ruiz, C. B., Higham, T., Devièse, T., 2018. Nitrogen content variation in archaeological bone and its implications for stable isotope

analysis and radiocarbon dating. *Journal of Archaeological Science* **93**, 68-73.

Jans, M.M.E., 2005. *Histological Characterization of Diagenetic Alteration of Archaeological Bone.* Doctoral thesis. Institute for Geo and Bioarchaeology, VU University Amsterdam.

Johnson, C.N., 2009. Determinants of loss of mammal species during the late Quaternary 'megafauna' extinctions: life history and ecology, but not body size. *Proceedings of the Royal Society B* **269**, 2221–2227.

Jones, A.M., O'Connell, T.C., Young, E.D., Scott, K., Buckingham, C.M., Iacumin, P., Brasier, M.D., 2001. Biogeochemical data from well preserved 200 ka collagen and skeletal remains. *Earth and Planetary Science Letters* **193** (1-2), 143-149.

Jürgensen, J., Drucker, D.G., Stuart, A.J., Schneider, M., Buuveibaatar, B., Bocherens, H., 2017. Diet and habitat of the saiga antelope during the late Quaternary using stable carbon and nitrogen isotope ratios. *Quaternary Science Reviews* **160**, 150–161.

Kahlke, R.D., 2015. The maximum geographic extension of Late Pleistocene *Mammuthus primigenius* (Proboscidea, Mammalia) and its limiting factors. *Quaternary International* **379**, 147-154.

Kamjan, S., Rosalind, G., Balasse, M., Çakirlar, C., Raemaekers, D. The role of specialized cattle farming in the Neolithic Dutch Delta: results from stable isotope (δ^{18}O, δ^{13}C, δ^{15}N) and zooarchaeological analyses. Forthcoming.

Keigwin, L.D., Donnelly, J.P., Cook, M.S., Driscoll, N.W., Brigham-Grette, J., 2006. Rapid sea-level rise and Holocene climate in the Chukchi Sea. *Geology* **34**, 861-864.

van Klinken, G.J., 1999. Bone collagen quality indicators for palaeodietary and radiocarbon measurements. *Journal of Archaeological Science* **26**, 687-695.

van Klinken, G.J., van der Plicht, J., Hedges, R.E.M, 1994. Bone ^{13}C/^{12}C ratios reflect (paleo-) climatic variations. *Geophysical Research Letters* **21**, 445-448.

Koch, P.L. 2007. Isotopic study of the biology of modern and fossil vertebrates. In: Michener R., Lajtha, K. (Eds.) *Stable isotopes in Ecology and Environmental Science.* Blackwell Publishing (Oxford), 99-154.

Koch, P.L., Barnosky, A.D., 2006. Late Quaternary extinctions: state of the debate. *Annual Review of Ecology, Evolution, and Systematics* **37**, 215-250.

Kohn, M.J., 1999. You are what you eat. *Science* **283**, 335-336.

Kohn, M.J., 2010. Carbon isotope composition of terrestrial C3 plants as indicators of (paleo)ecology and (paleo) climate. *Proceedings of the National Academy of Sciences* **107**, 19691-19695.

van Kolfschoten, T., 2012. The Schöningen mammalian fauna in biostratigraphical perspective. In: Behre, K.-E. (Ed.). *Die chronologische Einordnung der paläolithischen Fundstelle von Schöningen/The chronological setting of the Palaeolithic sites of Schöningen.* Verlag des Römisch-Germanischen Zentralmuseums (Mainz), 113-124.

van Kolfschoten, T., 2014. The Palaeolithic locality Schöningen (Germany): a review of the mammalian record. *Quaternary International* **326-327**, 469-480.

van Kolfschoten, T., van Asperen, E., Voormolen, B., 2007. Die Großsäugerfauna von Schöningen. In: Thieme, H. (Ed.). Die Schöninger Speere. *Mensch und Jagd von 400*

000 Jahren. Konrad Theiss Verlag GmbH (Stuttgart/Niedersächsisches Landesamt für Denkmalpflege Hannover), 76-86.

van Kolfschoten, T., Buhrs, E., Verheijen, I. 2015. The larger mammal fauna from the Lower Paleolithic Schöningen Spear site and its contribution to hominin subsistence. *Journal of Human Evolution* **89**, 138-153.

van Kolfschoten, T., Laban, C., 1995. Pleistocene terrestrial mammal faunas from the North Sea Area. *Mededelingen Rijks Geologische Dienst* **52**, 135-151.

van Kolfschoten, T., Parfitt, S.A., Serangeli, J., Bello, S.M., 2015b. Lower Paleolithic bone tools from the 'Spear Horizon' at Schöningen (Germany). *Journal of Human Evolution* **89**, 226-263.

Kosintsev, P., Mitchell, K.J., Devièse, T., van der Plicht, J., Kuitems, M., Petrova, E., Tikhonov, A., Higham, T., Comeskey, D., Turney, C., Cooper, A., van Kolfschoten, T., Stuart, A.J., Lister, A.M., 2019. Evolution and extinction of the giant rhinoceros *Elasmotherium sibiricum* sheds light on late Quaternary megafaunal extinctions. *Nature Ecology & Evolution* **3** (1), 31-38.

Kuitems, M., De Loecker, D., van Kolfschoten, T., Borst, W., van Doesburg, J., van der Es, H.P. Opdebeeck, J., Otte, A., Reumer, J.W.F., van Tongeren, O., Weerts, H.J.T., Wesselingh, F., 2013. *Succesvol botvangen. Rapport 4 van het geo-archeologisch en paleontologisch onderzoek zandwingebied en buitencontour Maasvlakte 2.* Faculty of Archaeology, Leiden University (Leiden).

Kuitems, M., van Kolfschoten, T., De Loecker, D., Busschers, F.S., 2015b. Geoarchaeological and palaeontological research in the Maasvlakte 2 sand extraction zone and on the artificially created Maasvlakte 2 beach: a synthesis. *BOORrapporten* **48**.

Kuitems, M., van Kolfschoten, T., van der Plicht, J., 2015c. Elevated $\delta^{15}N$ values in mammoths: a comparison with modern elephants. *Archaeological and Anthropological Sciences* **7** (3), 289-295.

Kuitems, M., van Kolfschoten, T., Tikhonov, A.N., van der Plicht, J., 2019. Woolly mammoth $\delta^{13}C$ and $\delta^{15}N$ values remained amazingly stable throughout the last ~50,000 years in north-eastern Siberia. *Quaternary International* **500**, 120-127.

Kuitems, M., van der Plicht, J., Drucker, D.G., van Kolfschoten, T., Palstra, S.W.L., Bocherens, H., 2015a. Carbon and Nitrogen isotopes of well-preserved Middle Pleistocene bone collagen from Schöningen (Germany) and their palaeoecological implications. *Journal of Human Evolution* **89**, 105-113.

Kuitems, M., van der Plicht, J., forthcoming. Fossil Bones from the North Sea: Stable Isotopes. Paleontos, accepted.

Lang, J., Böhner, U., Polom, U., Serangeli, J., Winsemann, J., 2015. The Middle Pleistocene tunnel valley at Schöningen as a Paleolithic archive. *Journal of Human Evolution* **89**, 18-26.

Lang, J., Winsemann, J., Steinmetz, D., Polom, U., Pollok, L., Böhner, U., Serangeli, J., Brandes, C., Hampel, A., Winghart, S., 2012. The Pleistocene of Schöningen,

Germany: a complex tunnel valley fill revealed from 3D subsurface modelling and shear wave seismics. *Quaternary Science Reviews* **39**, 86-105.

Lanting, J.N., van der Plicht, J., 1998. Reservoir effects and apparent ^{14}C ages. *Journal of Irish Archaeology* **9**, 151-165.

Leshchinskiy, S., 2015. Enzootic diseases and extinction of mammoths as a reflection of deep geochemical changes in ecosystems of Northern Eurasia. *Archaeological and Anthropological Sciences* **7** (3), 297-317.

Lister, A.M., Sher, A.V., 2001. The Origin and Evolution of the Woolly Mammoth. *Science* **294**, 1094-1097.

Lister, A.M., Sher, A.V., 2015. Evolution and dispersal of mammoths across the Northern Hemisphere. *Science* 350, 805-809.

Lister, A.M., Sher, A.V., van Essen, H., Wei, G., 2005. The pattern and process of mammoth evolution in Eurasia. *Quaternary International* **126-128**, 49-64.

Lister, A.M., Stuart, A.J., 2008. The impact of climate change on large mammal distribution and extinction: evidence from the last glacial/interglacial transition. *Geoscience* **340**, 615-620.

Lister, A.M., Stuart, A.J., 2019. The extinction of the giant deer Megaloceros giganteus (Blumenbach): New radiocarbon evidence. *Quaternary International* **500**, 185-203.

Loose, H., 1975. Pleistocene Rhinocerotidae of W. Europe with reference to the recent two-horned species of Africa and S.E. Asia. *Scripta Geologica* **33**, 1-57.

Lorenzen, E.D., Nogués-Bravo, D., Orlando, L., Weinstock, J., Binladen, J., Marske, K.A., Ugan, A., Borregaard, M.K., Gilbert, M.T.P., Nielsen, R., Ho, S.Y.W., Goebel, T., Graf, K.E., Byers, D., Stenderup, J.T., Rasmussen, M., Campos, P.F., Leonard, J.A., Koepfli, K.-P., Froese, D., Zazula, G., Stafford Jr., T.W., Aaris-Sørensen, K., Batra, P., Haywood, A.M., Singarayer, J.S., Valdes, P.J., Boeskorov, G., Burns, J.A., Davydov, S.P., Haile, J., Jenkins, D.L., Kosintsev, P., Kuznetsova, T., Lai, X., Martin, L.D., McDonald, H.G., Mol, D., Meldgaard, M., Munch, K., Stephan, E., Sablin, M., Sommer, R.S., Sipko, T., Scott, E., Suchard, M.A., Tikhonov, A., Willerslev, R., Wayne, R.K., Cooper, A., Hofreiter, M., Sher, A., Shapiro, B., Rahbek, C., Willerslev, E., 2011. Species-specific responses of Late Quaternary megafauna to climate and humans. *Nature* **479**, 359–365.

Louwe Kooijmans, L.P., 2005. Jagerskampen in de moerassen. De donken bij Hardinxveld. In: *Nederland in de prehistorie*. Bert Bakker (Amsterdam), 183-186.

Louwe Kooijmans, L.P., Ball, E. A., Brinkkemper, O., van Wijngaarden, G.J., Bakels, C.C., Beerenhout, B., van Beurden, L.M., Bruineberg, M., van Gijn, A.L., Hakbijl, T., Hänninen, K., 2001. Hardinxveld-Giessendam De Bruin: een kampplaats uit het Laat-Mesolithicum en het begin van de Swifterbant-cultuur (5500-4450 v. Chr.). *Rapportage Archeologische Monumentenzorg* **88**.

Lovell, N.C., Nelson, D.E., Schwarcz, H.P., 1986. Carbon isotope ratios in palaeodiet: lack of age and sex effect. *Archaeometry* **28**, 51-55.

Lozhkin, A.V. 1993. Geochronology of late Quaternary events in northeastern Russia.

Radiocarbon **35**, 429-433.

Makarewicz, C.A., 2017. Stable isotopes in pastoralist archaeology as indicators of diet, mobility, and animal husbandry practices. In Isotopic Investigations of Pastoralism in Prehistory. Routledge, 149-166).

Mania, D., 1995. Die geologischen Verhältnisse im Gebiet von Schöningen. In: Thieme, H., Maier, R. (Eds.). *Archäologische Ausgrabungen im Braunkohlentagebau Schöningen.* (Hannover), 33-43.

Mania, D., 2007. Die fossilen Weichtiere (Mollusken) aus den Beckensedimenten des Zyklus Schöningen II (Reinsdorf-Warmzeit). In: Thieme, H. (Ed.). *Die Schöninger Speere. Mensch und Jagd von 400 000 Jahren.* Konrad Theiss Verlag GmbH. (Stuttgart/ Niedersächsisches Landesamt für Denkmalpflege Hannover), 99-104.

Mann, D.H., Groves, P., Gaglioti, B.V., Shapiro, B.A., 2018. Climate-driven ecological stability as a globally shared cause of Late Quaternary megafaunal extinctions: the Plaids and Stripes Hypothesis. *Biological Reviews* **94** (1), 328-352.

Mann, D.H., Groves, P., Reanier, R.E., Gaglioti, B.V., Kunz, M.L. and Shapiro, B., 2015. Life and extinction of megafauna in the ice-age Arctic. *Proceedings of the National Academy of Sciences* **112**, 14301-14306.

Marchant, G.H., Shoshani, J., 2007. Head muscles of Loxodonta africana and Elephas maximus with comments on *Mammuthus primigenius* muscles. *Quaternary International* **169**, 186-191.

Marshall, J.D., Brooks, J.R., Lajtha, K., 2007. Sources of variation in the stable isotopic composition of plants. *Stable isotopes in ecology and environmental science* **2**, 22-60.

Martin, P.S., 1984. Prehistoric overkill: the global model. In: Martin, P.S., Wright Jr., H.E. (Eds.). *Pleistocene extinctions: The search for a cause.* Yale University Press (New Haven), 75-120.

McMahon, K.W., McCarthy, M.D., 2016. Embracing variability in amino acid δ^{15}N fractionation: mechanisms, implications, and applications for trophic ecology. *Ecosphere* **7** (12), e01511.

Meiklejohn, C., Niekus, M.J.L.Th., van der Plicht, J., 2015. Radiocarbon dating of Mesolithic human remains in the Netherlands. *Mesolithic Miscellany* **23**, 3-48.

Meiri, M., Lister, A.M., Collins, M.J., Tuross, N., Goebel, T., Blockley, S., Zazula, G.D., van Doorn, N., Guthrie, R.D., Boeskorov, G.G., Baryshnikov, G.F., 2014. Faunal record identifies Bering isthmus conditions as constraint to end-Pleistocene migration to the New World. *Proceedings of the Royal Society B: Biological Sciences* **281** (1776), 20132167.

van der Merwe, N.W., Medina, E., 1991. The canopy effect, carbon isotope ratios and foodwebs in Amazonia. *Journal of Archaeological Science* **18**, 249-259.

Metcalfe, J.Z., Longstaffe, F.J., Hodgins, G., 2013. Proboscideans and paleoenvironments of the Pleistocene Great Lakes: landscape, vegetation, and stable isotopes. *Quaternary Science Reviews* **76**, 102–113.

Metcalfe, J.Z., Longstaffe, F.J., Jass, C.N., Zazula, G.D., Keddie, G., 2016. Taxonomy,

location of origin and health status of proboscideans from Western Canada investigated using stable isotope analysis. *Journal of Quaternary Science* **31**, 126-142.

Metcalfe, J.Z., Longstaffe, F.J., Zazula, G.D., 2010. Nursing, weaning, and tooth development in woolly mammoths from Old Crow, Yukon, Canada: implications for Pleistocene extinctions. *Palaeogeography, Palaeoclimatology, Palaeoecology* **298**, 257-270.

Meyer, M., Palkopoulou, E., Baleka, S., Stiller, M., Penkman, K.E., Alt, K.W., Ishida, Y., Mania, D., Mallick, S., Meijer, T. and Meller, H., 2017. Palaeogenomes of Eurasian straight-tusked elephants challenge the current view of elephant evolution. *eLife* **6**, 25413.

Michener, R., Lajtha, K., 2007. *Stable Isotopes in Ecology and Environmental Science*. Blackwell.

Minagawa, M., Wada, E., 1984. Stepwise enrichment of ^{15}N along food chains: Further evidence and the relation between δ^{15}N and animal age. *Geochimica et Cosmochimica Acta* **48**, 1135-1140.

Mol, D., de Vos J., 1995. Korren op de Oosterschelde: een zoogdierpaleontoloog als visser en wat de fossielen van de Oosterschelde ons vertellen. *Grondboor en Hamer* **49** (3/4), 57-61.

Mol, D., de Vos, J., van der Plicht, J., 2007. The presence and extinction of Elephas antiquus Falconer and Cautley, 1847, in Europe. *Quaternary International* **169-170**, 149-153.

Mol, D., Post, K., 2010. Gericht korren op de Noordzee voor de zoogdier paleontologie: een historisch overzicht van de uitgevoerde expedities. *Cranium* **27**, 14-28.

Mol, D., Tikhonov, A., van der Plicht, J., Kahlke, R.D., Debruyne, R., van Geel, B., van Reenen, G., Pals, J.P., de Marliave, C., Reumer, J.W., 2006. Results of the CERPOLEX/ *Mammuthus* Expeditions on the Taimyr Peninsula, Arctic Siberia, Russian Federation. *Quaternary International* **142-143**, 186-202.

Möller, P., Alexanderson, H., Funder, S., Hjort, C., 2015. The Taimyr Peninsula and the Severnaya Zemlya archipelago, Arctic Russia: a synthesis of glacial history and palaeo-environmental change during the Last Glacial cycle (MIS 5e-2). *Quaternary Science Reviews* **107**, 149-181.

Momber, G., Tomalin, D., Scaife, R., Satchell, J., Gillespie, J., 2011. Mesolithic occupation at Bouldnor Cliff and the submerged prehistoric landscapes of the Solent. *CBA research report*, 164.

Mook, W.G., 2006. *Introduction to isotope hydrology*. Taylor and Francis (London).

Mook, W.G., Streurman, H.J., 1983. Physical and chemical aspects of radiocarbon dating. *PACT Publications* **8**, 31-55.

Mook, W.G., van der Plicht, J., 1999. Reporting ^{14}C activities and concentrations. *Radiocarbon* **41**, 227-239.

Moree, J.M., Sier, M.M. (Eds.). 2015. Interdisciplinary Archaeological Research Programme Maasvlakte 2, Rotterdam. BOORrapporten 566. *Part 1: Twenty meters deep! The Mesolithic period at the Yangtze Harbour site - Rotterdam Maasvlakte, the Netherlands.* Bureau Oudheidkundig Onderzoek Rotterdam (Rotterdam).

Nadelhoffer, K., Shaver, G., Fry, B., Giblin, A., Johnson, L., McKane, R., 1996. [15]N natural abundances and N use by tundra plants. *Oecologia* **107**, 386–394.

Nardoto, G.B., Godoy, P.B.D., Ferraz, E.S.D.B., Ometto, J.P.H.B., Martinelli, L.A., 2006. Stable carbon and nitrogen isotopic fractionation between diet and swine tissues. *Scientia Agricola* **63** (6), 579-582.

Niekus, M.J.T., Kozowyk, P.R., Langejans, G.H., Ngan-Tillard, D., van Keulen, H., van der Plicht, J., Cohen, K.M., van Wingerden, W., van Os, B., Smit, B.I. and Amkreutz, L.W., 2019. Middle Paleolithic complex technology and a Neandertal tar-backed tool from the Dutch North Sea. *Proceedings of the National Academy of Sciences*, 201907828.

Nikolskiy, P.A., Sulerzhitsky, L.D., Pitulko, V.V., 2011. Last straw versus Blitzkrieg overkill: Climate-driven changes in the Arctic Siberian mammoth population and the Late Pleistocene extinction problem. *Quaternary Science Reviews* **30**, 2309–2328.

Noe-Nygaard, N., 1983. The importance of aquatic resources to Mesolithic man at inland sites in Denmark. *Animals and archaeology* **2**, 125-142.

Noe-Nygaard, N., 1988. δ^{13}C-values of dog bones reveal the nature of changes in man's food resources at the Mesolithic-Neolithic transition, Denmark. *Chemical Geology: Isotope Geoscience section* **73** (1), 87-96.

Noe-Nygaard, N., Price, T.D., Hede, S.U., 2005. Diet of aurochs and early cattle in southern Scandinavia: evidence from ^{15}N and ^{13}C stable isotopes. *Journal of Archaeological Science* **32**, 855-871.

O'Connell, J.F., Allen, J., Williams, M.A., Williams, A.N., Turney, C.S., Spooner, N.A., Kamminga, J., Brown, G., Cooper, A., 2018. When did Homo sapiens first reach Southeast Asia and Sahul?. *Proceedings of the National Academy of Sciences* **115** (34), 8482-8490.

O'Connell, T.C., Kneale, C.J., Tasevska, N., Kuhnle, G.G., 2012. The diet□ body offset in human nitrogen isotopic values: A controlled dietary study. *American Journal of Physical Anthropology* **149** (3), 426-434.

O'Connell, T.C., 2017. 'Trophic' and 'source' amino acids in trophic estimation: a likely metabolic explanation. *Oecologia* **184**, 317-326.

Olivier, R.C.D., 1982. Ecology and behavior of living elephants: bases for assumptions concerning the extinct woolly mammoths. In: Hopkins, D., Matthews, J.V., Jr., Schweger, C.E., Young, S.B. (Eds). *Paleoecology of Beringia*. Academic Press New York (New York, USA), 291–305.

Palkopoulou, E., Mallick, S., Skoglund, P., Enk, J., Rohland, N., Li, H., Omrak, A., Vartanyan, S., Poinar, H., Götherström, A., Reich, D., Dalén, L., 2015. Complete Genomes Reveal Signatures of Demographic and Genetic Declines in the Woolly Mammoth. *Current Biology* **25** (10), 1395-1400.

Palmqvist, P., Gröcke, D.R., Arribas, A., Fariñã, R.A., 2003. Paleoecological reconstruction of a lower Pleistocene large mammal community using biogeochemical (^{13}C, ^{15}N, ^{18}O, Sr:Zn) and ecomorphological approaches. *Paleobiology* **29**, 205-229.

Palmqvist, P., Pérez-Claros, J.A., Janis, C.M., Gröcke, D.R., 2008. Tracing the

ecophysiology of ungulates and predatoreprey relationships in an early Pleistocene large mammal community. *Palaeogeography, Palaeoclimatology, Palaeoecology* **266** (1-2), 95-111.

Parfitt, S.A., Ashton, N.M., Lewis, S.G., Abel, R.L., Coope, G.R., Field, M.H., Gale, R., Hoare, P.G., Larkin, N.R., Lewis, M.D., Karloukovski, V., Maher, B.A., Peglar, S.M., Preece, R.C., Whittaker J.E., Stringer, C.B., 2010. Early Pleistocene human occupation at the edge of the boreal zone in northwest Europe. *Nature* **466**, 229-233.

Parfitt, S.A., Barendregt, R.W., Breda, M., Candy, I., Collins, M.J., Coope, G.R., Durbridge, P., Field, M.H., Lee, J.R., Lister, A.M., Mutch, R., Penkman, K.E.H., Preece, R.C., Rose, J., Stringer, C.B., Symmons, R., Whittaker, J.E., Wymer, J.J., Stuart, A.J., 2005. The earliest record of human activity in northern Europe. *Nature* **438**, 1008-1012.

Pečnerová, P., Díez-del-Molino, D., Vartanyan, S., Dalén, L., 2016. Changes in variation at the MHC class II DQA locus during the final demise of the woolly mammoth. *Scientific Reports* **6**, 25274.

Peeters, H., Murphy, P., Flemming, N. (Eds). 2009. *North Sea Prehistory Research and Management Framework (NSPRMF) 2009*. Rijksdienst voor het Cultureel Erfgoed, (Amersfoort).

Peeters, J.H.M., 2011. How wet can we get? Approaches to submerged prehistoric sites and landscapes on the Dutch continental shelf. In: Benjamin, J., Bonsall, C., Pickard, C., Fischer, A. (Eds.). *Submerged Prehistory*. Oxbow books (Oxford), 55-64.

Philippsen, B., 2013. The freshwater reservoir effect in radiocarbon dating. *Heritage Science* **1**, 24.

Phillips, D.L., Inger, R., Bearhop, S., Jackson, A.L., Moore, J.W., Parnell, A.C., Semmens, B.X., Ward, E.J., 2014. Best practices for use of stable isotope mixing models in food-web studies. *Canadian Journal of Zoology* **92** (10), 823-835.

Pieters, M., Demerre, I., Lenaerts, T., Zeebroek, I., De Bie, M., de Clercq, W., Dickinson, B., Monsieur, P., 2010. De Noordzee: een waardevol archief onder water. Meer dan 100 jaaronderzoek van strandvondsten en vondsten uit zee in België: een overzicht. *Relicta* **6**, 177-218.

Pinter, N., Scott, A.C., Daulton, T.L., Podoll, A., Koeberl, C., Anderson, R.S., Ishman, S.E., 2011. The Younger Dryas impact hypothesis: A requiem. *Earth-Science Reviews* **106**, 247-264.

Pitulko, V.V., Kuzmin, Y.V., Glascock, M.D., Pavlova, E.Y., Grebennikov, A.V., 2019. 'They came from the ends of the earth': long-distance exchange of obsidian in the High Arctic during the Early Holocene. *Antiquity* **93** (367), 28-44.

Pitulko, V.V., Nikolskiy, P.A., Girya, E.Y., Basilyan, A.E., Tumskoy, V.E., Koulakov, S.A., Astakhov, S.N., Pavlova, E.Y., Anisimov, M.A., 2004. The Yana RHS site: humans in the arctic before the last glacial maximum. *Science* **303**, 52-56.

Pitulko, V.V., Tikhonov, A.N., Pavlova, E.Y., Nikolskiy, P.A., Kuper, K.E., Polozov, R.N., 2016. Paleoanthropology: early human presence in the Arctic: evidence from 45,000-year-old mammoth remains. *Science* **351**, 260-263

van der Plicht, J., Amkreutz, L.W.S.W., Niekus, M.J.L.Th., Peeters, J.H.M., Smit, B.I., 2016. Surf'n Turf in Doggerland: dating, stable isotopes and diet of Mesolithic human remains from the southern North Sea. *Journal of Archaeological Science Reports* **10**, 110-118.

van der Plicht, J., van Kolfschoten, T., Kuitems, M., 2011. *Isotopen in uniek Pleistoceen botmateriaal uit Schöningen*. Report Leiden University Fund, unpublished.

van der Plicht, J., Kuitems, M., forthcoming. Fossil Bones from the North Sea: Radiocarbon Dating. *Paleontos*, accepted.

van der Plicht, J., Palstra, S.W.L., 2016. Radiocarbon and mammoth bones: what's in a date. *Quaternary International* **406**, 246–251.

Polley, H.W., Johnson, H.B., Marino, B.D., Mayeux, H.S., 1993. Increase in C3 plant water-use efficiency and biomass over Glacial to present CO2 concentrations. *Nature* **361**, 61-64.

Prummel, W., Niekus, M.J.L.Th., 2011. Late Mesolithic hunting of a small female aurochs in the valley of the River Tjonger (the Netherlands) in the light of Mesolithic aurochs hunting in NW Europe. *Journal of Archaeological Science* **38**, 1456-1467.

Prummel, W., van der Plicht, J., Kootker, L., Arnoldussen, S. *Palaeohistoria*, forthcoming.

Pushkina, D., Bocherens, H. Ziegler, R., 2014. Unexpected palaeoecological features of the middle and late Pleistocene large herbivores in southwestern Germany revealed by stable isotopic abundances in tooth enamel. *Quaternary International* **339-340**, 164–178.

Putshkov, P.V., 2003. The impact of mammoths on their biome: a clash of two paradigms. In: Reumer, J.W.F., de Vos, J., Mol, D. (Eds.). Advances in mammoth research (Proceedings of the Second International Mammoth Conference, Rotterdam, May 16–20 1999). *Deinsea* **9**, 365-380.

Puzachenko, A.Y., Markova, A.K., Kosintsev P.A., van Kolfschoten, T., van der Plicht, J., Kuznetsova, T.V., Tikhonov, A.N., Ponomarev, D.V., Kuitems, M., Bachura, O.P., 2017. The Eurasian mammoth distribution during the second half of the Late Pleistocene and the Holocene: regional aspects. *Quaternary International* **445**, 71-88.

Rabanus-Wallace, M.T., Wooller, M.J., Zazula, G.D., Shute, E., Jahren, A.H., Kosintsev, P., Burns, J.A., Breen, J., Llamas, B., Cooper, A., 2017. Megafaunal isotopes reveal role of increased moisture on rangeland during late Pleistocene extinctions. *Nature Ecology & Evolution* **1**, 0125.

Raghavan, M., Espregueira Themudo, G., Smith, C.I., Zazula, G., Campos, P.F., 2014. Musk ox (*Ovibos moschatus*) of the mammoth steppe: tracing palaeodietary and palaeoenvironmental changes over the last 50,000 years using carbon and nitrogen isotopic analysis. *Quaternary Science Reviews* **102**, 192–201.

Rasmussen, S.O., Bigler, M. Blockley, S.P., Blunier, T., Buchardt, S.L., Clausen, H.B., Cvijanovic, I., Dahl-Jensen, D., Johnsen, S.J., Fischer, H., Gkinis, V., Guillevic, M., Hoek, W.Z., Lowe, J.J., Pedro, J.B., Popp, T., Seierstad, I.K., Steffensen, J.P., Svensson, A.M., Vallelonga, P., Vinther, B.M., Walker, M.J.C., Wheatley, J.J., Winstrup M., 2014.

A stratigraphic framework for abrupt climatic changes during the Last Glacial period based on three synchronized Greenland ice-core records: refining and extending the INTIMATE event stratigraphy. *Quaternary Science Reviews* **106**, 14-28.

Reimer, P.J., Bard, E., Bayliss, A., Beck, J.W., Blackwell, P.G., Bronk Ramsey, C., Buck, C.E., Edwards, R.L., Friedrich, M., Grootes, P.M., Guilderson, T.P., Haflidason, H., Hajdas, I., Hatté, C., Heaton, T.J., Hoffmann, D.L., Hogg, A.G., Hughen, K.A., Kaiser, K.F., Kromer, B., Manning, S.W., Niu, M., Reimer, R.W., Richards, D.A., Scott, E.M., Southon, J.R., Staff, R.A., Turney, C.S.M., van der Plicht, J., 2013. IntCal13 and Marine13 Radiocarbon age calibration curves 0-50,000 years cal BP. *Radiocarbon* **55**, 1869-1887.

Reynard, L.M., Tuross, N., 2015. The known, the unknown and the unknowable: weaning times from archaeological bones using nitrogen isotope ratios. *Journal of Archaeological Science* **53**, 618-625.

Richards, M.P., Hedges, R.E.M., 1999. Stable isotope evidence for similarities in the types of marine foods used by Late Mesolithic humans at sites along the Atlantic coast of Europe. *Journal of Archaeological Science* **26**, 717-722.

Richards, M.P., Hedges, R.E.M., 2003. Variations in bone collagen $\delta^{13}C$ and $\delta^{15}N$ values of fauna from Northwest Europe over the last 40000 years. *Palaeogeography, Palaeoclimatology, Palaeoecology* **193**, 261–267.

Richards, M.P., Pellegrini, M., Niven, L., Nehlich, O., Dibble, H., Turq, A., McPherron, S.J.P., 2017. Temporal variations in *Equus* tooth isotope values (C, N, O) from the Middle Paleolithic site of Combe Grenal, France (ca. 150,000 to 50,000 BP). *Journal of Archaeological Science: Reports* **14**, 189-198.

Richter, K.K., Wilson, J., Jones, A.K., Buckley, M., van Doorn, N., Collins, M.J., 2011. Fish'n chips: ZooMS peptide mass fingerprinting in a 96 well plate format to identify fish bone fragments. *Journal of Archaeological Science* **38**, 1502-1510.

Rijsdijk, K.F., Kroon, I.C., Meijer, T., Passchier, S., van Dijk, T.A.G.P., Bunnik, F.P.M., Janse, A.C., 2013. Reconstructing Quaternary Rhine-Meuse dynamics in the southern North Sea; architecture, seismo-lithofacies associations and malacological biozonation. *Journal of Quaternary Science* **28**, 453-466.

Rivals, F., Julien, M.A., Kuitems, M., Van Kolfschoten, T., Serangeli, J., Drucker, D.G., Bocherens, H., Conard, N.J., 2015. Investigation of equid paleodiet from Schöningen 13 II-4 through dental wear and isotopic analyses: Archaeological implications. *Journal of Human Evolution* **89**, 129-137.

Rivals, F., Lister, A.M., 2016. Dietary flexibility and niche partitioning of large herbivores through the Pleistocene of Britain. *Quaternary Science Reviews* **146**, 116–133.

Rivals, F., Mihlbachler, M.C., Solounias, N., Mol, D., Semprebon, G.M., de Vos, J., Kalthoff D.C., 2010. Palaeoecology of the Mammoth Steppe fauna from the late Pleistocene of the North Sea and Alaska: Separating species preferences from geographic influence in paleoecological dental wear analysis. *Palaeogeography, Palaeoclimatology, Palaeoecology* **286**, 42-54.

Rivals, F., Semprebon, G., Lister, A., 2012. An examination of dietary diversity patterns in Pleistocene proboscideans (*Mammuthus*, *Palaeoloxodon*, and *Mammut*) from Europe and North America as revealed by dental microwear. *Quaternary International* **255**, 188-195.

Rivals, F., Ziegler, R., 2018. High-resolution paleoenvironmental context for human occupations during the Middle Pleistocene in Europe (MIS 11, Germany). *Quaternary Science Reviews* **188**, 136-142.

Roebroeks, W., 2014. Terra incognita: The Palaeolithic record of northwest Europe and the information potential of the southern North Sea. *Netherlands Journal of Geosciences* **93**, 43-53.

Rogers, R.L., Slatkin, M., 2017. Excess of genomic defects in a woolly mammoth on Wrangel island. *PLoS genetics* **13** (3), e1006601.

Rountrey, A.N., Fisher, D.C., Vartanyan, S., Fox, D.L., 2007. Carbon and nitrogen isotope analyses of a juvenile woolly mammoth tusk: evidence of weaning. *Quaternary International* **169**, 166-173.

Rule, S., Brook, B.W., Haberle, S.G., Turney, C.S., Kershaw, A.P., Johnson, C.N., 2012. The aftermath of megafaunal extinction: ecosystem transformation in Pleistocene Australia. *Science* **335**, 1483-1486.

Saarinen, J., Eronen, J., Fortelius, M., Seppä, H., Lister, A.M., 2016. Patterns of diet and body mass of large ungulates from the Pleistocene of Western Europe, and their relation to vegetation. *Palaeontologia Electronica* **19**, 1–58.

Schild, R., 1976. The Final Paleolithic Settlements of the European Plain. *Scientific American* **234** (2), 88-100.

Schoeller, D.A., 1999. Isotope fractionation: Why aren't we what we eat? *Journal of Archaeological Science*, **26** (6), 667-673.

Schoeninger, M.J., Moore, K., 1992. Bone stable isotope studies in archaeology. *Journal of World Prehistory* **6** (2), 247–296.

Schoeninger, M.J., DeNiro, M.J., 1984. Nitrogen and carbon isotopic composition of bone collagen from marine and terrestrial animals. *Geochimica et Cosmochimica Acta* **48**, 625-639.

Schoeninger, M.J., DeNiro, M.J., Tauber, H., 1983. Stable nitrogen isotope ratios of bone collagen reflect marine and terrestrial components of prehistoric human diet. *Science* **220**, 1381–1383.

Schulting, R.J., Richards, M.P., 2002. Finding the coastal Mesolithic in southwest Britain: AMS dates and stable isotope results on human remains from Caldey Island, south Wales. *Antiquity* **76**, 1011-1025.

Schvyreva, A.K., 2014. *The rhinoceroses of the genus Elasmotherium in the biochronology of Eastern Europe*. In: Kostopoulos D.S., Vlachos E., Tsoukala E. (Eds.). Abstract Book of the VIth International Conference on Mammoths and their Relatives. S.A.S.G., 102. 180 – 181.

Schvyreva, A.K., 2015. On the importance of the representatives of the genus

Elasmotherium (Rhinocerotidae, Mammalia) in the biochronology of the Pleistocene of Eastern Europe. *Quaternary International* **379**, 128–134.

Schvyreva, A.K., 2016. *The Elasmotherii of Pleistocene Eurasia*. Pechatniy Dvor Publishers (Stavropol), 218. [in Russian]

Schwartz-Narbonne, R., Longstaffe, F.J., Metcalfe, J.Z., Zazula, G., 2015. Solving the woolly mammoth conundrum: amino acid ^{15}N-enrichment suggests a distinct forage or habitat. *Scientific reports* **5**, 9791.

Sealy, J., 2001. Body tissue chemistry and palaeodiet. In: Brotwell, D.R., Pollard, A.M. (Eds.). *Handbook of archaeological sciences*. Wiley (Chichester), 269–279.

Sealy, J.C., van der Merwe, N.J., Lee Thorp, J.A., Lanham, J.L. 1987. Nitrogen isotopic ecology in southern Africa: Implications for environmental and dietary tracing. *Geochimica et Cosmochimica Acta* **51**, 2707-2717.

Serangeli, J., Bigga, G., Böhner, U., Julien, M.-A., Lang, J., Stahlschmidt, M., 2012a. Ein Fenster ins Altpaläolithikum. *Archäologie in Deutschland* **4**, 6-12.

Serangeli, J., Böhner, U., Haßmann, H., Conard, N.J., 2012b. Die pleistozänen Fundstellen in Schöningen- eine Einführung. In: Behre, K.E. (Ed.). *Die chronologische Einordnung der paläolithischen Fundstelle von Schöningen/The chronological setting of the Palaeolithic sites of Schöningen*. Verlag des Römisch-Germanischen Zentralmuseums (Mainz), 1-22.

Shennan, S., 1997. *Quantifying Archaeology*. Edinburgh University Press (Edinburgh), 65-70.

Sher, A.V., Kuzmina, S.A., Kuznetsova, T.V., Sulerzhitsky, L.D., 2005. New insights into the Weichselian environment and climate of the East Siberian Arctic, derived from fossil insects, plants, and mammals. *Quaternary Science Reviews* **24**, 533-569.

Signor, P.W. III, Lipps, J.H., 1982. Sampling bias, gradual extinction patterns, and catastrophes in the fossil record. Geological Society of America **190**, 291-296.

Smith, C.I., Nielsen-Marsh, C.M., Jans, M.M.E., Collins, M.J., 2007. Bone diagenesis in the European Holocene I: patterns and mechanisms. *Journal of Archaeological Science* **34**, 1485–1493.

Smith, S.D., Kawash, J.K., Karaiskos, S., Biluck, I., Grigoriev, A., 2017. Evolutionary adaptation revealed by comparative genome analysis of woolly mammoths and elephants. *DNA Research* **24**, 359-369.

Soffer, O., Adovasio, J.M., Kornietz, N.L., Velichko, A.A., Gribchenko, Y.N., Lenz, B.R., Suntsov, V.Y., 1997. Cultural stratigraphy at Mezhirich, an Upper Palaeolithic site in Ukraine with multiple occupations. *Antiquity* **71** (271), 48-62.

Sponheimer, M., Robinson, T., Ayliffe, L., Hammer, J., Passey, B., West, A., Cerling, T., Dearing, D., Ehleringer, J., 2003a. Nitrogen isotopes in mammalian herbivores: hair δ^{15}N values from a controlled feeding study. *International Journal of Osteoarchaeology* **13**, 80–87.

Sponheimer, M., Robinson, T., Ayliffe, L., Passey, B., Roder, B., Shipley, L., Lopez, E., Cerling, T., Dearing, D., Ehleringer, J., 2003b. An experimental study of carbon-isotope fractionation between diet, hair, and feces of mammalian herbivores.

Canadian Journal of Zoology **81**, 871-876.

Stauch, G., Gualtieri, L., 2008. Late Quaternary glaciations in North-Eastern Russia. *Journal of Quaternary Science* **23**, 545-558.

Stevens, R.E., Hedges, R.E.M., 2004. Carbon and nitrogen stable isotope analysis of northwest European horse bone and tooth collagen, 40,000 BP-present: Palaeoclimatic interpretations. *Quaternary Science Reviews* **23**, 977-991.

Stewart, J.R., 2004. Neanderthal-modern human competition? A comparison between the mammals associated with Middle and Upper Palaeolithic Industries in Europe during OIS 3. *International Journal of Osteoarchaeology* **14**, 178-189.

Stewart, J.R., Allen, R.B., Jones, A.K., Kendall, T., Penkman, K.E.H., Demarchi, B., O'Connor, T., Collins, M.J., 2014. Walking on Eggshells: A Study of Egg Use in Anglo-Scandinavian York Based on Eggshell Identification Using ZooMS. *International Journal of Osteoarchaeology* **24**, 247-255.

Storm, P., 2010. Start onderzoek Homo sapiens resten Noordzee: micro-evolutie in de Lage landen. *Cranium* **27**, 63-66.

Stuart, A.J., 2005. The extinction of woolly mammoth (*Mammuthus primigenius*) and straight-tusked elephant (*Palaeoloxodon antiquus*) in Europe. *Quaternary International* **126-128**, 171-177.

Stuart, A.J., 2015. Late Quaternary megafaunal extinctions on the continents: a short review. *Geological Journal* **50** (3), 338-363.

Stuart, A.J., Lister, A.M., 2012. Extinction chronology of the woolly rhinoceros Coelodonta antiquitatis in the context of late Quaternary megafaunal extinctions in northern Eurasia. *Quaternary Science Reviews* **51**, 1–17.

Stuart, A.J., Sulerzhitsky, L.D., Orlova, L.A., Kuzmin, Y.V., Lister, A.M., 2002. The latest woolly mammoths (*Mammuthus primigenius* Blumenbach) in Europe and Asia: a review of the current evidence. *Quaternary Science Reviews* **21**, 1559–1569.

Sturt, F., Garrow, D., Bradley, S., 2013. New models of North West European Holocene palaeogeography and inundation. *Journal of Archaeological Science* **40**, 3963-3976.

Svoboda, J., Péan, S., Wojtal, P., 2005. Mammoth bone deposits and subsistence practices during Mid-Upper Palaeolithic in Central Europe: three cases from Moravia and Poland. *Quaternary International* **126**, 209-221.

Sykes, R.M.W., 2018. Isolation, Exploration or Seasonal Migration? Investigating Technological Organization in the Late Middle Palaeolithic of Britain During Marine Isotope Stage 3. In: Robinson, E., Sellet, F. (Eds.). *Lithic Technological Organization and Paleoenvironmental Change: Global and diachronic perspectives.* Springer, 123-161.

Synal, H.A., Schulze-König, T., Seiler, M., Suter, M., Wacker, L., 2013. Mass spectrometric detection of radiocarbon for dating applications. *Nuclear Instruments and Methods in Physics Research B* **294**, 349–352.

Szpak, P., 2014. Complexities of nitrogen isotope biogeochemistry in plant-soil systems: implications for the study of ancient agricultural and animal management practices. *Frontiers in Plant Science* **5**, 288.

Szpak, P., Gröcke, D.R., Debruyne, R., MacPhee, R.D.E., Guthrie, R.D., Froese, D., Zazula, G.D., Patterson, W.P., Poinar, H.N., 2010. Regional differences in bone collagen δ¹³C and δ¹⁵N of Pleistocene mammoths: Implications for paleoecology of the mammoth steppe. *Palaeogeography, Palaeoclimatology, Palaeoecology* **286**, 88–96.

Szpak, P., Metcalfe, J.Z., MacDonald, R.A., 2017. Best practices for calibrating and reporting stable isotope measurements in archaeology. *Journal of Archaeological Science* 13, 609-616.

Terberger, T., Gramsch, B., Heinemeijer, J., 2012. The underestimated fish? Early Mesolithic human remains from Northern Germany. In: Niekus, M.J.L.Th., Barton, R.N.E., Terberger, T. (Eds.). *A mind set on flint. Studies in honour of Dick Stapert.* Groningen Archaeological Studies 16, Barkhuis Publishing, Groningen, 343-354.

Thieme, H., 1997. Lower Palaeolithic hunting spears from Germany. *Nature* **385** (6619), 807-810.

Thieme, H., 1999. Altpaläolithische Holzgeräte aus Schöningen, Lkr. Helmstedt. Bedeutsame Funde zur Kulturentwicklung des frühen Menschen. *Germania* **77**, 451-487.

Tizzard, L., Bicket, A., De Loecker, D., Benjamin, J., 2015. Seabed prehistory: investigating the palaeogeography and early middle Palaeolithic archaeology in the Southern North Sea. *Wessex Archaeology*, 35.

Tizzard, L., Bicket, A.R., Benjamin, J., De Loecker, D., 2014. A Middle Palaeolithic site in the southern North Sea: investigating the archaeology and palaeogeography of Area 240. *Journal of Quaternary Science* **29** (7), 698-710.

Ugan, A., Coltrain, J., 2011. Variation in collagen stable nitrogen values in black-tailed jackrabbits (*Lepus californicus*) in relation to small-scale differences in climate, soil, and topography. *Journal of Archaeological Science* **38** (7), 1417-1429.

Ukraintseva, V.V., 1993. *Vegetation cover and environment of the "Mammoth Epoch" in Siberia.* Mammoth Site of Hot Springs (South Dakota).

Urban, B., 2007a. Interglacial pollen records from Schöningen, North Germany. In: Sirocko, F., Claussen, M., Sánchez-Goni, M.F., Litt, T. (Eds.). The Climate of Past Interglacials. *Developments in Quaternary Science* 7. Elsevier (Amsterdam), 417-444.

Urban, B., 2007b. Quartäre Vegetations- und Klimaentwicklung im Tagebau Schöningen. In: Thieme, H., Schöninger Speere, Die (Eds.). *Mensch und Jagd von 400 000 Jahren.* Konrad Theiss Verlag GmbH (Stuttgart/Niedersächsisches Landesamt für Denkmalpflege Hannover), 66-75.

Urban, B., Sierralta, M., Frechen, M., 2011. New evidence for vegetation development and timing of Upper Middle Pleistocene interglacials in Northern Germany and tentative correlations. *Quaternary International* **241**, 125-142.

Vachula, R.S., Huang, Y., Longo, W.M., Dee, S.G., Daniels, W.C., Russell, J.M., 2019. Evidence of Ice Age humans in eastern Beringia suggests early migration to North America. *Quaternary Science Reviews* **205**, 35-44.

Valente, A., 1983. Hair structure of the Woolly mammoth, *Mammuthus primigenius* and

the modern elephants, *Elephas maximus* and *Loxodonta africana*. J*ournal of Zoology* **199** (2), 271-274.

Vartanyan, S.L., Arslanov, K.A., Karhu, J.A., Possnert, G., Sulerzhitsky, L.D., 2008. Collection of radiocarbon dates on the mammoths (*Mammuthus primigenius*) and other genera of Wrangel Island, northeast Siberia, Russia. *Quaternary Research* **70**, 51-59.

Vartanyan, S.L., Garutt, V.E., Sher, A.V., 1993. Holocene dwarf mammoths from Wrangel Island in the Siberian Arctic. *Nature* **362**, 337-340.

Vereshchagin, N.K., Baryshnikov, G.F., 1982. Paleoecology of the mammoth fauna in the Eurasian Arctic. In: Hopkins, D.M., Matthews, J.V. Jr., Schweger, C.E., Young, S.B. (Eds.). *Paleoecology of Beringia*. Academic (New York), 267–280.

Vogel, J.C, van der Merwe, N.J., 1977. Isotopic evidence for early maize cultivation in New York state. American *Antiquity* **42**, 238-242.

Voormolen, B., 2008. *Ancient hunters, modern butchers: Schöningen 13II-4, a kill-butchery site dating from the northwest European Lower Palaeolithic*. PhD Thesis, Faculty of Archaeology, Leiden University.

Walker, P.L., DeNiro, M.J., 1986. Stable nitrogen and carbon isotope ratios in bone collagen as indices of prehistoric dietary dependence on marine and terrestrial resources in southern California. *American Journal of Physical Anthropology* **71**, 51-61.

Wan, X., Zhang, Z., 2017. Climate warming and humans played different roles in triggering Late Quaternary extinctions in east and west Eurasia. *Proceedings of the Royal Society B: Biological Sciences* **284** (1851), 20162438.

Wang, Y., Porter, W., Mathewson, P.D., Miller, P.A., Graham, R.W., Williams, J.W., 2018. Mechanistic modeling of environmental drivers of woolly mammoth carrying capacity declines on St. Paul Island. *Ecology* **99**, 2721-2730.

Welker, F., Soressi, M., Rendu, W., Hublin, J.J., Collins, M., 2015. Using ZooMS to identify fragmentary bone from the late Middle/Early Upper Palaeolithic sequence of Les Cottés, France. *Journal of Archaeological Science* **54**, 279-286.

Willerslev, E., Davison, J., Moora, M., Zobel, M., Coissac, E., Edwards, M.E., Lorenzen, E.D., Vestergård, M., Gussarova, G., Haile, J. and Craine, J., 2014. Fifty thousand years of Arctic vegetation and megafaunal diet. *Nature* **506** (7486), 47-51.

Wood, R.E., Higham, T.F., Buzilhova, A., Suvorov, A., Heinemeier, J., Olsen, J., 2013. Freshwater radiocarbon reservoir effects at the burial ground of Minino, northwest Russia. *Radiocarbon* **55**, 163-177.

Wooller, M.J., Saulnier-Talbot, É., Potter, B.A., Belmecheri, S., Bigelow, N., Choy, K., Cwynar, L.C., Davies, K., Graham, R.W., Kurek, J., Langdon, P., Medeiros, A., Rawcliffe, R., Wang, Y., Williams, J.W, 2018. A new terrestrial palaeoenvironmental record from the Bering Land Bridge and context for human dispersal. *Royal Society open science* **5** (6), 180145.

Yesner, D.R., 1987. Life in the "Garden of Eden": Causes and consequences of the adoption of marine diets by human societies. In: Harris, M., Ross, E.B. (Eds.). Food

and Evolution. Temple University Press (Philadelphia), 285-309.

Zhegallo, V., Kalandadze, N., Shapovalov, A., Bessudnova, Z., Noskova, N., Tesakova, E., 2005. On the fossil rhinoceros Elasmotherium (including the collections of the Russian Academy of Sciences). *Cranium* **22** (1), 17–40.

Zimov, S.A., Zimov, N.S., Tikhonov, A.N., Chapin III, F.S., 2012. Mammoth steppe: a high-productivity phenomenon. *Quaternary Science Reviews* **57**, 26-45.

Supplementary Information

Table SI Chapter 3.1

Results of the isotopic data and woolly mammoth sample information in chronological order.

Lab code[1]	Locality[2]	¹⁴C age (yr BP)	Sigma	% C	δ¹³C (‰)	% N	δ¹⁵N (‰)	C:N	Material[3]	% coll	Source[4]
GrA-43037	New Siberian Arch.	> 45000		46.5	−21.5	18.4	+7.51	3.0	b	7.4	1
GrA-60422	New Siberian Arch.	> 45000		44.9	−22.0	16.2	+8.63	3.2	b	16.2	1
Site 1 M. pr. 20	New Siberian Arch.	> 45000		40.0	−21.7	15.6	+7.60	3.0	b/t	14.1	2
Site 1 M. pr. 21	New Siberian Arch.	> 45000		42.6	−22.3	16.0	+9.30	3.1	b/t	16.1	2
95600	New Siberian Arch.	> 45000		43.2	−22.2	15.8	+9.20	3.2	b		3
UCIAMS38674	Sanga-Yuriakh	> 45000		35.9	−22.6	12.6	+10.90	3.3	b	18.6	4,5
UCIAMS38676	Ari Mas	> 45000		41.1	−21.8	15.2	+10.50	3.2	b	7.6	4,5
UCIAMS38677	Arilakh	> 45000		38.2	−22.0	13.4	+10.00	3.3	b	22.4	4,5
UCIAMS39109	Arilakh	> 45000		39.8	−23.2	12.8	+7.80	3.6	b	15.2	4,5
UCIAMS39111	Popigay	> 45000		32.0	−22.0	11.1	+7.50	3.4	b	23.4	4,5
UCIAMS39881	Arilakh	> 45000		38.8	−22.0	14.5	+11.40	3.1	b	24.0	4,5
Site 1 M. pr. 19	New Siberian Arch.	43600	1000	40.7	−23.2	14.6	+8.70	3.2	b/t	15.4	2
GrA-25856	Novaya R.	42040	830	45.9	−22.5	17.1	+8.46	3.1	b	16.0	1
GrA-57720	New Siberian Arch.	41650	+600/−500	43.5	−22.5	15.0	+10.02	3.4	t	0.9	1
GrA-17439	Novaya R.	41580	1190	43.3	−21.8	16.2	+9.94	3.1	b	6.0	1
UCIAMS39110	Taimyr Peninsula	41000	1400	35.0	−22.1	12.2	+8.10	3.3	b	22.3	4,5
20/415	Taymyr	40800	200	40.6	−22.2	13.7	+6.50	3.5	b	16.7	6
GrA-38905	Lena R.	40800	+650/−550	43.5	−21.3	15.0	+9.06	3.4	b	12.0	1
19/58	Sviatoy Site 1	40200	1800	44.2	−21.6	15.6	+11.20	3.3	b	19.2	6
Site 1 M. pr. 18	New Siberian Arch.	40200	900	42.2	−22.3	16.0	+9.60	3.1	b/t	16.8	2
UCIAMS38678	Baikura-Turku	40150	990	38.4	−21.7	13.6	+8.90	3.3	b	20.1	4,5
20/407	Taymyr	39800	600	42.6	−21.4	14.6	+8.20	3.4	b	23.1	6

20/412	Taymyr	39800	500	42.2	−21.4	14.2	+8.40	3.5	b	20.4	6
Site 1 M. pr. 17	New Siberian Arch.	39600	1000	41.6	−22.5	15.8	+9.40	3.1	b/t	10.2	2
GrA-62205	New Siberian Arch.	39460	+300/ −320	46.7	−22.6	17.1	+11.28	3.2	t	7.5	1
Site 1 M. pr. 16	New Siberian Arch.	37800	900	42.7	−21.9	15.5	+8.80	3.2	b/t	16.8	2
GrA-57021	Unspecified	37710	+430/ −370	42.9	−21.1	17.4	+10.25	2.9	t	2.2	1
GrA-57652	Wrangel Isl.	35870	+320/ −290	43.7	−21.6	16.1	+11.94	3.2	t	8.0	1
GrA-19528	Toll's Bay	35760	+280/ −370	39.8	−20.05				t	0.9	1
UCIAMS38680	Baikura-Turku	35380	550	35.4	−21.4	12.5	+8.70	3.3	b	14.7	4,5
GrA-19284	Oskar Pen.	34680	+350/ −340	39.2	−21.3				t	0.4	1
Site 2 M. pr. 23	Lena Delta	34600		42.1	−22.2	15.6	+9.10	3.1	b/t	10.7	2
GrA-53289	Yana-Indigirka lowl.	34300	+260/ −240	46.7	−22.85	15.9	+12.01	3.4	b	22.7	1
Site 2 M. pr. 15	Lena Delta	34000	500	39.6	−22.0	15.2	+8.60	3.0	b/t	16.1	2
Site 1 M. pr. A	New Siberian Arch.	32500	500	39.2	−22.6	15.9	+9.20	2.9	b/t	17.7	2
GrA-19523	Sabler C.	32180	+210/ −200	42.2	−22.35	16.2	+9.14	3.0	t	7.1	1
Site2-14	Lena Delta	31500	650	38.3	−21.7	14.9	+8.90	3.0	b/t	13.8	2
Site2-13	Lena Delta	30200	400	41.8	−22.1	15.3	+9.10	3.2	b/t	5.8	2
19/52	Sviatoy Site 1	30100	550	42.8	−22.1	14.8	+9.10	3.3	b	18.8	2
GrA-57019	Unspecified	29150	+190/ −180	38.1	−22.2	15.2	+9.10	2.9	t	12.1	1
UCIAMS39885	Lake Taimyr	28700	310	36.6	−21.9	12.9	+9.70	3.3	b	17.2	4,5
GrA-60044	New Siberian Arch.	28660	160	47.4	−22.0	17.3	+10.22	3.2	b	13.6	1
GrA-19275	Oskar Pen.	28370	200	40.5	−21.3	13.4	+10.78	3.5	t	1.3	1
GrA-19271	Oskar Pen.	28350	200	39.0	−21.8	15.6	+11.90	2.9	t	2.6	1
Beta-148643	Lake Taimyr	28260	170	40.5	−21.4	15.0	+9.40	3.2	b	12.2	4,5
Beta-148662	Arilakh	28210	210	39.1	−21.7	14.5	+10.70	3.1	b	14.7	4,5
Site 1 M. pr. 12	New Siberian Arch.	28000	180	40.7	−21.6	15.7	+9.00	3.0	b/t	14.4	2
Beta-210777	Baikura-Turku	27740	220	36.7	−21.9	13.6	+10.00	3.1	b	26.2	4,5
Site2-11	Lena Delta	27400	800	38.6	−21.9	15.8	+9.10	2.8	b/t	14.5	2
Site2-10	Lena Delta	25900	600	39.0	−22.5	14.8	+8.90	3.1	b/t	16.1	2
GrA-19311	Upper Taimyra R.	24990	150	42.3	−22.2	15.2	+10.08	3.3	b	8.3	1

GrA-19526	Upper Taimyra R.	24980	130	41.2	−22.3	13.8	+11.14	3.5	t	2.9	1
GrA-38941	Nordwik C.	24870	+130/−120	45.0	−21.8	16.6	+9.45	3.2	?	1.6	1
GrA-19273	Upper Taimyra R.	24740	150	40.0	−21.8	13.8	+9.66	3.4	b	3.0	1
GrA-19238	Upper Taimyra R.	24460	200	37.7	−21.6	14.2	+10.35	3.1	b	0.2	1
Site2-9	Lena Delta	24300	200	42.6	−22.3	16.1	+7.30	3.1	b/t	21.8	2
Site 1 M. pr. 8	New Siberian Arch.	22100	1000	41.8	−21.3	14.8	+8.30	3.3	b/t	19.8	2
GrA-17604	Taimyr Lake	20950	190	44.4	−22.3	16.0	+8.60	3.2	b	18.4	1
Site2-7	Lena Delta	20800	600	40.7	−21.7	15.2	+8.30	3.1	b/t	20.7	2
GrA-17347	Upper Taimyra R.	20500	90	45.7	−21.3	15.9	+11.21	3.3	b	14.1	1
UCIAMS39886	Sabler C.	20080	110	37.3	−20.8	13.1	+9.10	3.3	b	25.2	4,5
GrA-38930	Yana-Indigirka lowl.	19300	80	44.6	−21.9	16.3	+8.56	3.2	t	11.6	1
GrA-62207	New Siberian Arch.	19160	90	47.0	−21.8	17.1	+8.64	3.2	t	4.4	1
UCIAMS38679	Lake Taimyr	17300	60	39.0	−21.0	14.2	+10.70	3.3	b	20.0	4,5
Beta-148642	Sabler C.	15390	50	37.1	−21.0	13.7	+10.60	3.2	b	16.3	4,5
GrA-19264	Sabler C.	13919	70	38.6	−22.3				b	16.5	1
GrA-57617	Wrangel Isl.	13450	+60/−50	44.0	−21.5	15.6	+10.62	3.3	t	11.4	1
GrA-65681	New Siberian Arch.	13340	60	43.2	−21.9	15.0	+12.14	3.4	t	6.8	1
Site2-3	Lena Delta	13100	500	39.9	−22.7	15.4	+5.60	3.0	b/t	22.2	2
GrA-65517	New Siberian Arch.	13040	60	42.7	−21.1	14.3	+11.64	3.5	d	0.3	1
GrA-65689	New Siberian Arch.	13030	60	43.3	−22.2	15.4	+11.12	3.3	t	0.4	1
GrA-60423	Selliach R.	12470	50	41.7	−21.9	15.0	+8.78	3.2	b	14.4	1
UCIAMS38671	Berelekh	12350	35	37.8	−22.2	13.5	+9.40	3.3	b	18.2	4,5
GrA-65687	New Siberian Arch.	12330	60	46.6	−21.5	15.2	+9.82	3.6	t	2.3	1
UCIAMS38672	Berelekh	12295	40	37.8	−22.0	13.2	+9.40	3.3	b	23.4	4,5
UCIAMS38670	Berelekh	12125	30	43.7	−21.5	15.0	+9.20	3.4	b	11.9	4,5
Site 1 M. pr. 1	New Siberian Arch.	12030	60	41.3	−21.6	16.1	+5.70	3.0	b/t	22.4	2
Beta-148663	Arilakh	11900	40	38.2	−22.5	14.2	+9.10	3.1	b	10.7	4,5
GrA-65512	New Siberian Arch.	11250	50	50.1	−22.5	16.7	+8.81	3.5	b	2.6	1
20/411	Taymyr	11140		46.0	−22.4	15.4	+8.10	3.5	b	18.7	6

GrA-65686	New Siberian Arch.	10920	50	44.5	−22.6	15.2	+8.28	3.4	t	0.7	1
GrA-65685	New Siberian Arch.	10330	50	47.0	−22.5	15.9	+10.18	3.4	t	7.1	1
GrA-19231	Upper Taimyra R.	10230	60	39.4	−22.0	13.4	+9.50	3.4	t	10.3	1
GrA-17350	Bikada R.	9920	60	42.3	−22.8	14.9	+8.62	3.3	b	7.5	1
GrA-65680	New Siberian Arch.	9445	50	44.5	−22.1	15.8	+10.5	3.3	t	5.7	1
GrA-57648	Wrangel Isl.	8395	45	45.2	−22.5	16.5	+9.71	3.2	t	13.2	1
GrA-57649	Wrangel Isl.	8000	40	43.8	−21.8	15.9	+8.90	3.2	t	13.5	1
GrA-57645	Wrangel Isl.	7505	40	44.7	−22.45	16.3	+11.20	3.2	t	12.5	1
GrA-57711	Wrangel Isl.	7300	35	?	−22.6	16.8	+8.47		t	13.5	1
GrA-57647	Wrangel Isl.	7175	40	43.1	−22.5	15.7	+10.32	3.2	t	5.3	1
GrA-57622	Wrangel Isl.	7030	40	46.5	−22.23	16.8	+9.55	3.2	t	6.3	1
GrA-57650	Wrangel Isl.	6455	40	46.3	−21.82	16.9	+9.50	3.2	t	7.6	1
GrA-57725	Wrangel Isl.	6180	35	39.3	−22.55	14.3	+9.12	3.2	d	4.9	1
GrA-57623	Wrangel Isl.	6000	40	48.0	−22.06	17.3			t	15.8	1
GrA-57646	Wrangel Isl.	5615	35	43.8	−21.73	16.0	+8.77	3.2	t	7.3	1
GrA-57726	Wrangel Isl.	5400	40	45.5	−21.94	16.3	+8.68	3.3	t	12.3	1
GrA-57731	Wrangel Isl.	4955	35	48.1	−21.80	17.2	+8.16	3.3	t	14.3	1
GrA-57729	Wrangel Isl.	4870	35	47.6	−21.85	17.5	+9.38	3.2	t	8.1	1
GrA-57709	Wrangel Isl.	4770	35	42.7	−21.71	15.4	+10.08	3.2	t	14.7	1
GrA-57621	Wrangel Isl.	4535	35	47.8	−21.80	17.2	+9.71	3.2	t	13.9	1
GrA-57741	Wrangel Isl.	4495	35	45.3	−22.28	16.5	+9.80	3.2	t	14.2	1
UCIAMS38673	Wrangel Isl.	4420	15	37.9	−22.20	13.6	+8.60	3.3	b	15.5	4,5
GrA-57742	Wrangel Isl.	4410	35	47.5	−21.47	17.3	+9.03	3.2	d	8.9	1
GrA-57727	Wrangel Isl.	4155	35	43.9	−21.91	15.9	+9.73	3.2	t	8.7	1
GrA-57712	Wrangel Isl.	4115	30	41.4	−22.18	15.0	+9.11	3.2	t	5.4	1
GrA-57796	Wrangel Isl.	4030	35	40.1	−22.25	15.2	+10.56	3.1	t	7.2	1
GrA-57619	Wrangel Isl.	4020	35	48.4	−22.18	17.2	+9.10	3.3	t	9.3	1
GrA-57654	Wrangel Isl.	3960	35	46.7	−21.97	17.0	+9.25	3.2	t	12.2	1
GrA-57710	Wrangel Isl.	3955	30	46.7	−22.00	17.3	+8.70	3.1	t	5.7	1

[1]Used abbreviations: GrA = Groningen University, Groningen, NL, Beta = Beta Analytic, Miami, USA, UCIAMS = University of California, Irvine, USA. In cases that the lab code is unknown, we mention the sample ID as referred to in the original publication.

[2] Used abbreviations: Arch = archipel, Isl = island, R = River, C = cave, Lowl = lowland, Pen = Peninsula.

[3] Used abbreviations: b = bone, t = tusk, d = dentine, ? = unspecified.

[4] Used data sources: 1 = current study, 2 = Iacumin *et al.*, 2010, 3 = Bocherens *et al.*, 1996, 4 = Szpak *et al.*, 2010 (stable isotopes), 5 = Debruyne *et al.*, 2008 (^{14}C dates), 6 = Iacumin *et al.*, 2000.

Table SI Chapter 3.2

Isotopic data and sample information from woolly mammoth samples used to define the ranges for 'Alaska' in Fig. 3.4.

Lab code[iii]	Locality[i]	¹⁴C age, yr BP	±	δ¹³C (‰)	δ¹⁵N (‰)	C:N	Source[ii]
AA14939	Ester Cr.	> 45000		−20.5	+5.0	3.2	1,2
AA14855	Cripple Cr.	26022	640	−20.8	+6.4	3.5	1,2
AA14904	Cleary Cr.	43239	1878	−20.8	+4.4	3.5	1,2
AA17538	Eldorado Cr.	30000	1000	−20.7	+7.8	3.2	1,2
AA17535	Dawson	37920	2700	−20.6	+7.9	3.4	1,2
UCIAMS-41486	Paron's L.	> 45000		−21.3	+5.8	3.4	1,2
UCIAMS-39883	Dawson	> 45000		−20.4	+8.7	3.3	1,2
UCIAMS-39884	Dawson	> 45000		−20.3	+6.9	3.3	1,2
UCIAMS-39891	Quartz Cr.	36690	810	−20.5	+6.6	3.3	1,2
UCIAMS-38675	Whitman G.	32140	370	−20.7	+8.1	3.1	1,2
UCIAMS-39116	Sulphur Cr.	> 45000		−20.8	+7.5	3.3	1,2
UCIAMS-39892	Whitman G.	39899	1200	−20.5	+7.3	3.3	1,2
UCIAMS-39112	Finning	29030	310	−20.5	+7.2	3.3	1,2
UCIAMS-39113	Finning	> 45000		−20.6	+6.4	3.4	1,2
UCIAMS-39114	Finning	29170	320	−20.9	+7.1	3.3	1,2
UCIAMS-39887	Finning	44700	2200	−20.6	+5.7	3.3	1,2
UCIAMS-39115	Finning	28960	310	−20.6	+6.8	3.3	1,2
UCIAMS-39889	Hunker Cr.	32470	480	−20.6	+6.9	3.1	1,2
UCIAMS-39888	Hunker Cr.	> 45000		−20.7	+9.0	3.3	1,2
UCIAMS-39890	Indian R.	30630	870	−20.9	+6.4	3.2	1,2
UCIAMS-41490	VGFN Foot	> 45000		−21.2	+9.3	3.1	1,2
AA14935	Cleary Cr.	18379	124	−21.0	+7.0	3.2	1,2
AA17574	Tanana	23150	460	−21.0	+9.7	3.1	1,2
UCIAMS-41487	Hunker Cr.	22430	140	−21.0	+9.4	3.3	1,2
AA14888	Sullivan Cr.	12677	142	−20.8	+5.9	3.3	1,2
UCIAMS-149817	St. Paul Isl.	4750	20	−20.5	+8.1	3.2	3
UCIAMS-148202	St. Paul Isl.	5050	20	−20.7	+7.3	3.4	3
UCIAMS-148200	St. Paul Isl.	5095	20	−20.3	+6.3	3.2	3
UCIAMS-149816	St. Paul Isl.	5200	20	−20.3	+7.6	3.3	3
UCIAMS-149818	St. Paul Isl.	5405	20	−19.7	+7.1	3.2	3

UCIAMS-119831	St. Paul Isl.	5715	30	−19.5	+8.3	3.3	3
UCIAMS-149815	St. Paul Isl.	5960	20	−19.2	+7.2	3.2	3
UCIAMS-148201	St. Paul Isl.	6490	20	−19.2	+7.8	3.3	3
UCIAMS-148199	St. Paul Isl.	7145	25	−20.2	+6.8	3.2	3
UCIAMS-149811	St. Paul Isl.	7610	20	−19.1	+4.4	3.3	2
UCIAMS-149812	St. Paul Isl.	7785	25	−20.7	+3.5	3.3	3
UCIAMS-119830	St. Paul Isl.	8210	35	−20.9	+4.2	3.3	3
UCIAMS-149814	St. Paul Isl.	8370	20	−19.0	+7.6	3.2	3
UCIAMS-149813	St. Paul Isl.	8350	25	−19.1	+6.7	3.2	3

[i] Used abbreviations: Cr = Creek, G = Gulch, Isl = island, L = Lake, R = River.

[ii] Used data sources: 1 = Szpak *et al.*, 2010 [stable isotopes], 2 = Debruyne *et al.*, 2008 [14C dates], 3 = Graham *et al.*, 2016.

[iii] Used abbreviations: AA = University of Arizona AMS, USA, UCIAMS = University of California, Irvine, USA.

Table SI Chapter 4

Results of the isotopic data and sample information arranged per species.

lab code	locality	age (¹⁴C yr BP)	±	C%	δ¹³C (‰)	N%	δ¹⁵N (‰)	C/N ratio	species	skeletal element
GrA-54021	Zuid-Holland, Zandmotor	31140	200	32.3	-21.3				*Lepus species*	mandible
GrA-30722	Brown Bank	8910	50	45.1	-21.1	16.5	4.8	3.2	*Castor fiber*	femur
GrA-22183	Eurogully	>45000		43.4	-19.4	15.4	7.7	3.3	*Canis lupus*	femur
GrA-24209	Eurogully	8780	50	47.7	-25.6	16.7	10.2	3.3	*Canis species*	cranium
GrA-69520	Zuid-Holland, Zandmotor	29900	550	34.3	-20.7	12.5	8.5	3.2	*Alopex lagopus*	unknown
GrA-50465	Brown Bank	>45000		43	-20.3	14.3	7.7	3.5	*Ursus arctos*	mandible
GrA-25816	Eurogully	>45000		35.9	-22.3	14.2	3.5	3	*Ursus species*	unknown
GrA-11643	Brown Bank	40660	350	39.3	-20.1				*Crocuta c. spelaea*	ulna
GrA-23151	Eurogully	>45000		39.9	-19.2	15.7	8.7	3	*Panthera spelaea*	ulna
GrA-31471	North Sea	39970	360	41.5	-19.4	13.9	8.2	3.5	*Panthera spelaea*	scapula
GrA-34644	Brown Bank	10730	60	33.9	-21.2				*Gulo gulo*	mandible
GrA-52432	Eurogully	8825	45	39.4	-24.8				*Lutra lutra*	cranium
GrA-52433	Zuid-Holland, Maasvlakte 2	8300	40	32	-26.2	13.3	8.6	2.8	*Lutra lutra*	mandible
GrA-22178	Eurogully	>45000		45.6	-12.5	14.6	11.5	3.6	*Odobenus rosmarus*	cranium
GrN-28548	Southern Bight	>45000		41.9	-14.1				*Odobenus rosmarus*	femur
GrA-59468	Eurogully	>45000		42.2	-13.3	15.5	11.2	3.2	*Odobenus rosmarus*	mandible
GrA-64644	Denmark, Holmgren	40360	240	39.1	-13.9	15.3	12	3	*Odobenus rosmarus*	atlas
GrA-57505	Eurogully	2070	30	43.7	-12.9	16.9	13.6	3	*Odobenus rosmarus*	tooth
GrA-65933	Zuid-Holland, Maasvlakte 2	25130	130	26.2	-15.5	9.3	14.5	3.3	*Halichoerus grypus*	unknown
GrN-28551	Southern Bight	7180	60	38.7	-11.7				*Halichoerus grypus*	bone
GrN-28546	Southern Bight	>45000		43.9	-15.8				*Pagophilus groenlandica*	humerus

Lab code	Location	Date BP	±		δ13C				Species	Element
GrN-28547	Southern Bight	43500		40.1	-15				*Pagophilus groenlandica*	humerus
GrA-59476	Brown Bank	>45000		42.7	-21.4	15.4	7.8	3.2	*Mammuthus primigenius*	tusk
GrA-50851	Eurogully	>45000		47.9	-22.3	15.9	6.1	3.5	*Mammuthus primigenius*	tibia
GrA-50847	Eurogully	>45000		46.9	-22.1	15.8	6.2	3.5	*Mammuthus primigenius*	tibia
GrA-50854	Brown Bank	>45000		40	-21.7	14.8	7.2	3.1	*Mammuthus primigenius*	tooth
GrA-50860	Brown Bank	>45000		41.3	-21.5	14.3	9	3.4	*Mammuthus primigenius*	tooth
GrA-50848	North Sea	>45000		43.2	-22.2	13.4	8.3	3.7	*Mammuthus primigenius*	tooth
GrA-52416	Brown Bank	>45000		46	-21.6	15.9	9.1	3.4	*Mammuthus primigenius*	tooth
GrA-50846	Brown Bank	>45000		40.3	-22.4	15.2	8	3.1	*Mammuthus primigenius*	tooth
GrA-50843	Brown Bank	>45000		45.1	-22.4	14.1	8.4	3.7	*Mammuthus primigenius*	tooth
GrA-11640	Brown Bank	>45000		47.9	-22.4				*Mammuthus primigenius*	epistropheus
GrA-56656	Brown Bank	>45000		40.3	-21.9	14.9	5.9	3.2	*Mammuthus primigenius*	unknown
GrA-56660	Eurogully	>45000		39.6	-21.9	14.6	5.6	3.2	*Mammuthus primigenius*	humerus
GrA-56661	Eurogully	>45000		41.4	-21.8	15.1	5.7	3.2	*Mammuthus primigenius*	humerus
GrA-56675	Zuid-Holland, Maasvlakte	>45000		41.8	-21.6	15.4	5	3.2	*Mammuthus primigenius*	femur
GrA-56662	Eurogully	43910	550	43.4	-21.8	15.9	6.5	3.2	*Mammuthus primigenius*	ulna
GrA-20134	Eurogully	43800	600	39.7	-22.4				*Mammuthus primigenius*	fibula
GrA-50866	Brown Bank	42690	550	39.1	-21.4	14.8	6.6	3.1	*Mammuthus primigenius*	tooth
GrA-50858	Brown Bank	41450	490	44.7	-22.4	13.7	8.8	3.8	*Mammuthus primigenius*	tooth
GrA-56655	North Sea	41090	400	36.4	-22.1	13.3	6.1	3.2	*Mammuthus primigenius*	unknown
GrA-50864	North Sea	39970	440	34.9	-21.7	13.3	7.9	3.1	*Mammuthus primigenius*	tooth
GrA-56658	Brown Bank	39860	350	41.2	-21.5	15.1	7.2	3.2	*Mammuthus primigenius*	femur
GrA-50852	Eurogully	38960	400	38.6	-22.4	13.8	7.3	3.3	*Mammuthus primigenius*	vertebra
GrN-27410	Eurogully	37580	810	45.6	-21.7				*Mammuthus primigenius*	cranium
GrA-39962	Great Yarmouth	37240	280	27.5	-22.6				*Mammuthus primigenius*	vertebra
GrA-30740	Zeeland, Westerschelde	>45000		46.9	-20.7	17.5	7.5	3.1	*Palaeoloxodon antiquus*	unknown

Lab code	Location								Species	Element
GrA-30590	Zeeland, Westerschelde	>45000		48.7	-21.2	17.3	8.1	3.3	*Palaeoloxodon antiquus*	unknown
GrA-30591	Zeeland, Westerschelde	>45000		45.5	-20.6	15.7	10.1	3.4	*Palaeoloxodon antiquus*	unknown
GrA-30592	Zeeland, Westerschelde	>45000		41.6	-20.6	13.7	11.2	3.5	*Palaeoloxodon antiquus*	unknown
GrA-56664	Zuid-Holland, Maasvlakte	>45000		39.1	-20.2	14.1	9.8	3.2	*Palaeoloxodon antiquus*	cranium
GrA-52410	Eurogully	>45000		35.3	-20.8	16.4	11.6	2.5	*Palaeoloxodon antiquus*	molar root
GrA-40013	Zeeland, Westerschelde	42400	1100	36.6	-20.5	13.1	11.1	3.3	*Palaeoloxodon antiquus*	mandible
GrA-56674	Zuid-Holland, Maasvlakte	>45000		40	-21.3	14.8	3	3.2	*Palaeoloxodon antiquus*	tibia
GrA-42704	Southern Bight	>45000		36.4	-21.4	12.7	6.4	3.3	*Equus species*	metacarpal
GrA-23582	Brown Bank	44780	1635	40.7	-21.4	14.4	5.4	3.3	*Equus species*	tibia
GrA-22585	Eurogully	43550	1200	44.5	-22	16.5	2.3	3.1	*Equus caballus*	ulna
GrA-39964	Great Yarmouth	42960	500	38.2	-21.4	14.1	4.1	3.2	*Equus species*	metacarpal
GrA-37558	Stekels	37860	355	41.9	-19.9	16.3	4.8	3	*Equus caballus*	metacarpal
GrN-32392	Eurogully	>45000		44.4	-20.7				*Coelodonta antiquitatis*	unknown
GrA-39965	Great Yarmouth	>45000		42	-20.6	4.8	4.5	3.3	*Coelodonta antiquitatis*	mandible
GrN-27411	Eurogully	39910	1070	45.8	-20.8				*Coelodonta antiquitatis*	pelvis
GrA-66408	Yerseke	2190	30	39.4	-16.7	13.4	9.3	3.4	*Balaenidae*	bulla
GrA-34338	Southern Bight	>45000		40.9	-14.8	12.7	14.3	3.3	*Balaena mysticetus*	radius
GrA-37034	Southern Bight	>45000		46	-12.6				*Balaenoptera physalus*	thoracic vertebra
GrA-22182	Eurogully	>45000		42.2	-14.4	14.8	13.3	3.3	*Eschrichtius robustus*	vertebra
GrA-34348	Zuid-Holland, Scheveningen	>45000		44.3	-14.8	16.6	12.9	3.1	*Eschrichtius robustus*	vertebra
GrA-34381	Southern Bight	>45000		42.1	-13.3	16.2	14.8	3	*Eschrichtius robustus*	axis
GrN-28549	Southern Bight	42800	4100	42.3	-15.4				*Eschrichtius robustus*	vertebra
GrA-34349	Eurogullly	39100	360	1.6	-14	13.3	12.2	3.6	*Eschrichtius robustus*	atlas
GrA-34378	North Sea	4815	40	40.4	-14	16.2	13.9	2.9	*Eschrichtius robustus*	cranium
GrA-34380	Southern Bight	4230	35	46.8	-15	14.6	14.5	3.7	*Eschrichtius robustus*	vertebra
GrN-31093	Noord-Holland, Andijk	4130	40	39.1	-14.1				*Eschrichtius robustus*	unknown

GrA-34761	Southern Bight	4055	35	46.7	-14.6	13.8	16	3.4	*Eschrichtius robustus*	unknown
GrA-34379	North Sea	3925	35	42.2	-13.1	16.6	14	3	*Eschrichtius robustus*	cranium
GrA-34385	Southern Bight	3650	35	47.2	-13.4	17.4	14.6	3.2	*Eschrichtius robustus*	vertebra
GrA-34383	Southern Bight	2270	35	45	-14.6	16.1	12.5	3.3	*Eschrichtius robustus*	axis
GrA-34369	White Bank	1870	35	43.6	-15.1	17	16.1	3	*Eschrichtius robustus*	mandible
GrA-34368	North Sea	1865	30	42.8	-14.9	15.6	15.9	3.2	*Eschrichtius robustus*	vertebra
GrA-25852	Southern Bight	3120	40	39.8	-12	14.7	15.6	3.2	*Lagenorhynchus albirostris*	mandible
GrA-37555	Stekels	2505	35	43.2	-12.4	15	16.2	3.4	*Lagenorhynchus albirostris*	vertebra
GrA-34342	Wadden Sea (G)	4550	35	45.2	-12.3	17.1	15.4	3.1	*Orcinus orca*	maxila
GrA-25820	Southern Bight	3900	45	38.7	-11.6	14.4	17.4	3.1	*Orcinus orca*	unknown
GrA-25851	Southern Bight	8135	45	40	-11.4	15.6	15.9	3	*Tursiops truncatus*	mandible
GrA-25850	Southern Bight	7390	50	43.5	-12.4	16	14.9	3.2	*Tursiops truncatus*	mandible
GrN-28544	Southern Bight	>45000		40.5	-16.5	16.5			*Delphinapterus leucas*	vertebra
GrA-22179	Eurogully	>45000		40.9	-14.8	12.8	13.9	3.7	*Delphinapterus leucas*	axis
GrA-25849	Borkumrif	>45000		44.6	-14.4	17.3	16.5	3	*Delphinapterus leucas*	vertebra
GrA-34337	Zeeland, Yerseke	40550	400	40.5	-16.4	14.7	15.1	3.1	*Delphinapterus leucas*	mandible
GrA-34339	Southern Bight	8860	40	39.1	-21.9	15.1	4	3.2	*Sus scrofa*	mandible
GrA-32600	Eurogully	8710	45	41.7	-21.2	15.1	6.2	2.8	*Sus scrofa*	humerus
GrA-30721	Eurogully	7780	50	31.9	-21.9	13.4	6.6	3.3	*Sus scrofa*	atlas
GrA-38353	Eurogully	>45000		43	-20.6	15.2		3.6	*Megaloceros giganteus*	cranium
GrA-32601	Eurogully	>45000		45.7	-19.5	14.9	2.5	3.2	*Megaloceros giganteus*	antler
GrA-32685	Eurogully	>45000		40.5	-19.8	19.8			*Megaloceros giganteus*	unknown
GrA-32599	Eurogully	40750	440	38.7	-20.1	14.2	5.5	3.5	*Megaloceros giganteus*	antler
GrA-36110	Brown Bank	10000	50	44.4	-21.1	14.8	3.7	3.3	*Cervus elaphus*	antler
GrA-37796	Stekels	9815	40	42.9	-21.2	15.1	3.5	3.1	*Cervus elaphus*	antler
GrA-37795	Stekels	9675	40	43.7	-20.8	16.5	4.1		*Cervus elaphus*	antler

GrA-25514	North Sea	9500	180	41.5	-21.5				Cervus elaphus	antler
GrA-30732	Brown Bank	9070	50	40.6	-21.9	14.5	5	3.3	Cervus elaphus	tibia
GrA-40524	Eurogully	9070	45	38.1	-21.6	13.7	3.2	3.2	Cervus elaphus	antler
GrA-29204	Brown Bank	8870	50	42.4	-22.2				Cervus elaphus	antler
GrA-37561	Stekels	8830	40	44.2	-21.7	15.2	2.5	3.4	Cervus elaphus	antler
GrA-36113	Brown Bank	8710	50	39.7	-22.5	13.4	2.2	3.5	Cervus elaphus	antler
GrA-25568	Southern Bight	8600	50	36.6	-21.8	13.9	2.1	3.1	Cervus elaphus	antler
GrA-22999	Eurogully	8070	50	38.5	-20.4	16	3.4	2.8	Cervus elaphus	antler
GrA-20280	Zeeland, Roompot	4030	60	32.2	-22.6				Cervus elaphus	antler
GrA-50510	North Sea	3540	40	42.5	-22.6	14.6	5.1	3.4	Cervus elaphus	antler
*	Zeeland, Roompot	1352	34	37.1	-20.9				Cervus elaphus	antler
GrA-23581	Brown Bank	44560	1665	43.9	-20.4	15.3	4.7	3.3	Alces alces	antler
GrA-27206	Brown Bank	9910	50	39.9	-20.9	16.6	1.7	2.8	Alces alces	antler
GrA-37004	Brown Bank	9520	50	39.7	-21.7	14.1	3.4	2.8	Alces alces	antler
GrA-68250	Zuid-Holland	9510	50	44.3	-20.6	16.2	2.2	3.2	Alces alces	antler
GrA-30731	Brown Bank	8240	50	45.8	-21.2	16.4	4.2	3.3	Alces alces	antler
GrA-20475	Brown Bank	>45000		32.4	-19.6				Rangifer tarandus	bone
GrA-20303	Brown Bank	>45000		39.7	-19.6				Rangifer tarandus	metacarpal
GrA-20475	Brown Bank	>45000		32.4	-19.6	15.2	2.9	2.5	Rangifer tarandus	unknown
GrA-32597	Eurogully	45150	650	36.6	-19.1	15.1	2.9	2.8	Rangifer tarandus	metatarsal
GrA-20259	Brown Bank	42300	1000	36.3	-18.9	13.8	3.2	3.1	Rangifer tarandus	astragalus
*	Brown Bank	41604	645	39.8	-19.1	14.4	5.1	3.2	Rangifer tarandus	radius
*	Eurogully/Brown Bank	41832	612	41.1	-19.2				Rangifer tarandus	calcaneum
*	Brown Bank	39210	665	42.2	-19.1	14.7	4.4	3.3	Rangifer tarandus	metacarpal
GrA-20257	Eurogully	39200	700	35.9	-21.2	13.7	6.8	3.1	Rangifer tarandus	phalanx
GrA-20261	Brown Bank	39000	700	39	-19.2	14.1	4.3	3.2	Rangifer tarandus	epistropheus

GrA-31284	Brown Bank	38960	355	35.1	-19.8	13.2	3.6	3.1	*Rangifer tarandus*	antler
GrA-25570	Brown Bank	35160	315	36	-19.3	12.6	2.2	3.3	*Rangifer tarandus*	antler
GrA-39966	Great Yarmouth	31460	160	42.8	-19.5	14.4	2.5	3.5	*Rangifer tarandus*	antler
GrA-20294	Eurogully/Brown Bank	29460	250	38.5	-19.4	15.7	4.1	2.9	*Rangifer tarandus*	astragalus
GrA-20256	Brown Bank	8820	60	40.6	-22.7	16.8	4	2.8	*Rangifer tarandus*	phalanx
GrA-20353	Brown Bank	8350	50	30.6	-23.3				*Rangifer tarandus*	phalanx
GrA-31283	Brown Bank	8880	40	38.9	-22.2	12.8	2.4	3.6	*Capreolus capreolus*	tibia
GrA-33949	Eurogully	8405	45	36.8	-21.4	12.5	3	3.4	*Capreolus capreolus*	antler
GrA-37797	Stekels	>45000		45.9	-20.4	17.9	4.3	3	*Bos primigenius*	femur
GrA-51668	North Sea	8900	40	44.3	-22.4	15.6	5.2	3.3	*Bos primigenius*	unknown
GrA-25569	Brown Bank	8800	50	38.2	-22.3	14.7	5.2	3	*Bos primigenius*	metapodal
GrA-22998	Brown Bank	8780	60	36.2	-22.6	15.5	5.5	2.7	*Bos primigenius*	metacarpal
GrA-51786	Eurogully	8175	40	42.8	-22.8	16.6	6.1	3	*Bos primigenius*	horn pit
GrN-28261	Eurogully	>45000		50.7	-19.6				*Bison priscus*	lendal vertebra
GrA-39518	Great Yarmouth	39900	850	35.6	-20.9				*Bison species*	metacarpale
GrA-28364	Brown Bank	11560	50	37.9	-20.6	14.5	3.9	3.1	*Bison species*	metatarsus
GrA-34524	Brown Bank	>45000		37.5	-21.9	13.2	6.1	3.3	*Bovidae*	unknown
GrA-34531	Brown Bank	>45000		39.2	-21.7	14.3	5.4	3.2	*Bovidae*	unknown
GrA-34533	Brown Bank	>45000		42.1	-21.9	15.1	6.7	3.2	*Bovidae*	unknown
GrA-51667	North Sea	9220	40	38.6	-22.7	14.7	4.9	3.1	*Bovidae*	metacarpal
GrA-34526	Brown Bank	110	50	45.2	-21.8	15.9	5.1	3.3	*Bovidae*	unknown
GrA-11641	Brown Bank	36740	230	42.5	-20.1				*Ovibos moschatus*	metacarpal
*	Brown Bank	15183	36	37	-19.2	14.1	7.5	3	*Caprinae*	unknown
GrA-58271	Zuid-Holland, Maasvlakte	11050	45	41.6	-20.6	14.9	9.7	3.3	*Homo sapiens*	bone
GrA-42700	Southern Bight	10070	50	36	-24.7	13.3	11.2	3.2	*Homo sapiens*	cranium
GrA-42702	Southern Bight	9440	50	41.5	-24.2	15.6	13.6	3.1	*Homo sapiens*	cranium

GrA-57506	Eurogully/Brown Bank	9440	45	40.3	-24.4	15.1	12.2	3.1	Homo sapiens	femur
GrA-50459	Eurogully	9220	60	35.4	-22.8	13.1	10	3.2	Homo sapiens	femur
GrA-62470	Zuid-Holland, Maasvlakte	9180	50	42.7	-23	16.2	10.3	3.1	Homo sapiens	cranium
GrA-49638	North Sea	9150	50	44.5	-22.7	16.3	4.5	3.2	Homo sapiens	bone
GrA-27188	Brown Bank	9140	50	36.4	-23.1	15.4	10.2	2.8	Homo sapiens	humerus
GrA-30733	Brown Bank	9080	50	42.6	-22	15.3	11.6	3.2	Homo sapiens	bone
GrA-31287	Brown Bank	9035	40	33.2	-23.4	12.3	11.4	3.2	Homo sapiens	bone
GrA-35949	Brown Bank	9005	45	40.7	-23.3	14.1	10.8	3.4	Homo sapiens	humerus
GrA-62225	Eurogully	8945	45	40.4	-13.4	15	14.1	3.1	Homo sapiens	humerus
GrA-51669	North Sea	8910	40	43.7	-22.1	15.7	9.4	3.2	Homo sapiens	bone
GrA-49637	North Sea	8820	50	44.1	-22.5	13.9	9.3	3.7	Homo sapiens	bone
GrA-67124	Zuid-Holland, Zandmotor	8680	45	44	-23.6	16.1	12.4	3.2	Homo sapiens	cranium
GrA-45801	Brown Bank	8665	45	43.6	-16.5	15.3	15.7	3.3	Homo sapiens	femur
GrA-54735	North Sea	8660	50	43.1	-16.7	15.6	13.8	3.2	Homo sapiens	femur
M-21188	Zuid-Holland, Hoek van Holland	8630	25	51.3	-23.4	18	14.1	3.3	Homo sapiens	tooth
GrA-57501	Zuid-Holland, Maasvlakte	8565	45	37.3	-23.5	14	12.7	3.1	Homo sapiens	cranium
*	Eurogully	8610	36	43	-24.1	15.4	12.4	3.3	Homo sapiens	femur
GrA-65508	Slijtgeul	8560	50	30.5	-19.8	11.2	12.9	3.2	Homo sapiens	maxilla
GrA-56366	Zuid-Holland, Hoek van Holland	8425	40	37.4	-21.3	14.2	14.9	3.1	Homo sapiens	tooth
GrA-63432	Zuid-Holland, Hoek van Holland	8375	45	34	-23.1	12.8	12.5	3.1	Homo sapiens	cranium
GrA-11642	North Sea	8370	50	39	-15.6	14.3	15.7	3.2	Homo sapiens	mandible
GrA-56352	Zeeland, Burgh Haamstede	8290	40	42	-19.9	15.7	15	3.1	Homo sapiens	tooth
GrA-27205	Brown Bank	8180	45	40.6	-22.6	17.7	15.1	2.7	Homo sapiens	femur
GrA-65943	Zuid-Holland, Zandmotor	8140	45	39.1	-22.5	14	15.9	3.3	Homo sapiens	cranium
GrM-10211	Noord-Holland, Castricum	8000	45	43.2	-16.9	15.5	17.4	3.2	Homo sapiens	bone
GrA-51670	North Sea	7955	40	43.3	-21.5	15.6	14.6	3.2	Homo sapiens	bone

GrA-68069	North Sea	7950	45	43	-17.6	15.7	16.2	3.2	*Homo sapiens*	tooth
GrA-63431	Zuid-Holland, Monster	7885	45	38.4	-21.3	15	14.1	3	*Homo sapiens*	cranium
GrA-63799	Zuid-Holland, Maasvlakte	7870	45	40.8	-23.7	15	12.9	3.2	*Homo sapiens*	cranium
GrA-67123	Zuid-Holland, Zandmotor	7810	45	41.5	-20.9	15.1	15.6	3.2	*Homo sapiens*	cranium
GrA-65507	Zuid-Holland, Zandmotor	7760	45	36.3	-21.6	13.1	16.4	3.2	*Homo sapiens*	femur
GrA-68591	Zuid-Holland, Den Haag	7725	45	44.8	-23.2	16.3	13.9	3.2	*Homo sapiens*	cranium
GrM-10161	Wadden Sea, Texel	5020	25	45.8	-21	16.7	9.6	3.2	*Homo sapiens*	cranium
GrM-10748	Noord-Holland, Bloemendaal	3130	20	44.9	-20.2	16.4	13.4	3.2	*Homo sapiens*	vertebra
GrM-10746	Noord-Holland, Noordwijk	2985	20	46.3	-20.2	16.9	8	3.2	*Homo sapiens*	femur
GrM-12352	Noord-Holland, Noordwijk	2842	16	44	-20.2	16	9.5	3.2	*Homo sapiens*	humerus
GrA-65511	Wadden Sea, Terschelling	2740	35	40.5	-20.4	14.1	10.2	3.3	*Homo sapiens*	vertebra
GrM-13967	North Sea	2518	16	42.3	-20.3	15.3	8.5	3.2	*Homo sapiens*	phalanx
GrM-12977	Katwijk/Wassenaar	2515	16	44.7	-19.8	15.9	10.2	3.3	*Homo sapiens*	mandible
GrA-67067	North Sea	2285	30	42.3	-20.4	15.5	11.3	3.2	*Homo sapiens*	vertebra
GrA-68058	Zuid-Holland, Den Haag	2190	30	38	-19.6	13.9	12.2	3.2	*Homo sapiens*	tooth
GrM-12817	Wadden Sea, Texel	2156	15	44	-19.4	15.9	11.7	3.2	*Homo sapiens*	cranium
GrA-69134	Zuid-Holland, Katwijk	1995	30	45.2	-20.2	16.4	10.4	3.2	*Homo sapiens*	scapula
GrM-12923	Scheveningen	1838	15	47.3	-19.9	17.2	10	3.2	*Homo sapiens*	femur
GrA-63619	Wadden Sea, Terschelling	1830	30	44.2	-19.9	16.6	9.9	3.1	*Homo sapiens*	bone
GrM-12944	Noordwijk	1808	15	46.2	-19.7	16.9	12.1	3.2	*Homo sapiens*	vertebra
GrA-64747	Noord-Holland, Zaandam	1805	30	46.4	-20.2	16.9	9.9	3.2	*Homo sapiens*	femur
GrM-13316	Cadzand	1799	15	42.9	-18.7	15.7	9.8	3.2	*Homo sapiens*	mandible
GrA-64726	Zeeland, Borsele	1335	30	41.9	-19.4	15.2	12	3.2	*Homo sapiens*	tooth
GrA-50511	Southern Bight	1260	40	43.3	-20.3	12.7	8.8	4	*Homo sapiens*	bone
GrM-10157	Wadden Sea, Texel	1225	20	45.4	-20.1	16.6	9.6	3.2	*Homo sapiens*	cranium
GrM-10158	Wadden Sea, Texel	1205	20	45.5	-20	16.7	9.7	3.2	*Homo sapiens*	cranium

Lab ID	Location								Species	Element
GrM-12819	Wadden Sea, Texel	1212	15	43.3	-19.8	15.7	10.8	3.2	Homo sapiens	cranium
GrA-31286	Zeeland, Westerschelde	1200	25	49.6	-19.5	17.1	12	3.4	Homo sapiens	bone
GrA-65510	Zuid-Holland, Maasvlakte	1175	30	47	-20.6	16	10.8	3.4	Homo sapiens	cranium
GrM-12519	Zeeland	1141	13	46.5	-20	17	12.3	3.2	Homo sapiens	vertebra
GrM-10814	Zeeland	1115	12	42.5	-19.5	15.6	11.9	3.2	Homo sapiens	mandible
GrM-12518	Zeeland	1035	14	47.5	-20	17.4	9.4	3.2	Homo sapiens	cranium
GrA-66669	Zuid-Holland, Den Haag	1015	30	46.2	-19.7	16.7	10.9	3.2	Homo sapiens	vertebra
GrM-12512	Zeeland	986	14	46.7	-19.9	17.2	10.6	3.2	Homo sapiens	mandible
GrM-12513	Zeeland	975	13	45.8	-19.7	16.7	10	3.2	Homo sapiens	vertebra
GrM-12594	Zeeland	951	13	46.4	-20.3	16.8	12.2	3.2	Homo sapiens	cranium
GrM-10150	Wadden Sea, Texel	905	20	43.9	-18	16	13.6	3.2	Homo sapiens	humerus
GrA-67125	Zuid-Holland, Den Haag	875	30	44.4	-19.1	16.1	11.3	3.2	Homo sapiens	humerus
GrM-10156	Wadden Sea, Texel	840	20	43.8	-19.7	15.9	14	3.2	Homo sapiens	mandible
GrM-10172	North Sea	791	17	40.5	-19.4	14.6	12.4	3.2	Homo sapiens	bone
GrM-10162	Wadden Sea, Texel	730	20	43	-19.2	15.7	10.7	3.2	Homo sapiens	femur
GrA-68787	Zuid-Holland, Monster	730	30	45.4	-19.4	16.6	12.5	3.2	Homo sapiens	mandible
GrM-10163	Wadden Sea, Texel	695	20	43.5	-19.8	15.8	12.9	3.2	Homo sapiens	femur
GrM-12511	Zeeland	654	13	46.7	-19.6	17.2	11.8	3.2	Homo sapiens	cranium
GrM-10160	Wadden Sea, Texel	630	20	42.5	-20	15.4	12.7	3.2	Homo sapiens	cranium
GrA-69069	Noord-Holland, Noordwijk	585	30	42.8	-18.3	15.5	14.6	3.2	Homo sapiens	scapula
GrA-68049	North Sea	540	30	42.5	-19.9	15.4	11.5	3.2	Homo sapiens	mandible
GrA-61784	Noord-Holland, Wijk aan Zee	485	35	43.4	-18.5	15.5	13.7	3.3	Homo sapiens	mandible
GrM-12592	Wadden Sea, Griend	477	13	46	-17.2	16.8	15.2	3.2	Homo sapiens	pelvis
GrA-62687	Zuid-Holland, Biesbosch	470	30	13.3	-19.9	4.5	13.5	3.5	Homo sapiens	cranium
GrA-67126	Zuid-Holland, Den Haag	450	30	41.7	-18.9	15.1	13.4	3.2	Homo sapiens	femur
GrM-11117	Wadden Sea	374	17	35.7	-20.1	13	12.2	3.2	Homo sapiens	tooth

GrM-12514	356	Zeeland	13	47.9	-19.4	17.6	14.1	3.2	Homo sapiens	cranium
GrA-66670	355	Zuid-Holland, Den Haag	30	47.3	-20.1	17.1	11.4	3.2	Homo sapiens	vertebra
GrM-10351	340	Schiermonnikoog	15	43.8	-18.5	16.3	13.1	3.1	Homo sapiens	bone
GrM12013	338	North Sea	11	45.9	-20.5	16.3	10.7	3.3	Homo sapiens	bone
GrA-69720	335	Wadden Sea, Texel	35	41.9	-19.9	15.2	12.9	3.2	Homo sapiens	vertebra
GrM-12590	334	Zeeland, Domburg	13	46.8	-18.5	17.1	11.6	3.2	Homo sapiens	femur
GrM-10152	310	Wadden Sea, Texel	25	42.6	-21.6				Homo sapiens	femur
GrA-69722	300	Wadden Sea, Texel	35	43.4	-20.1	15.9	13.6	3.2	Homo sapiens	vertebra
GrA-37072	280	Eurogully	35	40.9	-18.2	13.5	12.2	3.5	Homo sapiens	humerus
GrA-68584	250	Zeeland, Vlissingen	30	41	-19.5	14.8	13.5	3.2	Homo sapiens	cranium
GrA-68309	248	North Sea	28	44.8	-19.9	16.2	12.3	3.2	Homo sapiens	mandible
GrM-10159	235	Wadden Sea, Texel	20	46.2	-19.5	16.9	11.3	3.2	Homo sapiens	cranium
GrA-64893	225	North Sea	30	44.1	-17	15.5	15.1	3.3	Homo sapiens	tibia
GrA-67581	225	Zeeland, Oostkapelle	30	44.9	-18	16.3	11.2	3.2	Homo sapiens	cranium
GrM-12348	223	Wadden Sea, Terschelling	14	45.6	-13.4	16.5	13.4	3.2	Homo sapiens	tibia
GrM-10149	220	Wadden Sea, Texel	20	43.1	-18.4	15.5	12.8	3.2	Homo sapiens	humerus
GrA-67523	210	Wadden Sea, Holwerd	30	46.9	-18.1	17	11.8	3.2	Homo sapiens	tibia
GrM-10200	207	North Sea	13	45.3	-19.7	16.4	11.6	3.2	Homo sapiens	bone
GrA-63668	205	North Sea	30	46.8	-17.2	17.3	11.1	3.2	Homo sapiens	bone
GrA-64239	200	North Sea	30	47	-19.6	17	11.9	3.2	Homo sapiens	bone
GrA-64895	195	North Sea	30	44.6	-19.2	15.1	11.3	3.5	Homo sapiens	tibia
GrM-10173	191	North Sea	16	42.9	-19.2	15.5	13.4	3.2	Homo sapiens	bone
GrA-68059	191	North Sea	30	39.8	-18.6	14.4	10.6	3.2	Homo sapiens	cranium
GrA-68655	190	Zuid-Holland, Wassenaar	30	45.6	-17.7	16.7	12.1	3.2	Homo sapiens	vertebra
GrM-10168	190	Wadden Sea, Texel	20	45	-17.8	16.3	11.8	3.2	Homo sapiens	femur
GrM-12516	178	Zeeland	13	46.9	-18.5	17.2	12.1	3.2	Homo sapiens	fibula

GrA-68310	North Sea	175	30	45.1	-19.5	16.3	11.8	3.2	*Homo sapiens*	mandible
GrA-69018	Zeeland, Sluis	170	30	47.5	-19.5	17	12.6	3.3	*Homo sapiens*	humerus
GrA-65315	Noord-Holland, Bergen aan Zee	165	30	41.6	-17.4	14.5	11.6	3.3	*Homo sapiens*	humerus
GrA-69724	Wadden Sea, Texel	165	30	45.2	-19.3	16.6	10.9	3.2	*Homo sapiens*	femur
GrA-69020	Zeeland, Sluis	160	30	43.8	-19.9	15.6	12.6	3.3	*Homo sapiens*	pelvis
GrM-10151	Wadden Sea, Texel	160	20	45.3	-19.6	16.4	10.1	3.2	*Homo sapiens*	humerus
GrM-10164	Wadden Sea, Texel	160	20	39.8	-19.9	14.6	12.6	3.2	*Homo sapiens*	femur
GrM-12346	Wadden Sea, Schiermonnikoog	159	14	44.6	-19.2	16.1	13.6	3.2	*Homo sapiens*	tibia
GrA-69723	Wadden Sea, Texel	155	35	45.1	-18.5	16.5	12.1	3.2	*Homo sapiens*	femur
GrM-12589	Zeeland, Domburg	144	12	46.9	-19.3	17.2	11.8	3.2	*Homo sapiens*	mandible
GrA-69019	Zeeland, Sluis	140	30	47.4	-19.6	17	12.6	3.3	*Homo sapiens*	cranium
GrM-10199	North Sea	130	14	45.8	-20	16.7	11.6	3.2	*Homo sapiens*	bone
GrA-64894	North Sea	120	30	40.8	-18.2	14.4	11.7	3.3	*Homo sapiens*	tibia
GrA-64891	Wadden Sea	115	30	43.8	-19.9	15.7	11.2	3.2	*Homo sapiens*	cranium
GrA-64892	Wadden Sea	75	30	45.3	-19.6	16.2	12.3	3.3	*Homo sapiens*	cranium
GrA-69016	North Sea	0	25	48.8	-19.6	17	12.4	3.4	*Homo sapiens*	cranium
GrA-69725	Zuid-Holland	0	25	44.2	-19.8	16.1	12.2	3.2	*Homo sapiens*	humerus
GrA-64453	Zuid-Holland, Hoek van Holland	43290	380	39.9	-14.9	14.5	17.6	3.2	*Pinguinus impennis*	humerus
GrA-64384	Zuid-Holland, Zandmotor	6480	40	35.5	-14.3	12.9	17.7	3.2	*Pinguinus impennis*	humerus
GrA-65546	Zuid-Holland, Zandmotor	3505	35	39.4	-14.2	13.8	16	3.3	*Pinguinus impennis*	unknown
GrA-43620	Stekels	>45000		36.6	-23	13.7	4.6	3.1	*unknown*	unknown
GrA-40522	Brown Bank, SW	>45000		38.9	-20.6	14.4	5.2	3.2	*unknown*	cf tibia
GrA-43612	Stekels	8945	45	34.8	-22.8	13.9	5.4	2.9	*unknown*	bone
GrA-59743	Zuid-Holland, Maasvlakte	8680	60	37.8	-19.6	13.9	4.2	3.2	*unknown*	unknown
GrA-30795	Brown Bank	8660	50	45.7	-21.9	16.1	5.3	3.3	*unknown*	metapodal
GrA-42195	Zuid-Holland, Rockanje	8295	45	42.4	-22.1	13.1	6.3	3.8	*unknown*	unknown

SI Chapter 7

OxCal code used to establish the final extinction date of the woolly mammoth.

```
Plot()
{
 Outlier_Model("General",T(5),U(0,4),"t");
 Sequence()
 {
  Boundary("Start Mammoth Wrangel Island");
  Phase("Mammoth Wrangel Island ")
  {
   R_Date("AA-60048", 8980, 90)
   {
    Outlier("General", 0.05);
   };
   R_Date("AA-60049", 8870, 100)
   {
    Outlier("General", 0.05);
   };
   R_Date("Ua-17609", 8850, 95)
   {
    Outlier("General", 0.05);
   };
   R_Date("Ua-17614", 8710, 95)
   {
    Outlier("General", 0.05);
   };

   R_Date("Ua-13363", 8640, 80)
   {
    Outlier("General", 0.05);
   };
   R_Date("Ua-17615", 8445, 100)
   {
    Outlier("General", 0.05);
   };
   R_Date("GrA-57648", 8395, 45)
   {
    Outlier("General", 0.05);
   };
   R_Date("GIN-8655", 8150, 60)
   {
    Outlier("General", 0.05);
   };
   R_Date("Ua-17624", 8135, 80)
   {
    Outlier("General", 0.05);
   };
   R_Date("Ua-17619", 8085, 85)
   {
    Outlier("General", 0.05);
   };
   R_Date("Ua-13377", 8030, 75)
   {
    Outlier("General", 0.05);
   };
   R_Date("GrA-57649", 8000, 40)
   {
    Outlier("General", 0.05);
   };
   R_Date("Ua-13370", 7910, 80)
   {
    Outlier("General", 0.05);
   };
   R_Date("LU-4473", 7850, 80)
   {
    Outlier("General", 0.05);
   };
   R_Date("Ua-17612", 7835, 85)
   {
    Outlier("General", 0.05);
   };
   R_Date("LU-4450", 7820, 220)
   {
    Outlier("General", 0.05);
   };
   R_Date("OxA-30122", 7711, 36)
   {
    Outlier("General", 0.05);
   };
   R_Date("GIN-6995", 7710, 40)
   {
    Outlier("General", 0.05);
   };
   R_Date("GIN-6996", 7620, 30)
   {
    Outlier("General", 0.05);
   };
   R_Date("Ua-13372", 7510, 80)
   {
    Outlier("General", 0.05);
   };
   R_Date("GrA-57645", 7505, 40)
   {
    Outlier("General", 0.05);
   };
   R_Date("Ua-17630", 7420, 90)
   {
    Outlier("General", 0.05);
   };
   R_Date("LU-2444", 7390, 30)
   {
    Outlier("General", 0.05);
   };
   R_Date("LU-2559", 7360, 50)
   {
    Outlier("General", 0.05);
   };
```

```
R_Date("GrA-57711", 7300, 35)
{
 Outlier("General", 0.05);
};
R_Date("LU-3743", 7300, 120)
{
 Outlier("General", 0.05);
};
R_Date("GIN-6991", 7280, 40)
{
 Outlier("General", 0.05);
};
R_Date("GIN-6986", 7270, 60)
{
 Outlier("General", 0.05);
};
R_Date("LU-2809", 7250, 60)
{
 Outlier("General", 0.05);
};
R_Date("LU-3514", 7190, 70)
{
 Outlier("General", 0.05);
};
R_Date("GrA-57647", 7175, 40)
{
 Outlier("General", 0.05);
};
R_Date("Ua-17621", 7130, 85)
{
 Outlier("General", 0.05);
};
R_Date("Ua-17622", 7060, 80)
{
 Outlier("General", 0.05);
};
R_Date("LU-2746", 7040, 60)
{
 Outlier("General", 0.05);
};
R_Date("GrA-57622", 7030, 40)
{
 Outlier("General", 0.05);
};
R_Date("Ua-17634", 6910, 75)
{
 Outlier("General", 0.05);
};
R_Date("GIN-6994", 6900, 60)
{
 Outlier("General", 0.05);
};
R_Date("LU-2810", 6890, 50)
{
 Outlier("General", 0.05);
};
R_Date("LU-3515", 6830, 40)
{
 Outlier("General", 0.05);
};
R_Date("LU-2736", 6760, 50)
{
 Outlier("General", 0.05);
};
R_Date("GIN-6990", 6750, 30)
{
 Outlier("General", 0.05);
};
R_Date("GIN-8654", 6720, 50)
{
 Outlier("General", 0.05);
};
R_Date("GIN-6997", 6690, 60)
{
 Outlier("General", 0.05);
};
R_Date("GIN-7692", 6650, 40)
{
 Outlier("General", 0.05);
};
R_Date("LU-2558", 6610, 50)
{
 Outlier("General", 0.05);
};
R_Date("LU-3740", 6590, 70)
{
 Outlier("General", 0.05);
};
R_Date("LU-4449", 6560, 60)
{
 Outlier("General", 0.05);
};
R_Date("Ua-13361", 6560, 75)
{
 Outlier("General", 0.05);
};
R_Date("Ua-13360", 6530, 70)
{
 Outlier("General", 0.05);
};
R_Date("AA-40666", 6499, 66)
{
 Outlier("General", 0.05);
};
R_Date("GrA-57650", 6455, 40)
{
 Outlier("General", 0.05);
};
R_Date("Ua-13374", 6410, 90)
{
 Outlier("General", 0.05);
};
R_Date("Ua-13367", 6405, 65)
{
```

```
 Outlier("General", 0.05);
};
R_Date("LU-3741", 6390, 70)
{
 Outlier("General", 0.05);
};
R_Date("LU-2799", 6260, 50)
{
 Outlier("General", 0.05);
};
R_Date("Ua-17625", 6245, 80)
{
 Outlier("General", 0.05);
};
R_Date("LU-4471", 6220, 50)
{
 Outlier("General", 0.05);
};
R_Date("LU-4468", 6190, 70)
{
 Outlier("General", 0.05);
};
R_Date("GrA-57725", 6180, 35)
{
 Outlier("General", 0.05);
};
R_Date("OxA-30117", 6148, 32)
{
 Outlier("General", 0.05);
};
R_Date("Ua-13371", 6090, 75)
{
 Outlier("General", 0.05);
};
R_Date("LU-3739", 6070, 70)
{
 Outlier("General", 0.05);
};
R_Date("GrA-57623", 6000, 40)
{
 Outlier("General", 0.05);
};
R_Date("LU-4474", 5910, 50)
{
 Outlier("General", 0.05);
};
R_Date("Ua-13356", 5875, 70)
{
 Outlier("General", 0.05);
};
R_Date("GrA-57646", 5615, 35)
{
 Outlier("General", 0.05);
};
R_Date("GIN-6988", 5610, 40)
{
 Outlier("General", 0.05);
```

```
};
R_Date("Ua-17626", 5570, 85)
{
 Outlier("General", 0.05);
};
R_Date("LU-2535", 5480, 50)
{
 Outlier("General", 0.05);
};
R_Date("Ua-17629", 5475, 75)
{
 Outlier("General", 0.05);
};
R_Date("Ua-17627", 5470, 85)
{
 Outlier("General", 0.05);
};
R_Date("GrA-57726", 5400, 40)
{
 Outlier("General", 0.05);
};
R_Date("Ua-17631", 5375, 85)
{
 Outlier("General", 0.05);
};
R_Date("LU-2742", 5310, 90)
{
 Outlier("General", 0.05);
};
R_Date("Ua-13359", 5285, 65)
{
 Outlier("General", 0.05);
};
R_Date("LU-2744", 5250, 40)
{
 Outlier("General", 0.05);
};
R_Date("LU-2745", 5200, 30)
{
 Outlier("General", 0.05);
};
R_Date("Ua-17628", 5185, 80)
{
 Outlier("General", 0.05);
};
R_Date("LU-2794", 5110, 40)
{
 Outlier("General", 0.05);
};
R_Date("Ua-17617", 5010, 75)
{
 Outlier("General", 0.05);
};
R_Date("Ua-13357", 4985, 65)
{
 Outlier("General", 0.05);
};
```

```
R_Date("GIN-7693", 4960, 120)
{
 Outlier("General", 0.05);
};
R_Date("GrA-57731", 4955, 35)
{
 Outlier("General", 0.05);
};
R_Date("Ua-17613", 4955, 80)
{
 Outlier("General", 0.05);
};
R_Date("LU-2740", 4900, 40)
{
 Outlier("General", 0.05);
};
R_Date("GrA-57729", 4870, 35)
{
 Outlier("General", 0.05);
};
R_Date("Ua-13358", 4860, 70)
{
 Outlier("General", 0.05);
};
R_Date("Ua-13376", 4860, 75)
{
 Outlier("General", 0.05);
};
R_Date("AA-60047", 4860, 60)
{
 Outlier("General", 0.05);
};
R_Date("Ua-17620", 4800, 75)
{
 Outlier("General", 0.05);
};
R_Date("GrA-57709", 4770, 35)
{
 Outlier("General", 0.05);
};
R_Date("GIN-6992", 4750, 50)
{
 Outlier("General", 0.05);
};
R_Date("LU-2556", 4740, 40)
{
 Outlier("General", 0.05);
};
R_Date("Ua-13368", 4730, 65)
{
 Outlier("General", 0.05);
};
R_Date("Ua-13373", 4675, 75)
{
 Outlier("General", 0.05);
};
R_Date("Ua-17623", 4615, 75)

{
 Outlier("General", 0.05);
};
R_Date("Ua-17616", 4585, 70)
{
 Outlier("General", 0.05);
};
R_Date("GrA-57621", 4535, 35)
{
 Outlier("General", 0.05);
};
R_Date("AA-60621", 4530, 60)
{
 Outlier("General", 0.05);
};
R_Date("GIN-7694", 4500, 50)
{
 Outlier("General", 0.05);
};
R_Date("GrA-57741", 4495, 35)
{
 Outlier("General", 0.05);
};
R_Date("LU-3742", 4490, 80)
{
 Outlier("General", 0.05);
};
R_Date("Ua-13378", 4475, 60)
{
 Outlier("General", 0.05);
};
R_Date("UCIAMS38673", 4420, 15)
{
 Outlier("General", 0.05);
};
R_Date("GrA-57742", 4410, 35)
{
 Outlier("General", 0.05);
};
R_Date("LU-2768", 4410, 50)
{
 Outlier("General", 0.05);
};
R_Date("LU-2756", 4400, 40)
{
 Outlier("General", 0.05);
};
R_Date("AA-40667", 4389, 46)
{
 Outlier("General", 0.05);
};
R_Date("GIN-6984", 4370, 30)
{
 Outlier("General", 0.05);
};
R_Date("GIN-6989", 4370, 40)
{
```

```
 Outlier("General", 0.05);
 };
 R_Date("GIN-8249", 4370, 70)
 {
  Outlier("General", 0.05);
 };
 R_Date("LU-3513", 4350, 60)
 {
  Outlier("General", 0.05);
 };
 R_Date("Ua-13364", 4335, 60)
 {
  Outlier("General", 0.05);
 };
 R_Date("Ua-13362", 4260, 75)
 {
  Outlier("General", 0.05);
 };
 R_Date("GIN-6993", 4230, 30)
 {
  Outlier("General", 0.05);
 };
 R_Date("Ua-13375", 4210, 70)
 {
  Outlier("General", 0.05);
 };
 R_Date("GrA-57727", 4155, 35)
 {
  Outlier("General", 0.05);
 };
 R_Date("LU-4448", 4120, 110)
 {
  Outlier("General", 0.05);
 };
 R_Date("GrA-57712", 4115, 30)
 {
  Outlier("General", 0.05);
 };
 R_Date("OxA-11181", 4091, 36)
 {
  Outlier("General", 0.05);
 };
 R_Date("Ua-13369", 4085, 65)
 {
  Outlier("General", 0.05);
 };
 R_Date("LU-2808", 4040, 30)
 {
  Outlier("General", 0.05);
 };
 R_Date("GrA-57796", 4030, 35)
 {
  Outlier("General", 0.05);
 };
 R_Date("GrA-57619", 4020, 35)
 {
  Outlier("General", 0.05);
```

```
 };
 R_Date("LU-2798", 4010, 50)
 {
  Outlier("General", 0.05);
 };
 R_Date("GrA-57654", 3960, 35)
 {
  Outlier("General", 0.05);
 };
 R_Date("GrA-57710", 3955, 30)
 {
  Outlier("General", 0.05);
 };
 R_Date("GIN-6983", 3920, 30)
 {
  Outlier("General", 0.05);
 };
 R_Date("GIN-6985", 3920, 40)
 {
  Outlier("General", 0.05);
 };
 R_Date("AA-40665", 3905, 47)
 {
  Outlier("General", 0.05);
 };
 R_Date("LU-2741", 3730, 40)
 {
  Outlier("General", 0.05);
 };
 R_Date("Ua-13366", 3685, 60)
 {
  Outlier("General", 0.05);
 };
 };
 Boundary("End Mammoth Wrangel Island ");
 };
 };
```

Acknowledgements

Rianne Simons, Karen van der Veen and Ivo Verheijen. I really appreciate the time we have had together and would like to thank you for your contribution to my research. In particular, I am grateful to André for everything he taught me about animal bone morphology and for allowing me to sample material at his laboratory. And I thank Inge for her discussions and advice. Furthermore, I thank Dimitri De Loecker, Gerrit Dusseldorp, Mike Field, Yvonne Haring, Jaap Hoff, Richard Jansen, Wim Kuijper, Geeske Langejans, Bouke van der Meer, Claudia Regoor, Rachel Schats, Femke Tomas and Olga Yates, for their support and contribution.

I am thankful also for the valuable input from my co-authors and the interesting discussions we had together. Prof. dr. Hervé Bocherens and Dr. Dorothée Drucker are especially acknowledged for sharing their stable isotope expertise, their valuable insights, and for welcoming me at their institute in Tübingen (Germany).

Thanks are owed to those who supplied me with samples and useful data or other relevant information, in particular to my Russian colleagues Anastasia Markova, Andrey Puzachenko, Alexei Tikhonov, Pavel Kosintsev, Dimitri Ponomarev, Olga Bachura and Tatiana Kuznetsova, and to Dick Mol (the Netherlands).

I am very grateful to the ECHOES team for their inspiration during the last phase of my PhD: Michael Dee, Andreas Neocleous and Andrea Scifo. Especially, I thank Mike very much for his trust, patience, encouragement, and for enabling me to finish the dissertation and combine work in a manageable way. And for teaching me copious numbers of synonyms.

On a more personal note, I would like to express my gratitude to Marijke Meima, Susanne, Elise and Lidewij Broekema and Michiel van der Plicht for their endless hospitality and warmth during my stay in Groningen, when I was still living in the Randstad. In particular, I thank Marijke for her tasty dinners and personal concern for my well-being.

I would like to thank my family and friends for their interest in the progress of my research. They assisted, supported or inspired me in various ways. First, I am deeply indebted to my parents. Dear Wim and Monique Kuitems, without your unconditional support, involvement and endless babysitting, the realization of this thesis would never have been possible. Further, I am thankful to my partner Hermen Visser for his support in my scientific career, which is seldom limited to normal office hours. I also thank him for teaching me valuable tips and tricks concerning scientific communication, and for the proofreading and lay-out of this dissertation. Loes, thank you for accepting that I was regularly away from home for research and that I had to work on my dissertation during weekends and holidays. The dissertation is now really ready! I am very pleased with your beautiful cover design. Finally, a special word of thanks go to Maaike de Boer, Hiltje Osinga, Claasje Reijers and Anna Sparreboom for their support and advice.

Last, but not least, various people played an important role at the very last stage of the process. Thanks are owed to the assessment committee for thoroughly examining my

About the author

Margot Kuitems was born in Houten on 7 October 1985 and was raised in Opperdoes, the Netherlands. She studied Archaeology at Leiden University. Both her Bachelors and Masters were focused on archaeological sciences and prehistory, and her theses involved stable carbon and nitrogen analysis of animal tissue. After her graduation in 2009, Margot worked part-time as analyst at the Centre of Isotope Research (CIO), University of Groningen. In addition, she continued working as a researcher in the field of archaeological sciences. At the Faculty of Archaeology, Leiden University, she was among others involved in the NWO-funded Dutch Russia Research Cooperation on the 'Collapse of the Mammoth Steppe Ecosystem' (COMSEC), in the geo-archaeological and palaeontological research that was carried out as part of the creation of the Maasvlakte 2 harbour area of Rotterdam, and in the determination and molecular investigation of fossil bones from the archaeological site Schöningen (Germany). Her PhD thesis presents a compilation of a number of stable isotope case studies executed by Margot during the past years. Since 2017, she is employed within the ERC-funded project 'Exact Chronology of Early Societies' (ECHOES), based at the CIO, University of Groningen. She works on a new approach to radiocarbon dating, one that is accurate to the exact calendar year. The technique is built on the recent discovery of annual rises, or 'Miyake Events', in the concentration of radiocarbon in the atmosphere. Margot is using this novel method for radiocarbon dating archaeological sites at an unprecedented precision.

Scientific publications

Related to the PhD research

Kosintsev, P., Mitchell, K.J., Devièse, T., van der Plicht, J., **Kuitems, M.**, Petrova, E., Tikhonov, A., Higham, T., Comeskey, D., Turney, C., Cooper, A., van Kolfschoten, T., Stuart, A.J., Lister, A.M., 2019. Evolution and extinction of the giant rhinoceros *Elasmotherium sibiricum* sheds light on late Quaternary megafaunal extinctions. *Nature Ecology & Evolution* **3** (1), 31-38.

Kuitems, M., van Kolfschoten, M., van der Plicht, J., 2015. Elevated δ^{15}N values in mammoths: a comparison with modern elephants. *Archaeological and Anthropological Sciences*, **7** (3), 289-295.

Kuitems, M., van Kolfschoten, T., 2014. Het Maasvlakte 2 zandwingebied: een bron van informatie. *Grondboor en Hamer* **4/5**, 166-172.

Kuitems, M., van Kolfschoten, T., Tikhonov, A.N., van der Plicht, J., 2019. Woolly mammoth δ^{13}C and δ^{15}N values remained amazingly stable throughout the last ~50,000 years in north-eastern Siberia. *Quaternary International* **500**, 120-127.

Kuitems, M., van der Plicht, J., 2019. Fossil bones from the North Sea: stable isotopes. *Paleontos*, accepted.

Kuitems, M., van der Plicht, J., Drucker, D.G., van Kolfschoten, T., Palstra, S.W.L., Bocherens, H., 2015. Carbon and nitrogen stable isotopes of well-preserved, Middle Pleistocene bone collagen from Schöningen (Germany) and their palaeoecological implications. *Journal of Human Evolution* **89**, 105-113.

Kuitems, M., van der Plicht, J., van Kolfschoten, T., 2019. *Elasmotherium sibiricum*: de uitgestorven Siberische Eenhoorn - uitkomsten van opzienbarend onderzoek. *Cranium* **36** (1), 34-43.

Markova, A.K., Puzachenko, A.Yu., van Kolfschoten, T., Kosintsev, P.A., Kuznetsova, T.V., Tikhonov, A.N., Bachura, O.N., Ponomarev, D.V., van der Plicht, J., **Kuitems, M.**, 2015. Changes in the Eurasian distribution of the musk ox (*Ovibos moschatus*) during the last 50 ka BP. *Quaternary International* **378**, 99-110.

Markova, A.K., Puzachenko, A.Yu., van Kolfschoten, T., Kosintsev, P.A., Kuznetsova, T.V., Tikhonov, A.N., Bachura, O.N., Ponomarev, D.V., van der Plicht, J., **Kuitems, M.**, 2013. Dynamics of Northern Eurasian Musk Ox and Primitive Bison Ranges During the Second Part of Late Pleistocene – Holocene. *IZVESTIYA RAN. The Geographic series*, 110-121.

van der Plicht, J., **Kuitems, M.**, 2019. Fossil bones from the North Sea: radiocarbon dates. *Paleontos*, accepted.

Puzachenko, A.Y., Markova, A.K., Kosintsev, P.A., van Kolfschoten, T., van der Plicht, J., Kuznetsova, T.V., Tikhonov, A.N., Ponomarev, D.V., **Kuitems, M.**, Bachura, O.P., 2017. The Eurasian mammoth distribution during the second half of the Late Pleistocene and the Holocene: Regional aspects. *Quaternary International* **445**, 71-88.

Rivals, F., Julien, M.A., **Kuitems, M.**, van Kolfschoten, T., Serangeli, J., Bocherens, H., Drucker, D.G., Conard, N.J., 2015. Investigation of the horse paleodiet from Schöningen 13 II-4 through dental wear and isotopic analyses and its archaeological implications. *Journal of Human Evolution* **89**, 129-137.

Miscellaneous

Dee, M.W., **Kuitems, M.**, 2019. Duration of activity inestimable due to imprecision of the data. *Proceedings of the National Academy of Sciences* **116** (46), 22907.

Dee, M.W., Palstra, S.W.L., Aerts-Bijma, A.Th., Bleeker, M.O., de Bruijn, S., Ghebru, F., Jansen, H.G., **Kuitems, M.**, Paul, D., Richie, R.R., Spriensma, J.J., Scifo, A., van Zonneveld, D., Verstappen-Dumoulin, B.M.A.A., Wietzes-Land, P., Meijer, H.A.J., 2019. Radiocarbon Dating at Groningen: New and Updated Chemical Pretreatment Procedures. *Radiocarbon*, 1-12. DOI:10.1017/RDC.2019.101.

Kuitems, M., Panin, A., Scifo, A., Arzhantseva, I., Kononov, Y., Doeve, P., Neocleous, A., Dee, M. Radiocarbon-based approach capable of subannual precision resolves the origins of the site of Por-Bajin. *Proceedings of the National Academy of Sciences*, accepted.

Kuitems, M., van der Plicht, J., Jansma, E., 2020. Wood from the Netherlands around the time of the Santorini eruption dated by dendrochronology and radiocarbon.

Radiocarbon, in press.

Neocleous, A., Azzopardi, G., **Kuitems, M.**, Scifo, A., Dee, M., 2019. Trainable Filters for the Identification of Anomalies in Cosmogenic Isotope Data. *IEEE Access* **7**, 24585-24592.

Neocleous, A., **Kuitems, M.**, Scifo, A., Dee, M., 2019. CHRONOscope: Application for the interactive visualization of carbon-14 and Beryllium-10 atmospheric data. *Radiocarbon*, 1-6. DOI: 10.1017/RDC.2019.135.

Scifo, A., **Kuitems, M.**, Neocleous, A., Pope, B.J.S., Miles, D., Jansma, E., Doeve, P., Smith, A.M., Miyake, F., Dee, M.W., 2019. Radiocarbon production events and their potential Relationship with the Schwabe cycle. *Scientific reports* **9** (1), 1-8.

Wacker, L., Scott, E.M., Bayliss, A., Brown, D., Bard, E., Bollhalder, S., Bronk Ramsey, C., Friedrich, M., Capano, M., Cherkinsky, A., Chivall, D., Culleton, B.J., Dee, M.W., Friedrich, R., Hodgins, G.W.L., Hogg, A., Kennett, D.J., Knowles, T.D.J., **Kuitems, M.**, Lange, T.E., Miyake, F., Nadeau, M.-J., Nakamura, T., Naysmith, J.P., Olsen, J., Omori, T., Petchey, F., Philippsen, B., Ravi Prasad, G.V., Seiler, M., Southon, J., Staff, R., Tuna, T., 2020. Findings from an in-depth annual tree ring radiocarbon intercomparison. *Radiocarbon*, in press.